NPS ARCHIVE
1964
MACVEAN, C.

THESIS

A SIMPLIFIED CELL THEORY APPLIED TO THE CALCULATION OF THERMAL NEUTRON SPECTRA IN LIGHT WATER LATTICES

CHARLES ROBERT MAC VEAN

1964

Library
U. S. Naval Postgraduate School
Monterey, California

A SIMPLIFIED CELL THEORY APPLIED TO THE CALCULATION OF THERMAL NEUTRON SPECTRA IN LIGHT WATER LATTICES

A Thesis

Presented to the Faculty of the Graduate School

of Cornell University for the Degree of

Doctor of Philosophy

by

Charles Robert Mac Vean

September, 1964

Library
U. S. Naval Postgraduate School
Monterey, California

ABSTRACT

A simplified polyenergetic cell theory is formulated to determine spatially averaged energy dependent thermal fluxes in the moderator, cladding, and fuel regions within the unit cell of a reactor lattice. The derived spectra are then utilized in the calculations of the thermal integral parameters and average cross sections required for reactor computations.

The cell theory, as formulated, postulates an infinite moderator region with the absorption cross section of this region appropriately modified to account for the neutron leakage into and absorption by the fuel element. The modifications to the moderator absorption cross section are formulated both in terms of the net current at the fuel element-moderator interface and in terms of energy dependent moderator and fuel element escape probabilities, the latter approach offering physical transparency and ease of calculation.

Analytic expressions for the escape probabilities are presented, integral transport theory being applied to the fuel element region, while diffusion theory is utilized in the moderator region. Using these analytic expressions, the theory is applied to actual lattices in the form of the light water moderated and uranium dioxide fueled cores of the Cornell University Zero Power Reactor. Room temperature parameters and their temperature coefficients are determined using both the monatomic gas model and the Nelkin water kernel to describe the energy transfer process in the moderator. Calculations are made with PROGRAM COUTH, a Fortran-63 program written for use with the Control Data Corporation 1604 digital computer. A typical lattice calculation including the computation of the spatially averaged fuel, cladding, and moderator spectra and the thermal integral properties and average cross sections takes approximately thirty-five seconds of computer time. This figure is exclusive of the compiling time and the time required to calculate the moderator scattering kernel.

In an attempt to estimate the accuracy of the calculational results, the method is applied to the Brookhaven National Laboratory uranium dioxide cores and the results are then compared with those predicted by Honeck's THERMOS code. Disadvantage factors agree to within 1.0% while the thermal utilizations agree to within 0.5%. A study of the sensitivity of the calculated integral parameters to variations in the input data leads to the assignment of rather small uncertainties in the results calculated with the simplified cell theory.

NOTICE

Lieutenant C. R. Mac Vean, U. S. Navy, attended Cornell University under the provisions of the Junior Line Officers Advanced Scientific Educational Program which is sponsored by the U. S. Navy Bureau of Personnel and the U. S. Naval Postgraduate School, Monterey, California.

ACKNOWLEDGMENTS

The author wishes to gratefully acknowledge his association with Professor K. Bingham Cady. The initial impetus provided by his suggestion of this thesis topic and the continuing enthusiasm generated by him with regard to this topic have been the underlying factors contributing to the completion of this work. His guidance has proved invaluable. To Professor David D. Clark, the author's academic adviser, thanks are expressed for the support, direction, and assistance provided during the author's four years at Cornell. The helpful and constructively critical discussions with Professor Mark S. Nelkin led to the improvement of several facets of this work and they are acknowledged with gratitude.

The Commanding Officers of the U. S. Naval R.O.T.C. Unit at Cornell during the author's tour of duty there, Captains R. B. Bretland and C. V. Zalewski, who along with their staffs have provided a wealth of administrative and cooperative support, are wholeheartedly acknowledged. The author is privileged to have served under them.

The author is indebted to the U. S. Navy Bureau of Personnel and the U. S. Naval Postgraduate School in Monterey, California, who jointly sponsor the Junior Line Officers Advanced Scientific Educational Program. In particular, the author wishes to express his gratitude to Mrs. C. M. Gumz of the Bureau of Personnel for the courteous and meaningful liaison which she has provided.

The efforts and cooperation of the Cornell Computing Center are gratefully acknowledged, and the author wishes to thank Mrs. Betty Blake and Mrs. Barbara Boettcher for their skillful preparation of the final manuscript.

Several of the Cornell graduate students in the field of Nuclear Science and Engineering have provided assistance in this work and the discussions with Donald H. Bryce, Floyd E. Gelhaus, William E. Schilling, Robert A. Shaw, and Lt. Walter P. Wynn, Jr., U.S.N. are acknowledged with thanks.

Finally, the author wishes to thank his wife, Ellen, for the constant and continuing encouragement and motivation which she has contributed during this work.

TABLE OF CONTENTS

CHAPTER		PAGE
1	INTRODUCTION	1
2	A SIMPLIFIED CELL THEORY	6
	2.1 General Formulation	6
	2.2 A Practical Approximation of Heterogeneous Effects	12
	2.3 Formulation in Terms of Escape Probabilities	17
3	MODERATOR ESCAPE PROBABILITIES	21
	3.1 $P_s(E)$	21
	3.2 $P_m(E)$	24
4	THE FUEL ELEMENT ESCAPE PROBABILITY	27
	4.1 The Fuel Rod Escape Probability	27
	4.2 Void Considerations	31
	4.3 Cladding Effects	33
5	MODELS FOR THE SCATTERING KERNEL	41
	5.1 The Monatomic Gas Model	41
	5.2 The Nelkin Water Kernel	46
6	THERMAL LATTICE SPECTRA AND INTEGRAL PROPERTIES	61
7	APPLICATION OF THE METHOD TO ACTUAL LATTICES .	73
	7.1 Room Temperature Calculations	73
	7.2 Temperature Coefficients	94
8	ACCURACY OF THE RESULTS	102
9	SUMMARY AND CONCLUSIONS	113

Chapter Page

APPENDIX A. LATTICE PARAMETERS FOR THE CORNELL UNIVERSITY ZERO POWER REACTOR 117

APPENDIX B. NUMERICAL RESULTS FOR THE CORNELL UNIVERSITY ZERO POWER REACTOR 121

APPENDIX C. NUMERICAL METHODS IN COUTH 150

APPENDIX D. INPUT-OUTPUT FOR COUTH 160

APPENDIX E. FORTRAN LISTING OF COUTH 170

APPENDIX F. NOTATION 189

WORKS CITED 196

LIST OF TABLES

TABLE		PAGE
8.1	Percentage Changes in Input Parameters Required to Change Integral Properties by +0.1 Percent . . .	109
A.1	Cornell University Zero Power Reactor Fuel Element Parameters	118
A.2	Cornell University Zero Power Reactor Lattice Parameters	119
A.3	Cornell University Zero Power Reactor Material Concentrations and Cross Sections	120
B.1	Energy, Velocity, and Lethargy Mesh Utilized by COUTH	122
B.2	Nelkin Water Model for the Scattering Matrix at 20°C	123
B.3	Nelkin Water Model for the Scattering Matrix at 40°C	129
B.4	Energy Dependent Cross Sections	134
B.5	Energy Dependent Cross Sections	135
B.6	Spatially Averaged Thermal Spectra for the Cornell ZPR 1:1 Core	136
B.7	Spatially Averaged Thermal Spectra for the Cornell ZPR 1.5:1 Core	137
B.8	Spatially Averaged Thermal Spectra for the Cornell ZPR 2:1 Core	138
B.9	Spatially Averaged Thermal Spectra for the Cornell ZPR 3:1 Core	139
B.10	Spatially Averaged Thermal Spectra for the Cornell ZPR 4:1 Core	140
B.11	Cornell University Zero Power Reactor Integral Properties	141
B.12	Cornell University Zero Power Reactor Integral Property Temperature Coefficients	143

Table Page

B.13 Cornell University Zero Power Reactor Effective Cross Sections 144

B.14 Cornell University Zero Power Reactor Effective Cross Section Temperature Coefficients . . . 145

B.15 Cornell University Zero Power Reactor Mean Cross Sections 147

B.16 Cornell University Zero Power Reactor Mean Cross Section Temperature Coefficients . . . 148

LIST OF ILLUSTRATIONS

FIGURE		PAGE
2.1	The Fuel Element and Moderator Escape Probabilities	18
3.1	The Moderator Escape Probability, $P_s(E)$ . .	23
3.2	The Moderator Escape Probability, $P_m(E)$ . .	25
4.1	The Fuel Rod Escape Probability, $P_r(E)$ . .	32
4.2	The Fuel Element Escape Probability, $P_e(E)$.	38
4.3	The Ratio of the Fuel Rod Absorption Rate to the Fuel Element Absorption Rate . . .	40
5.1	Approximations Used in the Calculation of the Nelkin Water Kernel	53
5.2	The Average Cosine of the Scattering Angle and the Transport Cross Section for Water	57
7.1	Apparent Lattice Absorption Cross Section .	79
7.2	Spatially Averaged Moderator Thermal Spectra	80
7.3	Comparison of the Moderator Spectra Predicted with the Nelkin Water and Monatomic Gas Models	81
7.4	Spatially Averaged Cell Spectra	83
7.5	Average Neutron Velocities	84
7.6	Average Neutron Velocity for the Homogenized Cell	86
7.7	Neutron Density Disadvantage Factors . . .	86a
7.8	Thermal Utilization	88
7.9	Integral Properties, η and ηf	89
7.10	Thermal Lifetime	90
7.11	Effective and Mean Absorption Cross Sections for the Homogenized Cell	92

Figure		Page
7.12	Thermal Diffusion Coefficient and Length for the Homogenized Cell	93
7.13	Temperature Coefficient of the Average Neutron Velocity for the Homogenized Cell	96
7.14	Temperature Coefficients of the Neutron Density Disadvantage Factors	97
7.15	Temperature Coefficients of the Integral Properties, f and ηf	99
7.16	Temperature Coefficients of the Thermal Diffusion Coefficient and Length for the Homogenized Cell	100
8.1	Thermal Utilization	104
8.2	Integral Property, η	105
8.3	Neutron Density Moderator Disadvantage Factor	107

CHAPTER 1

INTRODUCTION

The analysis and design of any thermal reactor requires an accurate knowledge of the various and competing neutron reaction rates within the reactor assembly. This, in turn, implies a knowledge of the distribution of thermal neutrons in space and energy. In the calculation of the thermal neutron spectra one must consider the two processes which affect these distributions in a heterogeneous reactor lattice. The first of these is the moderation process wherein a neutron is scattered by a moderator atom or molecule with a subsequent change in energy. The second process is the transport or diffusion mechanism whereby the neutrons are carried into regions of relatively different absorption characteristics. Although the time independent Boltzmann's equation or the integral transport equation[1] correctly describes both the moderation and transport phenomena, the difficulty in obtaining solutions to these equations have led previous investigators to develop their work along one of two lines. Initial attempts to characterize the distribution of thermal neutrons were done for infinite homogeneous media[2,3] where

---

[1] A. M. Weinberg and E. P. Wigner, The Physical Theory of Neutron Chain Reactors, pp. 221-234, The University of Chicago Press, Chicago, 1958.

[2] M. J. Poole, M. S. Nelkin, and R. S. Stone, "The Measurement and Theory of Reactor Spectra," Progress in Nuclear Energy, Series I, Vol. 2, pp. 91-164, Pergamon Press, New York, London, Paris, and Los Angeles, 1958.

there is no net transport or diffusion and the spatial variable is of no consequence. This approach allows concentration on the moderation or energy transfer process and sophisticated mathematical models may be incorporated into the calculation.

The other approach, as exemplified by multigroup diffusion calculations,[4] attempts to consider spatial effects at the expense of the details of the moderation process. In these calculations, the scattering kernel is often characterized by a simple model which allows ease of mathematical description but which may lack accuracy in its approximation of the energy transfer process.

More recently, interest has been focused on the use of transport theory[5] for dealing with the heterogeneities present in a reactor lattice. This approach is embodied in the work of Honeck[6,7] where both the spatial and

---

3/ Neutron Spectra in Lattices and Infinite Media, Proceedings of the Brookhaven Conference on Neutron Thermalization, BNL 719, Vol. II, Brookhaven National Laboratory (1962).

4/ A. Hassitt, "Methods of Calculation for Heterogeneous Reactors," Progress in Nuclear Energy, Series I, Vol. 2, pp. 271-313, Pergamon Press, New York, London, Paris, and Los Angeles, 1958.

5/ Neutron Spectra in Lattices and Infinite Media, see Footnote 3.

6/ H. C. Honeck, "THERMOS -- A Thermalization Transport Theory Code for Reactor Lattice Calculations" BNL 5826, Brookhaven National Laboratory (1961).

moderation effects on the spectra are considered through a space and energy calculation utilizing integral transport theory with only slight restrictions on the complexity of the scattering model used.

Still another approach is that found in the work of Leslie.[8,9] In this formulation the effect of moderation and heterogeneity are both considered, but the spatial effects are mathematically subordinated by consideration of only the spatially averaged fluxes in the moderator and the fuel. This method of attack leads to physical transparency while allowing one to maintain and concentrate on the importance of the moderator scattering model.

This work is an extension of Leslie's ideas, culminating in a computer code which provides for the rapid calculation of the spatially averaged thermal neutron spectra in the moderator, fuel, and cladding regions of a reactor lattice. The simplified cell theory utilized in these calculations is formulated in Chap. 2. A general formulation is presented as well as a formulation in terms of escape probabilities defined for the fuel element and the moderator regions. The escape probabilities utilized are a polyenergetic generalization of those defined by Amouyal,

---

7/ H. C. Honeck, "The Calculation of the Thermal Utilization and Disadvantage Factor in Uranium/Water Lattices," Nucl. Sci. Eng. 18, 49-68 (1964).

8/ D. C. Leslie, "The Spectrox Method for Thermal Spectra in Lattice Cells," AEEW-M211, United Kingdom Atomic Energy Authority (1962).

Benoist, and Horowitz[10] in their one velocity thermal utilization theory. Chapter 3 deals with the escape probabilities defined for the moderator region, while Chap. 4 details the calculational methods available for the determination of the fuel element escape probability. Mathematical models for the energy transfer or scattering kernel are discussed in Chap. 5. Emphasis is placed on the models actually used for calculational purposes; the monatomic gas kernel[11,12] and the Nelkin water kernel.[13] Chapter 6 defines the calculations necessary in the determination of spatially averaged, energy dependent thermal fluxes for the moderator, cladding, and fuel regions in a lattice utilizing the simplified cell theory. Integral thermal properties are defined as are the averaged cross sections necessary for the accurate calculation of reaction rates. In Chap. 7 the formulated theory is applied to actual lattices. A study is made of the low enrichment, high density, uranium dioxide fueled and light water moderated Cornell University Zero

---

9/ D. C. Leslie, "The Calculation of Thermal Spectra in Lattices," Proceedings of the Brookhaven Conference on Neutron Thermalization, BNL 719, Vol. II, pp. 592-609, Brookhaven National Laboratory (1962).

10/ A. Amouyal, P. Benoist, and J. Horowitz, "Nouvelle Méthode de Determination du Facteur d'Utilization Thermique d'une Cellule," J. Nucl. Energy 6, 79 (1957).

11/ E. P. Wigner and J. E. Wilkins, Jr., "Effect of the Temperature of the Moderator on the Velocity Distribution of Neutrons with Numerical Calculations for H as the Moderator," AECD-2275 (1944).

Power Reactor cores.[14] Temperature effects are predicted through the use of temperature dependent models for the scattering kernel. The accuracy of these results are discussed in Chap. 8. This chapter also includes a comparison of the results predicted with the simplified cell theory to those calculated by Honeck with THERMOS[15] for the Brookhaven light water moderated, and uranium dioxide fueled lattices. Chapter 9 contains a summary of the work undertaken as well as the conclusions which may be drawn from it.

12/ J. E. Wilkins, Jr., "Effect of Temperature of the Moderator on the Velocity Distribution of Neutrons for a Heavy Moderator," CP-2481 (1944).

13/ M. S. Nelkin, "Scattering of Slow Neutrons by Water," Phys. Rev. 119, 741-746 (1960).

14/ D. D. Clark, "The Cornell University Nuclear Reactor Laboratory," CURL-1, Cornell University (1961).

15/ H. C. Honeck, see Footnote 7.

CHAPTER 2

A SIMPLIFIED CELL THEORY

2.1 General Formulation

Recognizing that the neglect or oversimplification of the spatial effects in a heterogeneous lattice leads to answers which have little relationship to the physical processes taking place, one is prompted to overemphasize the spatial variations by resorting to multigroup diffusion[16] or transport[17] codes. However, these codes consume a considerable amount of computer time, particularly if the more complex models of the scattering kernel are used.

Thus, there is a need for a simple polyenergetic formulation for determining the thermal distribution of neutrons in the various regions of a heterogeneous lattice. Hopefully one could retain the calculational ease of the homogeneous, infinite medium thermal spectrum computation, thereby offering only slight limitations on the complexity of the scattering model used, while still accounting for the heterogeneities of the lattice in a meaningful way.

This section formulates a simplified cell theory for use in the calculation of thermal spectra and parameters in a lattice composed of uniformly arrayed unit cells. The

---

[16] R. S. Varga, "Numerical Methods for Solving Multi-Dimensional Multigroup Diffusion Equations," Proceedings of Symposia in Applied Mathematics, Vol. XI, pp. 164-189, Nuclear Reactor Theory, American Mathematical Society, Providence (1961).

heterogeneous effects due to neutron transport within the cell are formulated in a physically transparent manner, thereby allowing sufficient emphasis to be placed on the moderation process in any calculation.

Consider first the neutron balance equation to be solved in the case of an infinite, homogeneous, moderating medium:[18]

$$\left[\Sigma_a^m(E) + \Sigma_s^m(E) \right] \varphi^m(E) = S(E) + \int_o^{E_c} \Sigma(E' \rightarrow E) \varphi^m(E') dE' . \tag{2.1}$$

E_c is the thermal cutoff energy above which the moderator flux per unit energy, $\varphi^m(E)$, is assumed to be 1/E, while $\Sigma(E' \rightarrow E)$ is the energy transfer or scattering kernel expressed in $(\text{cm-eV})^{-1}$. $\Sigma_a^m(E)$ and $\Sigma_s^m(E)$ are the macroscopic absorption and scattering cross sections respectively of the moderator, $\Sigma_s^m(E)$ being defined by

$$\Sigma_s^m(E) = \int_o^{E_c} \Sigma(E \rightarrow E') dE' . \tag{2.2}$$

---

[17] H. C. Honeck, "THERMOS -- A Thermalization Transport Theory Code for Reactor Lattice Calculations," BNL-5826, Brookhaven National Laboratory (1961).

[18] M. J. Poole, M. S. Nelkin, and R. S. Stone, "The Measurement and Theory of Reactor Spectra," Progress in Nuclear Energy, Series I, Vol. 2, pp. 91-164, Pergamon Press, New York, London, Paris, and Los Angeles, 1958.

The source of thermal neutrons, S(E), due to down scattering from energies above E_c is given by

$$S(E) = \int_{E_c}^{\infty} \Sigma(E' \rightarrow E)\varphi_c^m(E')dE' \ , \qquad (2.3)$$

where $\varphi_c^m(E)$ is proportional to 1/E.

Neutron conservation requires that

$$\int_o^{E_c} S(E)dE = \int_o^{E_c} \Sigma_a^m(E)\ \varphi^m(E)dE \ , \qquad (2.4)$$

which is obtained by integrating Eq. (2.1) over energy from 0 to E_c.

The problem as stated places no restrictions on the form of the scattering kernel, $\Sigma(E' \rightarrow E)$, however, we require that it satisfy detailed balance:

$$\Sigma(E' \rightarrow E)M(E') = \Sigma(E \rightarrow E')M(E) \ , \qquad (2.5)$$

where the Maxwellian distribution, M(E), is given by

$$M(E) = E/(kT)^2 \exp(-E/kT) \ . \qquad (2.6)$$

The moderator temperature in electron volts is equal to kT, T being the moderator physical temperature while k is Boltzmann's constant.

There are of course practical limitations which restrict the complexity of the kernel and the number of energy points to be utilized in the computer solution of Eq. (2.1).

The infinite medium calculation is now extended to the heterogeneous lattice utilizing the ideas embodied in Leslie's SPECTROX method.[19] Since the only effect which the fuel element has upon the spectrum in the moderator of a lattice cell is to modify the transport process in the vicinity of the fuel element, while contributing very little to the moderation process itself, one may postulate an infinite moderator region with a contrived energy dependent absorption cross section which includes the heterogeneous properties of the lattice. In other words, if the absorption cross section of the moderator can be appropriately modified to account for the neutron leakage into and absorption by the fuel element, one can then turn his attention to the choice of a proper scattering kernel. The calculational ease of Eq. (2.1) is still available along with the fact that the non moderating part of the reactor lattice has been accounted for.

Considering the energy dependent absorption rates, one defines

$$f(E) = \frac{\text{absorption rate in the fuel element at energy E, per eV}}{\text{absorption rate in the lattice cell at energy E, per eV}} . \qquad (2.7)$$

The "fuel element" includes the fuel rod and its cladding, and in the case where there is no neutron absorption in the cladding, f(E) can be considered to be the energy dependent thermal utilization. In terms of f(E) the neutron

[19] D. C. Leslie, "The SPECTROX Method for Thermal Spectra in Lattice Cells," AEEW-M211, United Kingdom Atomic Energy Authority (1962).

loss rate per unit volume of the moderator due to leakage into and absorption by the fuel element may be expressed as $\Sigma_a^m(E)\overline{\varphi}^m(E)f(E)/[1-f(E)]$, where $\overline{\varphi}^m(E)$ is the spatially averaged flux in the moderator region having a volume of V^m:

$$\overline{\varphi}^m(E) = \frac{1}{V^m} \int \varphi^m(\vec{r},E)dV \quad . \tag{2.8}$$

Equation (2.1) may now be rewritten for the cell in a heterogeneous lattice as

$$\left(\Sigma_s^m(E) + \Sigma_a^m(E) \left[1 + \frac{f(E)}{1-f(E)} \right] \right) \overline{\varphi}^m(E) = \overline{S}(E) + \int_0^{E_c} \Sigma(E' \rightarrow E)\overline{\varphi}^m(E')dE' \quad . \tag{2.9}$$

$\overline{S}(E)$ is now the spatially averaged slowing source of neutrons which appear in dE at E due to scattering collisions at energies greater than E_c.

$$\overline{S}(E) = \frac{1}{V^m} \int S(\vec{r},E)dV \quad . \tag{2.10}$$

As it stands, Eq. (2.9) is correct for an infinite reactor lattice and it could be modified to include the effects of thermal leakage out of the reactor assembly. However, since one is usually interested in the intensive properties of the lattice, conventional approaches neglect

this thermal leakage calculation. In addition, Eq. (2.9) becomes approximate as soon as one postulates appropriate mathematical models for the scattering kernel, $\Sigma(E' \rightarrow E)$, and for the relative fuel element absorption, $f(E)/[1-f(E)]$, in the quest for a practical and economic computer solution.

The most general formulation for the relative fuel element absorption may be obtained by considering a unit cell in an infinite reactor lattice. Assume a source of neutrons in dE at energy E and position $\vec{r}$, $N(\vec{r},E)$, so that the spatially average source of neutrons, N(E), per unit volume, V, is expressed by:

$$N(E) = \frac{1}{V} \int N(\vec{r},E)dV \ . \qquad (2.11)$$

Given $N(\vec{r},E)$, one can in principle calculate the net current into the fuel element, $J_n(E)$, at each energy. The total number of neutrons absorbed by the fuel element at energy E is then $AJ_n(E)$, where A is the surface area of the fuel element. Since the total number of neutrons produced at E must equal the total number absorbed, the number of neutrons absorbed by the moderator is $VN(E)-AJ_n(E)$. The relative fuel element absorption is then expressed as:

$$\frac{f(E)}{1-f(E)} = \frac{AJ_n(E)}{VN(E)-AJ_n(E)} \ . \qquad (2.12)$$

In the assumption of a spatially dependent neutron source, $N(\vec{r},E)$, and the subsequent calculation of the net

current into the fuel element, any of several means may be utilized including the use of multigroup transport codes, integral transport theory, or energy dependent diffusion theory. The accuracy of the results is directly related to the effort expended on these calculations, and this fact must be reconciled with the desire to produce economy in the use of the computer along with the knowledge that certain errors will be introduced with the use of mathematical models for the scattering kernel.

It is to be noted that by incorporating and concentrating all of the heterogeneous effects into the function f(E), the calculational simplicity of the infinite, homogeneous case has been retained as is seen in Eq. (2.9). A discussion of practical approximations for f(E) is found in Secs. (2.2) and (2.3).

2.2 A Practical Approximation of Heterogeneous Effects

In formulating an analytic approximation for f(E), the function which takes into account all of the heterogeneous effects in the lattice cell, one is forced to compromise between accuracy and computational ease. As an initial approach, the following simple model is postulated in an attempt to investigate the feasibility of this method in determining the thermal spectra within a lattice cell. In this work we have restricted ourselves to systems with cylindrical symmetry, recognizing that analogous results for spheres and slabs are obtainable.

Consider a cylindrical unit cell situated in the regular, rectangular or hexagonal, array of a lattice. It is characterized by the fuel element radius, r_o, and the moderator radius, r_1. In determining r_1 from the actual lattice parameters, the Wigner-Seitz criterion[20] is applied. A spatially flat source of neutrons in the moderator, N(E), is assumed. The validity of this assumption for the calculation of integral properties has been discussed by Pomraning.[21] Leslie[22] has indicated that multigroup transport calculations yield moderator flux shapes which compare favorably with those predicted by one group diffusion theory. In light of this it is proposed to calculate the net current into the fuel element, $J_n(E)$, through the extension of monoenergetic diffusion theory to the polyenergetic case. The flux shape in the cell moderator at any energy E is assumed to be spatially distributed in a manner given by solution of the constant cross section diffusion theory approximation, using cross sections evaluated at the energy E:

$$D_m(E)\nabla^2\varphi^m(r,E)-\Sigma_a^m(E)\varphi^m(r,E) + N(E) = 0 \ . \qquad (2.13)$$

---

[20] S. Glasstone and M. C. Edlund, The Elements of Nuclear Reactor Theory, p. 265, D. Van Nostrand Company, Inc., Princeton, Toronto, London, and New York, 1952.

[21] G. C. Pomraning, "On the Validity of the Constant Source Assumption for the Cell Problem," Nucl. Sci. Eng. 18, 400-403 (1964).

[22] D. C. Leslie, see Footnote 19.

The boundary conditions applied are

$$\nabla\varphi^m(r_1,E) = 0 \ , \tag{2.14}$$

and

$$\frac{\varphi^m(r_o,E)}{\nabla\varphi^m(r_o,E)} = d(E) \ . \tag{2.15}$$

$D_m(E) = 1/3\Sigma^m_{tr}(E)$ is the moderator diffusion coefficient, $\Sigma^m_a(E)$ is the moderator macroscopic absorption cross section, and $d(E)$ is the energy dependent linear extrapolation length. The linear extrapolation length may be determined from $d_o(E)$, the linear extrapolation length into a black cylindrical hole,[23] by characterizing the fuel element with its escape probability, $P_e(E)$. This has the added advantage of eliminating the need to state anything explicit about the shape of the flux within the fuel element. The fuel element spatial flux is implied in any calculation of the escape probability, but by dealing strictly with $P_e(E)$ one can extract and utilize in a simple manner the accuracy of transport theory calculations.[24]

Considering the escape probability of the fuel element as its albedo,[25] and including the term in $\nabla^2\varphi$ which can

---

[23] A. M. Weinberg and E. P. Wigner, The Physical Theory of Neutron Chain Reactors , p. 765, The University of Chicago Press, Chicago, 1958.

[24] K. B. Cady and M. Clark, Jr., "Neutron Transport in Cylindrical Rods," Nucl. Sci. Eng., 18, 491-507 (1964).

[25] S. Glasstone and M. C. Edlund, p. 129, see Footnote 20.

be obtained in the derivation of Fick's Law,[26] one can write

$$P_e(E) = \frac{\varphi^m(r_o,E) - 2D_m(E)\nabla\varphi^m(r_o,E) + G(E)\nabla^2\varphi^m(r_o,E)}{\varphi^m(r_o,E) + 2D_m(E)\nabla\varphi^m(r_o,E) + G(E)\nabla^2\varphi^m(r_o,E)} \quad . \qquad (2.16)$$

For a black cylindrical hole, $P_e(E)$ is by definition zero so that G(E) is given by

$$G(E) = \frac{\nabla\varphi^m(r_o,E)}{\nabla^2\varphi^m(r_o,E)} \left[2D_m(E) - d_o(E) \right] . \qquad (2.17)$$

In the actual cell, where $P_e(E)$ is known from transport theory calculations, substitution of Eq. (2.17) into Eq. (2.16) yields with rearrangement

$$d(E) = \frac{\varphi^m(r_o,E)}{\nabla\varphi^m(r_o,E)} = \frac{4D_m(E)P_e(E)}{1-P_e(E)} + d_o(E) \quad . \qquad (2.18)$$

An approximate expression for $d_o(E)$ is given in Appendix C while the calculation of the fuel element escape probability is discussed in Chap. 4.

The relative fuel absorption, f(E)/[1-f(E)], may now be found from the solution of Eq. (2.13) utilizing the boundary conditions in Eqs. (2.14), (2.15), and (2.18). For a cylindrical cell, Eq. (2.12) may be expressed as

$$\frac{1-f(E)}{f(E)} = \frac{N(E)r_o(y^2-1)}{2D_m(E)\nabla\varphi^m(r_o,E)} - 1 \ , \qquad (2.19)$$

where $y = r_1/r_o$. Denoting $\Sigma_a^m(E)/D_m(E)$ by κ^2, it follows that

---

[26] A. M. Weinberg and E. P. Wigner, pp. 192-194, see Footnote 23.

$$\nabla\varphi^m(r_o,E) = \frac{N(E)/\Sigma_a^m(E)}{\chi(E)/\kappa + d_o(E) + \frac{4D_m(E)P_e(E)}{1-P_e(E)}} \quad , \qquad (2.20)$$

where

$$\chi(E) = \frac{K_1(\kappa r_1)I_o(\kappa r_o) + I_1(\kappa r_1)K_o(\kappa r_o)}{K_1(\kappa r_1)I_o(\kappa r_o) - I_1(\kappa r_1)K_1(\kappa r_o)} \quad . \qquad (2.21)$$

I_o, I_1, K_o, and K_1 are the modified Bessel functions of the first and second kind, respectively. Substitution into Eq. (2.19) yields

$$\frac{1-f(E)}{f(E)} = \frac{2r_o(y^2-1)\Sigma_a^m(E)P_e(E)}{1-P_e(E)} + \frac{r_o}{2}(y^2-1)\kappa\chi(E) + \frac{r_o(y^2-1)\Sigma_a^m(E)d_o(E)}{2D_m(E)} - 1 \quad . \qquad (2.22)$$

Insertion of Eq. (2.22) into Eq. (2.9) thus attempts to account for the heterogeneous effects in the lattice through use of diffusion theory in the moderator and transport theory in the fuel element. The formulation is not restricted to the use of diffusion theory in the moderator region but it is utilized because of its calculational ease and good approximation to one velocity transport theory.

2.3 Formulation In Terms of Escape Probabilities

The expression, Eq. (2.22), which approximates the relative fuel absorption, and hence, the heterogeneous effects in the cell may also be arrived at by the formulation of the energy dependent absorption rates in terms of moderator and fuel element escape probabilities. This approach is an extension of Amouyal, Benoist, and Horowitz's one velocity thermal utilization theory[27] to the polyenergetic case.

One begins by defining the following energy dependent escape probabilities, all of which are calculated assuming the adjacent region is black:

$P_e(E)$ is the escape probability of neutrons incident on the fuel element in the actual lattice directional distribution,

$P_s(E)$ is the escape probability of neutrons in the moderator at energy E due to collisions at other energies, and,

$P_m(E)$ is the escape probability of neutrons incident on the moderator from the fuel element.

These escape probabilities are schematically depicted in Fig. 2.1 for a Wigner-Seitz cylindrical cell. If one

---

[27] A. Amouyal, P. Benoist, and J. Horowitz, "Nouvelle Méthode de Determination du Facteur d'Utilization Thermique d'une Cellule," J. Nucl. Energy 6, 79 (1957).

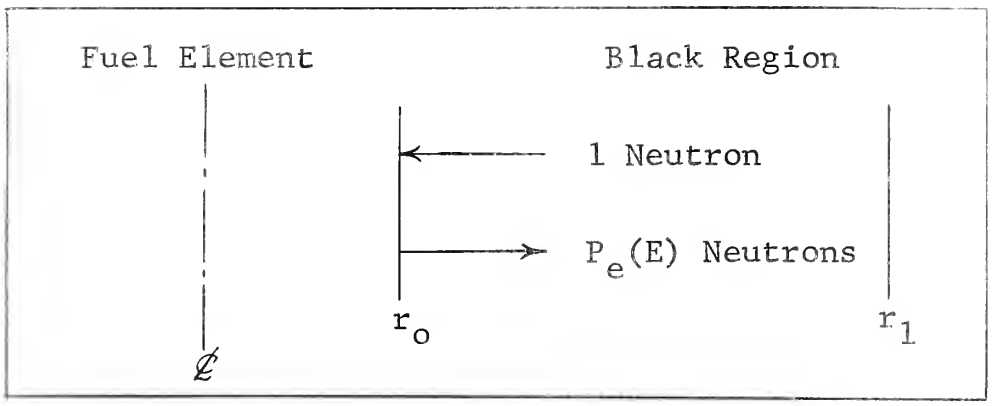

Fuel Element Escape Probability, $P_e(E)$

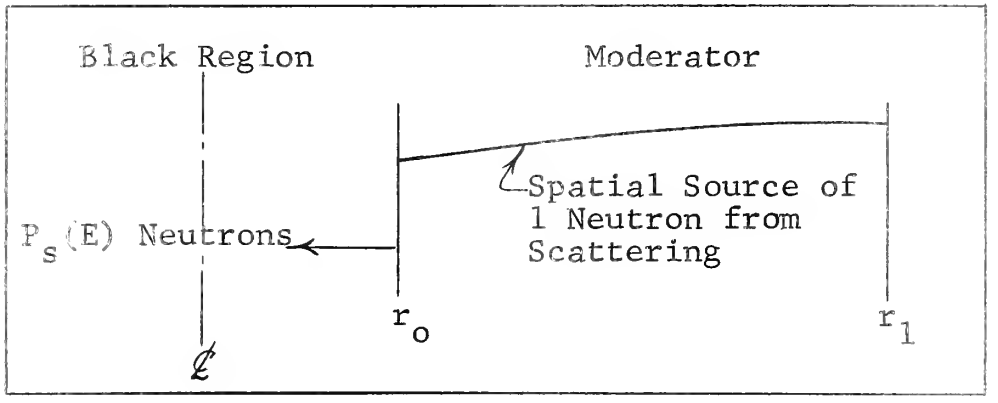

Moderator Escape Probability, $P_s(E)$

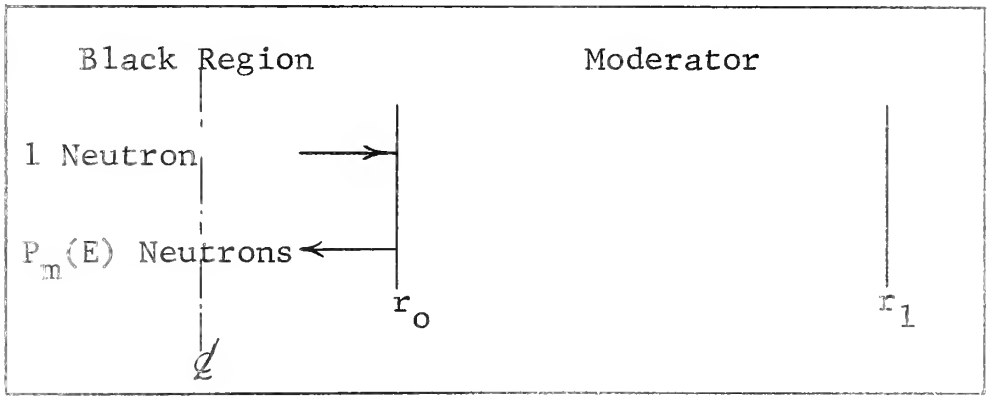

Moderator Escape Probability, $P_m(E)$

Figure 2.1 The Fuel Element and Moderator Escape Probabilities

considers a spatial source of neutrons from scattering which has been normalized to one:

$$\int N(\vec{r},E)dV = 1 \ , \tag{2.23}$$

then reference to Fig. 2.1 shows that the current into the fuel element, $J_-(E)$, may be expressed as

$$AJ_-(E) = P_s(E) + P_e(E)P_m(E)AJ_-(E) \ , \tag{2.24}$$

or,

$$AJ_-(E) = \frac{P_s(E)}{1-P_e(E)P_m(E)} \ , \tag{2.25}$$

where A is the surface area of the fuel element. The net current into the fuel element is given by

$$J_n(E) = J_-(E) - P_e(E)J_-(E) \ , \tag{2.26}$$

so that

$$AJ_n(E) = \frac{[1-P_e(E)]P_s(E)}{1-P_e(E)P_m(E)} \ . \tag{2.27}$$

Since the source has been normalized to one neutron, Eq. (2.27) is the ratio of the absorption rate in the fuel element to the absorption rate in the cell. Therefore,

$$f(E) = \frac{[1-P_e(E)]P_s(E)}{1-P_e(E)P_m(E)} \ . \tag{2.28}$$

Rearranging Eq. (2.28) or substituting Eq. (2.27) into Eq. (2.12) yields:

$$\frac{1-f(E)}{f(E)} = \frac{P_e(E)}{1-P_e(E)} \left[\frac{1-P_m(E)}{P_s(E)} \right] + \frac{1-P_s(E)}{P_s(E)} \quad . \qquad (2.29)$$

Writing the heterogeneous effects in terms of these escape probabilities has several advantages. In the first place a certain amount of physical transparency is gained by separating the contributions of the fuel and moderator into easily defined quantities. Secondly, $P_e(E)$ is a functional of the fuel element properties and its calculation depends only slightly on the moderator through the directional distribution of the current entering the fuel elements. $P_s(E)$ and $P_m(E)$ are functionals of the moderator and are very nearly independent of the fuel element properties. In addition, there are no restrictions on this simple model and the escape probabilities may be calculated with as much sophistication as is desirable. Calculational techniques for determining the moderator escape probabilities, $P_s(E)$ and $P_m(E)$, are discussed in Chap. 3, while the fuel element escape probability, $P_e(E)$, is discussed in Chap. 4.

CHAPTER 3

MODERATOR ESCAPE PROBABILITIES

3.1 $P_s(E)$

In this chapter the moderator escape probabilities, $P_s(E)$ and $P_m(E)$, as defined in Sec. 2.3 are discussed. It will be shown that by making appropriate assumptions, the formulation of the heterogeneous effects in terms of escape probabilities, Eq. (2.29), is identical to the expression derived utilizing diffusion theory in the moderator and characterizing the fuel element with its escape probability, $P_e(E)$, as given in Eq. (2.22).

The simplest model for $P_s(E)$ in cylindrical geometry is obtained by assuming, as in Sec. 2.2, a spatially flat source of neutrons in the moderator. Again as an expediency it is assumed that the flux shape in the moderator is given by one velocity diffusion theory applied at each energy. One finds $P_s(E)$ by calculating the net current into a black cylindrical hole of radius r_o. For a spatial source normalized to one neutron, $P_s(E)$ is given by

$$P_s(E) = AD_m(E)\nabla\varphi^m(r_o,E) \ . \tag{3.1}$$

Solving the diffusion equation, Eq. (2.13), with the boundary conditions given by

$$\nabla\varphi^m(r_1,E) = 0 \ , \tag{3.2}$$

and,

$$\frac{\varphi^m(r_o,E)}{\nabla\varphi^m(r_o,E)} = d_o(E) ,$$

yields

$$\nabla\varphi^m(r_o,E) = \frac{1/[V^m\Sigma_a^m(E)]}{\chi(E)/\kappa + d_o(E)} . \qquad (3.3)$$

V^m is the moderator volume, $\kappa^2 = \Sigma_a^m(E)/D_m(E)$, and $\chi(E)$ is given by Eq. (2.21). In accordance with Eq. (3.1), $P_s(E)$ is then given by

$$P_s(E) = \frac{2}{r_o(y^2-1)\kappa} \cdot \frac{1}{\chi(E) + \kappa d_o(E)} , \qquad (3.4)$$

or rearranging,

$$\frac{1-P_s(E)}{P_s(E)} = \frac{r_o}{2}(y^2-1)\kappa^2 d_o(E) + \frac{r_o}{2}(y^2-1)\kappa\chi(E) - 1 . \qquad (3.5)$$

As before, $y = r_1/r_o$. Figure 3.1 shows $P_s(E)$ as calculated for the Cornell University Zero Power Reactor cores. The effect of various water to uranium dioxide volume ratios is shown as well as the energy dependence. The parameters for the cores utilized in these calculations are given in Appendix A, while the cross section data incorporated in these computations are discussed in Chap. 7.

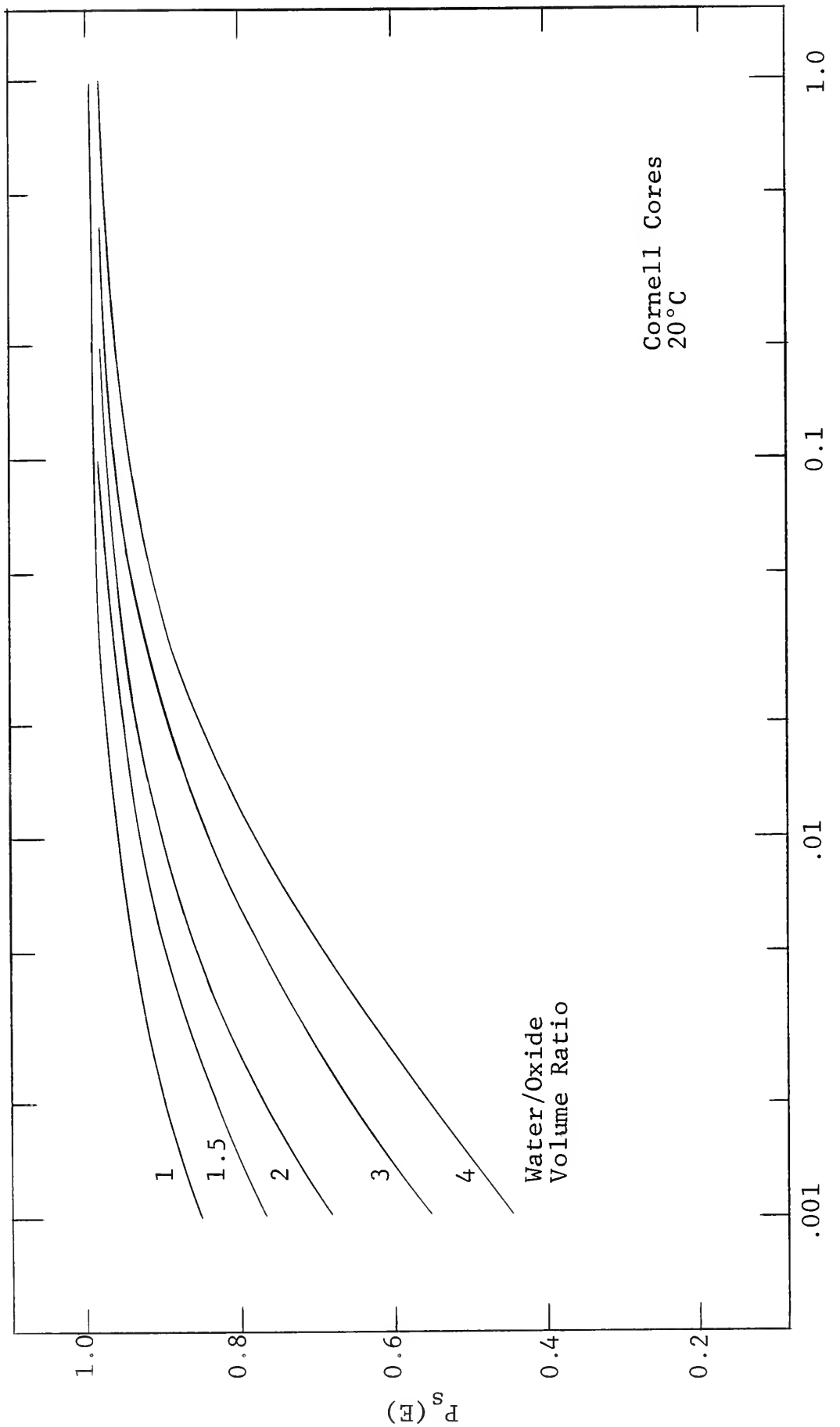

Figure 3.1 The Moderator Escape Probability, $P_s(E)$

3.2 $P_m(E)$

The moderator escape probability for neutrons incident on the moderator from the fuel element, $P_m(E)$, may be calculated from $P_s(E)$ through a reciprocity relationship under the following assumptions. If the flux in the moderator is isotropic, and if $P_s(E)$ is calculated using a spatially uniform source, as it has been, then $P_s(E)$ and $P_m(E)$ are related by[28,29]

$$\frac{1-P_m(E)}{P_s(E)} = 4\Sigma_a^m(E)\,\frac{V^m}{A}\,, \tag{3.6}$$

where for cylindrical cells

$$\frac{V^m}{A} = \frac{r_o}{2}(y^2-1)\,. \tag{3.7}$$

$P_m(E)$ is shown in Fig. 3.2 as calculated from Eq. (3.6) utilizing $P_s(E)$ as defined by Eq. (3.6) and depicted in Fig. 3.1.

Insertion of Eqs. (3.5), (3.6), (3.7) into Eq. (2.29) yields an expression for the relative fuel absorption:

$$\frac{1-f(E)}{f(E)} = \frac{2r_o(y^2-1)\Sigma_a^m(E)P_e(E)}{1-P_e(E)} + \frac{r_o}{2}(y^2-1)\kappa\chi(E) + \frac{r_o(y^2-1)\Sigma_a^m(E)d_o(E)}{2D_m(E)} - 1\,, \tag{3.8}$$

28/ K. M. Case, F. de Hoffmann, and G. Placzek, Introduction to the Theory of Neutron Diffusion, Vol. I, United States Government Printing Office, 1953.

29/ K. B. Cady, "Neutron Transport in Cylindrical Rods," Massachusetts Institute of Technology Thesis, 1962.

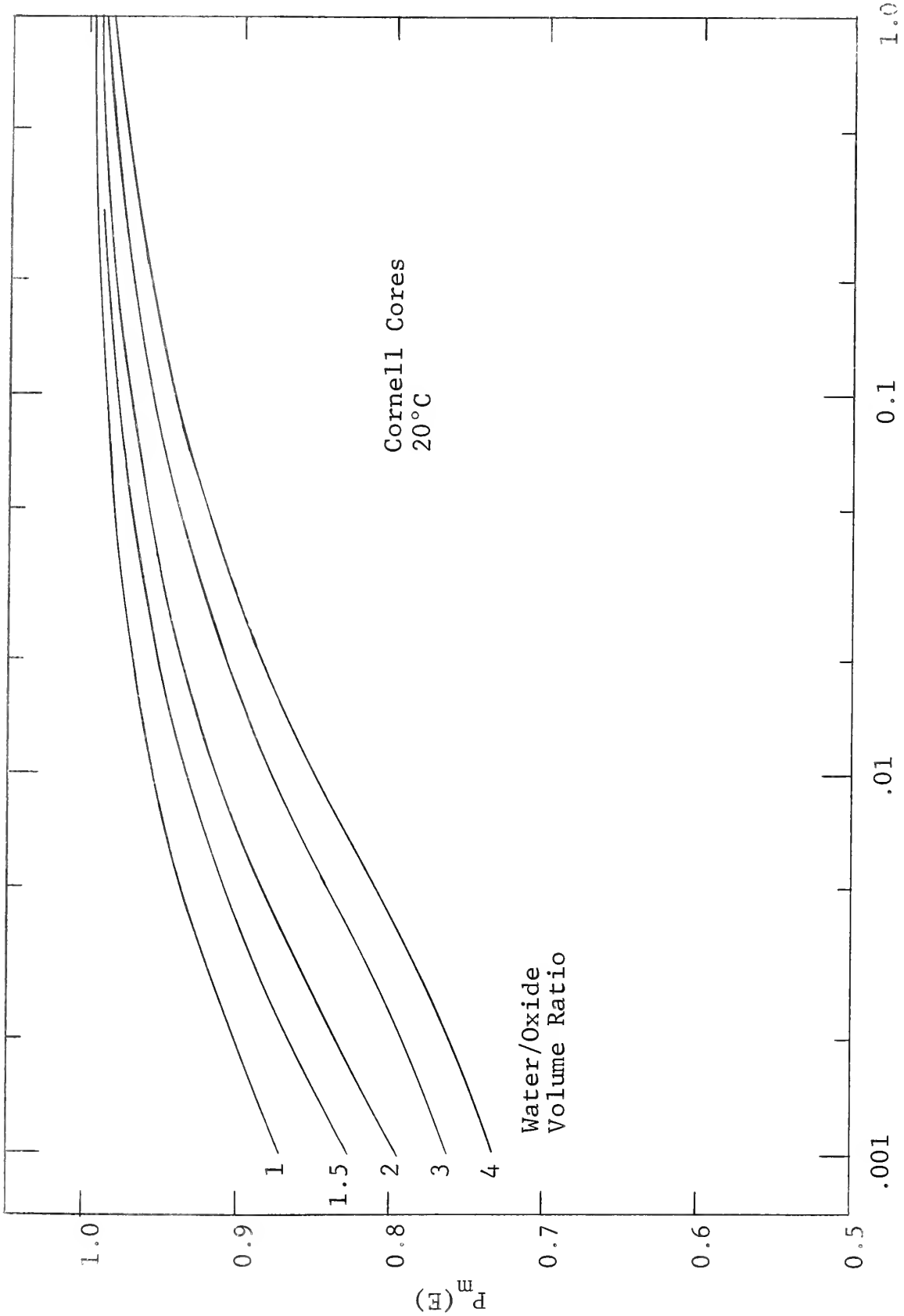

Figure 3.2 The Moderator Escape Probability, $P_m(E)$

which is identical with Eq. (2.22) as derived in Sec. 2.2. This is the expression which will be incorporated in the calculations discussed in Chap. 7 in an attempt to account for the heterogeneous effects of the lattice. Due to the physical transparency and separability of effects achieved through the consideration of the various escape probabilities, all future discussion will be in terms of them.

CHAPTER 4

THE FUEL ELEMENT ESCAPE PROBABILITY

4.1 The Fuel Rod Escape Probability

As was noted in Sec. 2.2, it is in many respects desirable to characterize the fuel element in terms of its escape probability, $P_e(E)$, thereby eliminating the need to explicitly define the flux in the various regions of the element. In addition, computation of $P_e(E)$ allows one to complete the calculation of the relative fuel absorption as defined in Eq. (3.8).

In the most general case, the fuel element is composed of a cladding region, a void region, and a fuel rod or fuel meat region. In the determination of $P_e(E)$, the fuel rod may be characterized by its escape probability, $P_r(E)$. The effect of the void may be accounted for by strictly geometric factors, while the cladding effects may be expressed in terms of several transmission factors. The results derived from the calculation of any of the above factors are of course dependent upon the assumption of an angular distribution of the current entering each respective region.

The fuel rod escape probability depends on the fuel rod radius, $a = \Sigma_t^f(E)r_f$, measured in mean free paths (mfp's) and the ratio, $c = \Sigma_s^f(E)/\Sigma_t^f(E)$ of the fuel scattering cross section to total cross section. The simplest expression for $P_r(E)$ is derived from diffusion theory and it is just the albedo of the rod:

$$P_r(E) = \frac{1-2D_f(E)\beta(E)}{1+2D_f(E)\beta(E)} \quad , \tag{4.1}$$

where

$$\beta(E) = \kappa_f \frac{I_1(\kappa_f r_f)}{I_o(\kappa_f r_f)} \quad . \tag{4.2}$$

I_o and I_1 are the modified Bessel functions of the first kind, while $\kappa_f^2 = \Sigma_a^f(E)/D_f(E)$, $D_f(E)$ being the diffusion coefficient of the fuel. The quantity κ_f may be obtained either from P-1 theory[30]

$$\kappa_f/\Sigma_t^f(E) = \sqrt{3(1-c)} \quad , \tag{4.3}$$

or from Wigner's "elementary theory,"

$$c \tanh^{-1}(\kappa_f/\Sigma_t^f(E)) = \kappa_f/\Sigma_t^f(E) \quad . \tag{4.4}$$

Transport theory expressions for the fuel rod escape probability have also been developed from Boltzmann's one velocity transport equation under the assumption of isotropic scattering in the laboratory system. This results in the integral transport or Peierl's equation:

$$\varphi(\vec{r}) = \varphi_u(\vec{r}) + c\Sigma_t \int \frac{d\vec{r}' \; e^{-\Sigma_t|\vec{r}-\vec{r}'|} \varphi(\vec{r}')}{4\pi|\vec{r}-\vec{r}'|^2} \quad , \tag{4.5}$$

---

[30] A. M. Weinberg and E. P. Wigner, The Physical Theory of Neutron Chain Reactors, The University of Chicago Press, Chicago, 1958.

where $\varphi_u(\vec{r})$ is the uncollided flux due to incident surface sources. Escape probabilities in terms of the solution of Eq. (4.5) have been considered by several authors.[31,32,33] This work utilizes the treatment by Cady for an isotropic flux incident upon the fuel rod. The calculational techniques utilized in the computation of $P_r(E)$ are quoted below.[34]

For thin rods of less than 0.5 mfp's a very accurate expression results from the uniform flux approximation. In terms of Placzek's collision probability,[35] M_{oo}, this yields the following expression for $P_r(E)$:

$$P_r(E) = 1-2a(1-c)\left[\frac{1-M_{oo}}{1-cM_{oo}}\right]. \qquad (4.6)$$

M_{oo} is calculated in terms of the modified Bessel functions of the first and second kind with an argument of a:

$$M_{oo} = 1 - \frac{2}{3}\left(I_1K_1+1-2a[I_1K_o+1-a(I_1K_1+I_oK_o)]\right). \qquad (4.7)$$

For rods which have radii, a, greater than 0.5 mfp's, the parabolic flux approximation yields more accurate results. In this case

$$P_r(E) = 1-2a(1-c)\left\{1-(1-c)\left[\frac{M_{oo}-c(M_{oo}M_{22}-3M_{o2}^2)}{1-c(4M_{oo}+4M_{22}-6M_{o2})+c^2(4M_{oo}M_{22}-2M_{o2}^2)}\right]\right\}, \qquad (4.8)$$

where the following quantities are calculated in order:

31/ K. B. Cady, "Neutron Transport in Cylindrical Rods," Massachusetts Institute of Technology Thesis, 1962.

32/ K. B. Cady and M. Clark, Jr., "Neutron Transport in Cylindrical Rods," Nucl. Sci. Eng. 18, 491-507 (1964).

$$A = a[I_1(a)K_1(a) + I_o(a)K_o(a)] , \tag{4.9}$$

$$B = 2a(I_1K_o + 1 - A) , \tag{4.10}$$

$$C = \frac{2}{3}(I_1K_1 + 1 - B) , \tag{4.11}$$

$$D = \frac{2}{3}(I_2K_o - 1 + B + C) , \tag{4.12}$$

$$E = \frac{4}{5}(\frac{2I_2K_1}{a} + C - D) , \tag{4.13}$$

$$F = \frac{6}{7}(\frac{1}{a^2} - \frac{4I_2K_2}{a^2} + E) , \tag{4.14}$$

$$M_{oo} = 1 - C , \tag{4.15}$$

$$M_{o2} = 1 - 2C + E , \tag{4.16}$$

and,

$$M_{22} = 1 - 3C + 3E - F .$$

Consideration of the asymptotic expansions for the moments, M_{oo}, M_{o2}, and M_{22}, yields the following approximations for the fuel rod escape probability. For the uniform flux approximation,

$$P_r(E) \approx \frac{1}{1 + 2a(1-c)} = \frac{1}{1 + 2\Sigma_a^f(E)r_f} , \tag{4.17}$$

and for the parabolic flux approximation,

$$P_r(E) \approx \frac{1 + 2a(1-c)}{1+4a(1-c) + \frac{16}{3}a^2(1-c)^2 + \frac{32}{3}a^3(1-c)^4} . \tag{4.18}$$

33/ G. W. Stuart and R. W. Woodruff, "Method of Successive Generations," Nucl. Sci. Eng. 10, 388 (1961).

Figure 4.1 shows the fuel rod escape probability as calculated utilizing the expressions stated above. The effect of the 0.27 U^{235} resonance is plainly evident. The parameters used in the computations are those of the low enrichment, high density uranium dioxide fuel of the Cornell University Zero Power Reactor. These parameters are listed in Appendix A, while cross section data are discussed in Chap. 7. The numerical methods needed for calculation of the modified Bessel functions are outlined in Appendix C.

4.2 Void Considerations

Any void space which is present between the fuel rod and the cladding is accounted for by considering the fraction of neutrons entering the void space from the cladding which are heading toward the fuel rod. The escape probability for the fuel rod and the void, $P_{rv}(E)$, may then be expressed as

$$P_{rv}(E) = (1-\zeta) + \zeta P_r(E), \qquad (4.19)$$

where ζ is the fraction of the neutrons headed toward the fuel rod. For an assumed isotropic flux emergent from the cladding,[36]

$$\zeta = r_f/r_c \qquad (4.20)$$

---

[34] K. B. Cady, see Footnote 31.

[35] K. M. Case, F. de Hoffman, and G. Placzek, Introduction to the Theory of Neutron Diffusion, Vol. I, United States Government Printing Office, 1953.

[36] K. B. Cady, p. 161, see Footnote 31.

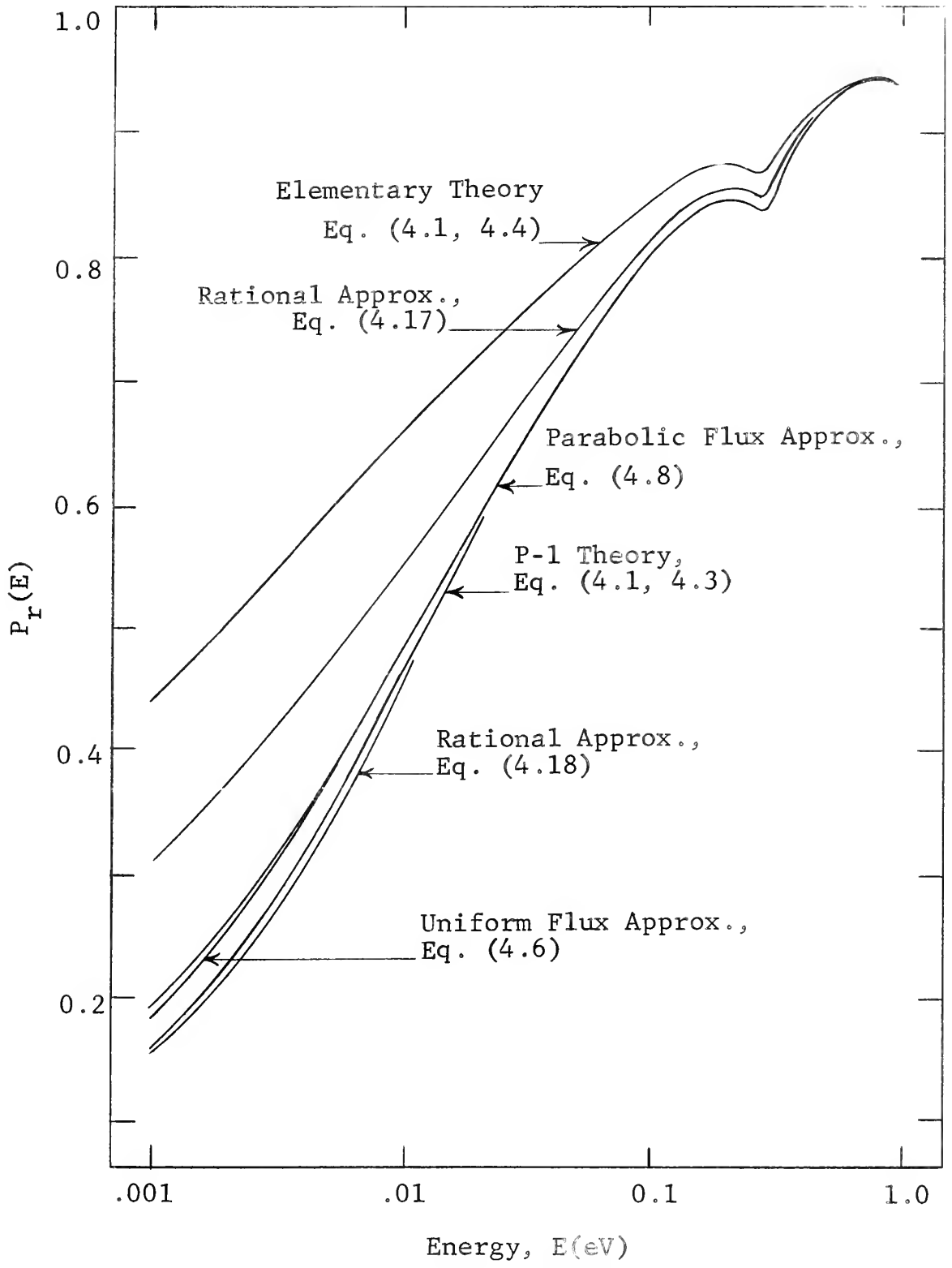

Figure 4.1 The Fuel Rod Escape Probability, $P_r(E)$

where r_f is the fuel rod radius and r_c is the inner radius of the cladding. Examination of Eqs. (4.19) and (4.20) shows that the correct limits exist in that $P_{rv}(E)$ goes to $P_r(E)$ as r_c goes to r_f, and $P_{rv}(E)$ goes to one as r_f goes to zero.

4.3 Cladding Effects

The fuel element cladding is treated in accordance with the cylindrical thin region theory developed by Cady.[37] The neutron reflection and transmission characteristics of the cladding can be divided into several fractions. For neutrons incident on the outer surface of the cladding,

1. g is the fraction of neutrons, which return uncollided to the moderator,
2. T is the fraction transmitted uncollided through the cladding,
3. r_{in} is the fraction scattered in and transmitted through the cladding,
4. r_{out} is the fraction scattered in and reflected out of the cladding back to the moderator, and
5. $1-(g+T+r_{in}+r_{out})$ is the remaining fraction which is absorbed in the cladding.

Similarly, for neutrons incident on the cladding from the fuel rod region,

---

[37] K. B. Cady, p. 63, see Footnote 31.

1. τ is the fraction transmitted uncollided through the cladding into the moderator,
2. ρ_{in} is the fraction scattered in the cladding and reflected back into the fuel rod and void region,
3. ρ_{out} is the fraction scattered in and transmitted through the cladding, and,
4. $1-(\tau+\rho_{in}+\rho_{out})$ is the remaining fraction which is absorbed in the cladding.

In terms of these energy dependent fractions, the escape probability for the entire fuel element may be expressed as

$$P_e(E) = g+r_{out} + (\tau+\rho_{out})J_o(E) \ . \qquad (4.21)$$

$J_o(E)$ is the net current entering the inner surface of the cladding from the fuel rod and is a function of $P_{rv}(E)$, the escape probability of the void and fuel rod region:

$$J_o(E) = \frac{(T+r_{in})P_{rv}(E)}{1-\rho_{in}P_{rv}(E)} \ . \qquad (4.22)$$

The computational receipes used for the calculation of the various fractions mentioned above are stated below. These schemes assume isotropic fluxes on both sides of the cladding and they are performed at each energy where applicable. The outer radius of the cladding is denoted by r_o, the inner cladding radius is r_c. Macroscopic cross sections refer to the cladding material.

$$\xi = r_c/r_o \ , \tag{4.23}$$

$$t = r_o - r_c \ , \tag{4.24}$$

$$\theta = 1 - \xi^2 \ , \tag{4.25}$$

$$F_o = \frac{2}{\pi} \sin^{-1} \xi \ , \tag{4.26}$$

$$F_1 = \xi \ , \tag{4.27}$$

$$F_2 = F_o + \frac{2}{\pi} \xi\sqrt{\theta} \ , \tag{4.28}$$

$$F_3 = \frac{3}{2} \xi \ (1-\xi^2/3) \ , \tag{4.29}$$

$$D_1 = \frac{\pi}{4} \xi^2 \ , \tag{4.30}$$

$$\Lambda = \ln(4/\sqrt{\theta}) \ , \tag{4.31}$$

$$D_2 = \frac{2}{3}\left[1 - \frac{3}{4}\theta - \frac{3}{16}(\Lambda - \frac{1}{4})\theta^2 - \frac{3}{64}(\Lambda - \frac{11}{12})\theta^3\right], \tag{4.32}$$

$$\bar{L}_1^1 = (F_2 - \frac{4}{\pi} D_1)/F_1 \ , \tag{4.33}$$

$$\bar{L}_1^2 = (\frac{8}{3} F_3 - 2\theta F_1 - 4D_2)/F_1 \ , \tag{4.34}$$

$$T = F_1 - \Sigma_t^c(E) r_o F_1 \bar{L}_1^1 + \frac{1}{2}(\Sigma_t^c(E) r_o)^2 F_1 \bar{L}_1^2 \ , \tag{4.35}$$

$$C_1 = (\frac{1}{2\xi})(\frac{\pi}{2} F_o + \xi\sqrt{\theta}) \ , \tag{4.36}$$

$$C_2 = D_2/\xi^2 \ , \tag{4.37}$$

$$\bar{\mathcal{L}}_1^1 = \frac{4}{\pi} C_1 - \xi \ , \tag{4.38}$$

$$\bar{\mathcal{L}}_1^2 = 2\theta - \frac{8}{3} \xi - 4\xi C_2 \ , \tag{4.39}$$

$$\tau = 1-\Sigma_t^c(E)r_o \bar{\mathscr{K}}_1^1 + \frac{1}{2}(\Sigma_t^c(E)r_o)^2 \bar{\mathscr{K}}_1^2 , \tag{4.40}$$

$$\gamma = 0.577215 \ldots, \text{ Euler's Constant,} \tag{4.41}$$

$$x = \Sigma_t^c(E)t , \tag{4.42}$$

$$P_u = \frac{x}{2}\left[\gamma + \ln(x) - \frac{3}{2}\right] + 1 - \frac{x^2}{6} + \frac{x^3}{48} - \frac{x^4}{360} + \frac{x^5}{2880} , \tag{4.43}$$

and,

$$P_{unif} = \frac{P_u}{1 - \frac{\Sigma_s^c(E)}{\Sigma_t^c(E)}(1-P_u)} . \tag{4.44}$$

For $x \leq .05$,

$$g = (1-F_1) - 2\Sigma_t^c(E)r_o(1-F_2) + \frac{1}{2}(\Sigma_t^c(E)r_o)^2 \cdot \frac{16}{3}(1-F_3) , \tag{4.45}$$

while for $.05 < x \leq 0.2$,

$$g = -.0212 - .0266\ \ln(x)/\xi^{2.2} . \tag{4.45}$$

$$r_{in} + r_{out} = \frac{\Sigma_s^c(E)}{\Sigma_t^c(E)}(1-g-T)P_{unif} , \tag{4.46}$$

$$\rho_{in} + \rho_{out} = \frac{\Sigma_s^c(E)}{\Sigma_t^c(E)}(1-\tau)\ P_{unif} , \tag{4.47}$$

$$f_{in} = \frac{1}{\pi}\ \sin^{-1}\left(\frac{2\xi}{1+\xi}\right) , \tag{4.48}$$

$$r_{in} = f_{in}(r_{in} + r_{out}) \ , \tag{4.49}$$

$$r_{out} = (r_{in} + r_{out}) - r_{in} \ , \tag{4.50}$$

$$\rho_{in} = f_{in} \ (\rho_{in} + \rho_{out}) \ , \tag{4.51}$$

and,

$$\rho_{out} = (\rho_{in} + \rho_{out}) - \rho_{in} \ . \tag{4.52}$$

Calculations have been made using the above techniques for the fuel elements of the Cornell University Zero Power Reactor, the specifications of which are given in Appendix A. The results of these computations in the form of the fuel element escape probability are shown in Fig. 4.2. In these calculations, the parabolic flux approximation, Eq. (4.8), was used for the calculation of $P_r(E)$. Again the effect of the U^{235} resonances can be seen.

In terms of previously defined quantities, the ratio of the number of neutrons absorbed in the fuel rod to the number absorbed in the fuel element is given by

$$\frac{\text{rod abs. rate}}{\text{element abs. rate}} = \frac{J_o(E)[1-P_{rv}(E)]}{P_{rv}(E)[1-P_e(E)]} \ . \tag{4.53}$$

Similarly the ratio of the number of neutrons absorbed in the cladding to the number absorbed in the fuel element can be defined by

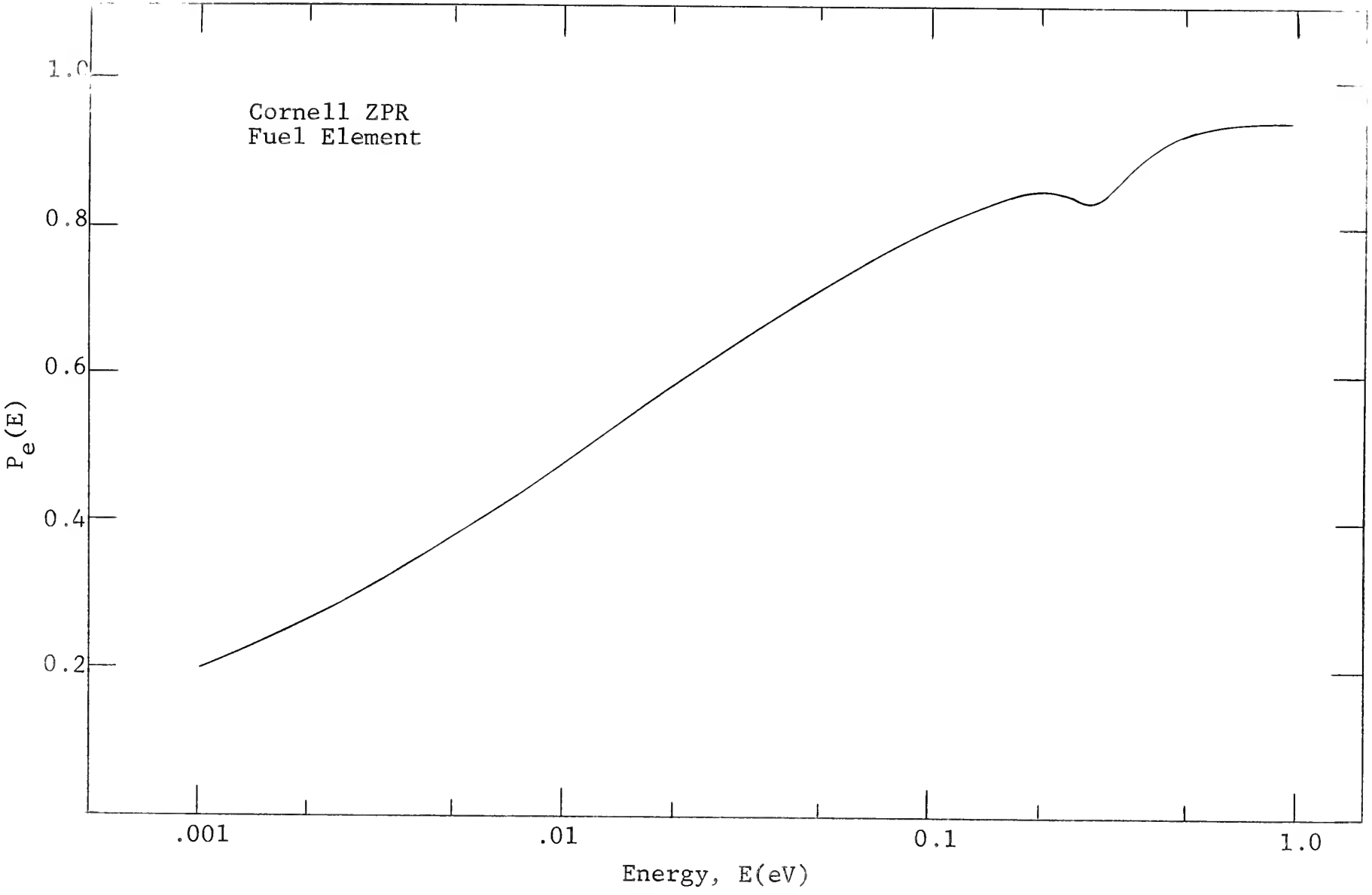

Figure 4.2 The Fuel Element Escape Probability, $P_e(E)$

$$\frac{\text{clad abs. rate}}{\text{element abs. rate}} = 1 - \frac{J_o(E)[1-P_{rv}(E)]}{P_{rv}(E)[1-P_e(E)]}, \qquad (4.54)$$

$$= \frac{\Sigma_a^c(E)}{\Sigma_a^c(E)+\Sigma_s^c(E)P_u}\,[(1-g-T)+J_o(E)(1-\tau)]. \qquad (4.55)$$

The results of performing the calculation expressed by Eq. (4.53) are shown in Fig. 4.3 for the Cornell fuel elements. Inspection of Fig. 4.3 shows that only about 1% of the neutrons absorbed by the fuel element are absorbed in the cladding. This is because of the low absorption cross section of the aluminum cladding. On the other hand, in the Brookhaven uranium dioxide fuel elements,[38] (see Chap. 8), where stainless steel is used as the cladding material, about 12% of the neutrons absorbed in the fuel element are lost to the cladding.

---

[38] H. C. Honeck, "The Calculation of Thermal Utilization and Disadvantage Factor in Uranium Water Lattices," Nucl. Sci. Eng. 18, 49-68 (1964).

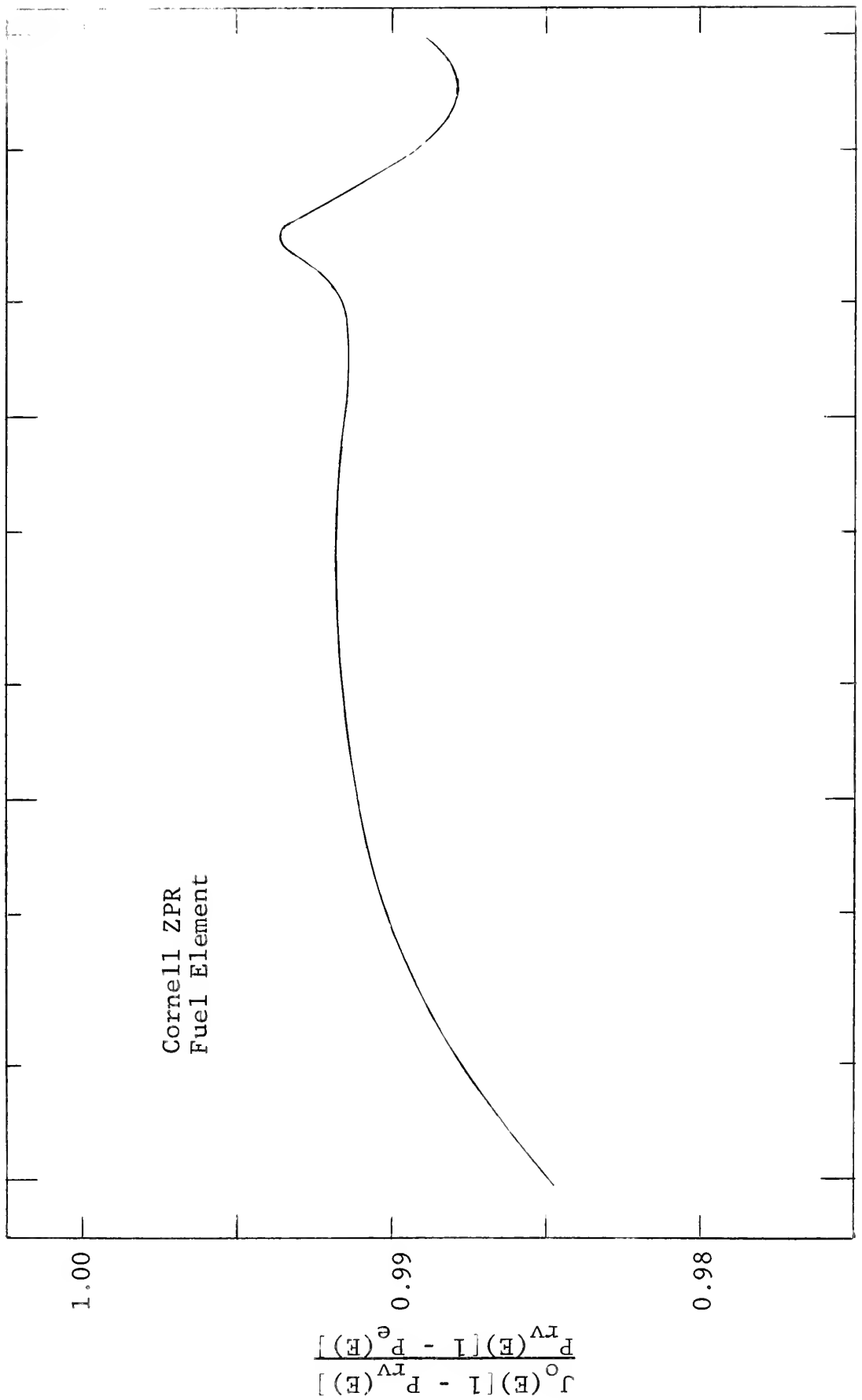

Figure 4.3 The Ratio of the Fuel Rod Absorption Rate to the Fuel Element Absorption Rate

CHAPTER 5

MODELS FOR THE SCATTERING KERNEL

5.1 The Monatomic Gas Model

By formulating the lattice heterogeneous effects in terms of contrived absorption rates as in Secs. 2.1 and 2.3, one is left free to incorporate as much sophistication as is desired into the calculation of the energy transfer or scattering kernel to be used in Eq. (2.9). With this type of an approach one can determine directly the effect of different mathematical models on the neutron spectra and lattice integral properties. One can then decide on the basis of computer time used and the accuracy of the results whether or not use of the more complicated models for the kernel is desirable for a particular computation.

Numerous mathematical models for the scattering kernel have been proposed.[39,40,41,42,43,44] In an attempt to bracket the degrees of computational difficulty and the accuracy of the results predicted with these many models, we have limited ourselves to calculations with only two of them; the Wigner-Wilkins monatomic gas model[45] and the Nelkin water kernel.[46]

---

[39] E. P. Wigner and J. E. Wilkins, Jr., "Effect of the Temperature of the Moderator on the Velocity Distribution of Neutrons with Numerical Calculations for H as the Moderator," AECD-2275 (1944).

[40] J. E. Wilkins, Jr., "Effect of Temperature of the Moderator on the Velocity Distribution of Neutrons for a Heavy Moderator," CP-2481 (1944).

The choice of the monatomic gas model is mainly dictated by its ease of calculation. This model treats the moderator as a free gas in thermal equilibrium at the temperature of the moderator. Although crystalline or molecular binding effects in the thermalization properties of the moderator are neglected, infinite homogeneous media calculations[47] with this model have yielded spectra which are essentially consistent with those measured experimentally.

The cross section for scattering from an energy E' to an energy E through an angle with a cosine of μ may be derived from the short collision time approximation[48] applied to the single oscillational mode of the translational motion of the scattering particle. For the situation where E' is greater than E, this results in[49]

$$\sigma(E' \longrightarrow E, \mu) = \frac{\sigma_b}{4}\left[\frac{EA}{E'\pi TX}\right]^{1/2} \exp\left[\frac{-A}{4TX}\left(E-E'+\frac{X}{A}\right)^2\right], \tag{5.1}$$

---

[41] M. S. Nelkin, "Scattering of Slow Neutrons by Water," Phys. Rev. 119, 741-746 (1960).

[42] A. Radkowsky, "Temperature Dependence of the Thermal Transport Mean Free Path," Physics Quarterly Report, (April, May, June, 1950), ANL-4476, p. 89, Argonne National Laboratory (July, 1950).

[43] H. D. Brown and D. S. St. John, "Neutron Energy Spectrum in D_2O," DP-33 (1954).

[44] The Scattering Law, Proceedings of the Brookhaven Conference on Neutron Thermalization, BNL 719, Vol. I, Brookhaven National Laboratory (1962).

where $\sigma(E' \rightarrow E,\mu)$ is in barns/(eV-unit cosine). The bound atom cross section in barns is σ_b, T is the moderator temperature in electron volts, and A is the ratio of the scattering nucleus mass to the neutron mass. The quantity X is related to the momentum transfer in that

$$X = E+E' - 2\mu\sqrt{EE'} \quad . \tag{5.2}$$

A similar result can be obtained for upscattering in energy by employing the principle of detailed balance, Eq. (2.5) as is discussed below.

The scattering kernel is found by the angular integration of Eq. (5.1),

$$\sigma(E' \rightarrow E) = \int_{-1}^{1} \sigma(E' \rightarrow E,\mu)d\mu \quad . \tag{5.3}$$

This operation can be carried out analytically and it results in the formulation of the Wilkins' heavy gas model[50] for the scattering kernel. For down scattering in energy,

---

[45] E. P. Wigner and J. E. Wilkins, Jr., see Footnotes 39 and 40.

[46] M. S. Nelkin, see Footnote 41.

[47] L. G. de Sobrino and M. Clark, Jr., "A Study of the Wilkins Equation," Nucl. Sci. Eng. 10, 388 (1961); "Comparison of the Wilkins Equation with Experiments on Water Systems," Nucl. Sci. Eng. 10, 377 (1961).

[48] M. S. Nelkin, see Footnote 41.

[49] F. D. Federighi and D. T. Goldman, "KERNEL and PAM - Programs for Use in the Calculation of the Thermal Scattering Matrix for Chemically Bound Systems," KAPL-2225, Knolls Atomic Power Laboratory (1962).

[50] J. E. Wilkins, Jr., see Footnote 40.

$E' \geq E$, the monatomic gas scattering kernel is expressed in barns/eV as[51]

$$\sigma(E' \longrightarrow E) = \frac{\sigma_f \eta^2}{2E'} \left(\mathrm{ERF}(\eta z - \rho z') + \mathrm{ERF}(\eta z + \rho z') + \exp(z'^2 - z^2)[\mathrm{ERF}(\eta z' - \rho z) - \mathrm{ERF}(\rho z + \eta z')] \right) , \quad (5.4)$$

where

$$z^2 = E/T , \quad (5.5)$$

$$z'^2 = E'/T , \quad (5.6)$$

$$\eta = \frac{1}{2}(A+1)A^{-1/2} , \quad (5.7)$$

and,

$$\rho = \frac{1}{2}(A-1)A^{-1/2} . \quad (5.8)$$

ERF(z) is the error function defined by

$$\mathrm{ERF}(z) = \frac{2}{\sqrt{\pi}} \int_0^z e^{-y^2} \, dy , \quad (5.9)$$

while σ_f is the free atom scattering cross section for the moderating medium.

$$\sigma_f = \sigma_b \left(\frac{A}{A+1} \right)^2 . \quad (5.10)$$

The scattering kernel for upscattering, $E' < E$, is calculated utilizing detailed balance as expressed in Eq. (2.5).

In the case where one is considering moderation by hydrogen, Eq. (5.4) reduces to the Wigner-Wilkins model for

a gas of mass one.[52] Then for $E' \geq E$,

$$\sigma(E' \rightarrow E) = \frac{\sigma_f}{E'} \, ERF(z) \quad . \tag{5.11}$$

The use of the monatomic gas model has another advantage in that the scattering cross section defined by

$$\sigma_s(E) = \int_0^\infty \sigma(E \rightarrow E')dE' \quad , \tag{5.12}$$

is an analytic function given by

$$\sigma_s(E) = \sigma_f \left[\left(1 + \frac{1}{2y^2}\right) ERF(z) + \frac{e^{-y^2}}{\sqrt{\pi}y} \right] , \tag{5.13}$$

where

$$y^2 = \frac{EA}{T} \quad . \tag{5.14}$$

This analytic function for the scattering cross section is useful because it allows one to check on the accuracy of the numerical integration scheme employed. This aspect is more fully discussed in Sec. 5.2.

The calculations performed utilizing the monatomic gas model for the scattering kernel are discussed in Chap. 7. Calculation of the error function necessary in the computations of this kernel is detailed in Appendix C.

51/ M. J. Poole, M. S. Nelkin, and R. S. Stone, "The Measurement and Theory of Reactor Spectra," Progress in Nuclear Energy, Series I, Vol. 2, pp. 91-164, Pergamon Press, New York, London, Paris, and Los Angeles, 1958.

52/ E. P. Wigner and J. E. Wilkins, Jr., see Footnote 39.

5.2 The Nelkin Water Kernel

The second mathematical model for the scattering kernel utilized in these calculations is that proposed by Nelkin[53] for protons bound in water. Although the computer calculation of the Nelkin water kernel takes a relatively long time, its use is justified in that infinite homogeneous media thermal spectra calculated with this model are in good agreement with those measured experimentally.[54] In addition, diffusion coefficients calculated with the Nelkin model[55] agree well with measured values.[56]

Physically, the mathematical approximation proposed by Nelkin for water treats the scattering molecule translation with the free gas model utilizing a translator mass (M) of 18. The effects of the atomic motions within the molecule are approximated by simple harmonic oscillations, the phonon frequencies of which determine the relative strength of the interaction with a particular oscillator. The oscillators treated are as follows: A hindered rotational oscillator of mass (M_r) 2.32 and frequency (Ω_r) corresponding to an energy ($\omega_r = \hbar\Omega_r$) of 0.06 eV, where $\hbar$ is Planck's Constant divided by 2π; a vibrational oscillator of mass (M_v) 5.84 and an energy (ω_1) of 0.205 eV; and a

---

[53] M. S. Nelkin, see Footnote 41.

[54] J. R. Beyster, et al., "Measurement of Neutron Spectra in Water, Polyethylene, and Zirconium Hydride," Nucl. Sci. Eng. 9, 168 (1961).

second vibrational oscillator of mass ($M_{v2} = M_v/2$) 2.92 and energy (ω_2) of 0.481 eV. Different mathematical approximations may be made to treat the translational, vibrational and rotational modes, dependent upon the incident neutron energy and the energy or momentum transfer. However, a single expression may be used to characterize the differential scattering kernel for scattering from an energy E' to an energy E ($E' \geq E$) through an angle with a cosine of μ. Parameters within the Nelkin water kernel then change dependent upon the specific approximation made,

$$\sigma(E' \longrightarrow E,\mu) = \frac{\sigma_b}{4}\sqrt{\frac{E}{E'\chi\xi\pi}}\; e^{-\frac{X}{A}} \sum_{m=0}^{mm} \frac{1}{m!}\left(\frac{2X}{M_v\omega_2}\right)^m$$

$$\sum_{\ell=0}^{\ell\ell} \frac{1}{\ell!}\left(\frac{X}{M_v\omega_1}\right)^\ell \sum_{n=-\infty}^{\infty} e^{\frac{n\omega}{2T}} I_n(z) \exp\left[-\frac{1}{4X\xi}(E-E'\right.$$

$$\left. + \frac{X}{M} + m\omega_2 + \ell\omega_1 + n\omega)^2\right] \quad . \qquad (5.15)$$

55/ G. P. Calame, "Diffusion Parameters of Water for Various Scattering Kernels," Nucl. Sci. Eng. 19, 189 (1964).

56/ E. Starr and J. Koppel, "Determination of Diffusion Hardening in Water," Nucl. Sci. Eng. 14, 224 (1962).

Equation (5.15) gives the differential scattering kernel in barns/(eV-unit cosine) with σ_b as the bound atom cross section in barns. The $I_n(z)$ are the modified Bessel functions of the first kind and order n. As before, the quantity X is given by

$$X = E+E'-2\mu\sqrt{EE'} \quad . \tag{5.16}$$

One may allow for all of the transitions for the translational and rotational modes, while utilizing a phonon expansion for the first (ω_1 = .205 eV) vibrational mode and the elastic (unexcited) limit for the second (ω_2 = .481 eV) vibrational mode by inserting the following values into Eq. (5.15):

$$\begin{aligned}
&\frac{1}{A} = \frac{1}{\omega_r M_r \tanh(\omega_r/2T)} + \frac{1}{M_v\omega_1} + \frac{2}{M_v\omega_2} \quad , \\
&\xi = T/M \quad , \\
&z = \frac{X}{M\omega\sinh(\omega/2T)} \quad , \\
&\frac{1}{\overline{M}} = \frac{1}{M} \quad , \\
&mm = 0 \quad , \\
&\ell\ell = 2 \quad , \\
&\omega = \omega_r \quad ,
\end{aligned} \tag{5.17}$$

and,

$$M = M_r \ ,$$

where T is the moderator temperature in eV. The phonon expansion for the second vibrational mode is included if mm is set equal to 2 in the above set of parameters.

To allow for all transitions of the translational and first vibrational modes, while treating the rotational mode with the short collision time approximation and the second vibrational mode with a phonon expansion, the following parameters are inserted into Eq. (5.15):

$$\begin{aligned}
\frac{1}{A} &= \frac{1}{M_v\omega_1} + \frac{2}{M_v\omega_2} \ , \\
\xi &= \frac{T}{M} + \frac{\omega_r}{M_r}\left(\frac{1}{e^{\omega_r/T}-1} + \frac{1}{2}\right), \\
z &= \frac{X}{M\omega\sinh(\omega/2T)} \ , \\
\frac{1}{\bar{M}} &= \frac{1}{M} + \frac{1}{M_r} \ , \\
mm &= 2 \ , \\
\ell\ell &= 0 \ , \\
\omega &= \omega_1
\end{aligned} \qquad (5.18)$$

and

$$M = M_v \ .$$

The oxygen present in the water is accounted for by adding the monatomic gas model with mass 16, Eq. (5.1), to the Nelkin water kernel, Eq. (5.15).

Angular integration of the differential scattering kernel, $\sigma(E' \rightarrow E,\mu)$, was performed numerically to obtain the scattering kernel in the form utilized in lattice calculations. For the non diagonal terms in the scattering matrix ($E' \neq E$), the Gauss quadrature formula was used for the angular integration:

$$\sigma(E' \rightarrow E) = \int_{-1}^{1} \sigma(E' \rightarrow E,\mu)d\mu$$

$$\approx \sum_{k=1}^{kk} w_k \left[\sigma(E' \rightarrow E,\mu_k) + \sigma(E' \rightarrow E,-\mu_k)\right], \tag{5.19}$$

where w_k is the weighting coefficient corresponding to μ_k, a zero of the Legendre polynomials.[57] For terms where the energy transfer is large ($E << E'$), an eight point ($kk = 4$) integration is used, while for small energy transfers where the fine structure of the differential kernel is a rapidly varying function of angle, a sixteen point ($kk = 8$) quadrature integration is performed.

Calculation of the scattering kernel diagonal terms ($E = E'$), where there is no energy transfer, requires some

---

[57] A. N. Lowan, N. Davis, and A. Levinson, "Tables of the Zeros of the Legendre Polynomials of Order 1-16 and the Weight Coefficients for Gauss's Mechanical Quadrature Formula," Bull. Am. Math. Soc. 48, 739 (1942).

modification of the above procedure. Inspection of Eq. (5.15) shows that for $E' = E$, $X = 2E(1-\mu)$, and there is a singularity in the differential scattering kernel at $\mu = 1$.

The use of the Gaussian quadrature angular integration scheme introduces numerical errors in this situation. Therefore the following calculational technique is utilized as suggested by Federighi and Goldman.[58] Equation (5.15) is considered in the limit as X goes to zero (μ goes to 1). The singularity is subtracted from the differential kernel and integrated analytically, the remainder being integrated with the sixteen point Gaussian quadrature rule. The analytically integrated singularity is then added to the result. This process is indicated below:

$$\sigma(E\longrightarrow E) = \int_{-1}^{1} f(\mu)d\mu + \frac{\sigma_b}{4\sqrt{\pi\xi}} \int_{-1}^{1} \frac{d\mu}{\sqrt{2E(1-\mu)}} , \qquad (5.20)$$

where,

$$f(\mu) = \sigma(E\longrightarrow E,\mu) - \frac{\sigma_b}{4\sqrt{\pi\xi X}} , \qquad (5.21)$$

and $X = 2E(1-\mu)$. The diagonal terms are then approximated by

---

[58] F. D. Federighi and D. T. Goldman, see Footnote 49.

$$\sigma(E \rightarrow E) = \sum_{k=1}^{8} w_k \left[f(\mu_k) + f(-\mu_k) \right] + \frac{\sigma_b}{2\sqrt{\pi \xi E}} \quad . \tag{5.22}$$

In the calculations of the Nelkin water kernel made for incorporation into the lattice studies Eqs. (5.17) were utilized for incident energies, E', less than 0.33 eV, while Eqs. (5.18) were used for E' greater than 0.33 eV. This is essentially the same approximation made by Honeck for the water kernel calculations incorporated in THERMOS.[59] The phonon expansion for the second vibrational mode along with Eqs. (5.17) is not used because only a small increase in accuracy at higher incident energies is accomplished with a large (by a factor of 3) increase in computer time through its utilization.

Figure 5.1 shows the results of a calculation which utilized both Eqs. (5.17) and (5.18) in Eq. (5.15) for an incident energy of 0.366 eV. The results are expressed in barns/unit lethargy, $E\sigma(E' \rightarrow E)$, for down scattering, $E' \geq E$. However, the basic difference between the two approximations is plainly evident in Fig. 5.1. By considering all transitions for the hindered rotator, Eqs. (5.17), a scattering kernel is predicted with a complicated fine energy structure having oscillations at energy

---

[59] H. C. Honeck, "THERMOS - A Thermalization Transport Theory Code for Reactor Lattice Calculations," BNL 5826, Brookhaven National Laboratory (1961).

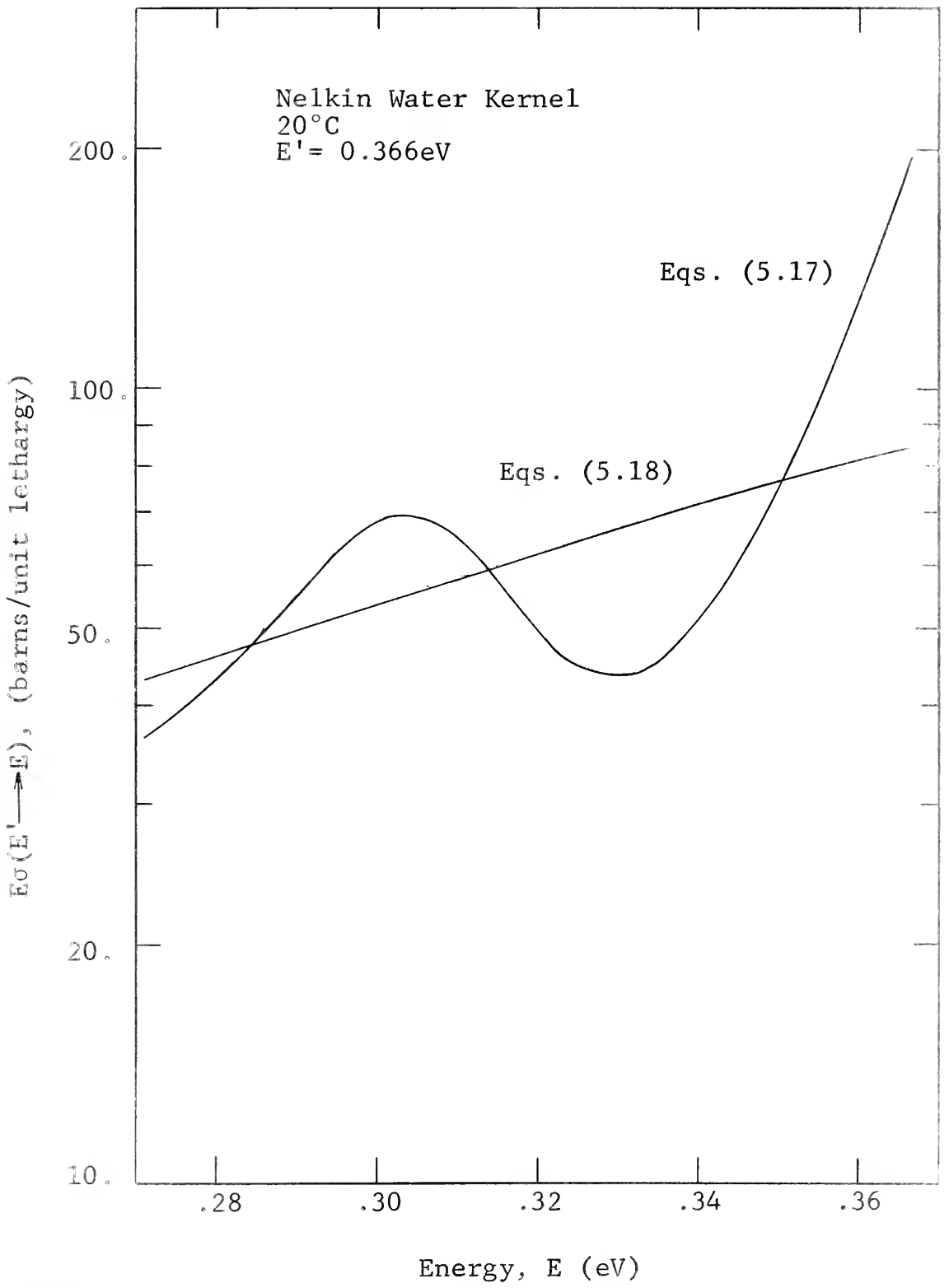

gure 5.1 Approximations Used in the Calculation of the Nelkin Water Kernel

intervals (E' — E) equal to the frequency of the rotator, ω_r = 0.06 eV. In going to the short collision time approximation for the hindered rotator, Eqs. (5.18), this fine structure is considerably smoothed, however the cross section derived by the energy integration of the kernel, Eq. (5.12), is essentially the same for both models. The choice of 0.33 eV as the energy above which Eqs. (5.18) will be used and below which Eqs. (5.17) will be used is made with this fact in mind, but primarily on the basis of computer economy. In order to predict accurate cross sections utilizing all transitions for the hindered rotator, it is necessary to use a fine energy mesh in the calculations ($\Delta E < .06$eV), but if one is interested in energies in the range up to 1.0 eV this means that an excessively large number of energy points must be used in the calculation. This problem is further discussed below and in Chap. 7.

The first moment of the scattering kernel, $\sigma_1(E' \rightarrow E)$ is calculated for down scattering utilizing the same techniques as above, where,

$$\sigma_1(E' \rightarrow E) = \int_{-1}^{1} \mu\sigma(E' \rightarrow E, \mu)d\mu \ . \qquad (5.23)$$

As before, a sixteen point Gaussian quadrature angular integration is made for the off diagonal terms when the energy transfer is small, while eight points is considered

sufficient for large energy transfers. The diagonal terms, E' = E, for the first moment are calculated using the function defined in Eq. (5.21):

$$\sigma_1(E \longrightarrow E) = \int_{-1}^{1} \mu f(\mu) d\mu + \frac{\sigma_b}{4\sqrt{\pi\xi}} \int_{-1}^{1} \frac{\mu d\mu}{\sqrt{2E(1-\mu)}} ,$$

$$\approx \sum_{k=1}^{8} w_k \left[\mu_k f(\mu_k) - \mu_k f(-\mu_k) \right] + \frac{\sigma_b}{6\sqrt{\pi\xi E}} . \qquad (5.23)$$

The upscattering terms for both the scattering kernel and its first moment are calculated using detailed balance, Eq. (2.5). It is to be noted that a slight, but acceptable inconsistency is introduced in this manner, since the use of detailed balance means that in the upscattering portion of the scattering matrices, the approximation used, Eqs. (5.17) or Eqs. (5.18), actually depends on the neutron final energy rather than its initial energy.

Energy integration was performed on the scattering kernel and its first moment to determine the average cosine of the scattering angle, $\bar{\mu}(E)$:

$$\bar{\mu}(E) = \frac{\int_0^{E_c} \sigma_1(E \longrightarrow E') dE'}{\int_0^{E_c} \sigma(E \longrightarrow E') dE'} . \qquad (5.24)$$

A trapezoidal rule numerical integration scheme, Appendix C, is used for this calculation and the results are shown in Fig. 5.2. Figure 5.2 also shows the transport cross section of water as calculated using the expression

$$\sigma_{tr}(E) = \sigma_a(E) + \sigma_s(E)[1-\bar{\mu}(E)] \quad . \tag{5.25}$$

In the energy integration of the scattering kernel, Eq. (5.12), to obtain the scattering cross section, $\sigma_s(E)$, certain numerical inaccuracies were encountered. Specifically, numerical integration of the Nelkin water utilizing the trapezoidal integration scheme discussed in Appendix C consistently yields scattering cross sections which were higher than those measured experimentally[60] for energies greater than 0.1 eV. Essentially the same percentage error is seen when the numerically integrated monatomic gas kernel is compared with the analytic expression for the cross section given by Eq. (5.13). These numerical errors are attributable to the fact that at higher incident energies, the diagonal terms of the scattering matrix are large compared with the first off diagonal terms for the energy mesh used in the calculation as discussed in Chap. 7. Use of the trapezoidal integration rule in this region therefore yields scattering cross sections for both kernels which are higher

---

[60] D. Hughes and B. Schwartz, "Neutron Cross Sections," BNL 325, 2nd ed., Brookhaven National Laboratory (1958).

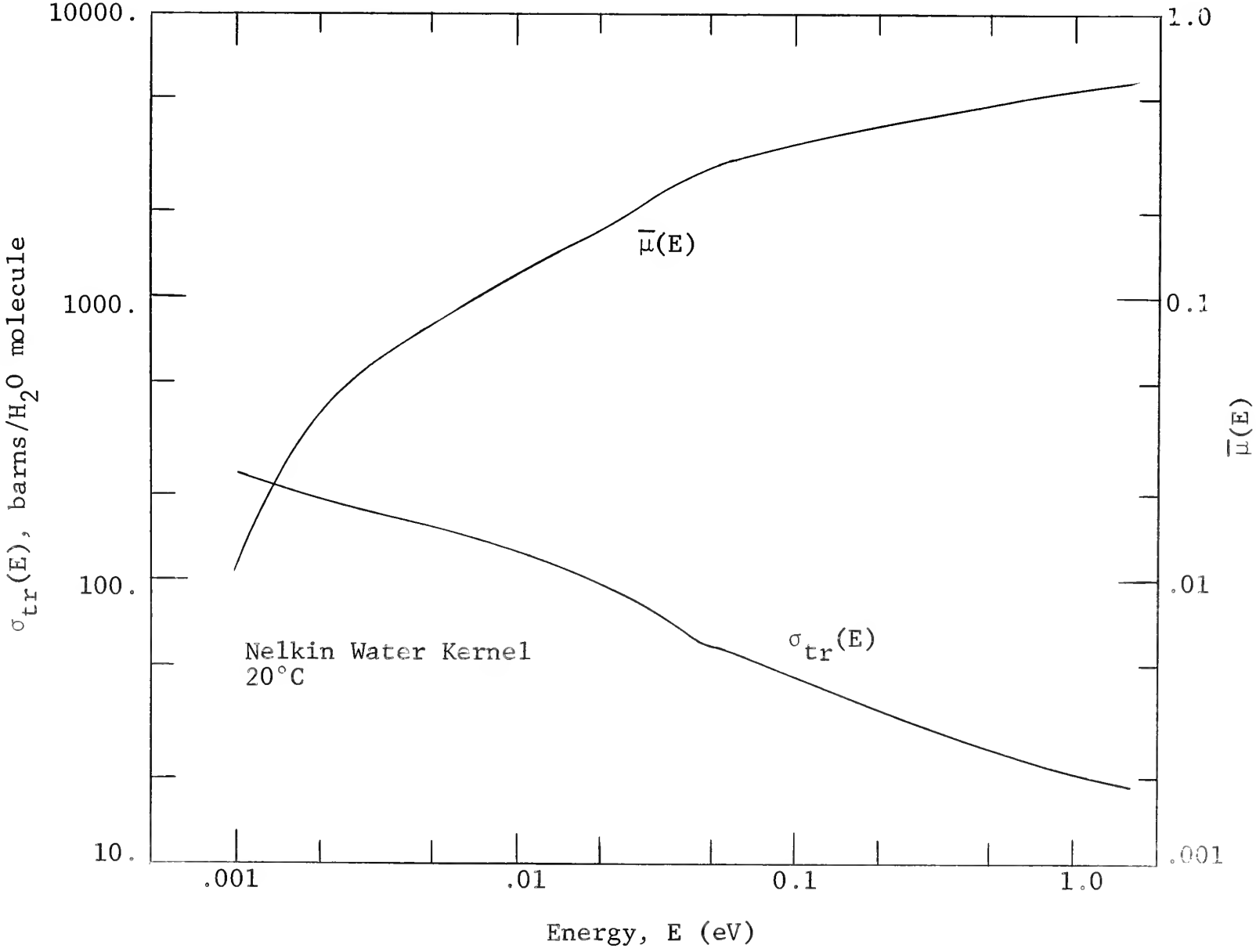

Figure 5.2 The Average Cosine of the Scattering Angle and the Transport Cross Section for Water

than experimentally measured or analytically calculated values. Auxiliary calculations showed that good agreement between $\sigma_s(E)$ calculated with the Nelkin water kernal and measured experimentally or between $\sigma_s(E)$ calculated by the monatomic gas model and $\sigma_s(E)$ given by Eq. (5.13) could be obtained by either utilizing a much finer energy mesh or by using more sophisticated integration schemes. However, both of these approaches create large increases in the computational time since the kernel calculation time is proportional to n^2 where n is the number of energy points considered, and the more complicated integration schemes which involve the fitting of exponentials or higher order polynomials to the calculated kernel points require additional computer time due to the uneven energy spacing used in the calculations. It is therefore desirable to retain the simplicity of the trapezoidal rule and correct for its inability to handle accurately the large diagonal terms encountered at high energies. This is done by recognizing that the actual value of the diagonal terms, $E' = E$, has no effect on the spectrum calculated with Eq. (2.1) or Eq. (2.9). This is seen by substituting the definition of the scattering cross section, Eq. (2.2) into Eq. (2.1) or (2.9) and letting E go to E'. Furthermore, integration of both sides of Eq. (2.1) or Eq. (2.9) over the energy variable E indicates the scattering cross section used in calculations must be the one derived from

the scattering kernel by the numerical integration scheme.

Since some of the integral properties that are to be calculated are strongly dependent upon the use of an accurate scattering cross section, we propose to modify the calculated diagonal terms in such a way that the scattering cross section calculated with the trapezoidal numerical integration scheme will equal the measured values for the Nelkin water kernel and Eq. (5.13) for the monatomic gas model. Thus, the diagonal terms, $\sigma^*(E \rightarrow E)$, utilized in the calculations will be given by:

$$\sigma^*(E \rightarrow E) = C(E)\sigma(E \rightarrow E) , \qquad (5.26)$$

where $\sigma(E \rightarrow E)$ is calculated using Eq. (5.22). The correction factors, C(E), are easily found for the trapezoidal integration rule from the difference between the measured or analytic scattering cross section and the scattering cross section using the diagonals, $\sigma(E \rightarrow E)$. These correction factors are assumed to be temperature independent and those calculated for room temperature may therefore be applied to the diagonals, $\sigma(E \rightarrow E)$ calculated at any temperature. It is to be noted that this technique is not applied to the calculation of $\bar{\mu}(E)$, Eq. (5.24), since the most important effect is the relative magnitude of the correctly calculated values of $\sigma_1(E' \rightarrow E)$ and $\sigma(E' \rightarrow E)$.

Appendix B gives a listing of the scattering matrix as calculated using the Nelkin water model. The physical

temperaturesof 20°C and 40°C are considered.

The source of thermal neutrons, S(E), due to down scattering from energies above the thermal cutoff energy, E_c, can be calculated in accordance with Eq. (2.3) by taking the short collision time approximation on all of the modes of oscillation in the Nelkin model. Assuming a 1/E flux above E_c and neglecting upscattering, Eq. (2.3) yields an unnormalized source of:

$$S(E) = ERF\sqrt{E/T_e} \ , \tag{5.27}$$

where ERF(z) is defined in Eq. (5.9).

The effective temperature, T_e, is given by:

$$T_e = \frac{T}{M} + \frac{\overline{E}_r}{M_r} + \frac{\overline{E}_1}{M_v} + \frac{2\overline{E}_2}{M_v} \ , \tag{5.28}$$

where the $\overline{E}$'s are given for each mode of oscillation as:

$$\overline{E} = \omega\left(\frac{1}{e^{\omega/T} - 1} + \frac{1}{2}\right). \tag{5.29}$$

Because of the relative magnitudes of ω_1 and ω_2, T_e may be approximated by:

$$T_e = \frac{T}{M} + \frac{\omega_1}{2M_v} + \frac{\omega_2}{M_v} + \frac{\omega_r}{M_r}\left(\frac{1}{e^{\omega_r/T} - 1} + \frac{1}{2}\right). \tag{5.30}$$

At a physical temperature of 20°C the effective temperature has a value of 0.1169 eV.

CHAPTER 6

THERMAL LATTICE SPECTRA AND INTEGRAL PROPERTIES

Having selected appropriate mathematical models for the scattering kernel, Eq. (5.4) or Eqs. (5.15) and (5.19), and for the relative fuel absorption, f(E)/[1-f(E)], Eqs. (3.8) and (4.21), one proceeds to look for solutions to Eq. (2.9), which is rearranged below.

$$\bar{\varphi}^m(E) = \frac{\bar{S}(E) + \int_0^{E_c} \Sigma(E' \longrightarrow E)\bar{\varphi}^m(E')dE'}{\Sigma_s^m(E) + \Sigma_a^m(E)\left[1 + \frac{f(E)}{1 - f(E)}\right]} , \qquad (6.1)$$

where $\bar{S}(E)$ is given in its unnormalized form by Eq. (5.27) and,

$$\Sigma(E' \longrightarrow E) = N\sigma(E' \longrightarrow E) , \qquad (6.2)$$

N being the number density of the moderator. Solution of Eq. (6.1) for the spatially averaged, energy dependent thermal flux in the moderator is accomplished with Program COUTH (Cornell University Thermalization), a Fortran 63 code written for use with the Control Data Corporation 1604 digital computer. A Fortran statement of COUTH appears in Appendix E, while the numerical methods employed are discussed in Appendix C. This chapter describes the lattice variables and integral parameters calculated in COUTH. The results of a set of actual lattice calculations are described in Chap. 7.

Determination of the spatially averaged flux in the moderator through the solution of Eq. (6.1) leads to the calculation of several other useful quantities. The spatially averaged thermal flux in the fuel, $\bar{\varphi}^f(E)$, and in the cladding, $\bar{\varphi}^c(E)$, may be determined from the moderator spectrum by equating absorption rates in the various regions. Utilizing the relationships in Eqs. (4.53) and (4.54),

$$\bar{\varphi}^f(E) = \frac{V^m}{V^f} \frac{\Sigma_a^m(E)}{\Sigma_a^f(E)} \left[\frac{f(E)}{1-f(E)}\right] \cdot \left[\frac{J_o(E)(1-P_{rv}(E))}{P_{rv}(E)(1-P_e(E))}\right] \bar{\varphi}^m(E) , \tag{6.3}$$

where V^m and V^f are the volumes of the moderator and fuel respectively, $\Sigma_a^f(E)$ is the fuel absorption cross section, $\Sigma_a^m f\bar{\varphi}^m/(1-f)$ is the absorption rate in the fuel element, and $J_o(1-P_{rv})/(1-P_e)P_{rv}$ is the ratio of absorptions in the fuel meat to absorptions in the fuel element. Similarly for the cladding:

$$\bar{\varphi}^c(E) = \frac{V^m}{V^c} \frac{\Sigma_a^m(E)}{\Sigma_a^c(E)} \left[\frac{f(E)}{1-f(E)}\right] \cdot \left[1 - \frac{J_o(E)(1-P_{rv}(E))}{P_{rv}(E)(1-P_e(E))}\right] \bar{\varphi}^m(E) , \tag{6.4}$$

where V^c is the cladding volume and $\Sigma_a^c(E)$ is the cladding absorption cross section.

Average neutron velocities in each region of the cell may now be defined utilizing the relationship between

neutron density and flux,

$$\bar{N}(E) = \bar{\varphi}(E)/v(E) \ , \tag{6.5}$$

where v(E) is the neutron velocity. The average velocity in the moderator, $\bar{v}_m$, is then expressed as

$$\bar{v}_m = \frac{\int_o^{E_c} v(E)\bar{N}^m(E)dE}{\int_o^{E_c} \bar{N}^m(E)dE} = \frac{\int_o^{E_c} \bar{\varphi}^m(E)dE}{\int_o^{E_c} \bar{\varphi}^m(E)/v(E)dE} \ . \tag{6.6}$$

Similar expressions define the average velocities in the fuel, $\bar{v}_f$, and in the cladding, $\bar{v}_c$.

Definitions of disadvantage factors follow directly by expressing the total spatially averaged neutron density, $\bar{N}$, as shown below for the moderator:

$$\bar{N}^m = \int_o^{E_c} \bar{N}^m(E)dE = \int_o^{E_c} \bar{\varphi}^m(E)/v(E)dE \ . \tag{6.7}$$

Using analogous expressions for the total densities in the fuel, $\bar{N}^f$, and the cladding, $\bar{N}^c$, one can calculate neutron density disadvantage factors for the moderator, δ_n^m;

$$\delta_n^m = \bar{N}^m/\bar{N}^f \ , \tag{6.8}$$

and for the cladding δ_n^c;

$$\delta_n^c = \bar{N}^c/\bar{N}^f \ . \tag{6.9}$$

The disadvantage factors are related to the familiar flux disadvantage factors through the relationships:

$$\delta_{\varphi}^{m} = \bar{\varphi}^{m}/\bar{\varphi}^{f} = \bar{v}_{m}\delta_{n}^{m}/\bar{v}_{f} \ , \tag{6.10}$$

and

$$\delta_{\varphi}^{c} = \bar{\varphi}^{c}/\bar{\varphi}^{f} = \bar{v}_{c}\delta_{n}^{c}/\bar{v}_{f} \ , \tag{6.11}$$

where m, c, and f again refer to moderator, cladding, and fuel, and

$$\bar{\varphi}^{m} = \int_{o}^{E_c} \bar{\varphi}^{m}(E)dE \ . \tag{6.12}$$

In terms of quantities already defined the thermal utilization, f, and the more basic quantity, ηf, may be determined, where

$$f = \frac{\text{thermal absorption rate in the fuel rod}}{\text{thermal absorption rate in the cell}} \ , \tag{6.13}$$

and,

$$\eta f = \frac{\text{thermal fission neutron production rate in the cell}}{\text{thermal absorption rate in the cell}} \ . \tag{6.14}$$

These definitions lead to the following expressions:

$$f = \frac{V^f \int_0^{E_c} \Sigma_a^f(E)\ \bar{\varphi}^f(E)dE}{V^m \int_0^{E_c} \Sigma_a^m(E) \left[1 + \frac{f(E)}{1-f(E)}\right] \bar{\varphi}^m(E)dE} , \qquad (6.15)$$

and,

$$\eta f = \frac{\nu\ V^f \int_0^{E_c} \Sigma_a^f(E)\ \bar{\varphi}^f(E)/[1+\alpha(E)]dE}{V^m \int_0^{E_c} \Sigma_a^m(E) \left[1 + \frac{f(E)}{1-f(E)}\right] \bar{\varphi}^m(E)dE} , \qquad (6.16)$$

where ν is the number of fission neutrons produced per thermal fission, and $\alpha(E)$ is the energy dependent capture to fission ratio for the fuel.

A thermal neutron lifetime, ℓ_t, may be defined as the ratio of the total number of thermal neutrons in the cell to the thermal absorption rate in the cell,

$$\ell_t = \frac{\bar{N}^m V^m + \bar{N}^c V^c + \bar{N}^f V^f}{V^m \int_0^{E_c} \Sigma_a^m(E) \left[1 + \frac{f(E)}{1-f(E)}\right] \bar{\varphi}^m(E)dE} , \qquad (6.17)$$

where $\bar{N}$ is defined by Eq. (6.7) for each region.

Since one of the prime concerns in reactor calculations is the accurate determination of various reaction rates, it is desirable to define average thermal cross sections which are suitable for use in calculations utilizing the thermal flux or the 2200 meter/second flux. In terms of the spatially averaged flux or neutron density in a given region, a reaction rate, RR, per unit volume of the region is expressed by:

$$RR = \int_0^{E_c} \Sigma(E)\overline{\varphi}(E)dE = \int_0^{E_c} \Sigma(E)\overline{N}(E)v(E)dE \quad . \qquad (6.18)$$

As before, superscripts on the variables will denote the region considered (m = moderator, c = cladding, f = fuel), while subscripts will denote the interaction considered (a = absorption, s = scattering, t = total, tr = transport, f = fission). Thus, the thermal absorption rate in the moderator will be given by

$$RR_a^m = \int_0^{E_c} \Sigma_a^m(E)\overline{\varphi}^m(E)dE = \int_0^{E_c} \Sigma_a^m(E)\overline{N}^m(E)v(E)dE \quad . \qquad (6.19)$$

In the notation of Wescott,[61] reaction rates may now be formulated in terms of an effective cross section, $\hat{\Sigma}$, and

---

[61] C. H. Wescott, "The Specification of Neutron Flux and Effective Cross Sections," AECL 352 (1956).

a mean cross section, $\bar{\Sigma}$, for use in a calculation with the spatially averaged 2200 meter per second flux, $\bar{\varphi}_o$, and the spatially averaged thermal flux, $\bar{\varphi}_T$, respectively. A given reaction rate is now defined by

$$RR = \hat{\bar{\Sigma}}\bar{\varphi}_o = \bar{\Sigma}\bar{\varphi}_T \ , \tag{6.20}$$

where,

$$\bar{\varphi}_o = \bar{N}v_o = v_o \int_o^{E_c} \bar{N}(E)dE = v_o \int_o^{E_c} \bar{\varphi}(E)/v(E)dE \ , \tag{6.21}$$

and,

$$\bar{\varphi}_T = \overline{Nv} = \int_o^{E_c} \bar{N}(E)v(E)dE = \int_o^{E_c} \bar{\varphi}(E)dE \ . \tag{6.22}$$

The velocity v_o denotes 2200 m/sec, while $\bar{v}$ is the mean velocity defined by Eq. (6.6). This leads to the definition of the effective cross section as:

$$\hat{\bar{\Sigma}} = \frac{\int_o^{E_c} \Sigma(E)\bar{\varphi}(E)dE}{v_o \int_o^{E_c} \bar{N}(E)dE} \ , \tag{6.23}$$

while the mean cross section is defined as

$$\bar{\Sigma} = \frac{\int_0^{E_c} \Sigma(E)\bar{\varphi}(E)dE}{\int_0^{E_c} \bar{\varphi}(E)dE} \quad . \tag{6.24}$$

Consideration of Eqs. (6.23) and (6.24) shows that $\hat{\Sigma}v_o = \overline{\Sigma v}$. Applying this nomenclature to absorption rate per unit volume of the moderator as an example yields:

$$RR_a^m = \hat{\Sigma}_a^m \bar{\varphi}_o^m = \bar{\Sigma}_a^m \bar{\varphi}_T^m \quad , \tag{6.25}$$

where

$$\hat{\Sigma}_a^m = \frac{\int_0^{E_c} \Sigma_a^m(E)\bar{\varphi}^m(E)dE}{v_o \int_0^{E_c} \bar{\varphi}^m(E)/v(E)dE} \quad , \tag{6.26}$$

$$\bar{\Sigma}_a^m = \frac{\int_0^{E_c} \Sigma_a^m(E)\bar{\varphi}^m(E)dE}{\int_0^{E_c} \bar{\varphi}^m(E)dE} \quad , \tag{6.27}$$

$$\bar{\varphi}_o^m = v_o \int_0^{E_c} \bar{\varphi}^m(E)/v(E)dE \quad , \tag{6.28}$$

$$\bar{\varphi}_T^m = \int_o^{E_c} \bar{\varphi}^m(E)dE \ , \tag{6.29}$$

and,

$$\hat{\Sigma}_a^m \ v_o = \bar{\Sigma}_a^m \ \bar{v}_m \quad . \tag{6.30}$$

This approach is extended to define effective and mean cross sections for the homogenized cell, $\hat{\Sigma}^h$ and $\bar{\Sigma}^h$, subscripts denoting the interaction considered. In this manner

$$\hat{\Sigma}^h = \frac{\int_o^{E_c} dE\left[V^m\Sigma^m(E)\bar{\varphi}^m(E) + V^c\Sigma^c(E)\bar{\varphi}^c(E) + V^f\Sigma^f(E)\bar{\varphi}^f(E)\right]}{v_o\int_o^{E_c} \frac{dE}{v(E)}\left[\ V^m\bar{\varphi}^m(E) + V^c\bar{\varphi}^c(E) + V^f\bar{\varphi}^f(E)\ \right]} \ , \tag{6.31}$$

and,

$$\bar{\Sigma}^h = \frac{\int_o^{E_c} dE\left[V^m\Sigma^m(E)\bar{\varphi}^m(E) + V^c\Sigma^c(E)\bar{\varphi}^c(E) + V^f\Sigma^f(E)\bar{\varphi}^f(E)\right]}{\int_o^{E_c} dE\left[V^m\bar{\varphi}^m(E) + V^c\bar{\varphi}^c(E) + V^f\bar{\varphi}^f(E)\ \right]} \ . \tag{6.32}$$

The mean velocity of neutrons in the homogenized cell is defined as

$$\bar{v}_h = \frac{\int_o^{E_c} dE \left[V^m \bar{\varphi}^m(E) + V^c \bar{\varphi}^c(E) + V^f \bar{\varphi}^f(E) \right]}{v_o \int_o^{E_c} \frac{dE}{v(E)} \left[V^m \bar{\varphi}^m(E) + V^c \bar{\varphi}^c(E) + V^f \bar{\varphi}^f(E) \right]} , \tag{6.33}$$

so that,

$$\hat{\Sigma}^h v_o = \bar{\Sigma}^h \bar{v}_h . \tag{6.34}$$

To complete the calculation of the thermal parameters, one would like to define a thermal diffusion area, L^2, for the homogenized cell in a meaningful way. In the one velocity, one region problem, L^2 may be defined unambiguously as

$$L^2 = D/\Sigma_a , \tag{6.35}$$

where $D = 1/3\Sigma_{tr}$. However, in the polyenergetic, homogenized cell problem, one must decide whether L^2 in Eq. (6.35) should be calculated utilizing mean or effective cross sections, and whether D should be calculated by averaging the transport cross section or the transport mean free path.

Larrimore[62] has indicated the desirability of utilizing the mean homogenized cross section, $\bar{\Sigma}_a^h$, in the calculation of L^2. He also notes that several authors[63,64,65] argue in favor of averaging the transport mean free path, while Sjöstrand[66] has shown a physical basis for averaging the transport cross section in the determination of D. The paradox between these two approaches has recently been clarified by Pomraning[67] and on the basis of that discussion this work averages the reciprocal of a homogenized transport cross section, $\Sigma_{tr}^h(E)$, over a homogenized spectrum in the determination of the diffusion coefficient, D. The homogenized transport cross section is defined as

$$\Sigma_{tr}^h(E) = \frac{\Sigma_{tr}^m(E)\bar{\varphi}^m(E)V^m + \Sigma_{tr}^c(E)\bar{\varphi}^c(E)V^c + \Sigma_{tr}^f(E)\bar{\varphi}^f(E)V^f}{\bar{\varphi}^m(E)V^m + \bar{\varphi}^c(E)V^c + \bar{\varphi}^f(E)V^f} \quad , \tag{6.36}$$

while the homogenized flux, $\bar{\varphi}^h(E)$, is defined by

$$\bar{\varphi}^h(E) = \frac{\bar{\varphi}^m(E)V^m + \bar{\varphi}^c(E)V^c + \bar{\varphi}^f(E)V^f}{V^m + V^c + V^f} \quad . \tag{6.37}$$

62/ J. A. Larrimore, "Temperature Coefficients of Reactivity in Homogenized Thermal Nuclear Reactors," Massachusetts Institute of Technology Thesis (1962).

63/ A. M. Weinberg and E. P. Wigner, The Physical Theory of Neutron Chain Reactors, p. 514, The University of Chicago Press, Chicago, 1958.

64/ C. D. Petrie, M. L. Storm, and P. F. Zweifel, "Calculation of Thermal Group Constants for Mixtures Containing Hydrogen," Nucl. Sci. Eng. 2, 728-744 (1957).

The diffusion coefficient is then expressed as

$$D = \frac{\frac{1}{3}\int_0^{E_c} \bar{\varphi}^h(E)/\Sigma^h_{tr}(E)dE}{\int_0^{E_c} \bar{\varphi}^h(E)dE} \quad . \tag{6.38}$$

The thermal diffusion area is calculated from

$$L^2 = D/\bar{\Sigma}^h_a \quad , \tag{6.39}$$

where $\bar{\Sigma}^h_a$ is defined by Eq. (6.32).

The calculation of all of the parameters and variables discussed in this chapter is carried out by program COUTH. The results derived from these calculations for an actual lattice system are discussed in Chap. 7.

65/ K. S. Singwi and L. S. Kothari, "Transport Cross Section of Thermal Neutrons in Solid Moderators," Second Geneva Conference Proceedings, 16, 325 (1958).

66/ N. G. Sjöstrand, "Definition of the Diffusion Constant in One-Group Theory," J. Nucl. Energy, Part A, Reactor Science, 151 (1960).

67/ G. C. Pomraning, "On the Energy Averaging of the Diffusion Coefficient," Nucl. Sci. Eng. 19, 250 (1964).

CHAPTER 7

APPLICATION OF THE METHOD TO ACTUAL LATTICES

7.1 Room Temperature Calculations

In this chapter we discuss the numerical results obtained with program COUTH when the cell theory formulated in Secs. 2.1 and 2.3 is applied to an actual lattice system. The aim of this work is to calculate at various temperatures, the spatially averaged thermal spectra, and the integral parameters defined in Chap. 6 for all of the cores incorporated in the Cornell University Zero Power Reactor facility.[68,69] The Cornell ZPR cores are light water moderated and utilize high density, low enrichment uranium dioxide fuel, clad in aluminum. Several water to uranium oxide volume ratios (nominally 1:1, 1.5:1, 2:1, 3:1 and 4:1) are provided with sets of grid plates which vary the spacing (lattice pitch) between the fuel elements arranged in a hexagonal array. More specifically, the fuel rods consist of 0.60 inch diameter uranium dioxide fuel of density 10.38 gm/cc, enriched to 2.096 atom per cent of U^{235}. The fuel rods, formed by 48 one inch long fuel pellets, are clad in 0.028 inch thick aluminum to form a fuel element with an outside diameter of 0.666 inches. A list of the parameters of the various lattices is given in Appendix A.

---

[68] D. D. Clark, "The Cornell University Nuclear Reactor Laboratory," CURL-1, Cornell University (1961).

Initial calculations have been carried out utilizing as a scattering kernel both the Nelkin water kernel, Eq. (5.15), and the monatomic gas model, Eq. (5.11), for a gas of mass one. The two physical temperatures of 20°C and 40°C have been considered. The results of an elementary study utilizing the monatomic gas model have previously been reported.[70]

In the solution of the neutron balance equation, Eq. (6.1), to determine the spatially averaged moderator flux, $\overline{\varphi}^m(E)$, the heterogeneous effects of the lattice are accounted for by the relative fuel absorption, $f(E)/[1-f(E)]$, as given in terms of escape probabilities by Eq. (2.29). The moderator escape probabilities, $P_s(E)$ and $P_m(E)$, are given by Eqs. (3.4) and (3.6), respectively. This yields Eq. (3.8) for the relative fuel absorption. The fuel element escape probability to be used in Eq. (3.8) is calculated by means of Eq. (4.21), which in turn requires the calculations indicated by Eqs. (4.22), (4.19), and (4.8). Equation (4.8) calculates the fuel rod escape probability utilizing the parabolic flux approximation.

---

[69] S. S. Berg, "Initial Experiments on the Cornell University Zero Power Reactor Cores," Cornell University Thesis (1964).

[70] K. B. Cady and C. R. Mac Vean, "A Simplified Formulation of Space-Energy Cell Theory," Trans. Am. Nucl. Soc. 6, 234-235 (1963).

The source of neutrons due to down scattering from energies above E_c is that given by Eq. (5.27), normalized to one neutron per second per unit volume of the moderator. That is,

$$\overline{S}(E) = \frac{\mathrm{ERF}\sqrt{E/T_e}}{\int_0^{E_c} \mathrm{ERF}\sqrt{E/T_e}} \quad . \tag{7.1}$$

The calculations were performed utilizing an energy mesh containing forty-five energy points ranging from 0.001 eV to a thermal cutoff energy, E_c, of 1.609 eV. In the stipulation of a useful energy mesh a compromise must be reached between several conflicting requirements. In the first place, a reasonable range of energies must be covered. Secondly, the total number of energy mesh points, n, may not be too large, since the computer time necessary for the calculation of the scattering kernel increases as n squared. Furthermore, it is desirable to have a finely spaced energy mesh in the region above the thermal energy, E_o = kT, where the 1/E tail joins that part of the spectrum resembling a Maxwellian. Finally, the use of the Nelkin water kernel places certain restrictions on the size of the energy spacing, ΔE, between the energy points in the mesh. With the use of the approximation allowing for all transitions of the hindered rotator, Eqs. (5.17) (utilized for incident neutron energies less than 0.33 eV) it is

necessary to use a ΔE which is less than the frequency (ω_r = 0.06 eV) of the hindered rotator. This requirement insures that the fine structure of the water kernel is preserved in the calculations and that energy integration of the scattering kernel will yield a fairly accurate scattering cross section. In order to satisfy this requirement, the energy spacings utilized in the calculations are less than one quarter of ω_r or .015 eV for all energies below 0.33 eV. In light of these restrictions, the energy mesh used in the calculations consists of 35 energy points below E = .33 eV with 34 energy intervals corresponding to equal intervals in velocity. Each of these low energy velocity intervals corresponds to 0.1 v_o or 220 m/sec. For energies above E = 0.33 eV the ten energy intervals correspond to velocity intervals which exponentially increase from 220 m/sec to 2200 m/sec as energy increases. A complete listing of the energy mesh utilized is given in Appendix B.

The U^{235} absorption and fission cross sections used are those compiled by Suich.[71] The absorption cross sections for U^{238}, the moderator and the cladding are all assumed to be 1/v and the 2200 m/s values of these cross sections are given in Appendix A. The scattering cross

---

[71] J. Suich, "Temperature Coefficients in Heterogeneous Reactor Lattices," Massachusetts Institute of Technology Thesis (1963).

sections for all of the materials other than the moderator are calculated utilizing the analytic expression, Eq. (5.13), derived from the monatomic gas model. Scattering cross sections for the moderator are computed by integration of the scattering kernel in accordance with Eq. (5.12). The use of the monatomic gas model yields a water scattering cross section given by Eq. (5.13), while the use of the Nelkin water kernel results in the scattering cross section given by BNL 325.[72] The free atom scattering cross sections used are given in Appendix A.

The transport cross sections are calculated using

$$\Sigma_{tr}(E) = \Sigma_a(E) + \Sigma_s(E) \left[1 - \bar{\mu}(E)\right] . \qquad (7.2)$$

The average cosine of the scattering angle, $\bar{\mu}(E)$, is calculated from the Nelkin water kernel, Eq. (5.24) and Fig. (5.2), for the water moderator. The water transport cross section derived from the Nelkin model is also used in the calculation of the moderator escape probabilities with use of the monatomic gas kernel. For all other materials $\bar{\mu}(E)$ is given by

$$\bar{\mu}(E) = \bar{\mu} = 2/3A , \qquad (7.3)$$

A being the mass number of the scattering material.

Calculation of the relative fuel absorption f(E)/[1-f(E)], Eq. (2.29), using the $P_s(E)$ shown in Fig. (3.1),

---

[72] D. Hughes and B. Schwartz, "Neutron Cross Sections," BNL 325, 2nd Ed., Brookhaven National Laboratory (1958).

the $P_m(E)$ shown in Fig. (3.2), and the $P_e(E)$ shown in Fig. (4.2), yields the apparent lattice absorption cross section, $\Sigma_a^m(E)\left[1 + f(E)/[1-f(E)]\right]$. This quantity is shown in Fig. 7.1 for the five Cornell ZPR cores. Comparison with the absorption cross section of pure water, $\Sigma_a^m(E)$, shows the non 1/v behavior of this apparent cross section as well as the effect of the 0.273 eV resonances in U^{235}. It is this non 1/v behavior which yields a temperature coefficient of the thermal utilization, f.

The apparent lattice absorption cross section shown in Fig. (7.1) is substituted into the neutron balance equation, Eq. (6.1), along with either the monatomic gas or Nelkin water scattering cross section. The computer solution of Eq. (6.1) is discussed in Appendix C, the result of the solution being the spatially averaged moderator spectrum, $\bar{\varphi}^m(E)$, evaluated at the discrete energy points in the energy mesh used. Figure 7.2 shows the results of this calculation utilizing the Nelkin water kernel for the five water to uranium oxide volume ratios of the Cornell ZPR. Since all of the results are normalized to one neutron per second slowing down per unit volume of the moderator, Fig. 7.2 shows the flux suppression as well as the spectral hardening experienced in the tighter (lower water to oxide volume ratios) cores. The difference between moderator spectra predicted with the monatomic gas model and the Nelkin water kernel is shown in Fig. 7.3 where the $\bar{\varphi}^m(E)$

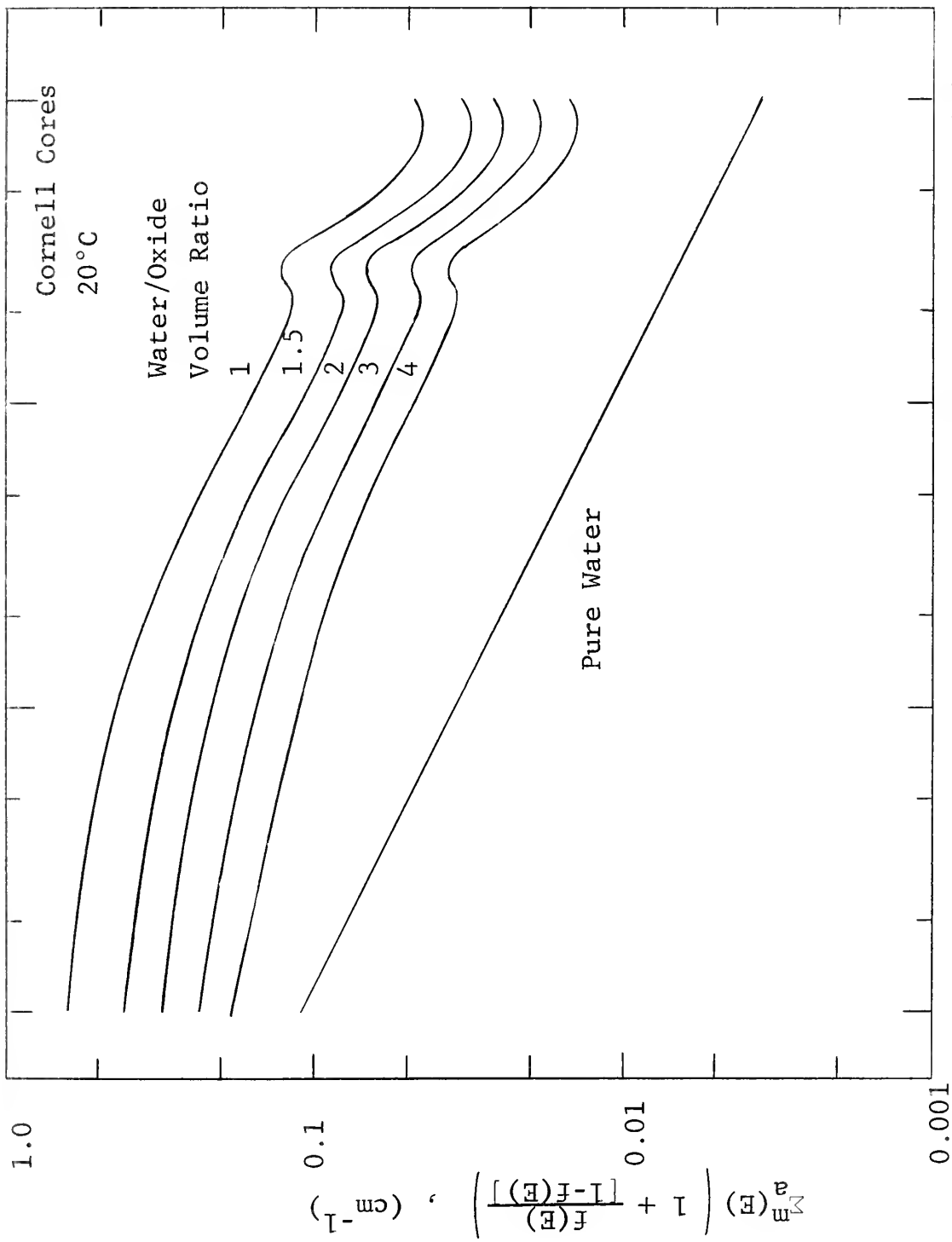

Figure 7.1 Apparent Lattice Absorption Cross Section

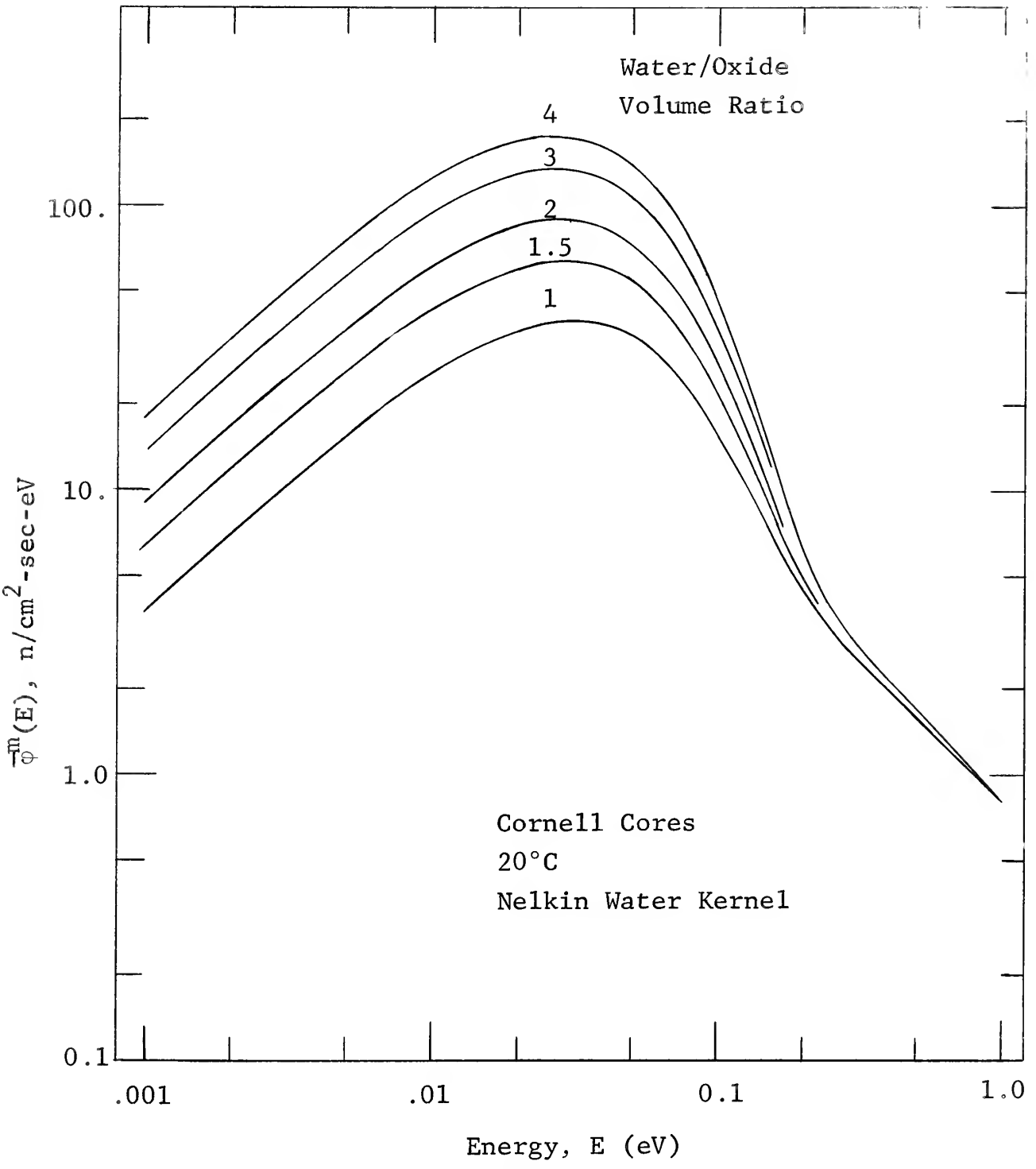

Figure 7.2 Spatially Averaged Moderator Thermal Spectra

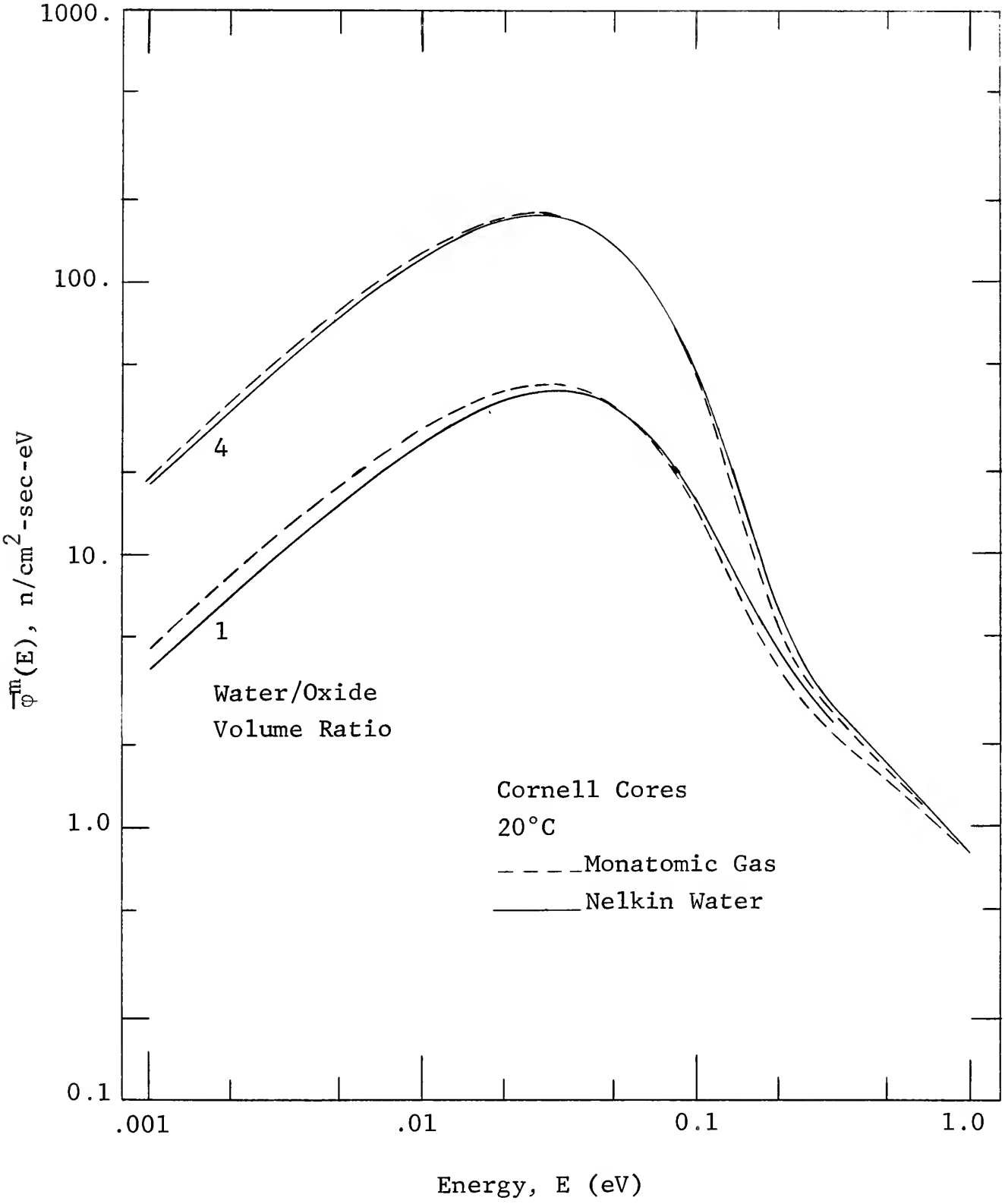

Figure 7.3 Comparison of the Moderator Spectra Predicted with the Nelkin Water and Monatomic Gas Models

predicted by these two models are plotted for the extreme lattices of the ZPR; that is the 1:1 and 4:1 water to oxide volume ratio cores. Figure 7.3 indicates that harder spectra are predicted with the use of the Nelkin water kernel than with the use of the monatomic gas kernel.

Using the spatially averaged moderator flux, the spatially averaged fluxes in the fuel, $\overline{\varphi}^{f}(E)$, and the cladding, $\overline{\varphi}^{c}(E)$, may be calculated using Eqs. (6.3) and (6.4) respectively. Results typical of this calculation using the Nelkin water kernel are shown in Fig. 7.4 where $\overline{\varphi}^{m}(E)$, $\overline{\varphi}^{c}(E)$, and $\overline{\varphi}^{f}(E)$ are plotted for the ZPR 3:1 core. Spectrum hardening as well as depression, giving rise to disadvantage factors, is experienced as one goes from the moderator to the cladding to the fuel.

The average neutron velocities in the moderator, cladding, and fuel as defined in Eq. (6.6) are shown in Fig. 7.5 for all of the ZPR cores, these calculations being made with the Nelkin water kernel. Again the spectral hardening produced in the tighter cores is evident. Figure 7.5 also shows that for the tighter cores $\overline{v}_c$ is well represented by the relationship which Honeck[73] has verified for the Brookhaven uranium metal cores,

---

[73] H. C. Honeck, "The Calculation of the Thermal Utilization and Disadvantage Factor in Uranium/Water Lattices," Nucl. Sci. Eng. 18, 49-68 (1964).

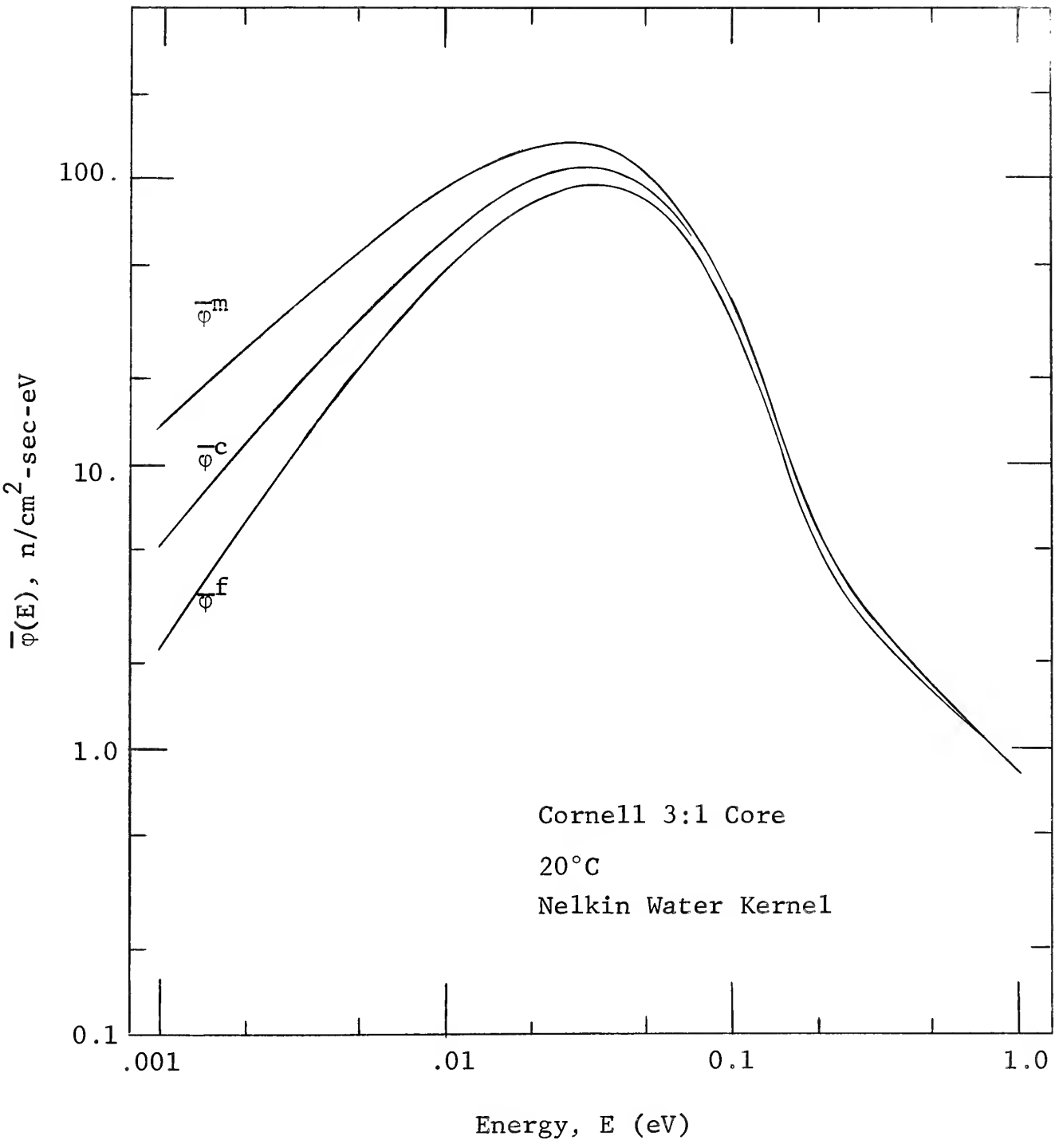

Figure 7.4 Spatially Averaged Cell Spectra

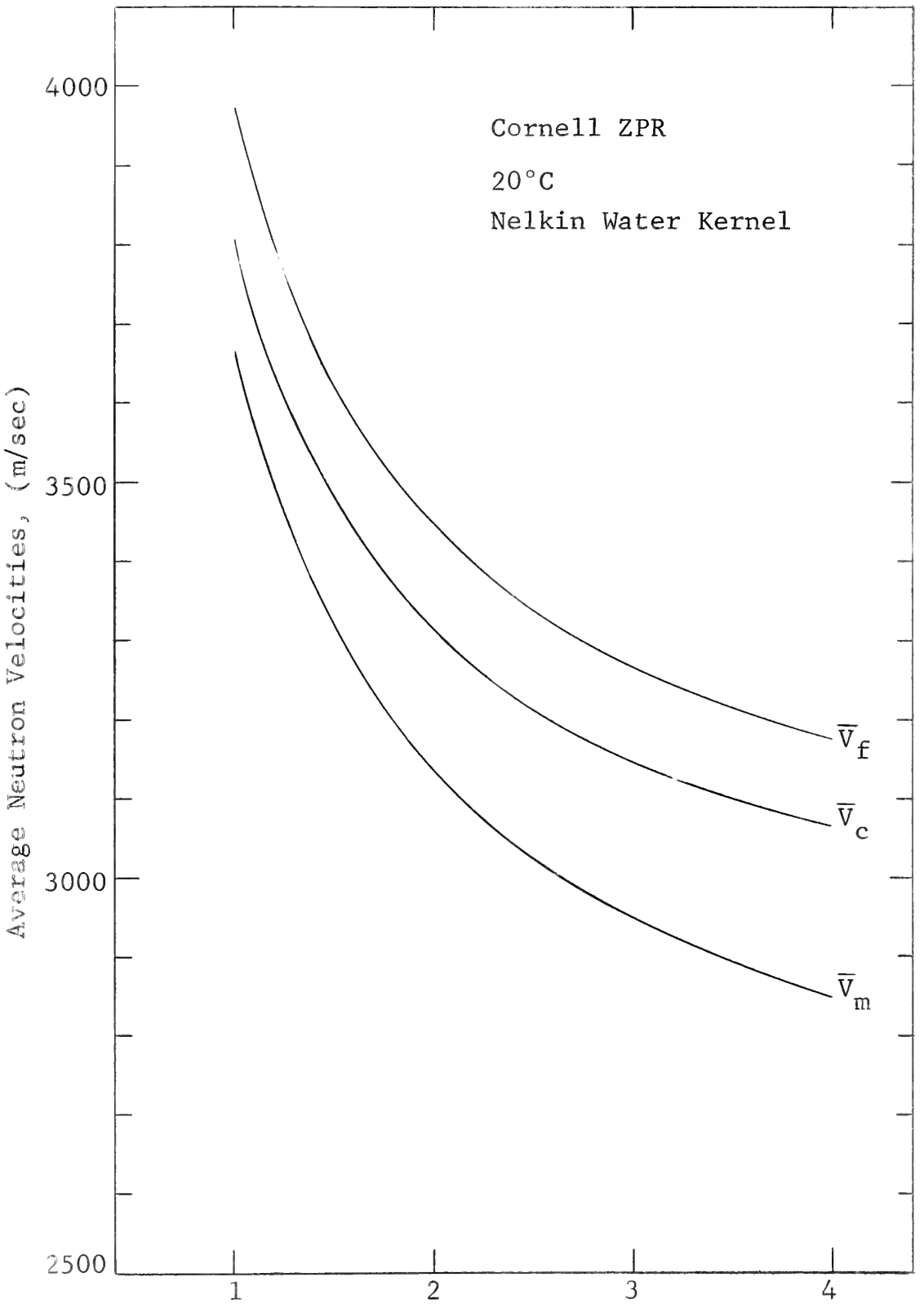

Figure 7.5 Average Neutron Velocities

$$\bar{v}_c = \frac{1}{2}(\bar{v}_f + \bar{v}_m) \quad . \tag{7.4}$$

The error in the result predicted by Eq. (7.4) increases with the water to oxide volume ratio to a maximum of 1.8% for the 4:1 core.

The average neutron velocities, $\bar{v}_h$, for the homogenized cell, Eq. (6.33), are shown for calculations with both the monatomic gas model and the Nelkin water kernel in Fig. 7.6. Again the harger spectra predicted by the Nelkin water kernel is evident as the average neutron velocities for the homogenized cell calculated with the monatomic gas model are lower than those given by the Nelkin model by 5.4% for the 1:1 core and 2.4% for the 4:1 core.

The neutron density disadvantage factors for the moderator, δ_n^m, and for the cladding, δ_n^c, as defined in Eqs. (6.8) and (6.9) respectively, are shown in Fig. 7.7 as calculated with both the monatomic gas kernel and the Nelkin water model. In this case, the discrepancies between the results computed with the two models is entirely attributed to the softer spectra produced with the monatomic gas model since the transport cross section for water used in both calculations was that calculated with the Nelkin water kernel. The δ_n^m predicted with the monatomic gas kernel are 1.4% higher for the 1:1 core and

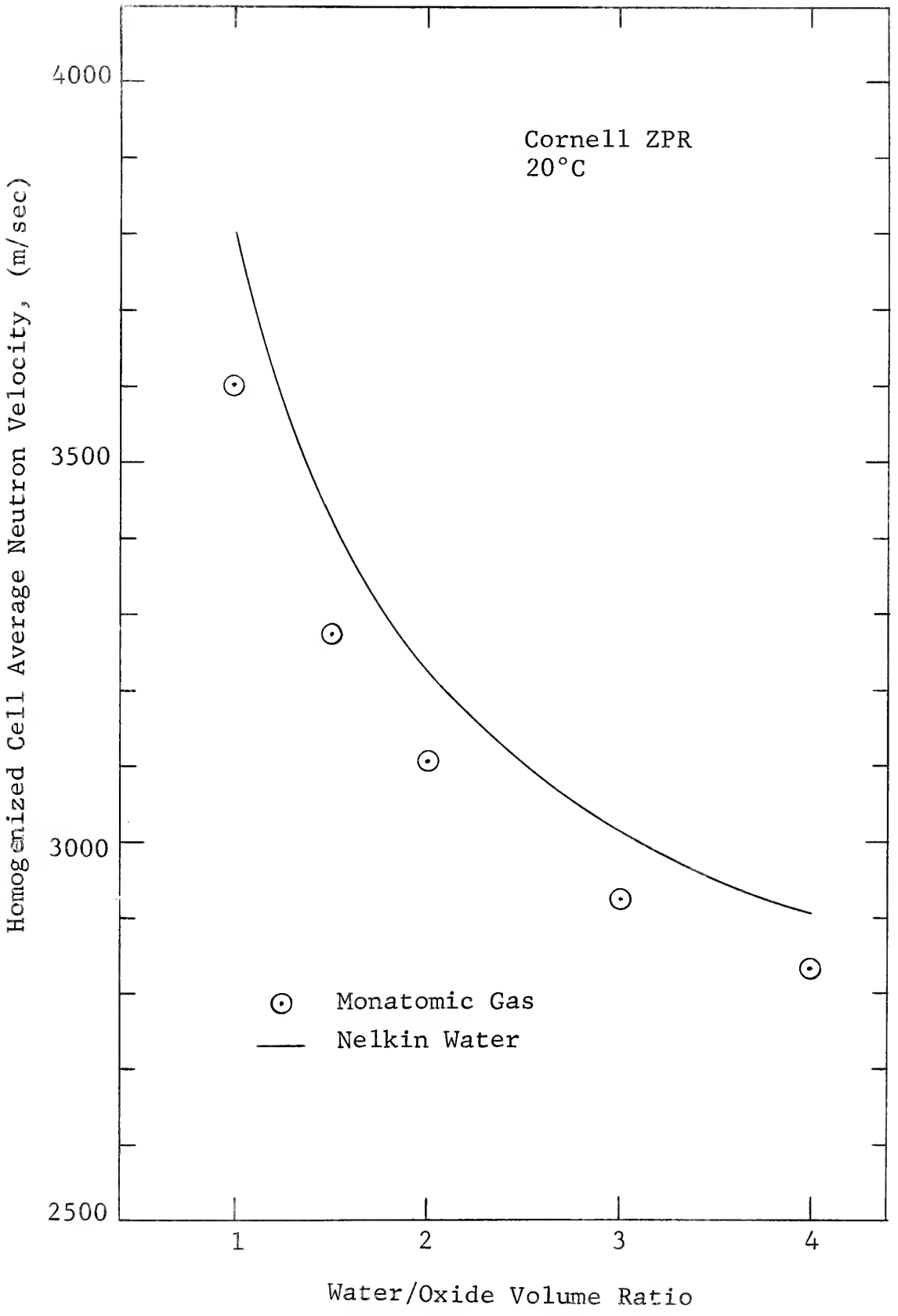

Figure 7.6 Average Neutron Velocity for the Homogenized Cell

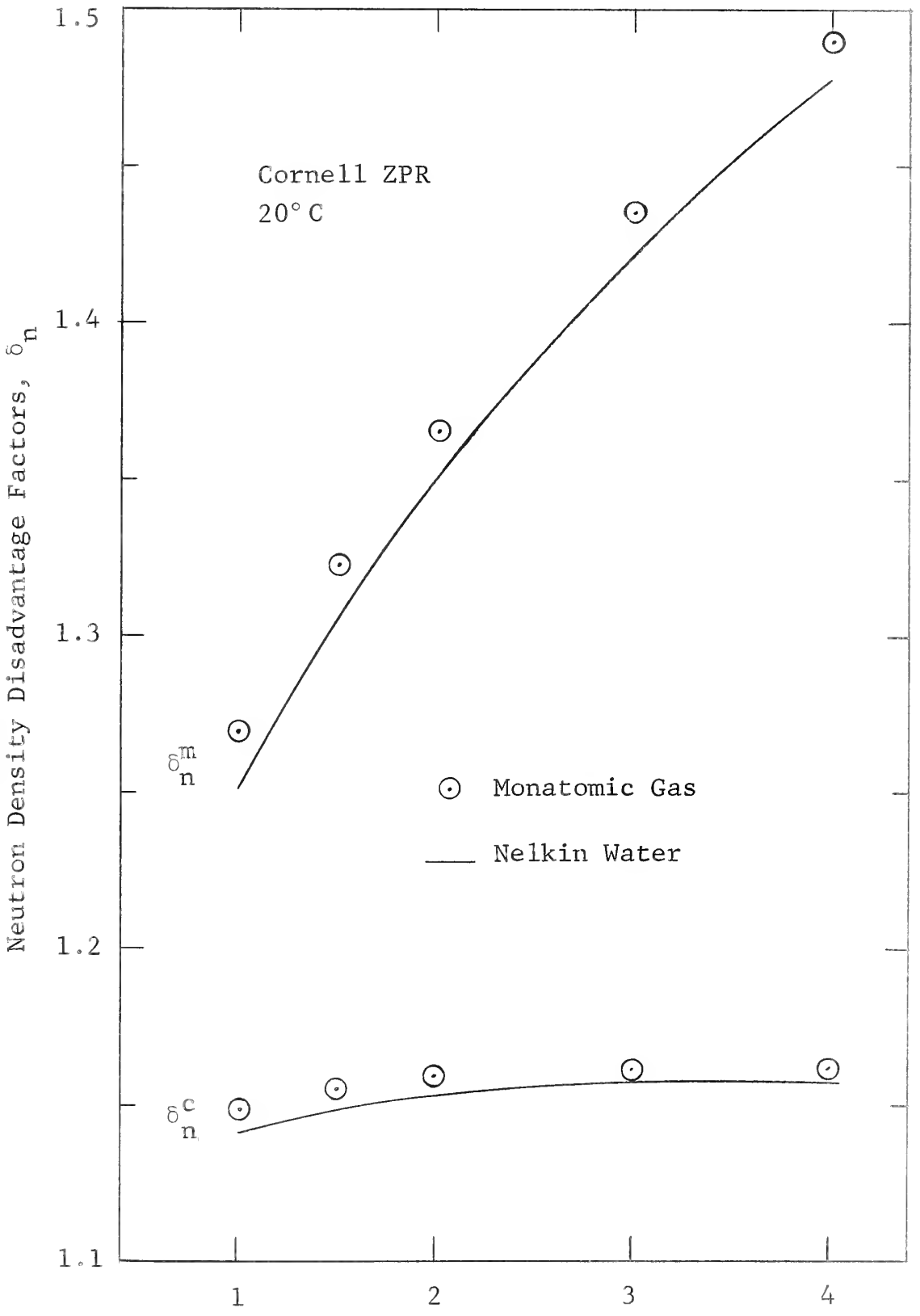

Figure 7 Neutron Density Disadvantage Factors

0.8% higher for the 4:1 core than those calculated with the Nelkin model. Similarly, the differences in the δ_n^c calculated by the two models is 0.8% for the 1:1 core and 0.3% for the 4:1 core. The fact that the disadvantage factors monotonically increase as a function of water to oxide volume ratio is expected[74] since a non-reflecting cylindrical cell boundary condition is incorporated in this formulation.

The results of the calculation of the thermal utilization, f, and ηf defined by Eqs. (6.15) and (6.16) respectively for the Nelkin water model are shown in Figs. 7.8 and 7.9. The results predicted with the monatomic gas model closely approximate those computed with the Nelkin water kernel, the differences being less than 0.2% for all cases of f, η, and ηf. This indicates that these integral properties are essentially insensitive to the scattering model used in the averaging process.

Figure 7.10 shows the variation of thermal lifetimes, Eq. (6.17), as a function of water to oxide volume ratio calculated with the Nelkin water kernel and the monatomic gas model. Again relatively small variations, always less than 0.4%, between the Nelkin water and monatomic gas kernel calculations are present. The lifetimes are seen to decrease in the tighter cores because of the increased apparent absorption, Fig. 7.1, present in these cores.

---

[74] H. C. Honeck, p. 56, see Footnote 73.

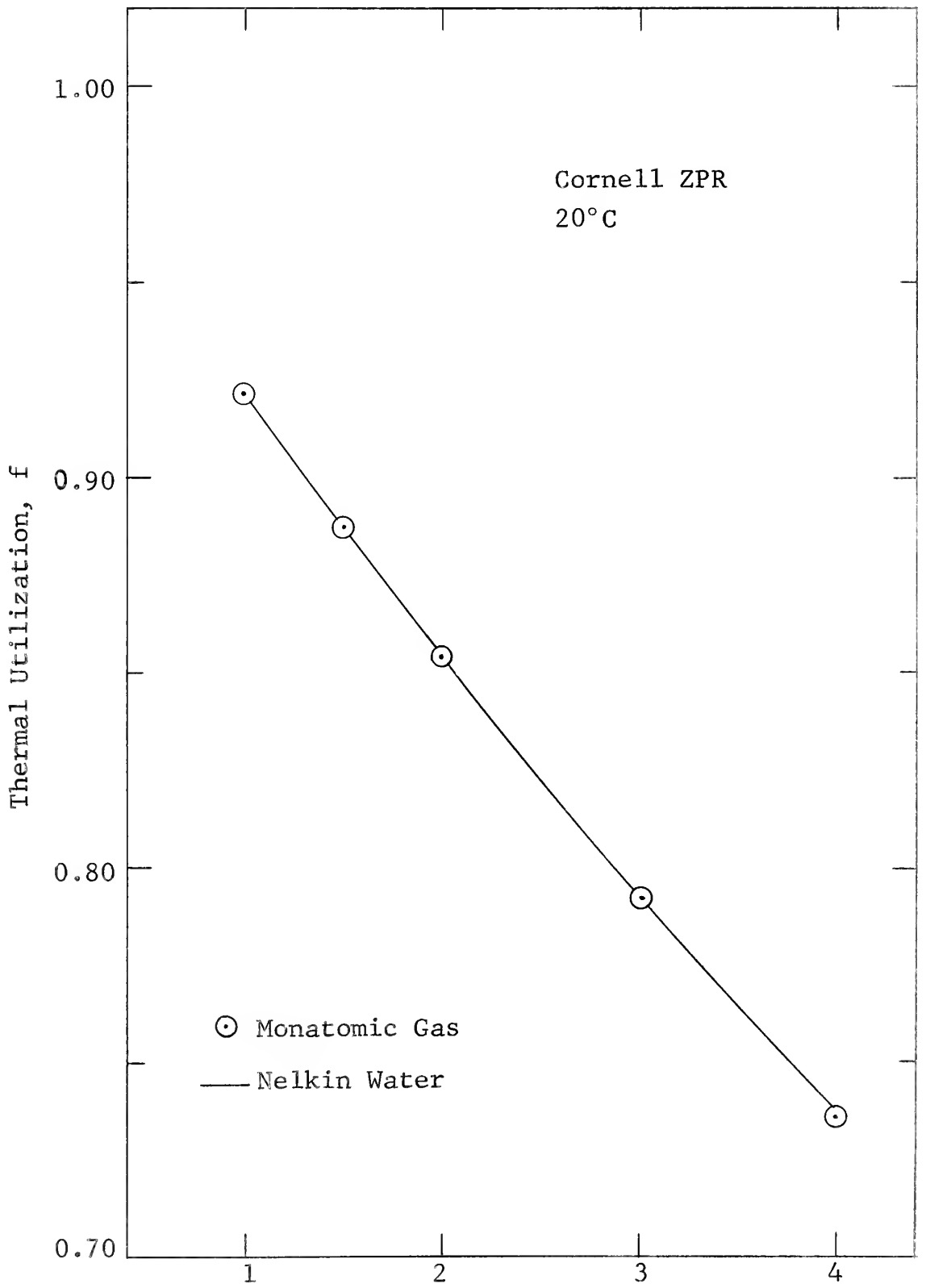

Figure 7.8 Thermal Utilization

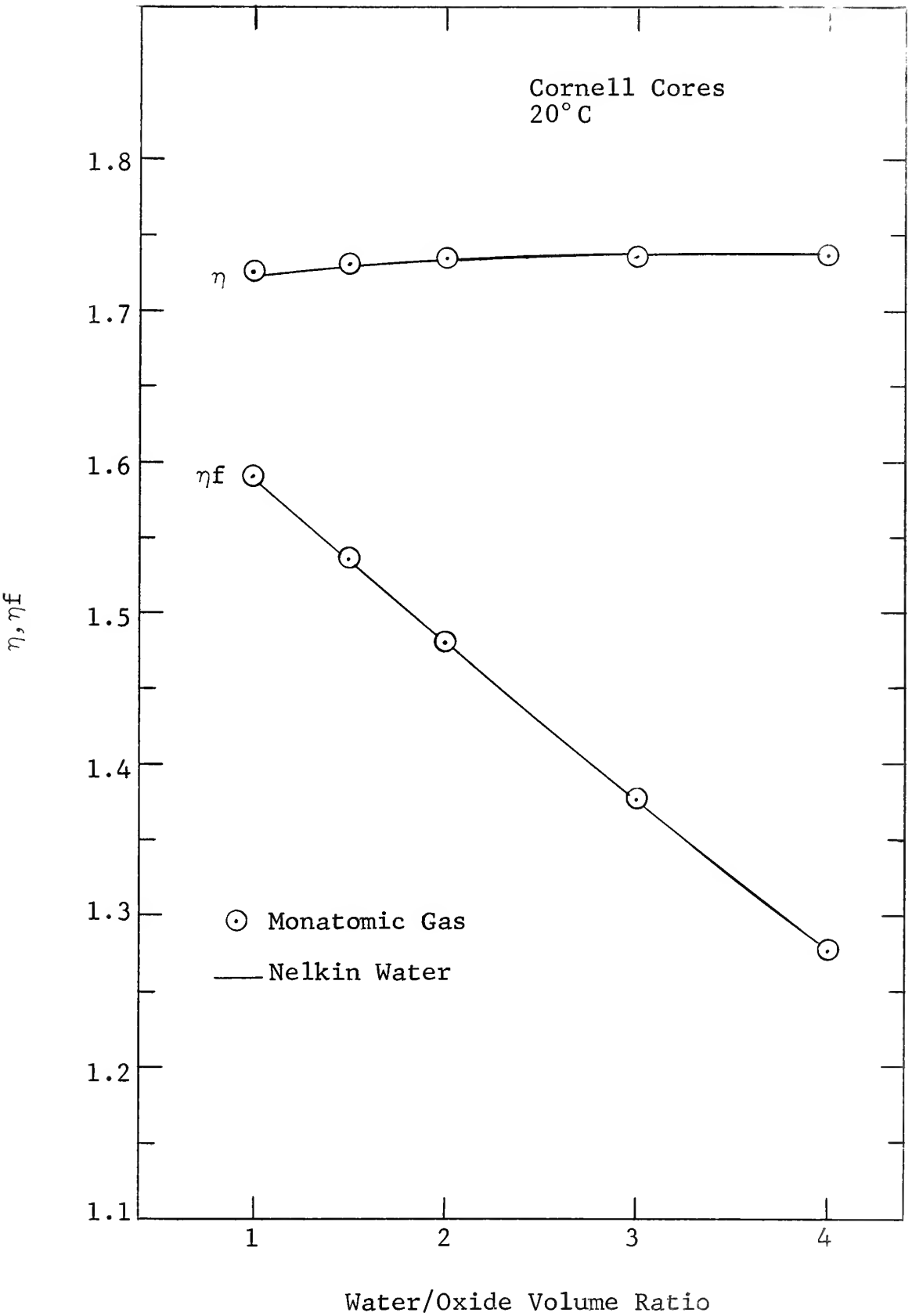

Figure 7.9 Integral Properties, η and

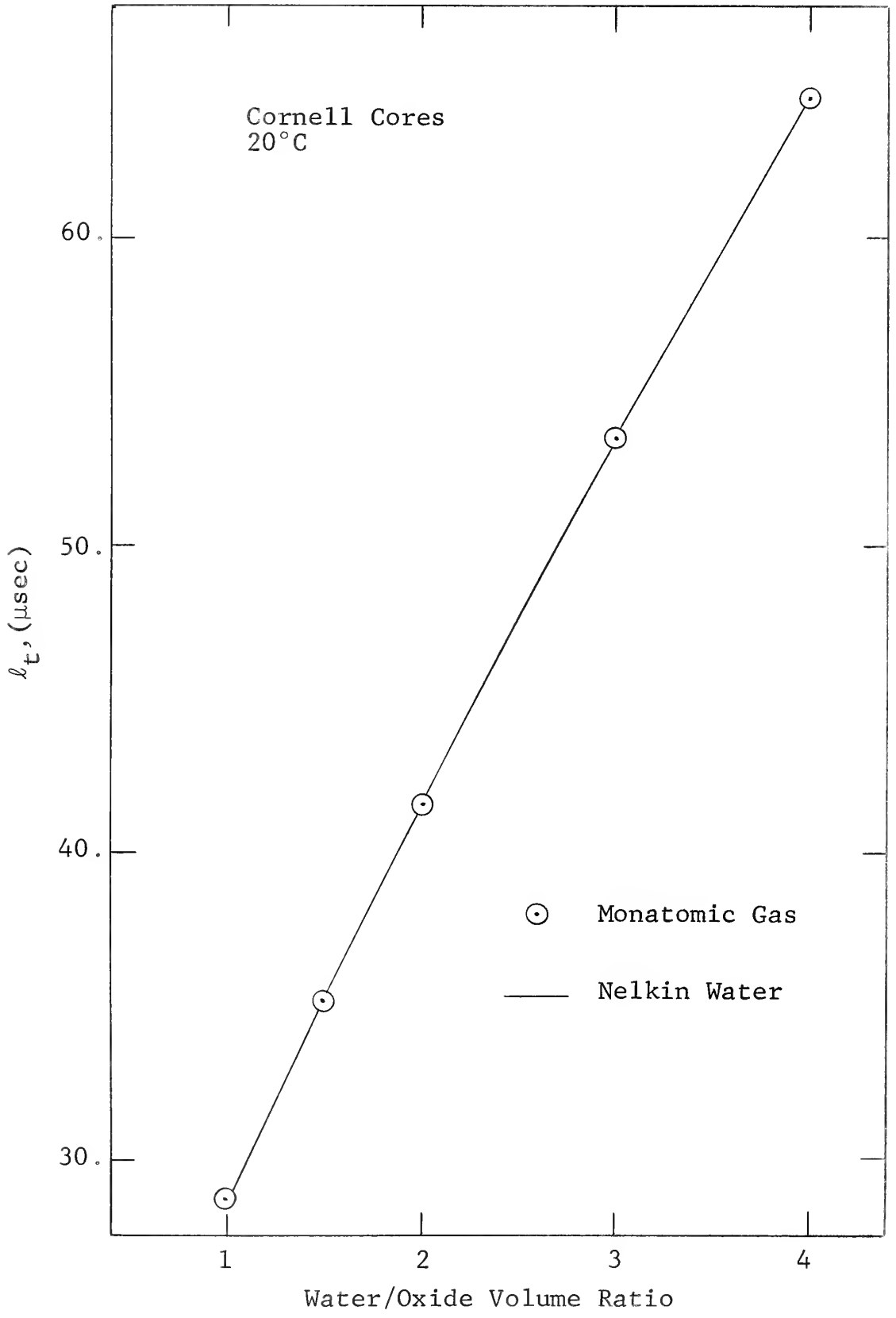

Figure 7.10 Thermal Lifetime

Figure 7.11 shows the effective absorption cross section, $\hat{\Sigma}_a^h$, Eq. (6.31), and the mean absorption cross section, $\bar{\Sigma}_a^h$, Eq. (6.32), for the homogenized cell as calculated using the Nelkin water and monatomic gas models. Variations encountered in the calculation of these results when the monatomic gas model was utilized were less than 0.4% for the effective absorption cross sections and 2.0% for the mean absorption cross sections.

The thermal diffusion coefficient, D, and the thermal diffusion length, L, as calculated by averaging a homogenized mean free path in accordance with Eq. (6.38) are shown in Fig. 7.12 using both the Nelkin water and monatomic gas kernels. From Fig. 7.12 it is seen that the monatomic gas model predicts a D which is about 3.0% less, and an L which is about 4.0% less than those calculated with the Nelkin water kernel. The differences between these results are strictly due to the relative hardness of the spectra predicted by the two models, since the transport cross sections utilized were the same in both cases. It is still not clear how these calculated diffusion lengths would compare with those measured in a buckling experiment; however, it is noteworthy that the minimum in L for the 2:1 core is the same phenomenon measured for the Brookhaven uranium metal lattices.[75]

---

[75] R. L. Hellens and H. C. Honeck, "Summary and Preliminary Analysis of the BNL Slightly Enriched Uranium, Water Moderated Lattice Measurements," Light Water Lattices, p. 54, International Atomic Energy Agency, Vienna (1962).

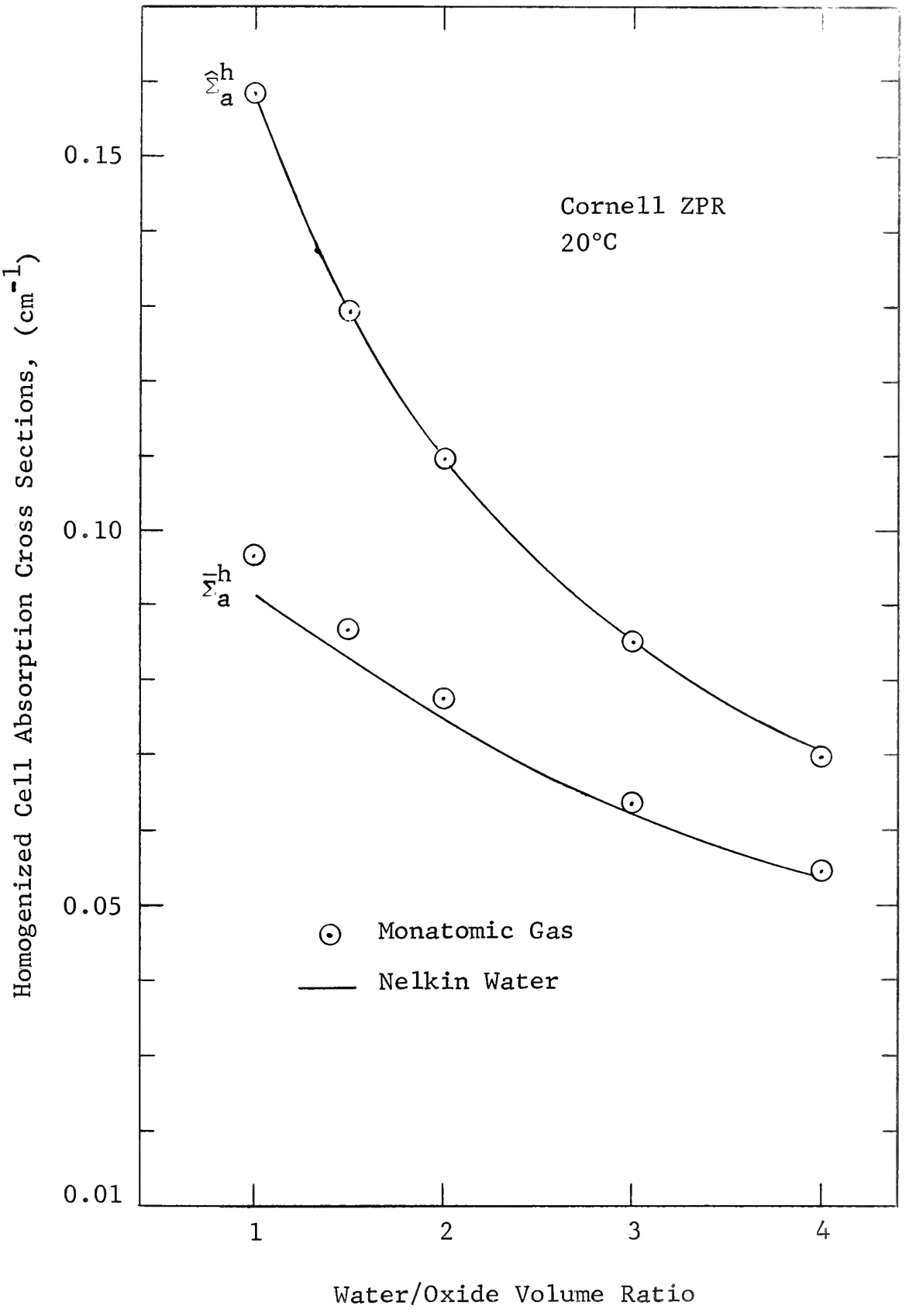

Figure 7.11 Effective and Mean Absorption Cross Sections for Homogenized Cell

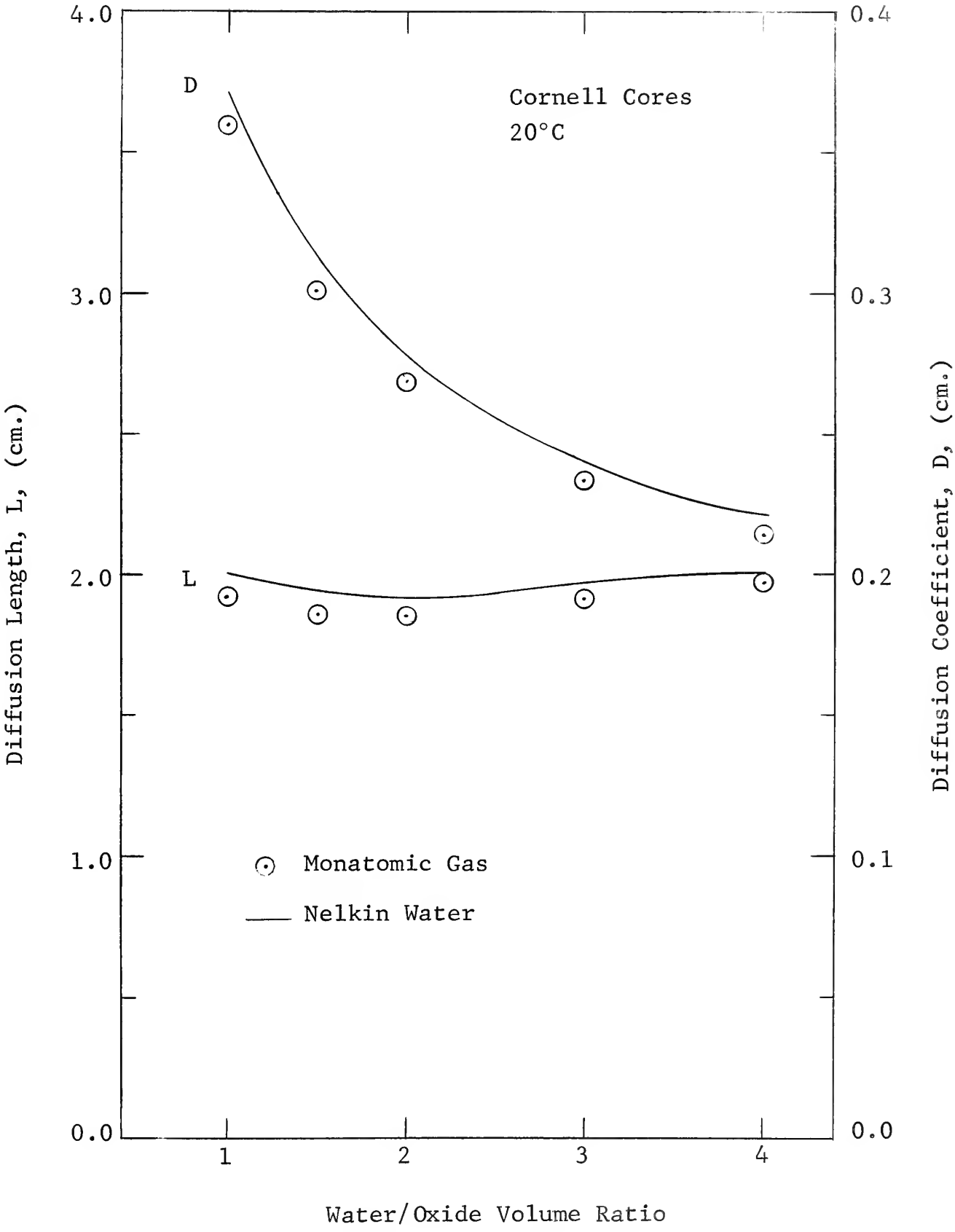

Figure 7.12 Thermal Diffusion Coefficient and Length for the Homogenized Cell

This also indicates that the customary receipe for calculating a homogenized diffusion area, $L^2 = (1-f) L_o^2$, [76] lacks validity in that it predicts a monotonically increasing L^2 with increasing water to oxide volume ratios.

A tabular listing of the parameters presented in this section appear in Appendix B as calculated with the Nelkin water kernel at 20°C. A discussion of the accuracy of these results is given in Chap. 8.

7.2 Temperature Coefficients

In order to estimate the effect of temperature on the various integral parameters defined in Chap. 6 and presented for 20°C in Sec. 7.1, all of the calculations were remade at a physical temperature of 40°C. In these calculations any changes in the fuel and cladding densities and dimensions have been neglected. In addition, the expansion of grid plate supporting the fuel elements leading to a change in the equivalent cell radius has also been neglected. All of the results are expressed in terms of temperature coefficients defined for a given variable, x, as

$$\frac{1}{x}\frac{\Delta x}{\Delta T} = \frac{1}{x(20°)} \cdot \frac{x(40°) - x(20°)}{20} \ °C^{-1} . \qquad (7.5)$$

---

[76] A. M. Weinberg and E. P. Wigner, The Physical Theory of Neutron Chain Reactors, p. 724, The University of Chicago Press, Chicago, 1958.

The temperature coefficient of the average neutron velocity in the homogenized cell, $\bar{v}_h$, Eq. (6.33), is shown in Fig. 7.13 for both models of the scattering kernel. This indicates that although the Nelkin model predicts a harder homogenized spectrum at room temperature, the monatomic gas spectra hardens at a faster rate with increasing temperature. It is therefore possible to postulate that at some elevated temperature the integral parameters dependent primarily on the degree of spectral hardening will be the same for both models of the scattering kernel. The temperature coefficient of $\bar{v}_h$ predicted with the monatomic gas model is 23.8% higher for the 1:1 core and 7.8% higher for the 4:1 core than those predicted by the Nelkin water kernel.

Figure 7.14 shows the temperature coefficients of the moderator and cladding disadvantage factors, δ_n^m and δ_n^c, these parameters having been defined in Eqs. (6.8) and (6.9) respectively. As expected, they are negative; the effects of harder spectra being seen in Fig. 7.7. The monatomic gas model predicts larger negative temperature coefficients because of the greater relative spectral hardening encountered with that model. The maximum difference between the scattering models occurs in the 1:1 core where the temperature coefficient of δ_n^m predicted by the monatomic gas model is 30% higher than the prediction by the Nelkin water kernel. In the case of δ_n^c the results differ by 20%.

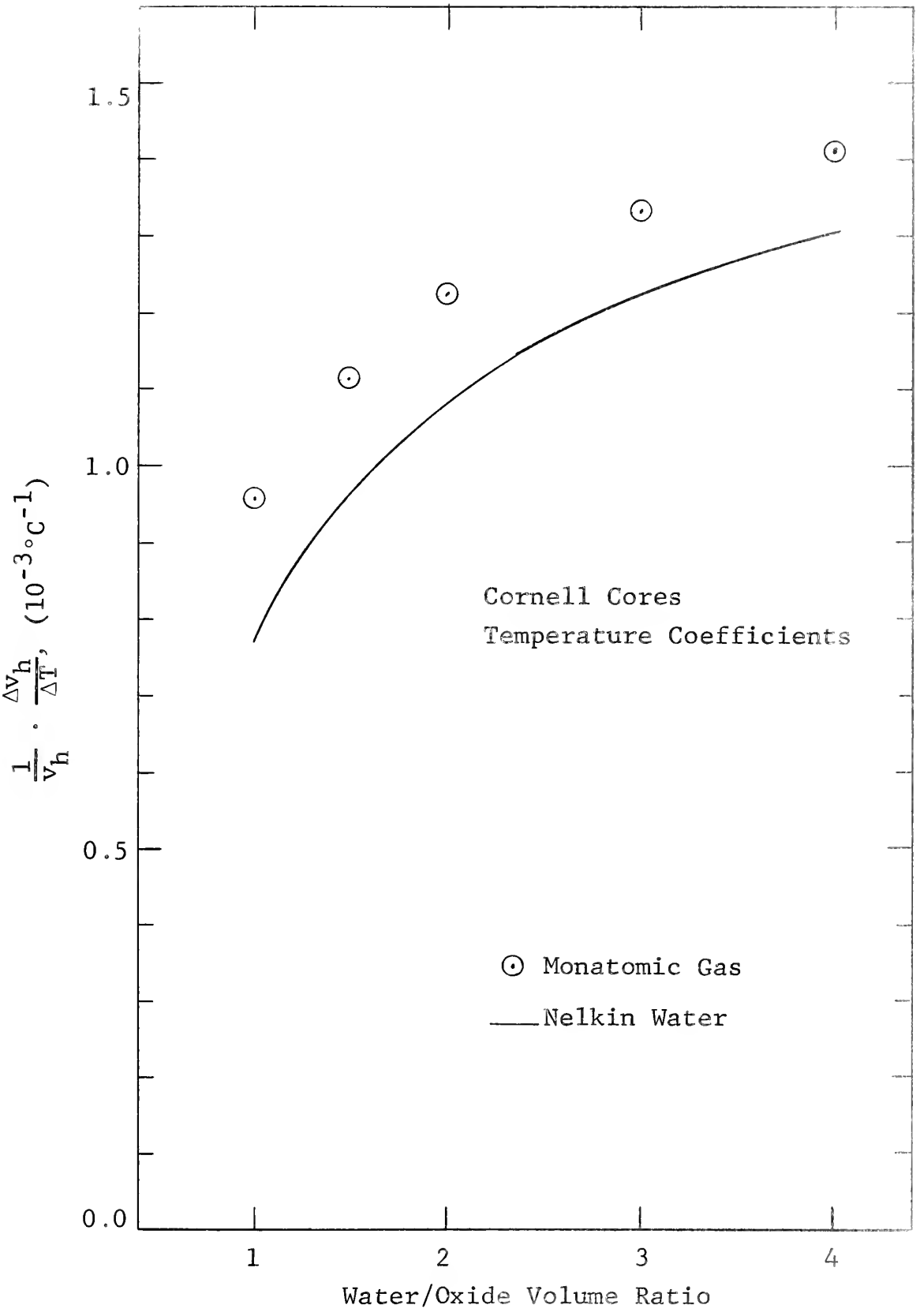

Figure 7.13 Temperature Coefficient of the Average Neutron Velocity for the Homogenized Cell

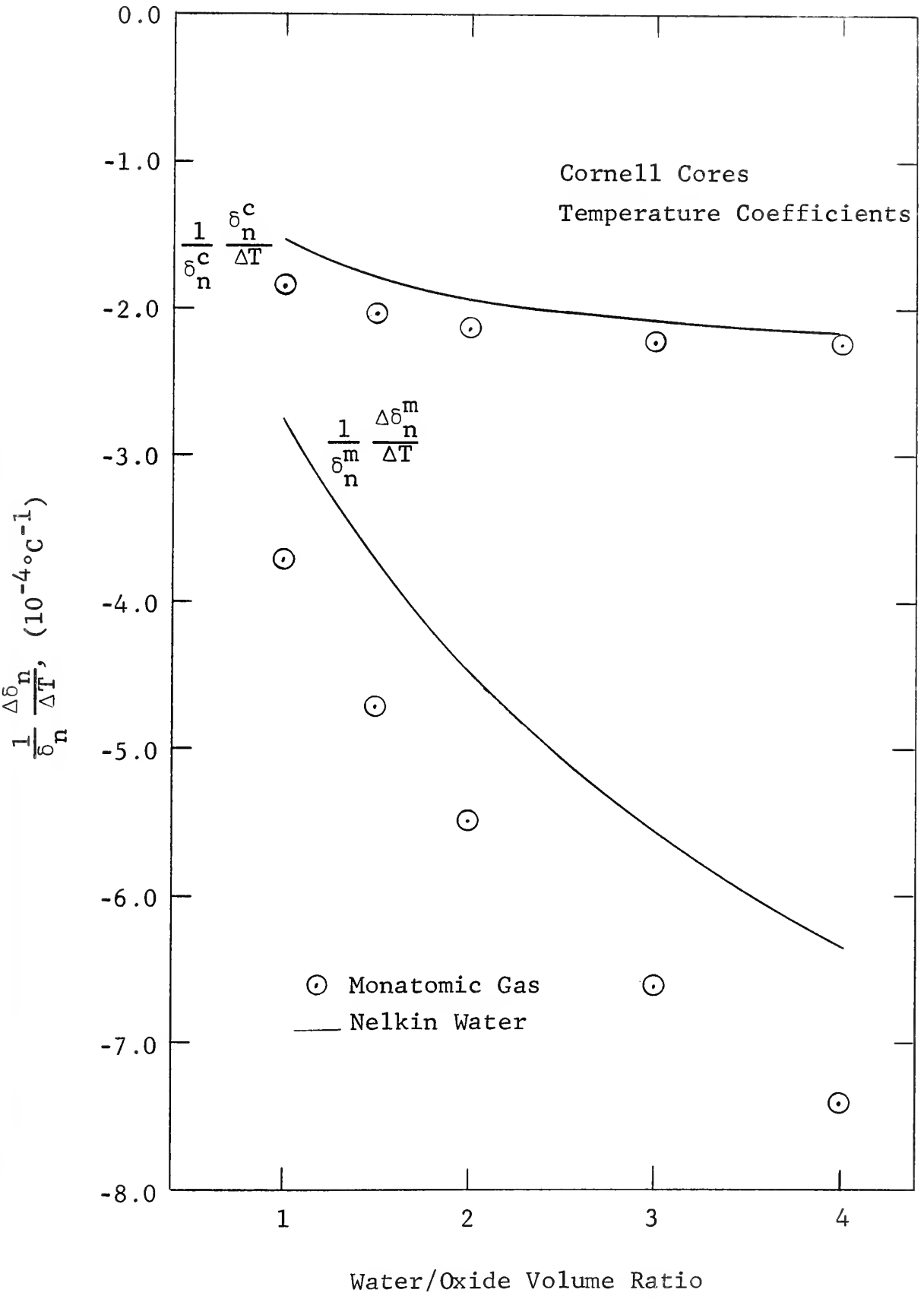

Figure 7.14 Temperature Coefficients of the Neutron Density Disadvantage Factors

The variation of the temperature coefficients of the thermal utilization, f, Eq. (6.15), and ηf, Eq. (6.16) is shown in Fig. 7.15, the difference between the two curves for each scattering model being equal to the temperature coefficient of η. Again the results predicted are more positive with the use of the monatomic gas model because of the greater relative spectral hardening given by that model. It is to be noted that the temperature coefficient of ηf is slightly negative for the 1:1 core.

The final temperature coefficients worthy of note are those of the diffusion coefficient, D, Eq. (6.38), and the thermal diffusion length, L, Eq. (6.39). These are shown in Fig. 7.16; the difference between the monatomic gas and the Nelkin water models being quite evident. Again, the temperature coefficients predicted by the monatomic gas model are higher than those produced by the Nelkin water kernel. The deviation is the most pronounced for the 1:1 core where the monatomic gas results are higher than the Nelkin water kernal results by the following percentages: temperature coefficient of D, 68%; and temperature coefficient of L, 34%.

The differences between the monatomic gas and the Nelkin water kernel results are more pronounced for the D and L temperature coefficient calculations than for any of the other parameters previously discussed. This may be attributed to the fact that these calculations are

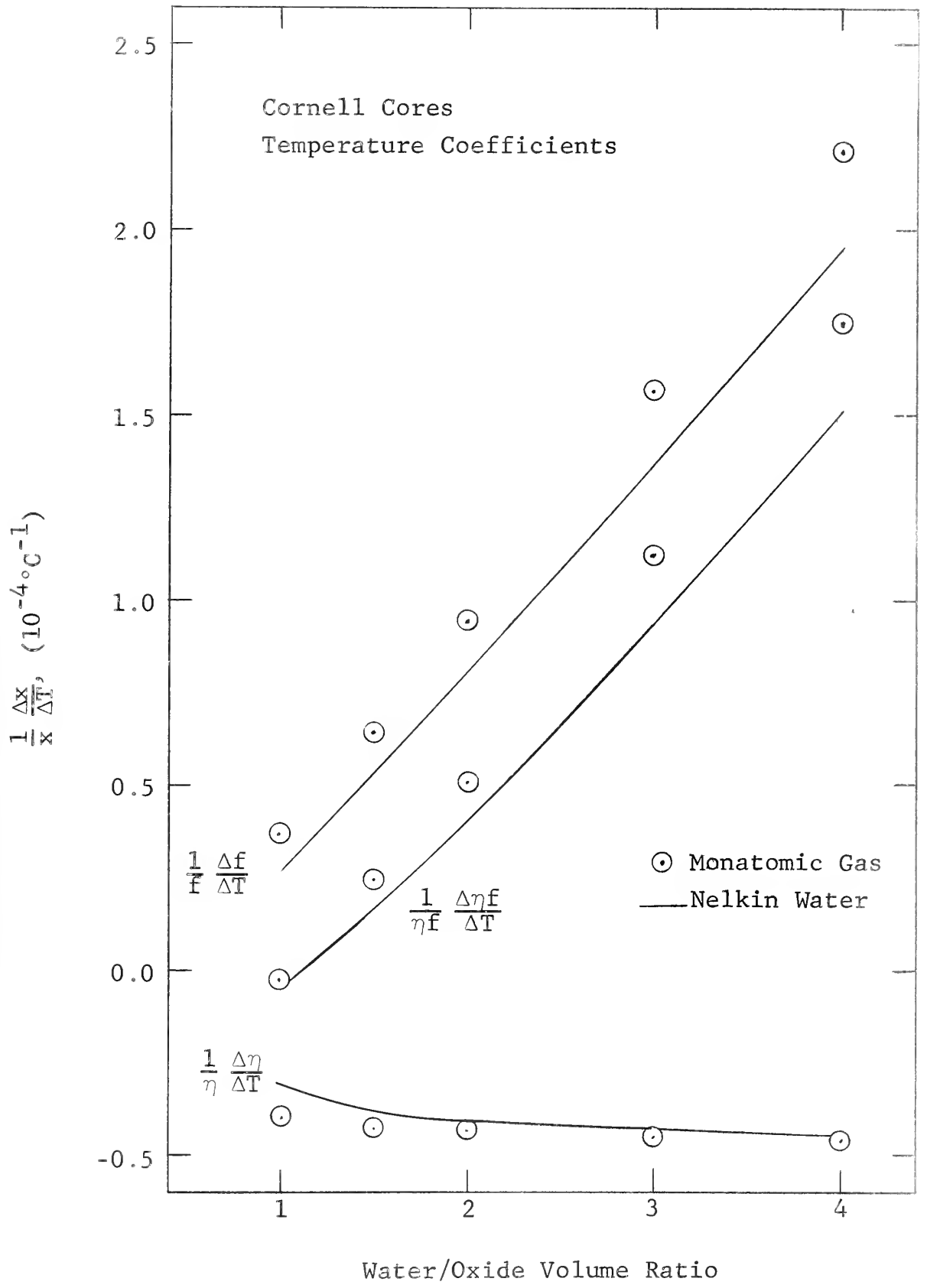

Figure 7.15 Temperature Coefficients of the Integral Properties, f and ηf

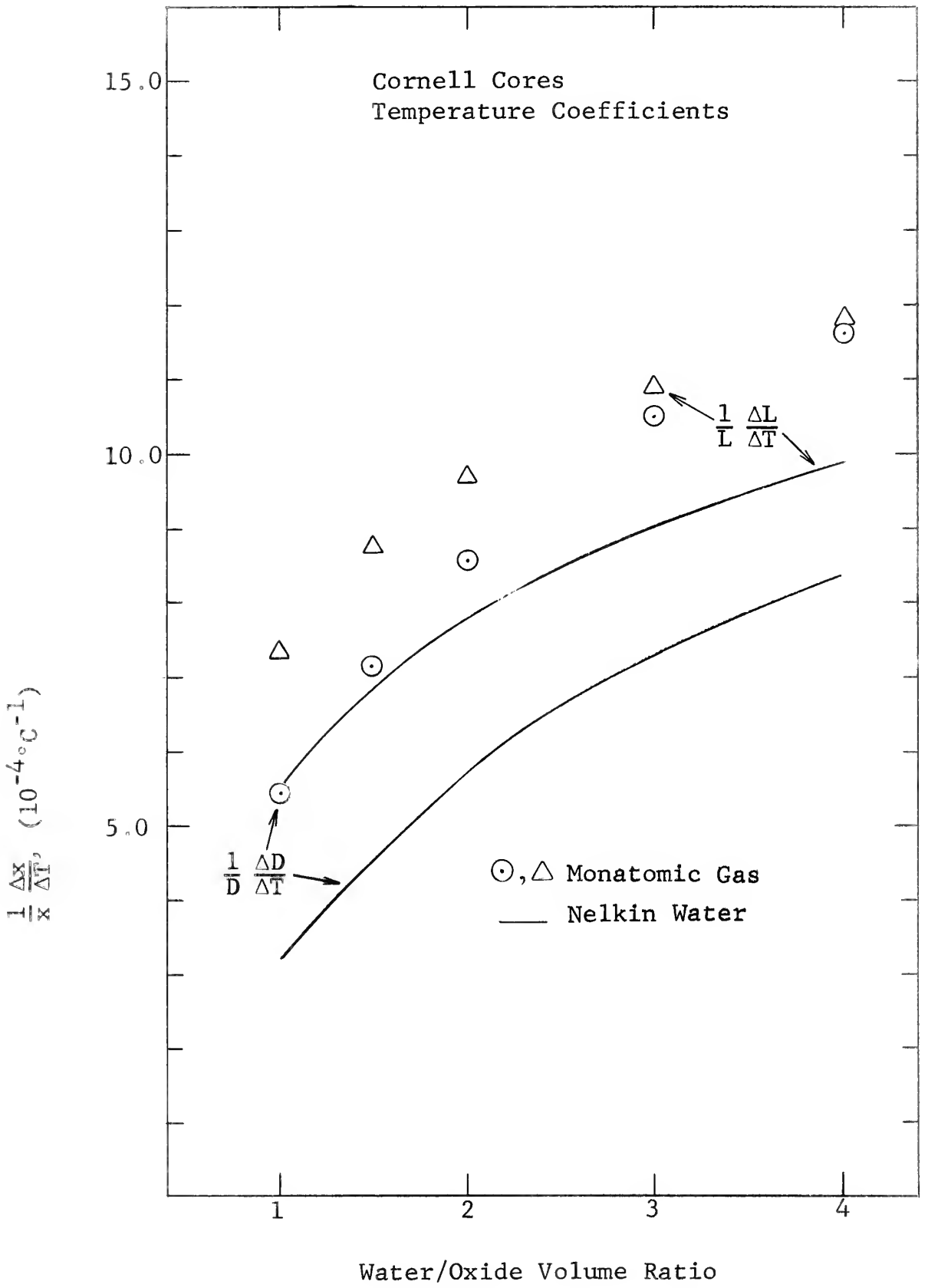

Figure 7.16 Temperature Coefficients of the Thermal Diffusion Coefficient and Length for the Homogenized Cell

doubly sensitive to the degree of spectral hardening predicted by the two models, since the homogenized cell transport cross section, $\Sigma^{h}_{tr}(E)$, Eq. (6.36), used in these calculations is derived by flux and volume weighting the transport cross sections of the various regions in the cell. The reciprocal of this homogenized transport cross section is then averaged over a homogenized spectrum, Eq. (6.37), making the resultant D highly sensitive to the degree of hardness in the spectra utilized in these averaging processes.

An estimate of the accuracy of the temperature coefficient calculations is discussed in Chap. 8, while a tabular listing of all of the temperature coefficients calculated with the Nelkin water kernel is given in Appendix B.

CHAPTER 8

ACCURACY OF THE RESULTS

In an attempt to estimate the accuracy of the results predicted with program COUTH, as presented in Chap. 7 and listed in Appendix B, two lines of approach have been utilized. The first of these involved the calculation by COUTH of several integral properties of the Brookhaven uranium dioxide lattices, a comparison then being made between these results and those calculated by Honeck[77] with the THERMOS transport theory code. The second of these was an investigation of the sensitivity of the Cornell ZPR results to changes in the inputs to the COUTH code such as the densities, cross sections, and dimensions of various regions within the lattice cell.

The Brookhaven cores[78] studied are generically related to the Cornell ZPR cores in that they are light water moderated and utilize low enrichment uranium dioxide fuel. Five water to uranium oxide volume ratios are provided, these being 1.291:1, 1.600:1, 2.050:1, 2.803:1, and 4.000:1. The fuel rods are 0.444 inches in diameter and clad with 0.028 inch thick stainless steel giving the fuel element an outside diameter of 0.500 inches. The uranium dioxide fuel is enriched to 3.0 atom per cent, its density being 9.3 gm/cc.

---

[77] H. C. Honeck, "The Calculation of the Thermal Utilization and Disadvantage Factor in Uranium/Water Lattices," Nucl. Sci. Eng. 18, 49-68 (1964).

The integral thermal parameters compared are the thermal utilization, f, the ratio of the number of fission neutrons produced to the number of thermal neutrons absorbed in the fuel, η, and the moderator neutron density disadvantage factor, δ_n^m. The THERMOS calculation of these parameters utilizes a thirty point energy mesh ranging from 0.00025 to 0.632 eV, while COUTH uses a 41 point energy mesh ranging from 0.001 to 0.645 eV, as discussed in Sec. 7.1. Both programs utilize the same cross section input data and both perform their calculations utilizing a Nelkin water model for the scattering kernel at 20°C.

A comparison between the results predicted by THERMOS, using integral transport theory, and COUTH, using the simplified cell theory, are shown in Fig. 8.1 for the thermal utilization, f. In Fig. 8.1 it is seen that the f's calculated with the two codes compare very well, the maximum deviation in the results occurring in the 4.0:1 core where the THERMOS f is 0.39% higher than the f calculated with COUTH.

The results of the calculation of η by COUTH and THERMOS are seen in Fig. 8.2 to be even closer than those for f. In this case the maximum difference between the results predicted by the two techniques is found in the 1:1 core, the THERMOS result here being 0.19% higher than the COUTH estimate.

78/ H. C. Honeck, see Footnote 77.

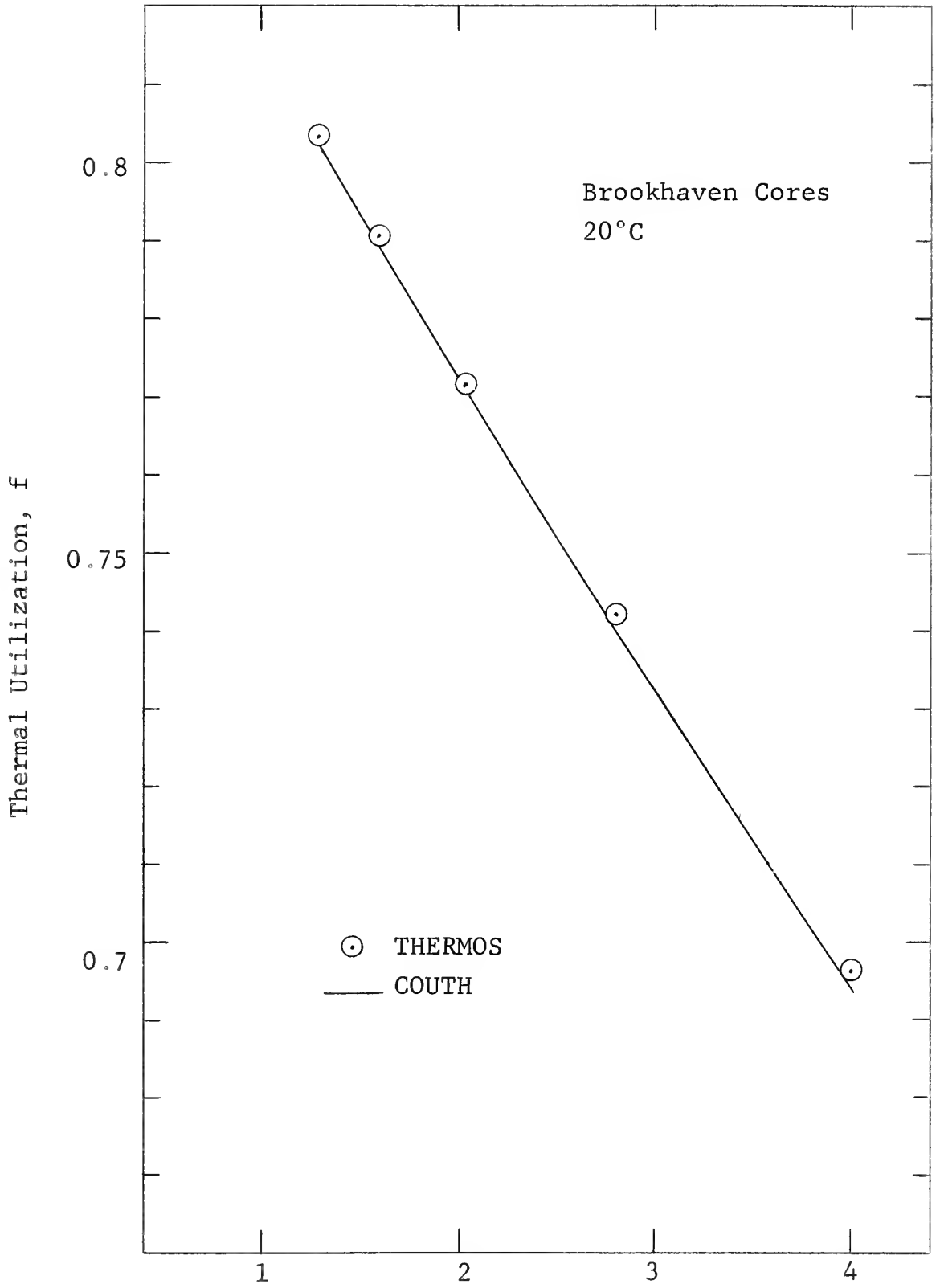

Figure 8.1 Thermal Utilization

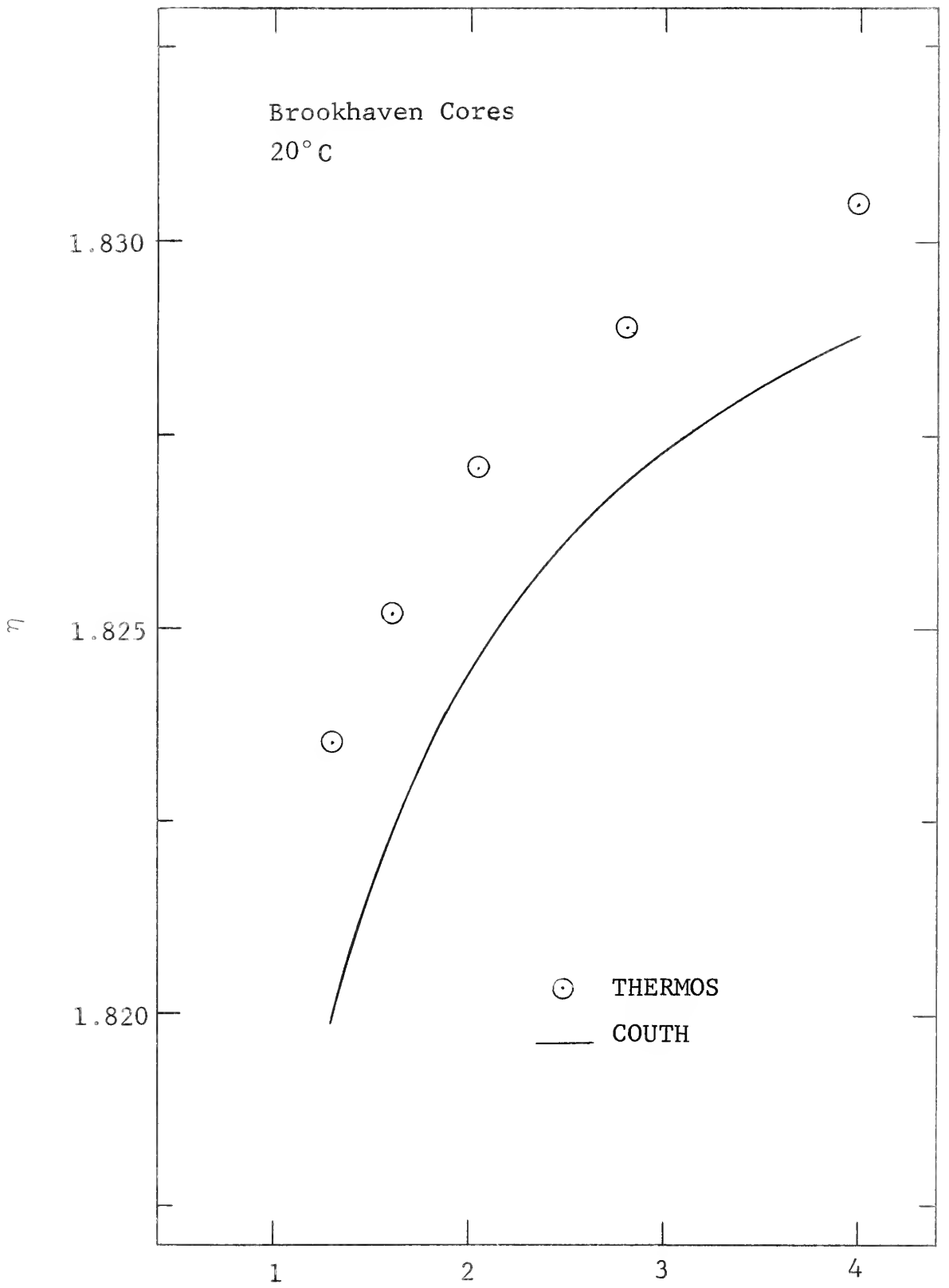

Figure 8.2 Integral Property, η

In the case of the moderator disadvantage factor, δ_n^m, the agreement between the two codes is not quite as close as in the calculations of f and η. Figure 8.3 shows the results derived, indicating that THERMOS predicts higher disadvantage factors for the tighter cores than COUTH, while this role is reversed with the larger water to oxide volume ratios. The THERMOS δ_n^m for the 1.29:1 core is 0.62% higher than the COUTH number, while for the 4.0:1 core the COUTH δ_n^m is 0.97% higher than that given by THERMOS. Honeck[79] assigns a combined uncertainty to the THERMOS calculation of the disadvantage factor of 1.5%, meaning the COUTH calculation of this parameter has an uncertainty less than 2.5%. The deviations between COUTH and THERMOS in this calculation are believed to be attributable to COUTH's use of simple diffusion theory in the moderator region, combined with an overestimation of the fuel element escape probability. Resolution of these differences requires further study and is discussed in Chap. 9.

The parametric study made on the Cornell ZPR for 20°C using the Nelkin water kernel investigated the sensitivity of the calculated parameters to changes in the input data. Changes where made in the fuel density, the fuel enrichment, the fuel rod radius, the cladding radius, the cladding scattering and absorption cross sections, the moderator density, and lattice spacing or pitch. In an attempt to

---

[79] H. C. Honeck, p. 60, see Footnote 77.

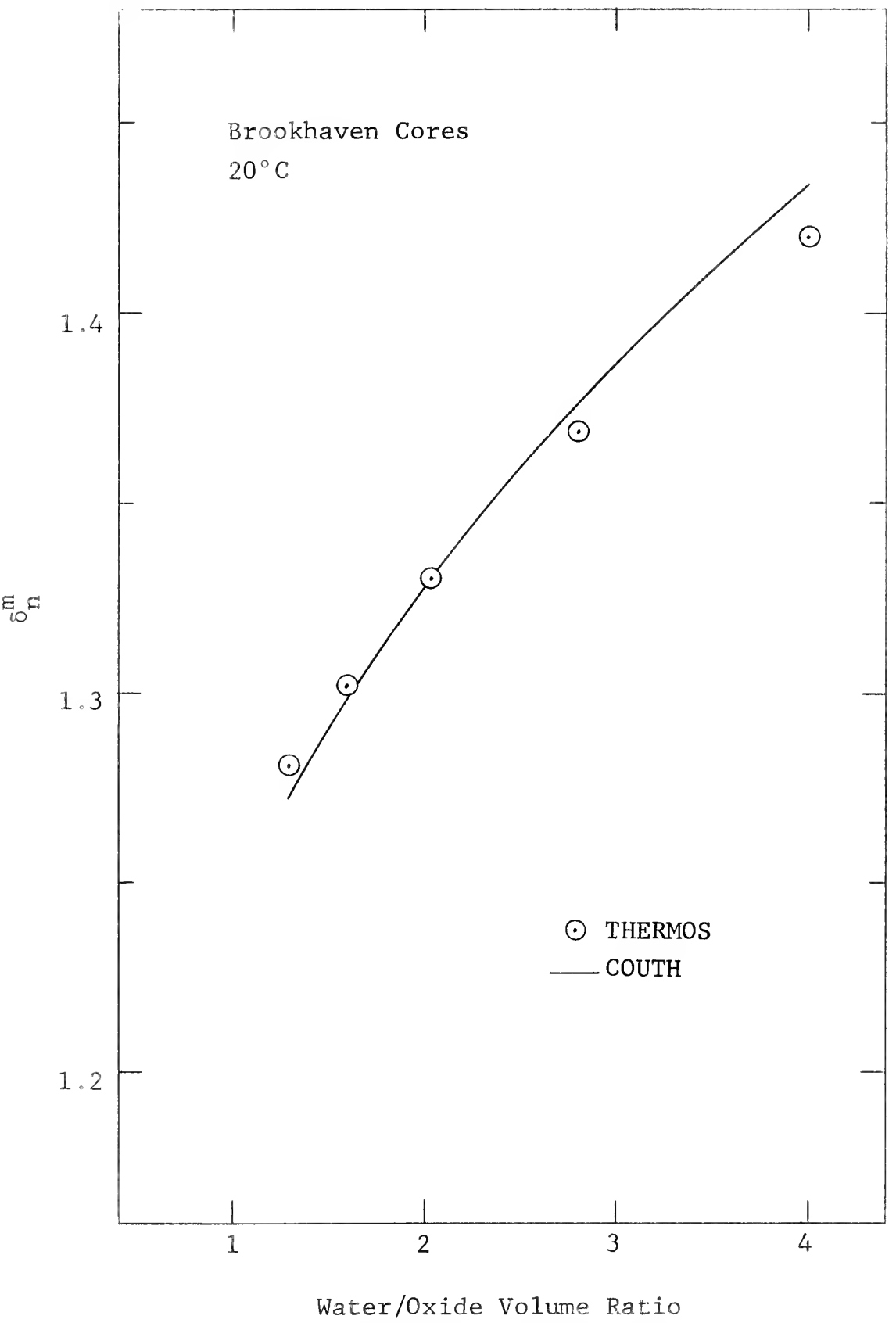

Figure 8.3 Neutron Density Moderator Disadvantage Factor

determine the effect of using various numerical integration schemes, the results utilizing an integration method which fit exponentials, i.e., straight lines on log paper, were also studied. The effect of these changes were noted for several parameters, these being: The thermal utilization, f; the ratio of the number of fission neutrons produced to the number of neutrons absorbed thermally in the cell, ηf; the moderator neutron density disadvantage factor, δ_n^m; the thermal diffusion length, L; the thermal lifetime ℓ_t; the mean neutron velocity for the homogenized cell, $\bar{v}_h$; and the mean total cross section for the homogenized cell, $\bar{\Sigma}_t^h$. The results of the parameter variation study are shown in Table 8.1 where the percentage changes in the input parameters required to produce a positive 0.1% change in the resultant integral properties are listed. The results presented in Table 8.1 represent the most sensitive cases, the error analysis having been carried out on the 1:1 and 4:1 ZPR cores. Thus the percentage changes shown which involve changes in the fuel element parameters come from the 1:1 core analysis, since a relatively large portion of the unit cell is composed of fuel for this core. The 1:1 core is also most sensitive to changes in lattice pitch. On the other hand results from the 4:1 core are given for the sensitivity of parameters to changes in the water density, water playing a relatively more important role in this core.

TABLE 8.1

PERCENTAGE CHANGES IN INPUT PARAMETERS REQUIRED TO CHANGE INTEGRAL PROPERTIES BY +0.1 PERCENT

INPUT PARAMETERS	INTEGRAL PROPERTIES						
	f	ηf	δ_n^m	L	ℓ_t	$\bar{v}_h$	$\bar{\Sigma}_t^h$
Fuel Density	+1.64	+1.92	+0.57	-0.28	-0.13	+0.47	+1.16
Fuel Enrichment	+1.89	+0.47	+0.74	-0.48	-0.15	+0.55	-5.56
Fuel Radius	+0.69	+0.81	-1.43	+0.85	-0.10	+0.19	-0.13
Cladding Radius	+1.25	+1.85	+0.45	+0.07	-1.47	+0.14	-0.04
Cladding Scattering Cross Section	-500.	-1000.	+58.8	-7.46	-100.	-333.	+17.85
Cladding Absorption Cross Section	-12.5	-12.3	+166.	-34.48	-14.49	+50.	-333.
Lattice Pitch	-0.10	-0.34	+0.23	-0.18	+0.05	-0.08	+0.04
Water Density	-1.35	-1.56	+1.14	-0.16	-1.45	-0.39	+0.10

The use of the numerical integration scheme involving the fitting of exponentials rather than straight lines as in the trapezoidal integration rule produces the following maximum percentage changes in the integral parameters: f, 0.004%; ηf, .009%; δ_n^m, 0.12%; L, 1.1%; ℓ_t, .069%; $\bar{v}_h$, 0.12%; and $\bar{\Sigma}_t^h$, 2.5%. The large percentage change in $\bar{\Sigma}_t^h$ may attribute to the fact that the numerical integration scheme using exponentials predicts scattering cross sections for water by integrating the scattering kernel which are as much as 3.0% higher than the experimentally measured values.

Table 8.1 shows that the numerical results are essentially insensitive to the cladding cross section data, while they are most sensitive to the lattice pitch. The actual tolerances given[80] for the Cornell ZPR lattice pitches are less than 0.10% so that the output parameters will vary no more than about 0.2% because of variations in this dimension. The fuel element parameter, density, enrichment, fuel rod radius, and fuel element radius are known to within 0.5% and reference to Table 8.1 indicates that in general variations of the thermal integral properties will be less than 0.5%.

In light of the results of comparing the predictions of the THERMOS and COUTH codes and the results of the input parametric studies, the following probable uncertainties may be assigned to the 20°C calculations performed

by COUTH utilizing the Nelkin water kernel as a scattering model.

1. f, η, and ηf; 0.5%.
2. Disadvantage factors for the moderator and cladding, 2.0%.
3. Thermal lifetimes; 3.0%.
4. Mean velocities; 3.0%.
5. Averaged cross sections, including the calculation of D and L; 5%.

With regard to the room temperature calculations made utilizing the monatomic gas model, the deviations from the Nelkin water kernel results were quoted in Chap. 7. Using these percentages, one can then assign the following probable uncertainties to the 20°C monatomic gas calculations.

1. f, η, and ηf; 0.8%.
2. Moderator and cladding disadvantage factors; 4.0%.
3. Thermal lifetimes; 4.0%.
4. Mean velocities; 8.0%.
5. Averaged cross sections, including the diffusion coefficient and length; 10.0%.

On the basis of these two sets of uncertainties, one must reconcile the accuracy obtained with the computer time required for a given calculation. A monatomic gas scattering kernel, in the form of a 45 by 45 matrix takes only two and one half minutes of computer calculation, while the Nelkin

water scattering kernel takes on the order of fifteen minutes. Thus if one is undertaking a detailed temperature study wherein multiple scattering kernels must be calculated, use of the monatomic gas model is advocated for one primarily interested in f and ηf. However, if emphasis is to be placed on the other integral parameters, and in particular the averaged cross sections, then the more complicated Nelkin model should be used.

The assignment of uncertainties to the temperature coefficients presented in Chap. 7 presents a slightly different problem. In this case one must estimate the uncertainties in a calculation at a given temperature and then estimate the uncertainty in the degree of spectral hardening predicted by a certain model. The fact that the THERMOS and COUTH results at room temperature are in agreement for all values of water to fuel volume ratios indicates that COUTH can adequately handle spectral hardening effects if the scattering kernel model can predict the appropriate temperature changes in the energy transfer process. We therefore, apriori, assign uncertainties to the temperature coefficient calculations as being twice those stated above for the room temperature calculations with both the Nelkin water model and the monatomic gas kernel.

80/ S. S. Berg, "Initial Experiments on the Cornell University Zero Power Reactor Cores," Cornell University Thesis (1964).

CHAPTER 9

SUMMARY AND CONCLUSIONS

A simplified polyenergetic cell theory has been formulated for use in the determination of the spatially averaged energy dependent thermal fluxes in the various regions of a lattice cell. The derived spectra are then utilized in the calculations of the thermal integral parameters and average cross sections required for reactor computations.

The cell theory, as formulated, postulates an infinite moderator region with the absorption cross section of this region appropriately modified to account for the neutron leakage into and absorption by the fuel element in the actual lattice. The modifications to the moderator absorption cross section, have been formulated both in general terms an in terms of moderator and fuel element escape probabilities, the latter approach offering physical transparency and ease of calculation.

Analytic expressions for the escape probabilities have been presented, integral transport theory having been applied in the fuel element region, while diffusion theory was utilized in the moderator region. Using these analytic expressions the theory was applied to actual lattices in the form of the Cornell University Zero Power Reactor cores to determine room temperature parameters and their temperature coefficients.

In an attempt to estimate the accuracy of these results, the method was also applied to the Brookhaven uranium dioxide cores and the results then compared with those predicted by multigroup transport methods. The remarkably good comparison between these two sets of calculations in conjunction with a parametric study which yielded a relative low sensitivity of the calculated parameters to changes in the input data has led to the assignment of rather small uncertainties in the results calculated with the simplified cell theory.

Although the estimated uncertainties tend to instill confidence in the calculational results, one must insure that these events are not just fortuitous and that the simplified cell theory is in fact predicting behaviors which closely approximate the physical processes taking place.

In this regard, there are three areas in which further work is necessary in the simplified cell theory as presently formulated. The first of these concerns the validity of the assumptions made in the calculations of the moderator escape probabilities, or alternatively, in the calculation of gradient of the moderator flux at the fuel element surface. In these calculations it was assumed that the shape of the flux in the moderator was given by monoenergetic diffusion theory applied at each energy point. Although multigroup transport calculations have given some

support to this assumption, its accuracy can certainly be questioned particularly in the tighter cores where fuel element spacing becomes comparable with a mean free path. Thus there is a need to accurately determine the flux gradient, or more precisely, the net current as a function of energy at the fuel element moderator interface. Any study such as this should include the effects of a non uniform spatial source of slowing down neutrons. The use of multigroup transport theory specificially oriented toward this problem is suggested for this future study.

The second area of concern involves the calculation of the fuel rod escape probability. In the expression utilized in these calculations an isotropic flux was assumed incident upon the fuel rod. This in turn leads to escape probabilities which are too large; the flux in an actual lattice is more peaked toward the rod. The use of smaller escape probabilities for the fuel rod would lead to larger values of f and ηf, along with larger values for the calculated disadvantage factors. Thus there is need for at least a parametric study utilizing all of the analytic approximations for the fuel rod escape probability presented. One could then turn his attention to variations caused with changes in angular distribution of the neutrons incident on the fuel element.

The final area where further study is needed concerns the calculation of temperature coefficients. The immediate need is to compare temperature coefficients calculated with integral transport theory with those predicted by the simplified cell theory as was done with the room temperature case. However, if both calculations utilize the same scattering model, it is believed the comparison of the temperature coefficient computations will be comparable with those for room temperature, since the simplified cell theory has demonstrated its ability to handle spectral hardening in five different cores at 20°C. The accuracy of the temperature coefficient results thus reduces to a question of how well the scattering model predicts spectral hardening as a function of temperature. This question is perhaps best answered by the comparison of pure moderator spectra predicted by the model at various temperatures with those measured experimentally.

APPENDIX A

LATTICE PARAMETERS FOR THE CORNELL UNIVERSITY ZERO POWER REACTOR

This section details the input parameters which were utilized by program COUTH in the calculations described in Chap. 7 for the Cornell University Zero Power Reactor cores. Appendix D deals with the Fortran FORMATS used in COUTH for reading data into the program.

Table A.1 lists the fuel element parameters for the Cornell ZPR while Table A.2 gives the dimensional parameters of the five hexagonal lattices of the ZPR. Material concentrations and cross sections are given in Table A.3. The absorption cross sections, σ_a, listed are evaluated at E_o = .0253 eV while the scattering cross sections given are the free atom values, σ_f. The number of neutrons produced per thermal fission for U^{235}, ν, is 2.43 while the value of the U^{235} fission cross section at E_o is 580.9 barns.[81] Appendix B gives a complete listing as a function of energy for the scattering and transport cross sections of water, the absorption, fission, and scattering cross sections of U^{235}, and the scattering cross sections of U^{238} and oxygen.

---

[81] H. C. Honeck, "The Calculation of Thermal Utilization and Disadvantage Factor in Uranium/Water Lattices," Nucl. Sci. Eng. 18, 66 (1964).

TABLE A.1

CORNELL UNIVERSITY ZERO POWER REACTOR FUEL ELEMENT PARAMETERS [a]

Fuel Material	Uranium Dioxide
Fuel Rod Diameter, in:	0.600±0.003
Fuel Density, gm/cc:	10.381±0.52%
Fuel Enrichment, Weight Percent U^{235}:	2.070±0.10
Fuel Enrichment, Atom Percent U^{235}:	2.096±0.90
Oxygen to Uranium Number Ratio:	2.01:1
Fuel Molecular Weight:	270.26(physical)
Cladding Material:	6061-76 aluminum
Cladding Density, gm/cc:	2.70
Cladding Inner Diameter, in:	0.610±0.002
Cladding Thickness, in:	0.028±0.003
Fuel Element Diameter, in:	0.666±.006

[a] S. S. Berg, "Initial Experiments on the Cornell University Zero Power Reactor Cores," Cornell University Thesis (1964).

TABLE A.2

CORNELL UNIVERSITY ZERO POWER REACTOR LATTICE PARAMETERS

	Nominal Water/Oxide Volume Ratio				
	1:1	1.5:1	2:1	3:1	4:1
Lattice Pitch, in.[a/]	0.8560	0.9470	1.0300	1.1770	1.3090
Equivalent Cell Radius, cm.	1.1416	1.2629	1.3736	1.5696	1.7457
Fuel Element Radius, cm.	0.8458	0.8458	0.8458	0.8458	0.8458
Fuel Rod Radius, cm.	0.7620	0.7620	0.7620	0.7620	0.7620
Water Area, cm^2.	1.8465	2.7632	3.6800	5.4927	7.3261
Cladding Area, cm^2.	0.3621	0.3621	0.3621	0.3621	0.3621
Fuel Rod Area, cm^2.	1.8242	1.8242	1.8242	1.8242	1.8242
Actual Water/Oxide Volume Ratio.	1.0122:1	1.5148:1	2.0174:1	3.0111:1	4.0162:1

[a/] D. D. Clark, "The Cornell University Nuclear Reactor Laboratory," CURL-1, Cornell University (1961).

TABLE A.3

CORNELL UNIVERSITY ZERO POWER REACTOR MATERIAL CONCENTRATIONS AND CROSS SECTIONS

Material	Concentration (atoms/barn-cm)	$\sigma_a(E_o)$[a] (barns)	σ_f[a] (barns)
U^{235}	4.8498×10^{-4}	679.0	10.0
U^{238}	2.2654×10^{-2}	2.71	8.3
Oxygen in UO_2	4.6510×10^{-2}	0.0	3.76
Aluminum	6.0205×10^{-2}	0.230	1.40
Hydrogen in H_2O		0.328	20.4
20°C	6.6746×10^{-2}		
40°C	6.6346×10^{-2}		
Oxygen in H_2O		0.0	3.76
20°C	3.3373×10^{-2}		
40°C	3.3173×10^{-2}		

[a] H. C. Honeck, "The Calculation of the Thermal Utilization and Disadvantage Factor in Uranium/Water Lattices," Nucl. Sci. Eng. 18, 66 (1964).

APPENDIX B

NUMERICAL RESULTS FOR THE CORNELL UNIVERSITY ZERO POWER REACTOR

Chapter 7 discussed some of the results of the calculations made on the Cornell University Zero Power Reactor using the simplified cell theory as incorporated in COUTH. This section presents all of the results in a tabular form derived from the calculations utilizing the Nelkin water model for the scattering kernel.

Table B.1 lists the energy, velocity and lethargy mesh used in the calculations by COUTH. The derivation of this mesh is discussed in Sec. 7.1, and all of the calculations are carried out using the lethargy mesh.

Table B.2 gives the scattering kernel in matrix form as derived from the Nelkin water model, Eq. (5.15), for a physical moderator temperature of 20°C. The scattering matrix is expressed in barns/unit lethargy and it is related to the scattering matrix in barns/eV by,

$$\sigma(u_j \longrightarrow u_i) = E_i \sigma(E_j \longrightarrow E_i) \ . \qquad \text{(B.1)}$$

The subscripted indices i and j correspond to the lethargy and energy points listed in Table B.1. The diagonal terms of the scattering matrix listed in Table B.2 are those calculated with Eq. (5.22) and they are not modified in accordance with Eq. (5.26).

TABLE B.1

ENERGY, VELOCITY, AND LETHARGY MESH UTILIZED BY COUTH

I	ENERGY	DELTA E	VELOCITY	DELTA V	LETHARGY	DELTA U
1	1.609E 000	3.782E-001	17547.0	2200.0	.0000	.2679
2	1.231E 000	2.644E-001	15347.0	1747.5	.2679	.2418
3	9.667E-001	1.873E-001	13599.5	1388.1	.5097	.2153
4	7.794E-001	1.344E-001	12211.4	1102.6	.7250	.1893
5	6.450E-001	9.770E-002	11108.7	875.8	.9143	.1642
6	5.473E-001	7.189E-002	10232.9	695.7	1.0785	.1408
7	4.754E-001	5.350E-002	9537.2	552.6	1.2194	.1194
8	4.219E-001	4.022E-002	8984.6	439.0	1.3387	.1002
9	3.817E-001	3.051E-002	8545.6	348.7	1.4389	.0833
10	3.512E-001	2.333E-002	8197.0	277.0	1.5222	.0687
11	3.279E-001	1.796E-002	7920.0	220.0	1.5910	.0563
12	3.099E-001	1.746E-002	7700.0	220.0	1.6473	.0580
13	2.924E-001	1.695E-002	7480.0	220.0	1.7053	.0597
14	2.755E-001	1.644E-002	7260.0	220.0	1.7650	.0615
15	2.590E-001	1.594E-002	7040.0	220.0	1.8265	.0635
16	2.431E-001	1.543E-002	6820.0	220.0	1.8900	.0656
17	2.277E-001	1.493E-002	6600.0	220.0	1.9556	.0678
18	2.128E-001	1.442E-002	6380.0	220.0	2.0234	.0702
19	1.983E-001	1.391E-002	6160.0	220.0	2.0936	.0727
20	1.844E-001	1.341E-002	5940.0	220.0	2.1663	.0755
21	1.710E-001	1.290E-002	5720.0	220.0	2.2418	.0784
22	1.581E-001	1.240E-002	5500.0	220.0	2.3203	.0816
23	1.457E-001	1.189E-002	5280.0	220.0	2.4019	.0851
24	1.338E-001	1.138E-002	5060.0	220.0	2.4870	.0889
25	1.224E-001	1.088E-002	4840.0	220.0	2.5759	.0930
26	1.116E-001	1.037E-002	4620.0	220.0	2.6690	.0976
27	1.012E-001	9.866E-003	4400.0	220.0	2.7666	.1026
28	9.132E-002	9.360E-003	4180.0	220.0	2.8691	.1081
29	8.196E-002	8.854E-003	3960.0	220.0	2.9773	.1143
30	7.311E-002	8.348E-003	3740.0	220.0	3.0916	.1212
31	6.476E-002	7.842E-003	3520.0	220.0	3.2128	.1291
32	5.692E-002	7.336E-003	3300.0	220.0	3.3419	.1380
33	4.958E-002	6.830E-003	3080.0	220.0	3.4799	.1482
34	4.275E-002	6.324E-003	2860.0	220.0	3.6281	.1601
35	3.643E-002	5.818E-003	2640.0	220.0	3.7882	.1740
36	3.061E-002	5.313E-003	2420.0	220.0	3.9622	.1906
37	2.530E-002	4.807E-003	2200.0	220.0	4.1529	.2107
38	2.049E-002	4.301E-003	1980.0	220.0	4.3636	.2356
39	1.619E-002	3.795E-003	1760.0	220.0	4.5991	.2671
40	1.240E-002	3.289E-003	1540.0	220.0	4.8662	.3083
41	9.107E-003	2.783E-003	1320.0	220.0	5.1745	.3646
42	6.324E-003	2.277E-003	1100.0	220.0	5.5391	.4463
43	4.048E-003	1.771E-003	880.0	220.0	5.9854	.5754
44	2.277E-003	1.265E-003	660.0	220.0	6.5608	.8109
45	1.012E-003	.000E 000	440.0	.0	7.3717	.0000

TABLE B.2

NELKIN WATER MODEL FOR THE SCATTERING MATRIX AT 20°C.

SCATTERING KERNEL, SIGMA(U(J) TO U(I))/UNIT LETHARGY, KT = .0253, J = 1 TO 10

I \ J =	1	2	3	4	5	6	7	8	9	10
1	8.644E 001	1.82[illegible]E-005	6.145E-010	4.580E-013	2.682E-015	6.589E-017	4.402E-018	5.963E-019	1.339E-019	4.340E-020
2	3.399E 001	8.636E 001	1.817E-003	1.038E-006	6.543E-009	1.626E-010	1.085E-011	1.467E-012	3.287E-013	1.063E-013
3	2.471E 001	3.929E 001	8.613E 001	4.016E-002	1.839E-004	4.115E-006	2.802E-007	3.913E-008	8.936E-009	2.920E-009
4	1.983E 001	2.418E 001	4.324E 001	8.580E 001	3.457E-001	6.742E-003	4.034E-004	5.159E-005	1.126E-005	3.620E-006
5	1.625E 001	2.132E 001	2.771E 001	4.837E 001	8.540E 001	1.573E 000	8.283E-002	1.009E-002	2.153E-003	6.758E-004
6	1.374E 001	1.823E 001	2.134E 001	3.247E 001	5.414E 001	8.498E 001	4.541E 000	5.053E-001	9.984E-002	3.038E-002
7	1.192E 001	1.580E 001	1.887E 001	2.523E 001	3.702E 001	5.897E 001	8.455E 001	9.590E 000	1.868E 000	5.384E-001
8	1.057E 001	1.398E 001	1.725E 001	2.112E 001	2.952E 001	4.295E 001	6.277E 001	8.416E 001	1.645E 001	4.809E 000
9	9.545E 000	1.260E 001	1.584E 001	1.854E 001	2.533E 001	3.413E 001	4.917E 001	6.616E 001	8.388E 001	2.456E 001
10	8.762E 000	1.154E 001	1.466E 001	1.688E 001	2.252E 001	2.941E 001	4.014E 001	5.477E 001	6.955E 001	8.349E 001
11	8.160E 000	1.074E 001	1.370E 001	1.574E 001	2.053E 001	2.656E 001	3.459E 001	4.649E 001	5.937E 001	7.274E 001
12	7.694E 000	1.012E 001	1.295E 001	1.492E 001	1.906E 001	2.460E 001	3.109E 001	4.086E 001	5.239E 001	6.320E 001
13	7.239E 000	9.510E 000	1.221E 001	1.414E 001	1.768E 001	2.280E 001	2.827E 001	3.612E 001	4.593E 001	5.596E 001
14	6.795E 000	8.922E 000	1.147E 001	1.339E 001	1.640E 001	2.112E 001	2.594E 001	3.219E 001	4.033E 001	4.913E 001
15	6.361E 000	8.350E 000	1.076E 001	1.265E 001	1.522E 001	1.953E 001	2.391E 001	2.895E 001	3.561E 001	4.304E 001
16	5.939E 000	7.793E 000	1.005E 001	1.191E 001	1.411E 001	1.802E 001	2.207E 001	2.629E 001	3.165E 001	3.783E 001
17	5.527E 000	7.252E 000	9.364E 000	1.117E 001	1.309E 001	1.659E 001	2.035E 001	2.402E 001	2.835E 001	3.343E 001
18	5.127E 000	6.727E 000	8.693E 000	1.043E 001	1.212E 001	1.523E 001	1.871E 001	2.202E 001	2.558E 001	2.972E 001
19	4.738E 000	6.218E 000	8.040E 000	9.696E 000	1.122E 001	1.395E 001	1.716E 001	2.018E 001	2.322E 001	2.659E 001
20	4.361E 000	5.724E 000	7.405E 000	8.969E 000	1.035E 001	1.274E 001	1.567E 001	1.846E 001	2.112E 001	2.392E 001
21	3.997E 000	5.246E 000	6.789E 000	8.253E 000	9.514E 000	1.160E 001	1.425E 001	1.682E 001	1.921E 001	2.159E 001
22	3.645E 000	4.785E 000	6.194E 000	7.551E 000	8.709E 000	1.052E 001	1.290E 001	1.525E 001	1.742E 001	1.949E 001
23	3.307E 000	4.342E 000	5.619E 000	6.866E 000	7.929E 000	9.496E 000	1.161E 001	1.376E 001	1.573E 001	1.756E 001
24	2.983E 000	3.917E 000	5.068E 000	6.203E 000	7.175E 000	8.532E 000	1.040E 001	1.233E 001	1.412E 001	1.576E 001
25	2.673E 000	3.511E 000	4.541E 000	5.564E 000	6.446E 000	7.621E 000	9.251E 000	1.098E 001	1.259E 001	1.406E 001
26	2.379E 000	3.125E 000	4.039E 000	4.952E 000	5.746E 000	6.762E 000	8.173E 000	9.702E 000	1.114E 001	1.245E 001
27	2.102E 000	2.760E 000	3.565E 000	4.370E 000	5.078E 000	5.952E 000	7.164E 000	8.501E 000	9.778E 000	1.094E 001
28	1.841E 000	2.418E 000	3.119E 000	3.822E 000	4.444E 000	5.193E 000	6.224E 000	7.381E 000	8.498E 000	9.515E 000
29	1.598E 000	2.098E 000	2.703E 000	3.310E 000	3.849E 000	4.486E 000	5.355E 000	6.343E 000	7.308E 000	8.191E 000
30	1.373E 000	1.802E 000	2.319E 000	2.835E 000	3.296E 000	3.832E 000	4.557E 000	5.389E 000	6.212E 000	6.969E 000
31	1.166E 000	1.530E 000	1.966E 000	2.399E 000	2.787E 000	3.232E 000	3.830E 000	4.522E 000	5.213E 000	5.853E 000
32	9.774E-001	1.283E 000	1.645E 000	2.003E 000	2.324E 000	2.689E 000	3.176E 000	3.742E 000	4.313E 000	4.844E 000
33	8.078E-001	1.060E 000	1.357E 000	1.648E 000	1.908E 000	2.203E 000	2.592E 000	3.048E 000	3.512E 000	3.946E 000
34	6.567E-001	8.613E-001	1.101E 000	1.333E 000	1.540E 000	1.773E 000	2.080E 000	2.440E 000	2.809E 000	3.156E 000
35	5.238E-001	6.869E-001	8.766E-001	1.058E 000	1.218E 000	1.399E 000	1.636E 000	1.915E 000	2.202E 000	2.473E 000
36	4.087E-001	5.359E-001	6.827E-001	9.209E-001	9.428E-001	1.080E 000	1.258E 000	1.469E 000	1.687E 000	1.894E 000
37	3.107E-001	4.073E-001	5.180E-001	6.208E-001	7.106E-001	8.113E-001	9.424E-001	1.097E 000	1.258E 000	1.412E 000
38	2.289E-001	3.001E-001	3.810E-001	4.551E-001	5.190E-001	5.907E-001	6.840E-001	7.942E-001	9.091E-001	1.019E 000
39	1.623E-001	2.127E-001	2.697E-001	3.211E-001	3.649E-001	4.140E-001	4.779E-001	5.534E-001	6.323E-001	7.081E-001
40	1.096E-001	1.437E-001	1.820E-001	2.159E-001	2.446E-001	2.766E-001	3.183E-001	3.676E-001	4.192E-001	4.690E-001
41	6.954E-002	9.115E-002	1.153E-001	1.364E-001	1.540E-001	1.736E-001	1.992E-001	2.295E-001	2.613E-001	2.919E-001
42	4.049E-002	5.307E-002	6.705E-002	7.912E-002	8.906E-002	1.002E-001	1.146E-001	1.317E-001	1.497E-001	1.671E-001
43	2.083E-002	2.731E-002	3.447E-002	4.059E-002	4.557E-002	5.113E-002	5.838E-002	6.696E-002	7.597E-002	8.469E-002
44	8.822E-003	1.156E-002	1.459E-002	1.715E-002	1.921E-002	2.152E-002	2.452E-002	2.808E-002	3.181E-002	3.543E-002
45	2.621E-003	3.436E-003	4.333E-003	5.085E-003	5.689E-003	6.362E-003	7.240E-003	8.280E-003	9.373E-003	1.043E-002

Table B.2 (continued)

SCATTERING KERNEL, SIGMA(U(J) TO U(I))/UNIT LETHARGY, KT = .0253, J = 11 TO 20

I	J = 11	12	13	14	15	16	17	18	19	20
1	1.842E-020	9.546E-021	5.054E-021	2.733E-021	1.509E-021	8.514E-022	4.905E-022	2.886E-022	1.734E-022	1.064E-022
2	4.507E-014	2.335E-014	1.235E-014	6.673E-015	3.684E-015	2.077E-015	1.197E-015	7.041E-016	4.232E-016	2.598E-016
3	1.243E-009	6.461E-010	3.428E-010	1.855E-010	1.027E-010	5.794E-011	3.342E-011	1.968E-011	1.184E-011	7.268E-012
4	1.538E-006	8.016E-007	4.275E-007	2.332E-007	1.300E-007	7.393E-008	4.292E-008	2.542E-008	1.537E-008	9.479E-009
5	2.807E-004	1.433E-004	7.479E-005	3.997E-005	2.188E-005	1.226E-005	7.038E-006	4.134E-006	2.488E-006	1.531E-006
6	1.250E-002	6.365E-003	3.320E-003	1.771E-003	9.663E-004	5.387E-004	3.070E-004	1.788E-004	1.065E-004	6.484E-005
7	2.114E-001	1.045E-001	5.345E-002	2.826E-002	1.536E-002	8.568E-003	4.891E-003	2.852E-003	1.701E-003	1.036E-003
8	1.86nE 000	8.986E-001	4.470E-001	2.295E-001	1.218E-001	6.681E-002	3.779E-002	2.197E-002	1.309E-002	7.987E-003
9	9.551E 000	4.634E 000	2.286E 000	1.156E 000	6.023E-001	3.235E-001	1.793E-001	1.026E-001	6.059E-002	3.675E-002
10	3.314E 001	1.583E 001	7.888E 000	3.990E 000	2.062E 000	1.095E 000	5.990E-001	3.378E-001	1.965E-001	1.179E-001
11	1.882E 002	3.816E 001	1.305E 001	1.007E 001	6.572E 000	2.681E 000	1.268E 000	8.241E-001	5.297E-001	2.945E-001
12	6.941E 001	1.880E 002	3.969E 001	1.354E 001	1.016E 001	7.310E 000	3.133E 000	1.451E 000	9.184E-001	6.291E-001
13	4.217E 001	7.054E 001	1.878E 002	4.131E 001	1.410E 001	1.026E 001	8.057E 000	3.671E 000	1.684E 000	1.026E 000
14	5.651E 001	4.176E 001	7.171E 001	1.875E 002	4.302E 001	1.473E 001	1.036E 001	8.774E 000	4.305E 000	1.983E 000
15	6.251E 001	5.314E 001	4.148E 001	7.292E 001	1.873E 002	4.481E 001	1.544E 001	1.048E 001	9.407E 000	5.045E 000
16	4.221E 001	6.326E 001	4.995E 001	4.132E 001	7.417E 001	1.870E 002	4.670E 001	1.623E 001	1.063E 001	9.914E 000
17	3.225E 001	4.380E 001	6.339E 001	4.695E 001	4.128E 001	7.545E 001	1.867E 002	4.869E 001	1.713E 001	1.081E 001
18	3.304E 001	3.197E 001	4.553E 001	6.269E 001	4.417E 001	4.134E 001	7.676E 001	1.864E 002	5.078E 001	1.812E 001
19	3.266E 001	3.113E 001	3.212E 001	4.731E 001	6.098E 001	4.162E 001	4.152E 001	7.810E 001	1.861E 002	5.298E 001
20	2.723E 001	3.198E 001	2.936E 001	3.268E 001	4.904E 001	5.823E 001	3.932E 001	4.180E 001	7.946E 001	1.857E 002
21	2.222E 001	2.772E 001	3.070E 001	2.791E 001	3.361E 001	5.057E 001	5.463E 001	3.728E 001	4.217E 001	8.083E 001
22	1.983E 001	2.241E 001	2.792E 001	2.891E 001	2.689E 001	3.483E 001	5.174E 001	5.051E 001	3.547E 001	4.263E 001
23	1.900E 001	1.911E 001	2.276E 001	2.765E 001	2.684E 001	2.635E 001	3.627E 001	5.232E 001	4.620E 001	3.391E 001
24	1.806E 001	1.773E 001	1.871E 001	2.311E 001	2.675E 001	2.478E 001	2.628E 001	3.781E 001	5.199E 001	4.196E 001
25	1.631E 001	1.686E 001	1.659E 001	1.862E 001	2.324E 001	2.517E 001	2.300E 001	2.665E 001	3.931E 001	5.044E 001
26	1.398E 001	1.552E 001	1.551E 001	1.572E 001	1.872E 001	2.293E 001	2.308E 001	2.167E 001	2.737E 001	4.057E 001
27	1.178E 001	1.355E 001	1.439E 001	1.416E 001	1.518E 001	1.881E 001	2.199E 001	2.079E 001	2.084E 001	2.835E 001
28	1.008E 001	1.136E 001	1.281E 001	1.305E 001	1.300E 001	1.492E 001	1.867E 001	2.034E 001	1.865E 001	2.051E 001
29	8.783E 000	9.440E 000	1.087E 001	1.175E 001	1.163E 001	1.214E 001	1.481E 001	1.804E 001	1.814E 001	1.691E 001
30	7.652E 000	7.930E 000	8.921E 000	1.013E 001	1.045E 001	1.035E 001	1.161E 001	1.461E 001	1.675E 001	1.574E 001
31	6.541E 000	6.729E 000	7.255E 000	8.365E 000	9.116E 000	9.061E 000	9.340E 000	1.129E 001	1.406E 001	1.482E 001
32	5.434E 000	5.687E 000	5.924E 000	6.698E 000	7.624E 000	7.883E 000	7.784E 000	8.668E 000	1.098E 001	1.295E 001
33	4.386E 000	4.717E 000	4.853E 000	5.288E 000	6.116E 000	6.651E 000	6.592E 000	6.788E 000	8.242E 000	1.041E 001
34	3.456E 000	3.805E 000	3.947E 000	4.155E 000	4.751E 000	5.386E 000	5.521E 000	5.441E 000	6.125E 000	7.855E 000
35	2.669E 000	2.976E 000	3.150E 000	3.250E 000	3.609E 000	4.183E 000	4.485E 000	4.398E 000	4.585E 000	5.694E 000
36	2.022E 000	2.258E 000	2.444E 000	2.513E 000	2.699E 000	3.130E 000	3.498E 000	3.509E 000	3.470E 000	4.040E 000
37	1.500E 000	1.664E 000	1.833E 000	1.902E 000	1.988E 000	2.267E 000	2.610E 000	2.715E 000	2.626E 000	2.838E 000
38	1.083E 000	1.188E 000	1.323E 000	1.394E 000	1.434E 000	1.593E 000	1.862E 000	2.013E 000	1.955E 000	1.980E 000
39	7.554E-001	8.184E-001	9.150E-001	9.803E-001	1.002E 000	1.083E 000	1.268E 000	1.419E 000	1.406E 000	1.362E 000
40	5.029E-001	5.392E-001	6.020E-001	6.545E-001	6.708E-001	7.076E-001	8.201E-001	9.424E-001	9.603E-001	9.095E-001
41	3.148E-001	3.349E-001	3.722E-001	4.093E-001	4.223E-001	4.374E-001	4.991E-001	5.838E-001	6.124E-001	5.766E-001
42	1.811E-001	1.917E-001	2.117E-001	2.346E-001	2.442E-001	2.498E-001	2.801E-001	3.309E-001	3.565E-001	3.373E-001
43	9.220E-002	9.730E-002	1.068E-001	1.189E-001	1.249E-001	1.268E-001	1.398E-001	1.658E-001	1.827E-001	1.746E-001
44	3.870E-002	4.078E-002	4.453E-002	4.972E-002	5.257E-002	5.319E-002	5.782E-002	6.862E-002	7.687E-002	7.433E-002
45	1.142E-002	1.203E-002	1.308E-002	1.462E-002	1.555E-002	1.570E-002	1.689E-002	2.002E-002	2.270E-002	2.217E-002

Table B.2 (continued)

SCATTERING KERNEL, SIGMA(U(J) TO U(I))/UNIT LETHARGY, KT = .0253, J = 21 TO 30

I	J = 21	22	23	24	25	26	27	28	29	30
1	6.673E-023	4.272E-023	2.794E-023	1.866E-023	1.273E-023	8.873E-024	6.321E-024	4.599E-024	3.422E-024	2.603E-024
2	1.629E-016	1.043E-016	6.821E-017	4.557E-017	3.109E-017	2.167E-017	1.543E-017	1.123E-017	8.353E-018	6.352E-018
3	4.558E-012	2.920E-012	1.909E-012	1.275E-012	8.697E-013	6.058E-013	4.311E-013	3.134E-013	2.328E-013	1.768E-013
4	5.966E-009	3.832E-009	2.512E-009	1.680E-009	1.147E-009	7.997E-010	5.690E-010	4.135E-010	3.069E-010	2.327E-010
5	9.624E-007	6.185E-007	4.059E-007	2.720E-007	1.860E-007	1.298E-007	9.252E-008	6.727E-008	4.994E-008	3.786E-008
6	4.039E-005	2.571E-005	1.673E-005	1.113E-005	7.569E-006	5.259E-006	3.732E-006	2.705E-006	2.003E-006	1.515E-006
7	6.443E-004	4.095E-004	2.656E-004	1.762E-004	1.193E-004	8.255E-005	5.834E-005	4.211E-005	3.105E-005	2.339E-005
8	4.978E-003	3.168E-003	2.061E-003	1.367E-003	9.270E-004	6.414E-004	4.531E-004	3.269E-004	2.408E-004	1.811E-004
9	2.286E-002	1.455E-002	9.474E-003	6.297E-003	4.274E-003	2.962E-003	2.096E-003	1.513E-003	1.115E-003	8.394E-004
10	7.278E-002	4.612E-002	2.995E-002	1.991E-002	1.352E-002	9.376E-003	6.642E-003	4.800E-003	3.541E-003	2.667E-003
11	1.644E-001	1.030E-001	7.113E-002	5.007E-002	3.442E-002	2.310E-002	1.570E-002	1.116E-002	8.333E-003	6.427E-003
12	3.730E-001	2.117E-001	1.301E-001	8.941E-002	6.472E-002	4.666E-002	3.284E-002	2.287E-002	1.629E-002	1.212E-002
13	7.341E-001	4.687E-001	2.754E-001	1.677E-001	1.132E-001	8.286E-002	6.198E-002	4.584E-002	3.334E-002	2.422E-002
14	1.159E 000	8.424E-001	5.808E-001	3.595E-001	2.205E-001	1.458E-001	1.059E-001	8.106E-002	6.255E-002	4.774E-002
15	2.365E 000	1.328E 000	9.557E-001	7.053E-001	4.665E-001	2.943E-001	1.924E-001	1.369E-001	1.050E-001	8.349E-002
16	5.889E 000	2.848E 000	1.553E 000	1.081E 000	8.362E-001	5.965E-001	3.945E-001	2.600E-001	1.813E-001	1.369E-001
17	1.028E 001	6.834E 000	3.453E 000	1.853E 000	1.234E 000	9.700E-001	7.451E-001	5.256E-001	3.573E-001	2.480E-001
18	1.106E 001	1.052E 001	7.852E 000	4.202E 000	2.255E 000	1.436E 000	1.111E 000	9.027E-001	6.862E-001	4.920E-001
19	1.923E 001	1.136E 001	1.066E 001	8.886E 000	5.115E 000	2.789E 000	1.712E 000	1.273E 000	1.061E 000	8.674E-001
20	5.529E 001	2.047E 001	1.174E 001	1.076E 001	9.843E 000	6.199E 000	3.493E 000	2.099E 000	1.483E 000	1.222E 000
21	1.853E 002	5.771E 001	2.184E 001	1.220E 001	1.082E 001	1.062E 001	7.446E 000	4.404E 000	2.643E 000	1.784E 000
22	8.221E 001	1.848E 002	6.024E 001	2.336E 001	1.276E 001	1.088E 001	1.114E 001	8.801E 000	5.561E 000	3.403E 000
23	4.316E 001	8.357E 001	1.843E 002	6.288E 001	2.502E 001	1.342E 001	1.096E 001	1.140E 001	1.014E 001	6.982E 000
24	3.255E 001	4.376E 001	8.491E 001	1.837E 002	6.563E 001	2.686E 001	1.420E 001	1.106E 001	1.145E 001	1.127E 001
25	3.793E 001	3.139E 001	4.439E 001	8.621E 001	1.830E 002	6.847E 001	2.887E 001	1.512E 001	1.122E 001	1.134E 001
26	4.754E 001	3.419E 001	3.040E 001	4.505E 001	8.743E 001	1.821E 002	7.139E 001	3.105E 001	1.618E 001	1.144E 001
27	4.134E 001	4.343E 001	3.078E 001	2.955E 001	4.572E 001	8.855E 001	1.811E 002	7.439E 001	3.342E 001	1.741E 001
28	2.943E 001	4.129E 001	3.856E 001	2.771E 001	2.882E 001	4.635E 001	8.954E 001	1.800E 002	7.745E 001	3.599E 001
29	2.061E 001	3.044E 001	4.001E 001	3.346E 001	2.496E 001	2.819E 001	4.694E 001	9.036E 001	1.785E 002	8.052E 001
30	1.571E 001	2.104E 001	3.112E 001	3.721E 001	2.850E 001	2.251E 001	2.762E 001	4.743E 001	9.095E 001	1.768E 002
31	1.355E 001	1.504E 001	2.163E 001	3.113E 001	3.298E 001	2.392E 001	2.034E 001	2.709E 001	4.780E 001	9.126E 001
32	1.250E 001	1.183E 001	1.483E 001	2.218E 001	3.003E 001	2.781E 001	1.981E 001	1.843E 001	2.657E 001	4.799E 001
33	1.123E 001	1.024E 001	1.069E 001	1.495E 001	2.238E 001	2.747E 001	2.239E 001	1.623E 001	1.675E 001	2.604E 001
34	9.368E 000	9.126E 000	8.399E 000	1.010E 001	1.518E 001	2.185E 001	2.347E 001	1.729E 001	1.317E 001	1.528E 001
35	7.250E 000	7.810E 000	7.057E 000	7.145E 000	9.909E 000	1.525E 001	2.016E 001	1.855E 001	1.285E 001	1.063E 001
36	5.279E 000	6.239E 000	5.977E 000	5.402E 000	6.459E 000	9.910E 000	1.478E 001	1.714E 001	1.354E 001	9.205E 000
37	3.666E 000	4.646E 000	4.853E 000	4.276E 000	4.331E 000	6.185E 000	9.804E 000	1.338E 001	1.312E 001	9.114E 000
38	2.453E 000	3.246E 000	3.693E 000	3.379E 000	3.029E 000	3.787E 000	6.072E 000	9.227E 000	1.091E 001	8.904E 000
39	1.588E 000	2.138E 000	2.616E 000	2.557E 000	2.173E 000	2.316E 000	3.565E 000	5.808E 000	7.884E 000	7.729E 000
40	9.936E-001	1.329E 000	1.721E 000	1.806E 000	1.540E 000	1.424E 000	1.999E 000	3.385E 000	5.089E 000	5.810E 000
41	5.940E-001	7.748E-001	1.046E 000	1.173E 000	1.033E 000	8.683E-001	1.072E 000	1.831E 000	2.973E 000	3.818E 000
42	3.316E-001	4.173E-001	5.789E-001	6.864E-001	6.325E-001	5.063E-001	5.443E-001	9.092E-001	1.567E 000	2.203E 000
43	1.660E-001	2.009E-001	2.828E-001	3.509E-001	3.380E-001	2.665E-001	2.537E-001	4.039E-001	7.275E-001	1.097E 000
44	6.914E-002	8.068E-002	1.143E-001	1.468E-001	1.469E-001	1.161E-001	1.008E-001	1.510E-001	2.804E-001	4.461E-001
45	2.035E-002	2.308E-002	3.273E-002	4.308E-002	4.432E-002	3.536E-002	2.891E-002	4.085E-002	7.722E-002	1.277E-001

Table B.2 (continued)

SCATTERING KERNEL, SIGMA(U(J) TO U(I))/UNIT LETHARGY, KT = .02699, J = 41 TO 45

I	J = 41	42	43	44	45
1	3.845E-23	4.197E-23	4.834E-23	6.060E-23	8.697E-23
2	3.601E-17	3.921E-17	4.527E-17	5.675E-17	8.144E-17
3	5.047E-13	5.490E-13	6.333E-13	7.933E-13	1.138E-12
4	4.014E-10	4.355E-10	5.014E-10	6.269E-10	8.983E-10
5	4.531E-08	4.903E-08	5.630E-08	7.027E-08	1.005E-07
6	1.376E-06	1.486E-06	1.702E-06	2.121E-06	3.030E-06
7	1.710E-05	1.841E-05	2.105E-05	2.617E-05	3.734E-05
8	1.128E-04	1.209E-04	1.379E-04	1.713E-04	2.441E-04
9	4.650E-04	4.987E-04	5.683E-04	7.047E-04	1.003E-03
10	1.362E-03	1.460E-03	1.661E-03	2.059E-03	2.929E-03
11	3.032E-03	3.260E-03	3.723E-03	4.624E-03	6.591E-03
12	5.627E-03	6.027E-03	6.866E-03	8.518E-03	1.214E-02
13	1.057E-02	1.127E-02	1.277E-02	1.578E-02	2.241E-02
14	1.926E-02	2.046E-02	2.350E-02	2.909E-02	4.135E-02
15	3.260E-02	3.521E-02	4.034E-02	5.022E-02	7.169E-02
16	5.413E-02	5.787E-02	6.591E-02	8.181E-02	1.166E-01
17	9.518E-02	1.003E-01	1.126E-01	1.382E-01	1.954E-01
18	1.671E-01	1.774E-01	1.999E-01	2.453E-01	3.463E-01
19	2.610E-01	2.835E-01	3.255E-01	4.051E-01	5.776E-01
20	3.638E-01	3.946E-01	4.590E-01	5.767E-01	8.290E-01
21	5.360E-01	5.619E-01	6.321E-01	7.795E-01	1.108E 00
22	9.431E-01	9.584E-01	1.043E 00	1.248E 00	1.732E 00
23	1.672E 00	1.738E 00	1.914E 00	2.300E 00	3.194E 00
24	2.440E 00	2.676E 00	3.069E 00	3.802E 00	5.392E 00
25	2.828E 00	3.207E 00	3.821E 00	4.893E 00	7.115E 00
26	3.061E 00	3.325E 00	3.902E 00	4.998E 00	7.314E 00
27	4.538E 00	4.368E 00	4.614E 00	5.460E 00	7.582E 00
28	8.770E 00	8.255E 00	8.340E 00	9.345E 00	1.233E 01
29	1.582E 01	1.571E 01	1.649E 01	1.895E 01	2.537E 01
30	2.225E 01	2.403E 01	2.693E 01	3.251E 01	4.507E 01
31	2.212E 01	2.672E 01	3.262E 01	4.194E 01	6.075E 01
32	1.514E 01	2.030E 01	2.737E 01	3.807E 01	5.826E 01
33	8.473E 00	1.096E 01	1.546E 01	2.300E 01	3.728E 01
34	6.705E 00	6.096E 00	6.929E 00	9.506E 00	1.530E 01
35	9.994E 00	6.832E 00	5.158E 00	4.643E 00	5.441E 00
36	1.817E 01	1.225E 01	8.545E 00	6.432E 00	5.738E 00
37	3.146E 01	2.221E 01	1.618E 01	1.266E 01	1.164E 01
38	4.957E 01	3.672E 01	2.816E 01	2.324E 01	2.253E 01
39	7.058E 01	5.443E 01	4.397E 01	3.816E 01	3.887E 01
40	9.010E 01	7.271E 01	6.117E 01	5.561E 01	5.928E 01
41	1.028E 02	9.585E 01	7.515E 01	7.125E 01	7.910E 01
42	4.590E 01	8.875E 01	8.042E 01	7.910E 01	9.101E 01
43	1.791E 01	3.584E 01	7.317E 01	7.425E 01	8.802E 01
44	5.736E 00	1.191E 01	2.509E 01	5.622E 01	6.827E 01
45	1.318E 00	2.837E 00	6.156E 00	1.413E 01	3.815E 01

Table B.2 (continued)

SCATTERING KERNEL, SIGMA(U(J) TO U(I))/UNIT LETHARGY, KT = .0253, J = 31 TO 40

I	J = 31	32	33	34	35	36	37	38	39	40
1	2.024E-024	1.610E-024	1.312E-024	1.095E-024	9.363E-025	8.219E-025	7.413E-025	6.882E-025	6.593E-025	6.536E-025
2	4.939E-018	3.931E-018	3.201E-018	2.670E-018	2.283E-018	2.004E-018	1.807E-018	1.678E-018	1.607E-018	1.593E-018
3	1.373E-013	1.090E-013	8.863E-014	7.381E-014	6.302E-014	5.521E-014	4.970E-014	4.606E-014	4.406E-014	4.364E-014
4	1.803E-010	1.429E-010	1.159E-010	9.622E-011	8.189E-011	7.148E-011	6.413E-011	5.924E-011	5.648E-011	5.575E-011
5	2.932E-008	2.320E-008	1.878E-008	1.555E-008	1.319E-008	1.149E-008	1.027E-008	9.454E-009	8.981E-009	8.837E-009
6	1.170E-006	9.239E-007	7.461E-007	6.163E-007	5.215E-007	4.529E-007	4.036E-007	3.703E-007	3.507E-007	3.440E-007
7	1.801E-005	1.417E-005	1.140E-005	9.390E-006	7.920E-006	6.851E-006	6.089E-006	5.569E-006	5.257E-006	5.140E-006
8	1.392E-004	1.093E-004	8.775E-005	7.210E-005	6.068E-005	5.236E-005	4.639E-005	4.233E-005	3.985E-005	3.886E-005
9	6.451E-004	5.066E-004	4.066E-004	3.338E-004	2.806E-004	2.418E-004	2.140E-004	1.948E-004	1.831E-004	1.782E-004
10	2.052E-003	1.611E-003	1.294E-003	1.062E-003	8.926E-004	7.690E-004	6.802E-004	6.185E-004	5.807E-004	5.647E-004
11	5.032E-003	3.967E-003	3.156E-003	2.553E-003	2.114E-003	1.802E-003	1.586E-003	1.443E-003	1.360E-003	1.329E-003
12	9.415E-003	7.552E-003	6.175E-003	5.112E-003	4.288E-003	3.660E-003	3.200E-003	2.879E-003	2.679E-003	2.591E-003
13	1.804E-002	1.398E-002	1.129E-002	9.424E-003	8.065E-003	7.039E-003	6.264E-003	5.697E-003	5.323E-003	5.142E-003
14	3.610E-002	2.744E-002	2.135E-002	1.722E-002	1.444E-002	1.256E-002	1.128E-002	1.042E-002	9.900E-003	9.703E-003
15	6.670E-002	5.294E-002	4.186E-002	3.338E-002	2.719E-002	2.287E-002	1.999E-002	1.817E-002	1.715E-002	1.686E-002
16	1.097E-001	9.060E-002	7.535E-002	6.263E-002	5.216E-002	4.390E-002	3.773E-002	3.341E-002	3.068E-002	2.943E-002
17	1.827E-001	1.445E-001	1.206E-001	1.037E-001	9.034E-002	7.927E-002	7.017E-002	6.308E-002	5.804E-002	5.511E-002
18	3.482E-001	2.537E-001	1.958E-001	1.611E-001	1.397E-001	1.254E-001	1.151E-001	1.075E-001	1.024E-001	9.983E-002
19	6.668E-001	4.942E-001	3.657E-001	2.789E-001	2.239E-001	1.906E-001	1.712E-001	1.606E-001	1.560E-001	1.564E-001
20	1.054E 000	8.742E-001	6.927E-001	5.365E-001	4.170E-001	3.329E-001	2.774E-001	2.439E-001	2.267E-001	2.222E-001
21	1.409E 000	1.234E 000	1.092E 000	9.353E-001	7.762E-001	6.358E-001	5.239E-001	4.417E-001	3.863E-001	3.549E-001
22	2.228E 000	1.663E 000	1.419E 000	1.298E 000	1.191E 000	1.070E 000	9.457E-001	8.326E-001	7.409E-001	6.761E-001
23	4.445E 000	2.892E 000	2.055E 000	1.657E 000	1.493E 000	1.423E 000	1.370E 000	1.314E 000	1.258E 000	1.215E 000
24	8.638E 000	5.841E 000	3.881E 000	2.691E 000	2.041E 000	1.736E 000	1.631E 000	1.624E 000	1.660E 000	1.721E 000
25	1.202E 001	1.039E 001	7.632E 000	5.313E 000	3.719E 000	2.727E 000	2.170E 000	1.912E 000	1.853E 000	1.928E 000
26	1.113E 001	1.229E 001	1.196E 001	9.766E 000	7.309E 000	5.343E 000	3.956E 000	3.053E 000	2.522E 000	2.277E 000
27	1.174E 001	1.085E 001	1.209E 001	1.301E 001	1.198E 001	9.884E 000	7.779E 000	6.071E 000	4.816E 000	3.964E 000
28	1.882E 001	1.215E 001	1.055E 001	1.154E 001	1.327E 001	1.380E 001	1.278E 001	1.110E 001	9.443E 000	8.079E 000
29	3.875E 001	2.045E 001	1.270E 001	1.025E 001	1.073E 001	1.272E 001	1.462E 001	1.532E 001	1.496E 001	1.417E 001
30	8.358E 001	4.171E 001	2.231E 001	1.344E 001	1.002E 001	9.765E 000	1.147E 001	1.412E 001	1.656E 001	1.828E 001
31	1.747E 002	8.657E 001	4.486E 001	2.444E 001	1.442E 001	9.952E 000	8.782E 000	9.798E 000	1.237E 001	1.581E 001
32	9.121E 001	1.722E 002	8.941E 001	4.816E 001	2.685E 001	1.571E 001	1.015E 001	7.946E 000	7.992E 000	9.790E 000
33	4.795E 001	9.071E 001	1.691E 002	9.203E 001	5.159E 001	2.959E 001	1.739E 001	1.075E 001	7.476E 000	6.422E 000
34	2.545E 001	4.760E 001	8.966E 001	1.654E 002	9.430E 001	5.508E 001	3.266E 001	1.953E 001	1.190E 001	7.616E 000
35	1.400E 001	2.475E 001	4.687E 001	8.794E 001	1.608E 002	9.608E 001	5.855E 001	3.604E 001	2.222E 001	1.373E 001
36	8.592E 000	1.287E 001	2.390E 001	4.566E 001	8.541E 001	1.552E 002	9.721E 001	6.188E 001	3.971E 001	2.550E 001
37	6.390E 000	7.008E 000	1.184E 001	2.282E 001	4.387E 001	8.193E 001	1.484E 002	9.748E 001	6.498E 001	4.366E 001
38	5.658E 000	4.355E 000	5.805E 000	1.083E 001	2.143E 001	4.139E 001	7.736E 001	1.403E 002	9.675E 001	6.773E 001
39	5.286E 000	3.242E 000	2.989E 000	4.882E 000	9.780E 000	1.966E 001	3.817E 001	7.161E 001	1.306E 002	9.486E 001
40	4.604E 000	2.705E 000	1.749E 000	2.129E 000	4.117E 000	8.599E 000	1.747E 001	3.415E 001	6.462E 001	1.194E 002
41	3.502E 000	2.225E 000	1.180E 000	9.451E-001	1.584E 000	3.399E 000	7.254E 000	1.487E 001	2.938E 001	5.640E 001
42	2.279E 000	1.625E 000	8.319E-001	4.528E-001	5.568E-001	1.186E 000	2.665E 000	5.760E 000	1.195E 001	2.396E 001
43	1.244E 000	9.884E-001	5.330E-001	2.306E-001	1.801E-001	3.548E-001	8.379E-001	1.915E 000	4.188E 000	8.817E 000
44	5.414E-001	4.680E-001	2.717E-001	1.085E-001	5.307E-002	8.633E-002	2.132E-001	5.169E-001	1.194E 000	2.646E 000
45	1.624E-001	1.489E-001	9.207E-002	3.663E-002	1.266E-002	1.519E-002	3.895E-002	1.001E-001	2.442E-001	5.691E-001

Table B.3 gives the Nelkin water kernel scattering matrix for a moderator physical temperature of 40°C. Its format is the same as that described for Table B.2.

Table B.4 lists as a function of energy the scattering cross section, Eq. (2.2), and the transport cross section, Eq. (5.25), for water. The energy dependent scattering cross sections for U^{235}, U^{238}, and oxygen are also listed in Table B.4 as calculated using Eq. (5.13) with the parameters listed in Table A.3.

Table B.5 gives as a function of energy the absorption and fission cross sections[82] for U^{235}, as well as the uranium dioxide fuel fission and absorption cross sections. One plus the capture to fission ratio, $[1+\alpha(E)]$, for the fuel is also listed in Table B.5, along with the normalized slowing down source of neutrons, $\overline{S}(E)$, Eq. (7.1), used in the calculations.

Table B.6 through B.10 list the energy dependent thermal spectra calculated by COUTH for a moderator physical temperature of 20°C. The moderator, Eq. (6.1), fuel, Eq. (6.3), and cladding, Eq. (6.4), spectra are given for the five Cornell ZPR cores.

Table B.11 gives the integral properties defined in Chap. 6 for the five ZPR cores at a temperature of 20°C,

---

[82] J. Suich, "Temperature Coefficients in Heterogeneous Reactor Lattices," Massachusetts Institute of Technology Thesis (1963).

TABLE B.3

NELKIN WATER MODEL FOR THE SCATTERING MATRIX AT 40°C.

SCATTERING KERNEL, SIGMA(U(J) TO U(I))/UNIT LETHARGY, KT = .02699, J = 1 TO 10

I	J = 1	2	3	4	5	6	7	8	9	10
1	8.607E 01	4.758E-05	3.120E-09	3.732E-12	3.070E-14	9.659E-16	7.740E-17	1.200E-17	2.982E-18	1.044E-18
2	3.401E 01	8.595E 01	3.536E-03	3.263E-06	2.878E-08	9.152E-10	7.328E-11	1.134E-11	2.812E-12	9.827E-13
3	2.472E 01	3.920E 01	8.569E 01	6.431E-02	4.152E-04	1.190E-05	9.717E-07	1.552E-07	3.920E-08	1.383E-08
4	1.984E 01	2.426E 01	4.313E 01	8.532E 01	4.836E-01	1.213E-02	8.704E-04	1.381E-05	3.481E-05	1.070E-05
5	1.625E 01	2.132E 01	2.774E 01	4.818E 01	8.488E 01	2.002E 00	1.271E-01	1.775E-02	4.189E-03	1.420E-03
6	1.375E 01	1.823E 01	2.138E 01	3.250E 01	5.384E 01	8.443E 01	5.409E 00	6.918E-01	1.518E-01	4.993E-02
7	1.193E 01	1.580E 01	1.890E 01	2.525E 01	3.701E 01	5.857E 01	8.398E 01	1.090E 01	2.357E 00	7.355E-01
8	1.058E 01	1.398E 01	1.726E 01	2.112E 01	2.955E 01	4.283E 01	6.233E 01	8.357E 01	1.809E 01	5.716E 00
9	9.540E 00	1.240E 01	1.584E 01	1.856E 01	2.533E 01	3.414E 01	4.895E 01	6.573E 01	8.321E 01	2.636E 01
10	8.765E 00	1.154E 01	1.465E 01	1.691E 01	2.252E 01	2.944E 01	4.006E 01	5.445E 01	6.911E 01	8.289E 01
11	8.162E 00	1.074E 01	1.370E 01	1.577E 01	2.051E 01	2.658E 01	3.458E 01	4.630E 01	5.897E 01	7.226E 01
12	7.696E 00	1.011E 01	1.295E 01	1.495E 01	1.904E 01	2.460E 01	3.111E 01	4.076E 01	5.211E 01	6.277E 01
13	7.240E 00	9.510E 00	1.220E 01	1.417E 01	1.767E 01	2.279E 01	2.830E 01	3.608E 01	4.575E 01	5.561E 01
14	6.795E 00	8.921E 00	1.147E 01	1.341E 01	1.640E 01	2.110E 01	2.595E 01	3.218E 01	4.023E 01	4.889E 01
15	6.362E 00	8.349E 00	1.075E 01	1.266E 01	1.522E 01	1.951E 01	2.391E 01	2.896E 01	3.555E 01	4.289E 01
16	5.939E 00	7.792E 00	1.005E 01	1.191E 01	1.412E 01	1.800E 01	2.205E 01	2.629E 01	3.163E 01	3.774E 01
17	5.527E 00	7.251E 00	9.358E 00	1.117E 01	1.310E 01	1.657E 01	2.032E 01	2.402E 01	2.834E 01	3.338E 01
18	5.126E 00	6.725E 00	8.686E 00	1.043E 01	1.213E 01	1.521E 01	1.868E 01	2.201E 01	2.558E 01	2.969E 01
19	4.737E 00	6.215E 00	8.033E 00	9.693E 00	1.123E 01	1.393E 01	1.712E 01	2.016E 01	2.321E 01	2.657E 01
20	4.360E 00	5.721E 00	7.398E 00	8.964E 00	1.036E 01	1.272E 01	1.563E 01	1.843E 01	2.110E 01	2.390E 01
21	3.995E 00	5.243E 00	6.782E 00	8.246E 00	9.521E 00	1.158E 01	1.422E 01	1.678E 01	1.918E 01	2.156E 01
22	3.643E 00	4.782E 00	6.186E 00	7.543E 00	8.714E 00	1.050E 01	1.286E 01	1.522E 01	1.739E 01	1.946E 01
23	3.304E 00	4.339E 00	5.612E 00	6.858E 00	7.933E 00	9.487E 00	1.158E 01	1.372E 01	1.569E 01	1.753E 01
24	2.980E 00	3.914E 00	5.061E 00	6.194E 00	7.177E 00	8.525E 00	1.037E 01	1.229E 01	1.408E 01	1.572E 01
25	2.671E 00	3.508E 00	4.534E 00	5.555E 00	6.447E 00	7.616E 00	9.227E 00	1.094E 01	1.255E 01	1.402E 01
26	2.377E 00	3.122E 00	4.033E 00	4.944E 00	5.746E 00	6.758E 00	8.152E 00	9.669E 00	1.111E 01	1.241E 01
27	2.100E 00	2.757E 00	3.559E 00	4.364E 00	5.078E 00	5.950E 00	7.147E 00	8.472E 00	9.743E 00	1.090E 01
28	1.839E 00	2.415E 00	3.114E 00	3.816E 00	4.444E 00	5.192E 00	6.211E 00	7.356E 00	8.466E 00	9.480E 00
29	1.596E 00	2.096E 00	2.699E 00	3.305E 00	3.849E 00	4.485E 00	5.345E 00	6.322E 00	7.281E 00	8.161E 00
30	1.371E 00	1.800E 00	2.315E 00	2.831E 00	3.296E 00	3.833E 00	4.550E 00	5.373E 00	6.190E 00	6.944E 00
31	1.164E 00	1.528E 00	1.962E 00	2.395E 00	2.788E 00	3.234E 00	3.826E 00	4.510E 00	5.195E 00	5.832E 00
32	9.761E-01	1.281E 00	1.642E 00	2.000E 00	2.325E 00	2.692E 00	3.173E 00	3.733E 00	4.299E 00	4.828E 00
33	8.067E-01	1.058E 00	1.355E 00	1.646E 00	1.909E 00	2.205E 00	2.592E 00	3.043E 00	3.502E 00	3.934E 00
34	6.557E-01	8.600E-01	1.099E 00	1.332E 00	1.541E 00	1.776E 00	2.081E 00	2.437E 00	2.803E 00	3.148E 00
35	5.231E-01	6.858E-01	8.749E-01	1.057E 00	1.220E 00	1.403E 00	1.638E 00	1.914E 00	2.199E 00	2.469E 00
36	4.081E-01	5.350E-01	6.814E-01	8.204E-01	9.446E-01	1.083E 00	1.261E 00	1.469E 00	1.686E 00	1.892E 00
37	3.103E-01	4.046E-01	5.170E-01	6.205E-01	7.122E-01	8.141E-01	9.448E-01	1.098E 00	1.258E 00	1.411E 00
38	2.286E-01	2.996E-01	3.803E-01	4.549E-01	5.204E-01	5.931E-01	6.862E-01	7.957E-01	9.101E-01	1.020E 00
39	1.621E-01	2.124E-01	2.692E-01	3.210E-01	3.660E-01	4.159E-01	4.798E-01	5.549E-01	6.335E-01	7.093E-01
40	1.095E-01	1.434E-01	1.816E-01	2.159E-01	2.454E-01	2.780E-01	3.198E-01	3.689E-01	4.204E-01	4.702E-01
41	6.944E-02	9.098E-02	1.150E-01	1.364E-01	1.545E-01	1.746E-01	2.003E-01	2.305E-01	2.622E-01	2.930E-01
42	4.043E-02	5.297E-02	6.690E-02	7.912E-02	8.940E-02	1.008E-01	1.153E-01	1.324E-01	1.504E-01	1.678E-01
43	2.080E-02	2.725E-02	3.439E-02	4.059E-02	4.575E-02	5.145E-02	5.874E-02	6.733E-02	7.637E-02	8.515E-02
44	8.810E-03	1.154E-02	1.455E-02	1.715E-02	1.929E-02	2.166E-02	2.468E-02	2.825E-02	3.200E-02	3.564E-02
45	2.617E-03	3.429E-03	4.322E-03	5.086E-03	5.714E-03	6.405E-03	7.290E-03	8.333E-03	9.431E-03	1.050E-02

Table B.3 (continued)

SCATTERING KERNEL, SIGMA(U(J) TO U(I))/UNIT LETHARGY, KT = .02699, J = 11 TO 20

I	J = 11	12	13	14	15	16	17	18	19	20
1	4.690E-19	2.549E-19	1.410E-19	7.959E-20	4.582E-20	2.690E-20	1.611E-20	9.846E-21	6.136E-21	3.900E-21
2	4.41AE-13	2.394E-13	1.324E-13	7.4A8E-14	4.298E-14	2.523E-14	1.511E-14	9.233E-15	5.755E-15	3.659E-15
3	6.25nE-09	3.398E-09	1.883E-09	1.064E-09	6.135E-10	3.606E-10	2.162E-10	1.322E-10	8.245E-11	5.244E-11
4	4.82AE-06	2.632E-06	1.467E-06	8.347E-07	4.846E-07	2.869E-07	1.731E-07	1.065E-07	6.673E-08	4.262E-08
5	6.25nE-04	3.339E-04	1.823E-04	1.017E-04	5.804E-05	3.387E-05	2.022E-05	1.234E-05	7.699E-06	4.906E-06
6	2.17AE-02	1.160E-02	6.320E-03	3.518E-03	2.000E-03	1.161E-03	6.878E-04	4.160E-04	2.569E-04	1.621E-04
7	3.060E-01	1.588E-01	8.496E-02	4.685E-02	2.654E-02	1.540E-02	9.135E-03	5.532E-03	3.419E-03	2.156E-03
8	2.35nE 00	1.190E 00	6.194E-01	3.322E-01	1.839E-01	1.050E-01	6.174E-02	3.726E-02	2.302E-02	1.453E-02
9	1.087E 01	5.526E 00	2.853E 00	1.509E 00	8.199E-01	4.588E-01	2.646E-01	1.573E-01	9.625E-02	6.046E-02
10	3.493E 01	1.745E 01	9.094E 00	4.808E 00	2.594E 00	1.436E 00	8.172E-01	4.788E-01	2.890E-01	1.795E-01
11	1.821E 02	3.973E 01	1.456E 01	1.145E 01	7.663E 00	3.316E 00	1.655E 00	1.102E 00	7.268E-01	4.213E-01
12	6.905E 01	1.819E 02	4.124E 01	1.507E 01	1.156E 01	8.470E 00	3.836E 00	1.877E 00	1.223E 00	8.549E-01
13	4.302E 01	7.012E 01	1.817E 02	4.282E 01	1.564E 01	1.166E 01	9.284E 00	4.450E 00	2.158E 00	1.361E 00
14	5.629E 01	4.260E 01	7.122E 01	1.815E 02	4.449E 01	1.629E 01	1.177E 01	1.006E 01	5.169E 00	2.514E 00
15	6.125E 01	5.314E 01	4.230E 01	7.235E 01	1.812E 02	4.624E 01	1.702E 01	1.191E 01	1.075E 01	5.998E 00
16	4.213E 01	6.191E 01	5.013E 01	4.211E 01	7.352E 01	1.809E 02	4.809E 01	1.783E 01	1.207E 01	1.130E 01
17	3.267E 01	4.356E 01	6.201E 01	4.729E 01	4.204E 01	7.472E 01	1.806E 02	5.002E 01	1.874E 01	1.227E 01
18	3.304E 01	3.237E 01	4.512E 01	6.134E 01	4.465E 01	4.206E 01	7.594E 01	1.803E 02	5.206E 01	1.976E 01
19	3.230E 01	3.127E 01	3.245E 01	4.673E 01	5.975E 01	4.221E 01	4.219E 01	7.719E 01	1.800E 02	5.419E 01
20	2.711E 01	3.165E 01	2.962E 01	3.291E 01	4.828E 01	5.720E 01	4.000E 01	4.242E 01	7.845E 01	1.796E 02
21	2.236E 01	2.749E 01	3.045E 01	2.824E 01	3.371E 01	4.965E 01	5.387E 01	3.801E 01	4.273E 01	7.973E 01
22	1.994E 01	2.245E 01	2.761E 01	2.879E 01	2.724E 01	3.478E 01	5.068E 01	5.003E 01	3.624E 01	4.311E 01
23	1.890E 01	1.925E 01	2.270E 01	2.731E 01	2.687E 01	2.668E 01	3.604E 01	5.115E 01	4.600E 01	3.469E 01
24	1.793E 01	1.778E 01	1.882E 01	2.293E 01	2.643E 01	2.494E 01	2.654E 01	3.739E 01	5.079E 01	4.199E 01
25	1.617E 01	1.678E 01	1.669E 01	1.866E 01	2.297E 01	2.494E 01	2.324E 01	2.679E 01	3.870E 01	4.930E 01
26	1.390E 01	1.538E 01	1.549E 01	1.583E 01	1.865E 01	2.261E 01	2.299E 01	2.193E 01	2.737E 01	3.979E 01
27	1.177E 01	1.343E 01	1.429E 01	1.421E 01	1.525E 01	1.865E 01	2.168E 01	2.084E 01	2.10AE 01	2.818E 01
28	1.009E 01	1.131E 01	1.268E 01	1.300E 01	1.308E 01	1.493E 01	1.842E 01	2.010E 01	1.880E 01	2.067E 01
29	8.777E 00	9.439E 00	1.078E 01	1.165E 01	1.165E 01	1.222E 01	1.472E 01	1.776E 01	1.804E 01	1.711E 01
30	7.620E 00	7.943E 00	8.886E 00	1.003E 01	1.040E 01	1.041E 01	1.164E 01	1.444E 01	1.650E 01	1.578E 01
31	6.495E 00	6.730E 00	7.258E 00	8.297E 00	9.035E 00	9.073E 00	9.414E 00	1.125E 01	1.384E 01	1.466E 01
32	5.392E 00	5.670E 00	5.939E 00	6.673E 00	7.547E 00	7.845E 00	7.842E 00	8.712E 00	1.086E 01	1.274E 01
33	4.358E 00	4.690E 00	4.862E 00	5.292E 00	6.067E 00	6.595E 00	6.610E 00	6.858E 00	8.227E 00	1.025E 01
34	3.442E 00	3.778E 00	3.946E 00	4.171E 00	4.731E 00	5.333E 00	5.506E 00	5.498E 00	6.169E 00	7.777E 00
35	2.665E 00	2.956E 00	3.140E 00	3.265E 00	3.612E 00	4.148E 00	4.455E 00	4.428E 00	4.647E 00	5.687E 00
36	2.024E 00	2.247E 00	2.432E 00	2.522E 00	2.712E 00	3.114E 00	3.467E 00	3.515E 00	3.523E 00	4.073E 00
37	1.504E 00	1.659E 00	1.822E 00	1.904E 00	2.002E 00	2.265E 00	2.587E 00	2.707E 00	2.662E 00	2.886E 00
38	1.08AE 00	1.188E 00	1.315E 00	1.393E 00	1.445E 00	1.599E 00	1.849E 00	2.000E 00	1.974E 00	2.024E 00
39	7.577E-01	8.201E-01	9.109E-01	9.776E-01	1.010E 00	1.092E 00	1.263E 00	1.407E 00	1.412E 00	1.394E 00
40	5.03AE-01	5.412E-01	6.003E-01	6.519E-01	6.747E-01	7.153E-01	8.204E-01	9.346E-01	9.607E-01	9.298E-01
41	3.152E-01	3.365E-01	3.718E-01	4.074E-01	4.240E-01	4.429E-01	5.012E-01	5.795E-01	6.106E-01	5.877E-01
42	1.812E-01	1.927E-01	2.119E-01	2.336E-01	2.448E-01	2.531E-01	2.823E-01	3.290E-01	3.546E-01	3.426E-01
43	9.221E-02	9.785E-02	1.070E-01	1.185E-01	1.250E-01	1.285E-01	1.413E-01	1.652E-01	1.814E-01	1.767E-01
44	3.87nE-02	4.101E-02	4.468E-02	4.954E-02	5.258E-02	5.389E-02	5.858E-02	6.849E-02	7.629E-02	7.501E-02
45	1.142E-02	1.209E-02	1.314E-02	1.458E-02	1.554E-02	1.590E-02	1.714E-02	2.002E-02	2.252E-02	2.232E-02

Table B.3 (continued)

SCATTERING KERNEL, SIGMA(U(J) TO U(I))/UNIT LETHARGY, KT = .02699, J = 21 TO 30

I	J = 21	22	23	24	25	26	27	28	29	30
1	2.529E-21	1.673E-21	1.128E-21	7.767E-22	5.453E-22	3.907E-22	2.856E-22	2.131E-22	1.623E-22	1.262E-22
2	2.373E-15	1.570E-15	1.059E-15	7.290E-16	5.119E-16	3.668E-16	2.681E-16	2.000E-16	1.523E-16	1.184E-16
3	3.402E-11	2.251E-11	1.519E-11	1.045E-11	7.335E-12	5.252E-12	3.836E-12	2.859E-12	2.175E-12	1.688E-12
4	2.774E-08	1.841E-08	1.245E-08	8.580E-09	6.029E-09	4.319E-09	3.155E-09	2.350E-09	1.786E-09	1.385E-09
5	3.192E-06	2.119E-06	1.435E-06	9.904E-07	6.970E-07	5.001E-07	3.657E-07	2.727E-07	2.073E-07	1.607E-07
6	1.044E-04	6.867E-05	4.613E-05	3.163E-05	2.214E-05	1.581E-05	1.152E-05	8.564E-06	6.494E-06	5.023E-06
7	1.387E-03	9.106E-04	6.098E-04	4.166E-04	2.904E-04	2.062E-04	1.499E-04	1.109E-04	8.379E-05	6.457E-05
8	9.356E-03	6.158E-03	4.130E-03	2.824E-03	1.970E-03	1.401E-03	1.016E-03	7.512E-04	5.666E-04	4.360E-04
9	3.880E-02	2.557E-02	1.716E-02	1.175E-02	8.208E-03	5.845E-03	4.244E-03	3.141E-03	2.371E-03	1.825E-03
10	1.14AE-01	7.502E-02	5.025E-02	3.440E-02	2.403E-02	1.713E-02	1.245E-02	9.223E-03	6.968E-03	5.367E-03
11	2.45AE-01	1.592E-01	1.126E-01	8.118E-02	5.734E-02	3.969E-02	2.782E-02	2.032E-02	1.550E-02	1.219E-02
12	5.25AE-01	3.113E-01	1.985E-01	1.399E-01	1.035E-01	7.630E-02	5.515E-02	3.957E-02	2.898E-02	2.208E-02
13	9.89AE-01	6.510E-01	3.980E-01	2.519E-01	1.750E-01	1.307E-01	9.979E-02	7.546E-02	5.626E-02	4.200E-02
14	1.527E 00	1.129E 00	7.962E-01	5.103E-01	3.253E-01	2.221E-01	1.650E-01	1.286E-01	1.012E-01	7.885E-02
15	2.963E 00	1.737E 00	1.274E 00	9.563E-01	6.513E-01	4.257E-01	2.881E-01	2.104E-01	1.645E-01	1.329E-01
16	6.93AE 00	3.525E 00	2.011E 00	1.435E 00	1.124E 00	8.204E-01	5.598E-01	3.818E-01	2.742E-01	2.115E-01
17	1.17AE 01	7.981E 00	4.221E 00	2.372E 00	1.628E 00	1.296E 00	1.011E 00	7.320E-01	5.133E-01	3.674E-01
18	1.25AE 01	1.196E 01	9.095E 00	5.074E 00	2.848E 00	1.877E 00	1.476E 00	1.213E 00	9.403E-01	6.919E-01
19	2.08AE 01	1.285E 01	1.213E 01	1.022E 01	6.101E 00	3.473E 00	2.213E 00	1.682E 00	1.416E 00	1.173E 00
20	5.642E 01	2.213E 01	1.324E 01	1.223E 01	1.125E 01	7.310E 00	4.285E 00	2.678E 00	1.945E 00	1.624E 00
21	1.791E 02	5.875E 01	2.350E 01	1.372E 01	1.231E 01	1.209E 01	8.684E 00	5.324E 00	3.320E 00	2.312E 00
22	8.100E 01	1.787E 02	6.118E 01	2.502E 01	1.429E 01	1.238E 01	1.266E 01	1.016E 01	6.627E 00	4.201E 00
23	4.357E 01	8.225E 01	1.781E 02	6.370E 01	2.668E 01	1.497E 01	1.246E 01	1.295E 01	1.161E 01	8.207E 00
24	3.337E 01	4.408E 01	8.347E 01	1.775E 02	6.632E 01	2.849E 01	1.577E 01	1.257E 01	1.301E 01	1.283E 01
25	3.814E 01	3.214E 01	4.462E 01	8.465E 01	1.767E 02	6.902E 01	3.047E 01	1.670E 01	1.273E 01	1.290E 01
26	4.65AE 01	3.458E 01	3.111E 01	4.518E 01	8.574E 01	1.759E 02	7.179E 01	3.262E 01	1.777E 01	1.296E 01
27	4.042E 01	4.272E 01	3.128E 01	3.022E 01	4.574E 01	8.674E 01	1.749E 02	7.462E 01	3.494E 01	1.900E 01
28	2.909E 01	4.027E 01	3.816E 01	2.828E 01	2.943E 01	4.627E 01	8.760E 01	1.736E 02	7.748E 01	3.744E 01
29	2.067E 01	3.992E 01	3.898E 01	3.334E 01	2.556E 01	2.873E 01	4.674E 01	8.829E 01	1.722E 02	8.036E 01
30	1.590E 01	3.095E 01	3.045E 01	3.631E 01	2.862E 01	2.313E 01	2.808E 01	4.712E 01	8.876E 01	1.705E 02
31	1.36AE 01	1.518E 01	2.140E 01	3.034E 01	3.232E 01	2.421E 01	2.095E 01	2.747E 01	4.738E 01	8.896E 01
32	1.24AE 01	1.200E 01	1.488E 01	2.179E 01	2.920E 01	2.746E 01	2.022E 01	1.900E 01	2.687E 01	4.747E 01
33	1.109E 01	1.033E 01	1.085E 01	1.487E 01	2.186E 01	2.672E 01	2.232E 01	1.670E 01	1.728E 01	2.625E 01
34	9.205E 00	9.095E 00	8.544E 00	1.019E 01	1.498E 01	2.125E 01	2.293E 01	1.744E 01	1.366E 01	1.575E 01
35	7.132E 00	7.708E 00	7.126E 00	7.290E 00	9.916E 00	1.494E 01	1.956E 01	1.829E 01	1.314E 01	1.111E 01
36	5.221E 00	6.130E 00	5.968E 00	5.524E 00	6.560E 00	9.816E 00	1.438E 01	1.667E 01	1.352E 01	9.553E 00
37	3.656E 00	4.545E 00	4.800E 00	4.342E 00	4.450E 00	6.215E 00	9.616E 00	1.297E 01	1.286E 01	9.264E 00
38	2.470E 00	3.201E 00	3.631E 00	3.395E 00	3.124E 00	3.867E 00	6.025E 00	8.979E 00	1.059E 01	8.853E 00
39	1.615E 00	2.122E 00	2.568E 00	2.543E 00	2.232E 00	2.398E 00	3.588E 00	5.694E 00	7.640E 00	7.566E 00
40	1.010E 00	1.329E 00	1.691E 00	1.784E 00	1.567E 00	1.487E 00	2.044E 00	3.353E 00	4.945E 00	5.643E 00
41	6.128E-01	7.821E-01	1.031E 00	1.153E 00	1.042E 00	9.085E-01	1.114E 00	1.835E 00	2.906E 00	3.699E 00
42	3.434E-01	4.249E-01	5.730E-01	6.734E-01	6.323E-01	5.276E-01	5.737E-01	9.235E-01	1.542E 00	2.136E 00
43	1.722E-01	2.061E-01	2.813E-01	3.441E-01	3.357E-01	2.759E-01	2.701E-01	4.158E-01	7.215E-01	1.067E 00
44	7.174E-02	8.329E-02	1.142E-01	1.440E-01	1.453E-01	1.194E-01	1.080E-01	1.574E-01	2.801E-01	4.350E-01
45	2.111E-02	2.394E-02	3.283E-02	4.229E-02	4.372E-02	3.618E-02	3.104E-02	4.299E-02	7.763E-02	1.249E-01

Table B.3 (continued)

SCATTERING KERNEL, SIGMA(U(J) TO U(I))/UNIT LETHARGY, KT = .02699, J = 31 TO 40

I	J = 31	32	33	34	35	36	37	38	39	40
1	1.002E-22	8.137E-23	6.752E-23	5.732E-23	4.982E-23	4.438E-23	4.057E-23	3.812E-23	3.692E-23	3.696E-23
2	9.405E-17	7.632E-17	6.332E-17	5.374E-17	4.669E-17	4.158E-17	3.801E-17	3.571E-17	3.458E-17	3.462E-17
3	1.330E-12	1.085E-12	8.985E-13	7.612E-13	6.603E-13	5.871E-13	5.357E-13	5.025E-13	4.859E-13	4.858E-13
4	1.096E-09	8.863E-10	7.322E-10	6.186E-10	5.350E-10	4.741E-10	4.312E-10	4.032E-10	3.886E-10	3.874E-10
5	1.271E-07	1.026E-07	8.463E-08	7.135E-08	6.154E-08	5.438E-08	4.931E-08	4.595E-08	4.414E-08	4.386E-08
6	3.965E-06	3.194E-06	2.629E-06	2.211E-06	1.902E-06	1.676E-06	1.515E-06	1.408E-06	1.349E-06	1.336E-06
7	5.079E-05	4.078E-05	3.345E-05	2.804E-05	2.405E-05	2.113E-05	1.904E-05	1.764E-05	1.685E-05	1.664E-05
8	3.423E-04	2.743E-04	2.245E-04	1.878E-04	1.607E-04	1.403E-04	1.266E-04	1.170E-04	1.114E-04	1.098E-04
9	1.439E-03	1.149E-03	9.387E-04	7.845E-04	6.705E-04	5.869E-04	5.268E-04	4.860E-04	4.621E-04	4.545E-04
10	4.216E-03	3.379E-03	2.765E-03	2.311E-03	1.974E-03	1.727E-03	1.549E-03	1.428E-03	1.357E-03	1.333E-03
11	9.716E-03	7.808E-03	6.336E-03	5.226E-03	4.410E-03	3.823E-03	3.415E-03	3.147E-03	2.996E-03	2.955E-03
12	1.750E-02	1.427E-02	1.185E-02	9.971E-03	8.502E-03	7.378E-03	6.551E-03	5.981E-03	5.640E-03	5.517E-03
13	3.200E-02	2.642E-02	2.090E-02	1.771E-02	1.536E-02	1.359E-02	1.223E-02	1.126E-02	1.065E-02	1.041E-02
14	6.100E-02	4.750E-02	3.782E-02	3.113E-02	2.655E-02	2.341E-02	2.126E-02	1.983E-02	1.901E-02	1.879E-02
15	1.080E-01	8.735E-02	7.051E-02	5.743E-02	4.777E-02	4.095E-02	3.635E-02	3.346E-02	3.193E-02	3.163E-02
16	1.724E-01	1.444E-01	1.219E-01	1.029E-01	8.721E-02	7.475E-02	6.539E-02	5.888E-02	5.491E-02	5.331E-02
17	2.780E-01	2.342E-01	1.898E-01	1.651E-01	1.455E-01	1.293E-01	1.160E-01	1.058E-01	9.867E-02	9.499E-02
18	5.042E-01	3.781E-01	2.989E-01	2.502E-01	2.195E-01	1.990E-01	1.843E-01	1.737E-01	1.669E-01	1.643E-01
19	9.200E-01	6.990E-01	5.316E-01	4.163E-01	3.417E-01	2.958E-01	2.687E-01	2.541E-01	2.484E-01	2.504E-01
20	1.414E 00	1.187E 00	9.587E-01	7.598E-01	6.054E-01	4.951E-01	4.217E-01	3.773E-01	3.550E-01	3.509E-01
21	1.861E 00	1.643E 00	1.466E 00	1.271E 00	1.073E 00	8.968E-01	7.551E-01	6.506E-01	5.810E-01	5.433E-01
22	2.844E 00	2.479E 00	1.883E 00	1.731E 00	1.599E 00	1.452E 00	1.300E 00	1.163E 00	1.053E 00	9.775E-01
23	5.395E 00	3.631E 00	2.659E 00	2.187E 00	1.987E 00	1.900E 00	1.838E 00	1.773E 00	1.713E 00	1.672E 00
24	1.002E 01	6.970E 00	4.777E 00	3.419E 00	2.664E 00	2.305E 00	2.179E 00	2.172E 00	2.223E 00	2.311E 00
25	1.363E 01	1.192E 01	8.963E 00	6.414E 00	4.625E 00	3.493E 00	2.850E 00	2.552E 00	2.490E 00	2.592E 00
26	1.268E 01	1.393E 01	1.361E 01	1.130E 01	8.655E 00	6.494E 00	4.944E 00	3.924E 00	3.323E 00	3.055E 00
27	1.326E 01	1.239E 01	1.374E 01	1.473E 01	1.370E 01	1.150E 01	9.243E 00	7.387E 00	6.009E 00	5.074E 00
28	2.942E 01	1.367E 01	1.206E 01	1.316E 01	1.503E 01	1.564E 01	1.464E 01	1.292E 01	1.119E 01	9.771E 00
29	4.012E 01	2.203E 01	1.422E 01	1.174E 01	1.230E 01	1.445E 01	1.654E 01	1.737E 01	1.711E 01	1.642E 01
30	8.321E 01	4.298E 01	2.387E 01	1.496E 01	1.149E 01	1.129E 01	1.316E 01	1.604E 01	1.872E 01	2.070E 01
31	1.684E 02	8.509E 01	4.602E 01	2.598E 01	1.593E 01	1.140E 01	1.023E 01	1.138E 01	1.420E 01	1.797E 01
32	8.885E 01	1.659E 02	8.863E 01	4.921E 01	2.837E 01	1.723E 01	1.158E 01	9.326E 00	9.438E 00	1.145E 01
33	4.734E 01	8.926E 01	1.629E 02	9.105E 01	5.252E 01	3.109E 01	1.894E 01	1.218E 01	8.803E 00	7.728E 00
34	2.556E 01	4.693E 01	8.719E 01	1.593E 02	9.314E 01	5.590E 01	3.414E 01	2.113E 01	1.338E 01	8.934E 00
35	1.446E 01	2.483E 01	4.616E 01	8.548E 01	1.549E 02	9.477E 01	5.926E 01	3.752E 01	2.389E 01	1.531E 01
36	9.027E 00	1.321E 01	2.393E 01	4.404E 01	8.301E 01	1.495E 02	9.577E 01	6.250E 01	4.120E 01	2.729E 01
37	6.738E 00	7.383E 00	1.212E 01	2.282E 01	4.317E 01	7.964E 01	1.430E 02	9.597E 01	6.551E 01	4.520E 01
38	5.874E 00	4.642E 00	6.115E 00	1.108E 01	2.143E 01	4.075E 01	7.524E 01	1.352E 02	9.520E 01	6.820E 01
39	5.367E 00	3.454E 00	3.235E 00	5.133E 00	9.990E 00	1.967E 01	3.760E 01	6.970E 01	1.260E 02	9.330E 01
40	4.594E 00	2.827E 00	1.916E 00	2.313E 00	4.320E 00	8.789E 00	1.750E 01	3.369E 01	6.295E 01	1.152E 02
41	3.441E 00	2.275E 00	1.281E 00	1.058E 00	1.719E 00	3.567E 00	7.428E 00	1.493E 01	2.902E 01	5.499E 01
42	2.221E 00	1.634E 00	8.858E-01	5.145E-01	6.282E-01	1.285E 00	2.803E 00	5.913E 00	1.202E 01	2.370E 01
43	1.218E 00	9.818E-01	5.569E-01	2.606E-01	2.114E-01	3.998E-01	9.103E-01	2.021E 00	4.310E 00	8.887E 00
44	5.251E-01	4.414E-01	2.798E-01	1.208E-01	6.430E-02	1.017E-01	2.406E-01	5.634E-01	1.264E 00	2.729E 00
45	1.574E-01	1.462E-01	9.392E-02	4.024E-02	1.960E-02	1.878E-02	4.580E-02	1.131E-01	2.665E-01	6.023E-01

Table B.3 (continued)

SCATTERING KERNEL, SIGMA(U(J) TO U(I))/UNIT LETHARGY, KT = .0253, J = 41 TO 45

I	J = 41	42	43	44	45
1	6.745E-025	7.294E-025	8.372E-025	1.045E-024	1.495E-024
2	1.644E-018	1.778E-018	2.041E-018	2.546E-018	3.643E-018
3	4.497E-014	4.857E-014	5.571E-014	6.948E-014	9.936E-014
4	5.728E-011	6.171E-011	7.064E-011	8.794E-011	1.256E-010
5	9.050E-009	9.721E-009	1.110E-008	1.378E-008	1.966E-008
6	3.511E-007	3.764E-007	4.285E-007	5.314E-007	7.565E-007
7	5.232E-006	5.591E-006	6.354E-006	7.863E-006	1.118E-005
8	3.946E-005	4.205E-005	4.770E-005	5.894E-005	8.369E-005
9	1.807E-004	1.922E-004	2.176E-004	2.685E-004	3.810E-004
10	5.716E-004	6.078E-004	6.872E-004	8.471E-004	1.201E-003
11	1.353E-003	1.446E-003	1.642E-003	2.031E-003	2.886E-003
12	2.618E-003	2.783E-003	3.152E-003	3.892E-003	5.529E-003
13	5.170E-003	5.462E-003	6.148E-003	7.553E-003	1.068E-002
14	9.870E-003	1.051E-002	1.188E-002	1.464E-002	2.073E-002
15	1.726E-002	1.834E-002	2.116E-002	2.624E-002	3.737E-002
16	2.959E-002	3.139E-002	3.555E-002	4.394E-002	6.245E-002
17	5.455E-002	5.686E-002	6.331E-002	7.716E-002	1.085E-001
18	1.006E-001	1.059E-001	1.184E-001	1.444E-001	2.028E-001
19	1.623E-001	1.754E-001	2.006E-001	2.487E-001	3.536E-001
20	2.291E-001	2.489E-001	2.875E-001	3.606E-001	5.179E-001
21	3.451E-001	3.578E-001	3.996E-001	4.904E-001	6.950E-001
22	6.411E-001	6.414E-001	6.889E-001	8.151E-001	1.123E 000
23	1.201E 000	1.234E 000	1.345E 000	1.602E 000	2.209E 000
24	1.818E 000	1.976E 000	2.254E 000	2.779E 000	3.926E 000
25	2.104E 000	2.392E 000	2.852E 000	3.653E 000	5.306E 000
26	2.258E 000	2.445E 000	2.872E 000	3.686E 000	5.406E 000
27	3.458E 000	3.261E 000	3.391E 000	3.970E 000	5.482E 000
28	7.108E 000	6.556E 000	6.497E 000	7.157E 000	9.324E 000
29	1.347E 001	1.318E 001	1.365E 001	1.551E 001	2.056E 001
30	1.953E 001	2.093E 001	2.326E 001	2.787E 001	3.841E 001
31	1.956E 001	2.365E 001	2.880E 001	3.693E 001	5.334E 001
32	1.310E 001	1.777E 001	2.411E 001	3.364E 001	5.153E 001
33	7.047E 000	9.227E 000	1.319E 001	1.981E 001	3.233E 001
34	5.499E 000	4.893E 000	5.560E 000	7.708E 000	1.253E 001
35	8.594E 000	5.611E 000	4.049E 000	3.516E 000	4.038E 000
36	1.639E 001	1.052E 001	7.091E 000	5.084E 000	4.307E 000
37	2.949E 001	2.012E 001	1.411E 001	1.058E 001	9.309E 000
38	4.797E 001	3.451E 001	2.560E 001	2.036E 001	1.899E 001
39	7.015E 001	5.300E 001	4.144E 001	3.481E 001	3.428E 001
40	9.173E 001	7.238E 001	5.942E 001	5.255E 001	5.442E 001
41	1.065E 002	8.735E 001	7.488E 001	6.938E 001	7.520E 001
42	4.703E 001	9.187E 001	8.183E 001	7.895E 001	8.904E 001
43	1.807E 001	3.668E 001	7.571E 001	7.561E 001	8.818E 001
44	5.682E 000	1.201E 001	2.566E 001	5.815E 001	6.968E 001
45	1.279E 000	2.813E 000	6.215E 000	1.447E 001	3.944E 001

TABLE B.4

ENERGY DEPENDENT CROSS SECTIONS

I	ENERGY	H2O SCATTERING CROSS SECTION (BARNS)	H2O TRANSPORT CROSS SECTION (BARNS)	U235 SCATTER CROSS SECTION (BARNS)	U238 SCATTER CROSS SECTION (BARNS)	O16 SCATTER CROSS SECTION (BARNS)
1	1.6093E 000	4.4500E 001	1.8595E 001	1.0000E 001	8.3003E 000	3.7619E 000
2	1.2311E 000	4.4500E 001	1.9453E 001	1.0000E 001	8.3004E 000	3.7624E 000
3	9.6667E-001	4.4599E 001	2.0356E 001	1.0001E 001	8.3005E 000	3.7631E 000
4	7.7041E-001	4.4701E 001	2.1218E 001	1.0001E 001	8.3006E 000	3.7638E 000
5	6.4501E-001	4.5000E 001	2.2092E 001	1.0001E 001	8.3007E 000	3.7646E 000
6	5.4731E-001	4.6000E 001	2.3281E 001	1.0001E 001	8.3008E 000	3.7655E 000
7	4.7542E-001	4.7500E 001	2.4711E 001	1.0001E 001	8.3009E 000	3.7663E 000
8	4.2192E-001	4.9000E 001	2.6133E 001	1.0001E 001	8.3011E 000	3.7671E 000
9	3.8170E-001	5.0500E 001	2.7239E 001	1.0001E 001	8.3012E 000	3.7678E 000
10	3.5119E-001	5.1400E 001	2.8140E 001	1.0002E 001	8.3013E 000	3.7685E 000
11	3.2786E-001	5.2400E 001	2.9057E 001	1.0002E 001	8.3014E 000	3.7691E 000
12	3.0990E-001	5.3001E 001	2.9658E 001	1.0002E 001	8.3014E 000	3.7697E 000
13	2.9244E-001	5.3800E 001	3.0377E 001	1.0002E 001	8.3015E 000	3.7702E 000
14	2.7549E-001	5.4500E 001	3.1048E 001	1.0002E 001	8.3016E 000	3.7709E 000
15	2.5905E-001	5.5400E 001	3.1785E 001	1.0002E 001	8.3017E 000	3.7716E 000
16	2.4311E-001	5.6200E 001	3.2585E 001	1.0002E 001	8.3018E 000	3.7723E 000
17	2.2768E-001	5.7100E 001	3.3454E 001	1.0002E 001	8.3020E 000	3.7732E 000
18	2.1275E-001	5.8001E 001	3.4333E 001	1.0003E 001	8.3021E 000	3.7741E 000
19	1.9833E-001	5.9000E 001	3.5283E 001	1.0003E 001	8.3022E 000	3.7751E 000
20	1.8442E-001	6.0000E 001	3.6246E 001	1.0003E 001	8.3024E 000	3.7762E 000
21	1.7101E-001	6.1000E 001	3.7282E 001	1.0003E 001	8.3026E 000	3.7775E 000
22	1.5811E-001	6.2100E 001	3.8395E 001	1.0003E 001	8.3028E 000	3.7789E 000
23	1.4571E-001	6.3499E 001	3.9773E 001	1.0004E 001	8.3030E 000	3.7806E 000
24	1.3382E-001	6.4500E 001	4.0795E 001	1.0004E 001	8.3033E 000	3.7824E 000
25	1.2244E-001	6.6400E 001	4.2532E 001	1.0004E 001	8.3036E 000	3.7845E 000
26	1.1156E-001	6.7999E 001	4.4176E 001	1.0005E 001	8.3040E 000	3.7868E 000
27	1.0119E-001	6.9501E 001	4.5855E 001	1.0005E 001	8.3044E 000	3.7896E 000
28	9.1325E-002	7.1000E 001	4.7635E 001	1.0006E 001	8.3049E 000	3.7928E 000
29	8.1965E-002	7.3500E 001	5.0055E 001	1.0007E 001	8.3054E 000	3.7965E 000
30	7.3110E-002	7.5499E 001	5.2032E 001	1.0007E 001	8.3061E 000	3.8010E 000
31	6.4762E-002	7.7500E 001	5.4045E 001	1.0008E 001	8.3069E 000	3.8062E 000
32	5.6920E-002	8.0500E 001	5.6793E 001	1.0010E 001	8.3078E 000	3.8126E 000
33	4.9583E-002	8.3500E 001	5.9926E 001	1.0011E 001	8.3090E 000	3.8204E 000
34	4.2753E-002	8.7000E 001	6.4021E 001	1.0013E 001	8.3104E 000	3.8301E 000
35	3.6429E-002	9.2500E 001	7.0206E 001	1.0015E 001	8.3122E 000	3.8422E 000
36	3.0610E-002	9.9000E 001	7.7626E 001	1.0018E 001	8.3145E 000	3.8578E 000
37	2.5298E-002	1.0700E 002	8.6477E 001	1.0021E 001	8.3176E 000	3.8784E 000
38	2.0491E-002	1.1600E 002	9.6555E 001	1.0026E 001	8.3217E 000	3.9062E 000
39	1.6191E-002	1.2500E 002	1.0683E 002	1.0033E 001	8.3274E 000	3.9450E 000
40	1.2396E-002	1.3500E 002	1.1813E 002	1.0044E 001	8.3358E 000	4.0016E 000
41	9.1072E-003	1.4400E 002	1.2884E 002	1.0060E 001	8.3488E 000	4.0888E 000
42	6.3244E-003	1.5600E 002	1.4267E 002	1.0086E 001	8.3702E 000	4.2332E 000
43	4.0476E-003	1.7200E 002	1.6110E 002	1.0134E 001	8.4098E 000	4.4960E 000
44	2.2768E-003	1.9500E 002	1.8825E 002	1.0238E 001	8.4951E 000	5.0391E 000
45	1.0119E-003	2.3700E 002	2.3914E 002	1.0536E 001	8.7390E 000	6.3850E 000

TABLE B.5

ENERGY DEPENDENT CROSS SECTIONS

I	ENERGY	U235 ABSORPTION CROSS SECTION (BARNS)	U235 FISSION CROSS SECTION (BARNS)	FUEL ABSORPTION CROSS SECTION (1/CM)	FUEL FISSION CROSS SECTION (1/CM)	1 + ALPHA	SLOWING DOWN SOURCE
1	1.6093E 00	1.8800E 01	1.5800E 01	1.6427E-02	7.6627E-03	2.1438E 00	1.0341E 00
2	1.2311E 00	4.8100E 01	4.2000E 01	3.2129E-02	2.0369E-02	1.5773E 00	7.9101E-01
3	9.6667E-01	7.1700E 01	6.2100E 01	4.4705E-02	3.0117E-02	1.4844E 00	6.2110E-01
4	7.7941E-01	6.2300E 01	5.3800E 01	4.1275E-02	2.6092E-02	1.5819E 00	5.0067E-01
5	6.4501E-01	6.9800E 01	6.1700E 01	4.6011E-02	2.9924E-02	1.5376E 00	4.1408E-01
6	5.4731E-01	8.1500E 01	7.1600E 01	5.2725E-02	3.4725E-02	1.5184E 00	3.5090E-01
7	4.7542E-01	1.0010E 02	8.7900E 01	6.2709E-02	4.2630E-02	1.4710E 00	3.0415E-01
8	4.2192E-01	1.2210E 02	1.0570E 02	7.4250E-02	5.1263E-02	1.4484E 00	2.6915E-01
9	3.8170E-01	1.4670E 02	1.2580E 02	8.6953E-02	6.1011E-02	1.4252E 00	2.4266E-01
10	3.5119E-01	1.7650E 02	1.4810E 02	1.0208E-01	7.1826E-02	1.4212E 00	2.2245E-01
11	3.2786E-01	2.0130E 02	1.6620E 02	1.1468E-01	8.0604E-02	1.4228E 00	2.0690E-01
12	3.0990E-01	2.2430E 02	1.8330E 02	1.2632E-01	8.8898E-02	1.4210E 00	1.9489E-01
13	2.9244E-01	2.3700E 02	1.8810E 02	1.3300E-01	9.1225E-02	1.4579E 00	1.8316E-01
14	2.7549E-01	2.3960E 02	1.8840E 02	1.3481E-01	9.1371E-02	1.4754E 00	1.7172E-01
15	2.5905E-01	2.3160E 02	1.7760E 02	1.3151E-01	8.6133E-02	1.5268E 00	1.6059E-01
16	2.4311E-01	2.2110E 02	1.6870E 02	1.2655E-01	8.1817E-02	1.5468E 00	1.4975E-01
17	2.2768E-01	2.1080E 02	1.6690E 02	1.2270E-01	8.0944E-02	1.5159E 00	1.3922E-01
18	2.1275E-01	2.0780E 02	1.6720E 02	1.2195E-01	8.1089E-02	1.5039E 00	1.2900E-01
19	1.9833E-01	2.1000E 02	1.7140E 02	1.2377E-01	8.3126E-02	1.4890E 00	1.1910E-01
20	1.8442E-01	2.1310E 02	1.7570E 02	1.2609E-01	8.5212E-02	1.4797E 00	1.0954E-01
21	1.7101E-01	2.1870E 02	1.8130E 02	1.2968E-01	8.7928E-02	1.4748E 00	1.0031E-01
22	1.5811E-01	2.2520E 02	1.8780E 02	1.3378E-01	9.1080E-02	1.4688E 00	9.1439E-02
23	1.4571E-01	2.3330E 02	1.9630E 02	1.3873E-01	9.5202E-02	1.4572E 00	8.2929E-02
24	1.3382E-01	2.4290E 02	2.0620E 02	1.4450E-01	1.0000E-01	1.4449E 00	7.4796E-02
25	1.2244E-01	2.5560E 02	2.1810E 02	1.5187E-01	1.0577E-01	1.4358E 00	6.7053E-02
26	1.1156E-01	2.7070E 02	2.3100E 02	1.6052E-01	1.1203E-01	1.4328E 00	5.9712E-02
27	1.0119E-01	2.8960E 02	2.4710E 02	1.7115E-01	1.1984E-01	1.4282E 00	5.2786E-02
28	9.1325E-02	3.0880E 02	2.6420E 02	1.8208E-01	1.2813E-01	1.4210E 00	4.6287E-02
29	8.1965E-02	3.3190E 02	2.8430E 02	1.9508E-01	1.3788E-01	1.4148E 00	4.0225E-02
30	7.3110E-02	3.5560E 02	3.0500E 02	2.0858E-01	1.4792E-01	1.4101E 00	3.4608E-02
31	6.4762E-02	3.8600E 02	3.3220E 02	2.2558E-01	1.6111E-01	1.4001E 00	2.9445E-02
32	5.6920E-02	4.1810E 02	3.6000E 02	2.4370E-01	1.7459E-01	1.3958E 00	2.4738E-02
33	4.9583E-02	4.5600E 02	3.9210E 02	2.6501E-01	1.9016E-01	1.3936E 00	2.0488E-02
34	4.2753E-02	4.9930E 02	4.2860E 02	2.8938E-01	2.0786E-01	1.3922E 00	1.6694E-02
35	3.6429E-02	5.4930E 02	4.7120E 02	3.1757E-01	2.2852E-01	1.3896E 00	1.3348E-02
36	3.0610E-02	6.0900E 02	5.2140E 02	3.5117E-01	2.5287E-01	1.3887E 00	1.0441E-02
37	2.5298E-02	6.7900E 02	5.8090E 02	3.9070E-01	2.8173E-01	1.3868E 00	7.9565E-03
38	2.0491E-02	7.6310E 02	6.5290E 02	4.3831E-01	3.1665E-01	1.3842E 00	5.8763E-03
39	1.6191E-02	8.6720E 02	7.4190E 02	4.9732E-01	3.5981E-01	1.3822E 00	4.1759E-03
40	1.2396E-02	9.9990E 02	8.5540E 02	5.7264E-01	4.1486E-01	1.3803E 00	2.8270E-03
41	9.1072E-03	1.1750E 03	1.0060E 03	6.7218E-01	4.8789E-01	1.3777E 00	1.7966E-03
42	6.3244E-03	1.4190E 03	1.2140E 03	8.1098E-01	5.8877E-01	1.3774E 00	1.0479E-03
43	4.0476E-03	1.7840E 03	1.5260E 03	1.0187E 00	7.4009E-01	1.3765E 00	5.3996E-04
44	2.2768E-03	2.3880E 03	2.0430E 03	1.3628E 00	9.9082E-01	1.3754E 00	2.2894E-04
45	1.0119E-03	3.5920E 03	3.0730E 03	2.0490E 00	1.4904E 00	1.3749E 00	6.8079E-05

TABLE B.6

SPATIALLY AVERAGED THERMAL SPECTRA FOR THE CORNELL ZPR 1:1 CORE

I	ENERGY	MODERATOR SPECTRUM	CLADDING SPECTRUM	FUEL SPECTRUM
1	1.6093E 00	5.4517E-01	5.4549E-01	5.3873E-01
2	1.2311E 00	6.1583E-01	6.1323E-01	6.0196E-01
3	9.6667E-01	8.0549E-01	7.9914E-01	7.8064E-01
4	7.7941E-01	1.0053E 00	9.9849E-01	9.7670E-01
5	6.4501E-01	1.2364E 00	1.2265E 00	1.1975E 00
6	5.4731E-01	1.4605E 00	1.4462E 00	1.4084E 00
7	4.7542E-01	1.6733E 00	1.6526E 00	1.6032E 00
8	4.2192E-01	1.8733E 00	1.8446E 00	1.7814E 00
9	3.8170E-01	2.0569E 00	2.0188E 00	1.9400E 00
10	3.5119E-01	2.2251E 00	2.1755E 00	2.0783E 00
11	3.2786E-01	2.4269E 00	2.3654E 00	2.2485E 00
12	3.0990E-01	2.5621E 00	2.4900E 00	2.3562E 00
13	2.9244E-01	2.6780E 00	2.5986E 00	2.4525E 00
14	2.7549E-01	2.8720E 00	2.7858E 00	2.6273E 00
15	2.5905E-01	3.1313E 00	3.0400E 00	2.8708E 00
16	2.4311E-01	3.3868E 00	3.2923E 00	3.1152E 00
17	2.2768E-01	3.6805E 00	3.5815E 00	3.3940E 00
18	2.1275E-01	4.0585E 00	3.9501E 00	3.7445E 00
19	1.9833E-01	4.5281E 00	4.4053E 00	4.1731E 00
20	1.8442E-01	5.0873E 00	4.9465E 00	4.6815E 00
21	1.7101E-01	5.7628E 00	5.5982E 00	5.2910E 00
22	1.5811E-01	6.6162E 00	6.4207E 00	6.0586E 00
23	1.4571E-01	7.7214E 00	7.4837E 00	7.0480E 00
24	1.3382E-01	9.1329E 00	8.8386E 00	8.3053E 00
25	1.2244E-01	1.0860E 01	1.0490E 01	9.8281E 00
26	1.1156E-01	1.2890E 01	1.2422E 01	1.1599E 01
27	1.0119E-01	1.5239E 01	1.4646E 01	1.3619E 01
28	9.1325E-02	1.7990E 01	1.7239E 01	1.5961E 01
29	8.1965E-02	2.1205E 01	2.0247E 01	1.8650E 01
30	7.3110E-02	2.4876E 01	2.3666E 01	2.1683E 01
31	6.4762E-02	2.8784E 01	2.7259E 01	2.4807E 01
32	5.6920E-02	3.2558E 01	3.0676E 01	2.7716E 01
33	4.9583E-02	3.5759E 01	3.3489E 01	3.0001E 01
34	4.2753E-02	3.8132E 01	3.5455E 01	3.1375E 01
35	3.6429E-02	3.9529E 01	3.6405E 01	3.1844E 01
36	3.0610E-02	3.9848E 01	3.6256E 01	3.1277E 01
37	2.5298E-02	3.8994E 01	3.4941E 01	2.9651E 01
38	2.0491E-02	3.6909E 01	3.2445E 01	2.6991E 01
39	1.6191E-02	3.3619E 01	2.8878E 01	2.3436E 01
40	1.2396E-02	2.9266E 01	2.4426E 01	1.9203E 01
41	9.1072E-03	2.4109E 01	1.9449E 01	1.4659E 01
42	6.3244E-03	1.8522E 01	1.4278E 01	1.0146E 01
43	4.0476E-03	1.2954E 01	9.3837E 00	6.1077E 00
44	2.2768E-03	7.8840E 00	5.2262E 00	2.9522E 00
45	1.0119E-03	3.7721E 00	2.1714E 00	9.4648E-01

TABLE B.7

SPATIALLY AVERAGED THERMAL SPECTRA FOR THE CORNELL ZPR 1.5:1 CORE

I	ENERGY	MODERATOR SPECTRUM	CLADDING SPECTRUM	FUEL SPECTRUM
1	1.6093E 00	5.4770E-01	5.4779E-01	5.4101E-01
2	1.2311E 00	6.2156E-01	6.1843E-01	6.0706E-01
3	9.6667E-01	8.1724E-01	8.0963E-01	7.9108E-01
4	7.7941E-01	1.0217E 00	1.0136E 00	9.9151E-01
5	6.4501E-01	1.2606E 00	1.2488E 00	1.2193E 00
6	5.4731E-01	1.4943E 00	1.4773E 00	1.4387E 00
7	4.7542E-01	1.7191E 00	1.6944E 00	1.6438E 00
8	4.2192E-01	1.9332E 00	1.8988E 00	1.8338E 00
9	3.8170E-01	2.1327E 00	2.0869E 00	2.0055E 00
10	3.5119E-01	2.3190E 00	2.2592E 00	2.1582E 00
11	3.2786E-01	2.5420E 00	2.4673E 00	2.3454E 00
12	3.0990E-01	2.6954E 00	2.6075E 00	2.4673E 00
13	2.9244E-01	2.8287E 00	2.7312E 00	2.5776E 00
14	2.7549E-01	3.0465E 00	2.9399E 00	2.7726E 00
15	2.5905E-01	3.3369E 00	3.2230E 00	3.0436E 00
16	2.4311E-01	3.6304E 00	3.5112E 00	3.3223E 00
17	2.2768E-01	3.9778E 00	3.8511E 00	3.6495E 00
18	2.1275E-01	4.4366E 00	4.2957E 00	4.0722E 00
19	1.9833E-01	5.0247E 00	4.8620E 00	4.6057E 00
20	1.8442E-01	5.7523E 00	5.5615E 00	5.2536E 00
21	1.7101E-01	6.6668E 00	6.4379E 00	6.0845E 00
22	1.5811E-01	7.8577E 00	7.5773E 00	7.1500E 00
23	1.4571E-01	9.4351E 00	9.0828E 00	8.5541E 00
24	1.3382E-01	1.1493E 01	1.1042E 01	1.0376E 01
25	1.2244E-01	1.4078E 01	1.3491E 01	1.2641E 01
26	1.1156E-01	1.7210E 01	1.6444E 01	1.5355E 01
27	1.0119E-01	2.0941E 01	1.9937E 01	1.8538E 01
28	9.1325E-02	2.5381E 01	2.4072E 01	2.2287E 01
29	8.1965E-02	3.0613E 01	2.8896E 01	2.6617E 01
30	7.3110E-02	3.6609E 01	3.4389E 01	3.1500E 01
31	6.4762E-02	4.3073E 01	4.0222E 01	3.6603E 01
32	5.6920E-02	4.9486E 01	4.5898E 01	4.1469E 01
33	4.9583E-02	5.5219E 01	5.0801E 01	4.5509E 01
34	4.2753E-02	5.9821E 01	5.4503E 01	4.8231E 01
35	3.6429E-02	6.2963E 01	5.6618E 01	4.9524E 01
36	3.0610E-02	6.4361E 01	5.6921E 01	4.9103E 01
37	2.5298E-02	6.3762E 01	5.5227E 01	4.6866E 01
38	2.0491E-02	6.0997E 01	5.1480E 01	4.2827E 01
39	1.6191E-02	5.6058E 01	4.5874E 01	3.7230E 01
40	1.2396E-02	4.9154E 01	3.8723E 01	3.0444E 01
41	9.1072E-03	4.0712E 01	3.0685E 01	2.3128E 01
42	6.3244E-03	3.1386E 01	2.2312E 01	1.5852E 01
43	4.0476E-03	2.1971E 01	1.4437E 01	9.3966E 00
44	2.2768E-03	1.3337E 01	7.8532E 00	4.4363E 00
45	1.0119E-03	6.3281E 00	3.1495E 00	1.3728E 00

TABLE B.8

SPATIALLY AVERAGED THERMAL SPECTRA FOR THE CORNELL ZPR 2:1 CORE

I	ENERGY	MODERATOR SPECTRUM	CLADDING SPECTRUM	FUEL SPECTRUM
1	1.6093E 00	5.4898E-01	5.4887E-01	5.4207E-01
2	1.2311E 00	6.2448E-01	6.2087E-01	6.0946E-01
3	9.6667E-01	8.2325E-01	8.1492E-01	7.9606E-01
4	7.7941E-01	1.0301E 00	1.0209E 00	9.9865E-01
5	6.4501E-01	1.2730E 00	1.2596E 00	1.2298E 00
6	5.4731E-01	1.5118E 00	1.4924E 00	1.4534E 00
7	4.7542E-01	1.7429E 00	1.7148E 00	1.6635E 00
8	4.2102E-01	1.9644E 00	1.9253E 00	1.8593E 00
9	3.8170E-01	2.1725E 00	2.1202E 00	2.0375E 00
10	3.5119E-01	2.3689E 00	2.3003E 00	2.1975E 00
11	3.2786E-01	2.6038E 00	2.5180E 00	2.3936E 00
12	3.0990E-01	2.7681E 00	2.6668E 00	2.5234E 00
13	2.9244E-01	2.9124E 00	2.7996E 00	2.6422E 00
14	2.7549E-01	3.1460E 00	3.0220E 00	2.8501E 00
15	2.5905E-01	3.4581E 00	3.3248E 00	3.1398E 00
16	2.4311E-01	3.7806E 00	3.6399E 00	3.4441E 00
17	2.2768E-01	4.1711E 00	4.0200E 00	3.8096E 00
18	2.1275E-01	4.6967E 00	4.5266E 00	4.2910E 00
19	1.9833E-01	5.3856E 00	5.1862E 00	4.9128E 00
20	1.8442E-01	6.2613E 00	6.0233E 00	5.7007E 00
21	1.7101E-01	7.3914E 00	7.0999E 00	6.7102E 00
22	1.5811E-01	8.8924E 00	8.5271E 00	8.0462E 00
23	1.4571E-01	1.0909E 01	1.0438E 01	9.8308E 00
24	1.3382E-01	1.3573E 01	1.2958E 01	1.2176E 01
25	1.2244E-01	1.6971E 01	1.6151E 01	1.5133E 01
26	1.1156E-01	2.1163E 01	2.0068E 01	1.8739E 01
27	1.0119E-01	2.6233E 01	2.4767E 01	2.3030E 01
28	9.1325E-02	3.2322E 01	3.0376E 01	2.8124E 01
29	8.1965E-02	3.9526E 01	3.6932E 01	3.4019E 01
30	7.3110E-02	4.7797E 01	4.4400E 01	4.0680E 01
31	6.4762E-02	5.6769E 01	5.2359E 01	4.7649E 01
32	5.6920E-02	6.5794E 01	6.0185E 01	5.4377E 01
33	4.9583E-02	7.4071E 01	6.7090E 01	6.0102E 01
34	4.2753E-02	8.0958E 01	7.2462E 01	6.4123E 01
35	3.6429E-02	8.5931E 01	7.5681E 01	6.6199E 01
36	3.0610E-02	8.8511E 01	7.6378E 01	6.5887E 01
37	2.5298E-02	8.8270E 01	7.4250E 01	6.3009E 01
38	2.0491E-02	8.4918E 01	6.9214E 01	5.7580E 01
39	1.6191E-02	7.8403E 01	6.1574E 01	4.9971E 01
40	1.2396E-02	6.8997E 01	5.1782E 01	4.0710E 01
41	9.1072E-03	5.7299E 01	4.0814E 01	3.0762E 01
42	6.3244E-03	4.4241E 01	2.9431E 01	2.0913E 01
43	4.0476E-03	3.0975E 01	1.8818E 01	1.2249E 01
44	2.2768E-03	1.8772E 01	1.0074E 01	5.6906E 00
45	1.0119E-03	8.8666E 00	3.9564E 00	1.7245E 00

TABLE B.9

SPATIALLY AVERAGED THERMAL SPECTRA FOR THE CORNELL ZPR 3:1 CORE

I	ENERGY	MODERATOR SPECTRUM	CLADDING SPECTRUM	FUEL SPECTRUM
1	1.6093E 00	5.5025E-01	5.4979E-01	5.4298E-01
2	1.2311E 00	6.2740E-01	6.2299E-01	6.1154E-01
3	9.6667E-01	8.2930E-01	8.1943E-01	8.0045E-01
4	7.7941E-01	1.0386E 00	1.0275E 00	1.0051E 00
5	6.4501E-01	1.2855E 00	1.2694E 00	1.2394E 00
6	5.4731E-01	1.5295E 00	1.5062E 00	1.4668E 00
7	4.7542E-01	1.7671E 00	1.7333E 00	1.6814E 00
8	4.2192E-01	1.9963E 00	1.9491E 00	1.8824E 00
9	3.8170E-01	2.2135E 00	2.1503E 00	2.0664E 00
10	3.5119E-01	2.4208E 00	2.3379E 00	2.2334E 00
11	3.2786E-01	2.6693E 00	2.5651E 00	2.4384E 00
12	3.0990E-01	2.8464E 00	2.7231E 00	2.5767E 00
13	2.9244E-01	3.0052E 00	2.8671E 00	2.7059E 00
14	2.7549E-01	3.2604E 00	3.1077E 00	2.9308E 00
15	2.5905E-01	3.6043E 00	3.4384E 00	3.2471E 00
16	2.4311E-01	3.9724E 00	3.7952E 00	3.5910E 00
17	2.2768E-01	4.4338E 00	4.2404E 00	4.0184E 00
18	2.1275E-01	5.0712E 00	4.8493E 00	4.5969E 00
19	1.9833E-01	5.9324E 00	5.6662E 00	5.3675E 00
20	1.8442E-01	7.0673E 00	6.7408E 00	6.3797E 00
21	1.7101E-01	8.5809E 00	8.1684E 00	7.7201E 00
22	1.5811E-01	1.0640E 01	1.0106E 01	9.5357E 00
23	1.4571E-01	1.3451E 01	1.2740E 01	1.1999E 01
24	1.3382E-01	1.7220E 01	1.6262E 01	1.5281E 01
25	1.2244E-01	2.2110E 01	2.0796E 01	1.9484E 01
26	1.1156E-01	2.8257E 01	2.6453E 01	2.4701E 01
27	1.0119E-01	3.5816E 01	3.3342E 01	3.1004E 01
28	9.1325E-02	4.4981E 01	4.1626E 01	3.8540E 01
29	8.1965E-02	5.5868E 01	5.1313E 01	4.7266E 01
30	7.3110E-02	6.8387E 01	6.2343E 01	5.7119E 01
31	6.4762E-02	8.2050E 01	7.4117E 01	6.7450E 01
32	5.6920E-02	9.5986E 01	8.5787E 01	7.7509E 01
33	4.9583E-02	1.0909E 02	9.6262E 01	8.6236E 01
34	4.2753E-02	1.2036E 02	1.0458E 02	9.2546E 01
35	3.6429E-02	1.2889E 02	1.0966E 02	9.5918E 01
36	3.0610E-02	1.3381E 02	1.1087E 02	9.5639E 01
37	2.5298E-02	1.3434E 02	1.0771E 02	9.1404E 01
38	2.0491E-02	1.2997E 02	1.0010E 02	8.3273E 01
39	1.6191E-02	1.2054E 02	8.8597E 01	7.1902E 01
40	1.2396E-02	1.0644E 02	7.3949E 01	5.8138E 01
41	9.1072E-03	8.8606E 01	5.7754E 01	4.3530E 01
42	6.3244E-03	6.8496E 01	4.1127E 01	2.9224E 01
43	4.0476E-03	4.7951E 01	2.5877E 01	1.6843E 01
44	2.2768E-03	2.9002E 01	1.3586E 01	7.6744E 00
45	1.0119E-03	1.3635E 01	5.2270E 00	2.2783E 00

TABLE B.10

SPATIALLY AVERAGED THERMAL SPECTRA FOR THE CORNELL ZPR 4:1 CORE

I	ENERGY	MODERATOR SPECTRUM	CLADDING SPECTRUM	FUEL SPECTRUM
1	1.6093E 00	5.5090E-01	5.5015E-01	5.4333E-01
2	1.2311E 00	6.2890E-01	6.2380E-01	6.1233E-01
3	9.6667E-01	8.3241E-01	8.2121E-01	8.0220E-01
4	7.7941E-01	1.0430E 00	1.0303E 00	1.0078E 00
5	6.4501E-01	1.2920E 00	1.2736E 00	1.2435E 00
6	5.4731E-01	1.5386E 00	1.5120E 00	1.4725E 00
7	4.7542E-01	1.7795E 00	1.7409E 00	1.6889E 00
8	4.2192E-01	2.0129E 00	1.9589E 00	1.8918E 00
9	3.8170E-01	2.2350E 00	2.1627E 00	2.0783E 00
10	3.5119E-01	2.4484E 00	2.3535E 00	2.2483E 00
11	3.2786E-01	2.7049E 00	2.5854E 00	2.4576E 00
12	3.0990E-01	2.8902E 00	2.7485E 00	2.6007E 00
13	2.9244E-01	3.0592E 00	2.9000E 00	2.7369E 00
14	2.7549E-01	3.3304E 00	3.1533E 00	2.9739E 00
15	2.5905E-01	3.6990E 00	3.5054E 00	3.3103E 00
16	2.4311E-01	4.1049E 00	3.8960E 00	3.6864E 00
17	2.2768E-01	4.6265E 00	4.3957E 00	4.1656E 00
18	2.1275E-01	5.3603E 00	5.0914E 00	4.8264E 00
19	1.9833E-01	6.3721E 00	6.0438E 00	5.7252E 00
20	1.8442E-01	7.7365E 00	7.3254E 00	6.9331E 00
21	1.7101E-01	9.5931E 00	9.0621E 00	8.5648E 00
22	1.5811E-01	1.2154E 01	1.1451E 01	1.0805E 01
23	1.4571E-01	1.5685E 01	1.4728E 01	1.3870E 01
24	1.3382E-01	2.0456E 01	1.9141E 01	1.7986E 01
25	1.2244E-01	2.6706E 01	2.4867E 01	2.3299E 01
26	1.1156E-01	3.4641E 01	3.2077E 01	2.9953E 01
27	1.0119E-01	4.4483E 01	4.0918E 01	3.8049E 01
28	9.1325E-02	5.6475E 01	5.1585E 01	4.7761E 01
29	8.1965E-02	7.0749E 01	6.4047E 01	5.8995E 01
30	7.3110E-02	8.7178E 01	7.8221E 01	7.1567E 01
31	6.4762E-02	1.0516E 02	9.3344E 01	8.4947E 01
32	5.6920E-02	1.2364E 02	1.0836E 02	9.7907E 01
33	4.9583E-02	1.4122E 02	1.2192E 02	1.0922E 02
34	4.2753E-02	1.5658E 02	1.3273E 02	1.1746E 02
35	3.6429E-02	1.6844E 02	1.3926E 02	1.2181E 02
36	3.0610E-02	1.7557E 02	1.4068E 02	1.2136E 02
37	2.5298E-02	1.7687E 02	1.3696E 02	1.1571E 02
38	2.0491E-02	1.7157E 02	1.2623E 02	1.0501E 02
39	1.6191E-02	1.5947E 02	1.1117E 02	9.0218E 01
40	1.2396E-02	1.4104E 02	9.2196E 01	7.2483E 01
41	9.1072E-03	1.1753E 02	7.1498E 01	5.3889E 01
42	6.3244E-03	9.0891E 01	5.0468E 01	3.5862E 01
43	4.0476E-03	6.3611E 01	3.1432E 01	2.0459E 01
44	2.2768E-03	3.8430E 01	1.6328E 01	9.2237E 00
45	1.0119E-03	1.8025E 01	6.2363E 00	2.7183E 00

TABLE B.11

CORNELL UNIVERSITY ZERO POWER REACTOR INTEGRAL PROPERTIES

Integral Properties	Water/Oxide Volume Ratio				
	1:1	1.5:1	2:1	3:1	4:1
f	.92185	.88785	.85480	.79331	.73687
η	1.72300	1.72867	1.73165	1.73461	1.73605
ηf	1.58835	1.53480	1.48021	1.37607	1.27925
δ_n^m	1.25149	1.30644	1.35120	1.42173	1.47787
δ_n^c	1.14087	1.14917	1.15325	1.15677	1.15807
D, cm.	.3699	.3110	.2770	.2402	.2206
L, cm.	2.0086	1.9356	1.9253	1.9659	2.0298
ℓ_t, μsec.	28.69	35.17	41.53	53.43	64.37
$\bar{v}_m$, m/sec.	3667.	3318.	3134.	2945.	2849.
$\bar{v}_c$, m/sec.	3802.	3478.	3310.	3146.	3067.
$\bar{v}_f$, m/sec.	3971.	3626.	3446.	3265.	3177.
$\bar{v}_h$, m/sec.	3802.	3426.	3223.	3012.	2902.

while Table B.12 gives their temperature coefficients as defined by Eq. (7.5).

The effective cross sections, Eqs. (6.23) and (6.31), are given at 20°C for the five cores in Table B.13, the temperature coefficients being given in Table B.14.

Table B.15 lists the 20°C values of the mean cross sections, Eqs. (6.24) and (6.32), while Table B.16 lists the temperature coefficients of these cross sections.

TABLE B.12

CORNELL UNIVERSITY ZERO POWER REACTOR INTEGRAL PROPERTY TEMPERATURE COEFFICIENTS

Temperature Coefficients (10^{-4}°C^{-1})	Water/Oxide Volume Ratio				
	1:1	1.5:1	2:1	3:1	4:1
$\dot{f}/f$	+.266	+.546	+.813	+1.37	+1.95
$\dot{\eta}/\eta$	-.310	-.386	-.411	-.429	-.440
$\dot{\eta f}/\eta f$	-.044	+.160	+.402	+.941	+1.51
$\dot{\delta}_n^m/\delta_n^m$	-2.76	-3.71	-4.46	-5.56	-6.35
$\dot{\delta}_n^c/\delta_n^c$	-1.53	-1.78	-1.94	-2.08	-2.16
$\dot{D}/D$	+3.23	+4.49	+5.76	+7.27	+8.38
$\dot{L}/L$	+5.51	+6.89	+7.82	+9.10	+9.90
$\dot{\ell}_t/\ell_t$	+.048	-.411	-.807	-1.34	-1.63
$\dot{\bar{v}}_m/\bar{v}_m$	+8.32	+10.1	+11.2	+12.6	+13.3
$\dot{\bar{v}}_c/\bar{v}_c$	+7.76	+9.34	+10.3	+11.4	+12.1
$\dot{\bar{v}}_f/\bar{v}_f$	+6.92	+8.55	+9.58	+10.7	+11.5
$\dot{\bar{v}}_h/\bar{v}_h$	+7.76	+9.63	+10.9	+12.3	+13.0

TABLE B.13

CORNELL UNIVERSITY ZERO POWER REACTOR EFFECTIVE CROSS SECTIONS

Effective Cross Sections (cm^{-1})	Water/Oxide Volume Ratio				
	1:1	1.5:1	2:1	3:1	4:1
$\hat{\Sigma}_a^m$	.0219	.0219	.0219	.0219	.0219
$\hat{\Sigma}_a^c$	.0139	.0139	.0139	.0139	.0139
$\hat{\Sigma}_a^f$	.3641	.3680	.3700	.3719	.3728
$\hat{\Sigma}_s^m$	4.1967	4.0195	3.9254	3.8295	3.7806
$\hat{\Sigma}_s^c$	.1470	.1346	.1283	.1220	.1190
$\hat{\Sigma}_s^f$	.6685	.6112	.5811	.5510	.5364
$\hat{\Sigma}_{tr}^m$	2.9376	2.8927	2.8688	2.8445	2.8322
$\hat{\Sigma}_{tr}^c$	.1572	.1451	.1389	.1328	.1298
$\hat{\Sigma}_{tr}^f$	1.0182	.9660	.9385	.9110	.8976
$\hat{\Sigma}_t^m$	4.2186	4.0414	3.9473	3.8513	3.8025
$\hat{\Sigma}_t^c$	.1609	.1485	.1421	.1358	.1328
$\hat{\Sigma}_t^f$	1.0327	.9792	.9511	.9230	.9092
$\hat{\Sigma}_f^f$	.2852	.2618	.2637	.2655	.2664
$\hat{\Sigma}_a^h$	.1584	.1292	.1095	.0851	.0706
$\hat{\Sigma}_s^h$	2.4138	2.6804	2.8600	3.0800	3.2103
$\hat{\Sigma}_{tr}^h$	1.9152	2.0965	2.2227	2.3807	2.4755
$\hat{\Sigma}_t^h$	2.5722	2.8097	2.9694	3.1651	3.2809
$\hat{\Sigma}_f^h$	.1036	.0816	.0667	.0482	.0372

TABLE B.14

CORNELL UNIVERSITY ZERO POWER REACTOR EFFECTIVE CROSS SECTION TEMPERATURE COEFFICIENTS

Temperature Coefficients (10^{-4}°C^{-1})	Water/Oxide Volume Ratio				
	1:1	1.5:1	2:1	3:1	4:1
$\dot{\hat{\Sigma}}^m_a/\hat{\Sigma}^m_a$	-2.97	-2.97	-2.97	-2.97	-2.97
$\dot{\hat{\Sigma}}^c_a/\hat{\Sigma}^c_a$	0.0	0.0	0.0	0.0	0.0
$\dot{\hat{\Sigma}}^f_a/\hat{\Sigma}^f_a$	0.0	0.0	0.0	0.0	0.0
$\dot{\hat{\Sigma}}^m_s/\hat{\Sigma}^m_s$	+2.09	+2.88	+3.34	+3.84	+4.11
$\dot{\hat{\Sigma}}^c_s/\hat{\Sigma}^c_s$	+8.92	+9.43	+10.4	+11.6	+12.2
$\dot{\hat{\Sigma}}^f_s/\hat{\Sigma}^f_s$	+7.06	+8.60	+9.62	+10.8	+11.5
$\dot{\hat{\Sigma}}^m_{tr}/\hat{\Sigma}^m_{tr}$	+1.29	+1.60	+1.78	+1.97	+2.07
$\dot{\hat{\Sigma}}^c_{tr}/\hat{\Sigma}^c_{tr}$	+7.19	+8.54	+9.39	+10.4	+10.9
$\dot{\hat{\Sigma}}^f_{tr}/\hat{\Sigma}^f_{tr}$	+4.07	+4.76	+5.19	+5.69	+5.97
$\dot{\hat{\Sigma}}^m_t/\hat{\Sigma}^m_t$	+2.07	+2.85	+3.31	+3.80	+4.06
$\dot{\hat{\Sigma}}^c_t/\hat{\Sigma}^c_t$	+7.21	+8.59	+9.43	+10.4	+10.9
$\dot{\hat{\Sigma}}^f_t/\hat{\Sigma}^f_t$	+4.12	+4.81	+5.26	+5.76	+6.04
$\dot{\hat{\Sigma}}^f_f/\hat{\Sigma}^f_f$	-1.63	-1.85	-1.99	-2.13	-2.21
$\dot{\hat{\Sigma}}^h_a/\hat{\Sigma}^h_a$	-.06	+.43	+.78	+1.35	+1.63
$\dot{\hat{\Sigma}}^h_s/\hat{\Sigma}^h_s$	+1.77	+2.28	+2.63	+3.10	+3.40
$\dot{\hat{\Sigma}}^h_{tr}/\hat{\Sigma}^h_{tr}$	+1.30	+1.34	+1.38	+1.48	+1.58

Table B.14 (continued)

Temperature Coefficients ($10^{-4}\,°C^{-1}$)	Water/Oxide Volume Ratio				
	1:1	1.5:1	2:1	3:1	4:1
$\dot{\hat{\Sigma}}^h_t/\hat{\Sigma}^h_t$	+1.66	+2.19	+2.56	+3.05	+3.37
$\dot{\hat{\Sigma}}^h_f/\hat{\Sigma}^h_f$	-.10	+.55	+1.20	+2.28	+3.23

TABLE B.15

CORNELL UNIVERSITY ZERO POWER REACTOR MEAN CROSS SECTIONS

Mean Cross Sections (cm^{-1})	Water/Oxide Volume Ratio				
	1:1	1.5:1	2:1	3:1	4:1
$\bar{\Sigma}_a^m$	.0131	.0145	.0154	.0164	.0169
$\bar{\Sigma}_a^c$	.0080	.0088	.0092	.0097	.0099
$\bar{\Sigma}_a^f$	.2017	.2233	.2363	.2506	.2582
$\bar{\Sigma}_s^m$	2.5177	2.6648	2.7560	2.8605	2.9190
$\bar{\Sigma}_s^c$	.0851	.0852	.0852	.0853	.0853
$\bar{\Sigma}_s^f$	.3704	.3708	.3710	.3713	.3714
$\bar{\Sigma}_{tr}^m$	1.7624	1.9178	2.0141	2.1248	2.1867
$\bar{\Sigma}_{tr}^c$	.0910	.0918	.0923	.0929	.0931
$\bar{\Sigma}_{tr}^f$	.5641	.5860	.5992	.6138	.6215
$\bar{\Sigma}_t^m$	2.5309	2.6794	2.7713	2.8768	2.9359
$\bar{\Sigma}_t^c$	.0931	.0939	.0944	.0950	.0953
$\bar{\Sigma}_t^f$	.5721	.5940	.6073	.6219	.6296
$\bar{\Sigma}_f^f$	.1430	.1588	.1684	.1789	.1844
$\bar{\Sigma}_a^h$	.0917	.0830	.0747	.0622	.0535
$\bar{\Sigma}_s^h$	1.3970	1.7214	1.9524	2.2499	2.4337
$\bar{\Sigma}_{tr}^h$	1.1084	1.3463	1.5174	1.7391	1.8766
$\bar{\Sigma}_t^h$	1.4887	1.8044	2.0271	2.3120	2.4872
$\bar{\Sigma}_f^h$	.0599	.0524	.0455	.0352	.0282

TABLE B.16

CORNELL UNIVERSITY ZERO POWER REACTOR MEAN CROSS SECTION TEMPERATURE COEFFICIENTS

Temperature Coefficients (10^{-4}°C^{-1})	Water/Oxide Volume Ratio				
	1:1	1.5:1	2:1	3:1	4:1
$\dot{\bar{\Sigma}}^m_a/\bar{\Sigma}^m_a$	-11.0	-12.7	-14.0	-15.0	-15.7
$\dot{\bar{\Sigma}}^c_a/\bar{\Sigma}^c_a$	-7.49	-9.13	-9.78	-10.8	-11.6
$\dot{\bar{\Sigma}}^f_a/\bar{\Sigma}^f_a$	-8.13	-9.78	-10.9	-12.2	-12.9
$\dot{\bar{\Sigma}}^m_s/\bar{\Sigma}^m_s$	-6.16	-7.11	-7.75	-8.51	-8.94
$\dot{\bar{\Sigma}}^c_s/\bar{\Sigma}^c_s$	+.16	+.14	+.12	+.11	+.10
$\dot{\bar{\Sigma}}^f_s/\bar{\Sigma}^f_s$	+.11	+.11	+.10	+.09	+.08
$\dot{\bar{\Sigma}}^m_{tr}/\bar{\Sigma}^m_{tr}$	-6.96	-8.36	-9.28	-10.3	-10.9
$\dot{\bar{\Sigma}}^c_{tr}/\bar{\Sigma}^c_{tr}$	-.60	-.76	-.92	-1.08	-1.18
$\dot{\bar{\Sigma}}^f_{tr}/\bar{\Sigma}^f_{tr}$	-2.83	-3.67	-4.23	-4.92	-5.31
$\dot{\bar{\Sigma}}^m_t/\bar{\Sigma}^m_t$	-6.19	-7.15	-7.78	-8.55	-8.98
$\dot{\bar{\Sigma}}^c_t/\bar{\Sigma}^c_t$	-.54	-.75	-.90	-1.05	-1.15
$\dot{\bar{\Sigma}}^f_t/\bar{\Sigma}^f_t$	-2.79	-3.61	-4.18	-4.85	-5.24
$\dot{\bar{\Sigma}}^f_f/\bar{\Sigma}^f_f$	-8.46	-10.2	-11.3	-12.6	-13.3
$\dot{\bar{\Sigma}}^h_a/\bar{\Sigma}^h_a$	-7.69	-8.97	-9.83	-10.6	-11.1
$\dot{\bar{\Sigma}}^h_s/\bar{\Sigma}^h_s$	-5.91	-7.19	-8.01	-8.93	-9.40
$\dot{\bar{\Sigma}}^h_{tr}/\bar{\Sigma}^h_{tr}$	-6.36	-8.11	-9.23	-10.5	-11.2

Table B.16 (continued)

Temperature Coefficients (10^{-4}°C^{-1})	Water/Oxide Volume Ratio				
	1:1	1.5:1	2:1	3:1	4:1
$\dot{\bar{\Sigma}}^h_t/\bar{\Sigma}^h_t$	-6.01	-7.28	-8.08	-8.97	-9.44
$\dot{\bar{\Sigma}}^h_f/\bar{\Sigma}^h_f$	-7.76	-8.87	-9.44	-9.66	-9.70

APPENDIX C

NUMERICAL METHODS IN COUTH

This appendix describes the computational methods employed by the COUTH code in solving Eq. (6.1) for the spatially averaged moderator flux $\overline{\varphi}^m(E)$, as well as the subsequent calculation of all of the parameters defined in Chap. 6. A Fortran listing of COUTH appears in Appendix E utilizing the Nelkin water model for the scattering kernel. The input to COUTH is discussed in Appendix D.

COUTH, as presently instrumented begins its calculations with the computation of the energy, velocity, and lethargy mesh as described in Sec. 7.1 and listed in Appendix B. Inspection of these meshes shows that the lethargy mesh has the finest relative spacing in the region of maximum interest, .025 eV $\leq$ E $\leq$ .6 eV, while both the velocity and energy mesh tend to have the finest spacing at low energy end of the mesh. For this reason all calculations in COUTH are done in lethargy, u, space utilizing the relationships

$$\varphi(u) = E\varphi(E) \ , \tag{C.1}$$

$$\sigma(u' \longrightarrow u) = E\sigma(E' \longrightarrow E) \ , \tag{C.2}$$

and

$$\Sigma(u) = \Sigma(E) \ . \tag{C.3}$$

The heterogeneous effects of the lattice, Sec. 2.3, are incorporated into COUTH in terms of the moderator and fuel element escape probabilities. The escape probability of source neutrons, $P_s(E)$, is calculated in the subprogram FUNCTION PSLOF utilizing diffusion theory as expressed by Eq. (3.4). $P_m(E)$, the moderator escape probability of neutrons incident from the fuel element is calculated utilizing the reciprocity relationship, Eq. (3.6), by the subprogram FUNCTION PMODF. The linear extrapolation length into a black hole, d_o, necessary for these calculations is approximated by[83]

$$d_o(E)\Sigma^m_{tr}(E) = \lambda = \frac{0.6229}{1+2.48\Sigma^m_{tr}(E)r_o} + 0.7104 , \qquad (C.4)$$

where r_o is radius of the black hole. This expression equals 4/3 at $\Sigma^m_{tr}\ r_o = 0$, Zaretsky's[84] value of 0.889 at $\Sigma^m_{tr}\ r_o = 1$, and 0.7104 for $\Sigma^m_{tr}\ r_o$ approaching infinity. Leslie's SPECTROX method[85] corresponds to the special case of $\lambda = 2/3$.

The fuel rod escape probability, $P_r(E)$, is calculated from the parabolic flux approximation, Eq. (4.8). This computation is carried out by the subprogram FUNCTION PRODF. The subprogram SUBROUTINE PESCF calculates the fuel element escape probability, $P_e(E)$, utilizing the thin region transport theory embodied in Eq. (4.21).

In the explicit calculation of escape probabilities, the modified Bessel functions of the first and second kind and of order 0, 1, and 2 are required. Calculation of the functions

$I_o(z)$, $I_1(z)$, $I_2(z)$, $K_o(z)$, $K_1(z)$, and $K_2(z)$ is accomplished by the subprogram SUBROUTINE BESS.

The modified Bessel functions of the first kind, $I_n(z)$, are computed in the following manner.[86] Noting that for any given z, $I_n(z)$ approaches zero as n gets very large, we set $I_n(z)$ equal to zero and $I_{n-1}(z)$ equal to $1x10^{-40}$ where for any z, n is determined as follows. For $z \leq 45$, n = [2z+10], where [x] is the largest integer contained in x. For $z > 45$, n is taken equal to 100. Lower order I's are then calculated utilizing the recurrence relationship[87]

$$I_{m-1}(z) = \frac{2m}{z} I_m(z) + I_{m+1}(z) \quad . \qquad (C.5)$$

Recognizing that the I's calculated in this manner bear the correct relationship to each other, but lack normalization, the results are normalized through the expression

$$e^z = \sum_{m=-\infty}^{\infty} I_m(z) \approx I_o(z) + 2 \sum_{m=1}^{n} I_m(z) \quad . \qquad (C.6)$$

This same technique is utilized in the calculation of the I_m's utilized in the computation of the Nelkin water kernel, Eq. (5.15).

The zero order modified Bessel function of the second kind, $K_o(z)$, is computed using the following approximations.[88]

---

[83] A. M. Weinberg and E. P. Wigner, The Physical Theory of Neutron Chain Reactors, p. 765, The University of Chicago Press, Chicago, 1958.

[84] D. F. Zaretsky, PICG 5, 529 (1955).

For $z \geq 5$:

$$K_o(z) \approx \left(\frac{\pi}{2z}\right)^{1/2} e^{-z} \left[1 - \frac{1^2}{1!8x} + \frac{1^2 \cdot 3^2}{2!(8x)^2} - \frac{1^2 \cdot 3^2 \cdot 5^2}{3!(8x)^3} + \ldots\right], \tag{C.7}$$

the number of terms used in this expansion being set equal to $2[z]$. For $z < 5$,

$$K_o(z) \approx \sum_{m=0}^{50} \delta_m I_{2m}(z) , \tag{C.8}$$

where

$$\delta_o = -(\gamma + \log z/2), \tag{C.9}$$

$$\gamma = \text{Euler's Constant} = 0.577215, \ldots, \tag{C.10}$$

$$\delta_1 = 2 , \tag{C.11}$$

and,

$$\delta_m = \frac{m-1}{m} \delta_{m-1} . \qquad m \geq 2 \tag{C.12}$$

The first and second order modified Bessel functions of the second kind are calculated using the Wronskian relationship,[89]

$$K_m(z)I_{m+1}(z) + K_{m+1}(z)I_m(z) = \frac{1}{z} . \tag{C.13}$$

---

[85] D. C. Leslie, "The SPECTROX Method for Thermal Spectra in Lattice Cells," AEEW-M211, United Kingdom Atomic Energy Authority (1962).

[86] F. D. Federighi and D. T. Goldman, "KERNEL and PAM-Programs for Use in the Calculation of the Thermal Scattering Matrix for Chemically Bound Systems," KAPL-2225, Knolls Atomic Power Laboratory (1962).

The calculation of the slowing down source, S(E), as given in Eq. (7.1), and of the monatomic gas model for the scattering kernel, Eq. (5.9), requires the evaluation of the error function for various arguments. The error function, ERF(z), is defined by

$$\mathrm{ERF}(z) = \frac{2}{\sqrt{\pi}} \int_0^z e^{-t^2}\, dt \ . \tag{C.14}$$

In the COUTH code, ERF(z) is calculated by FUNCTION ERF in the following manner.[90] For $|z| \geq 4$,

$$\mathrm{ERF}(z) \approx \frac{|z|}{z} \ , \tag{C.15}$$

while for $2 \leq |z| < 4$,

$$\mathrm{ERF}(z) \approx \frac{|z|}{z}\left[1 - \frac{e^{-z^2}}{|z|\sqrt{\pi}} \left(1 - \frac{1}{2z^2} + \frac{1.3}{2^2 z^4} - \frac{1.3.5}{2^3 z^6} + \frac{1.3.5.7}{2.2^4 z^8} \right) \right] . \tag{C.16}$$

For $|z| < 2$,

$$\mathrm{ERF}(z) \approx \frac{2z}{\sqrt{\pi}} \left[\sum_{n=1}^{20} \frac{(-1)^{n-1}}{(n-1)!} \frac{z^{2(n-1)}}{(2n-1)} + \frac{z^{40}}{2(20!)(41)} \right] . \tag{C.17}$$

87/ H. B. Dwight, Tables of Integrals and Other Mathematical Data, p. 189, The Macmillan Company, New York, 1961.

88/ M. Goldstein and R. M. Thaler, "Recurrence Techniques for Calculation of Bessel Functions," Mathematical Tables and Other Aids to Computation, 13, 102 (1959).

Numerical integration in the lethargy space used in COUTH is carried out by the subprogram FUNCTION TRAP. The trapezoidal rule is utilized to simplify the calculations with the uneven lethargy spacing encountered. Integration of an arbitrary function of lethargy, f(u), which has been evaluated at the discrete points $f(u_i)$, $i = 1,2,3,\ldots n$, is approximated by

$$\int_{u_1}^{u_n} f(u)du \approx \sum_{i=1}^{n-1} \frac{1}{2}\left[f(u_i)+f(u_{i+1})\right] \Delta u_i \ . \qquad (C.17)$$

The lethargy intervals, Δu_i, are defined by

$$\Delta u_i = u_{i+1}-u_i, \qquad i = 1,2,3,\ldots n-1 \ . \qquad (C.18)$$

Calculation of the scattering kernel using the monatomic gas model, Eq. (5.4), is performed by the subprogram SUBROUTINE FKERN. Only the down scattering in energy (or upscattering in lethargy) portion of the kernel is calculated in FKERN, the upscattering portion being calculated by detailed balance, Eq. (2.5), in the main program of COUTH. Calculation of the monatomic gas kernel in the form of a 45 by 45 matrix as needed with the lethargy mesh used takes about $2\frac{1}{2}$ minutes of computer time. If the Nelkin water kernel is used, then the scattering kernel, Eq. (5.15), is calculated with the subprogram SUBROUTINE WATER. Again, only the downscattering portion of the matrix is computed,

89/ M. Goldstein and R. M. Thaler, see Footnote 88.

the upscattering portion being calculated by detailed balance in the main body of COUTH. The actual methods used in the calculation of the Nelkin water kernel are discussed in Sec. 5.2. Since the calculation of 45 by 45 matrix representing the Nelkin water kernel takes approximately 15 minutes at a given temperature, the downscattering portion of the matrix for a physical temperature of 20°C has been reproduced on cards so that numerous lattice studies may be made at this temperature without necessitating the recomputation of the water kernel. Control cards read into COUTH (see Appendix D), determine whether the downscattering portion of scattering kernel shall be calculated using the Nelkin model, or whether the Nelkin results for 20°C shall be read directly in.

For calculations at temperatures above 20°C, the average cosine of the scattering angle for water, $\bar{\mu}(E)$, is decreased by $1x10^{-4}$ for every centigrade degree increase in temperature above 20°C at all energies. The slowing down source of neutrons, S(E), is calculated according to Eq. (7.1), while the moderator scattering cross section, $\Sigma_s^m(E)$, is calculated using Eq. (2.2) and as discussed in Sec. 7.1. The neutron balance equation, Eq. (6.1), rewritten below in terms of the lethargy mesh is then solved using an iterative process.[91]

[90] H. B. Dwight, p. 136, see Footnote 87.

[91] M. J. Poole, M. S. Nelkin, and R. S. Stone, "The Measurement and Theory of Reactor Spectra," Progress in Nuclear Energy, Series I, Vol. 2, p. 99, Pergamon Press, New York, London, Paris, and Los Angeles, 1958.

$$\bar{\varphi}^m(u_i) = \frac{\bar{S}(u_i) + \int_0^{u_c} \Sigma(u_j \rightarrow u_i)\, \bar{\varphi}^m(u_j)\, du_j}{\Sigma_s^m(u_i) + \Sigma_a^m(u_i)\left[1 + \frac{f(u_i)}{1-f(u_i)}\right]} \quad . \tag{C.19}$$

The cutoff lethargy, u_c, is 7.372 corresponding to a low energy of .00101 eV with the thermal cutoff energy, E_c, of 1.609 eV being the zero lethargy point. The relative fuel absorption f/[1-f] is calculated from the escape probabilities in accordance with Eq. (2.29).

An initial guess is made that the moderator spectrum is a constant in lethargy:

$$\bar{\varphi}^m(u_i) = 1 \ , \qquad i = 1,2,3,\ldots,n = 45 \ . \tag{C.20}$$

This guess is then normalized to satisfy neutron conservation as expressed in Eq. (2.4).

$$\hat{\varphi}_1^m(u_i) = \frac{\bar{\varphi}_1^m(u_i)}{\int_0^{u_c} \Sigma_a^m(u_i)\left[1 + \frac{f(u_i)}{1-f(u_i)}\right] \bar{\varphi}_1^m(u_i)\, du_i} \ , \quad i=1,2\ldots n. \tag{C.21}$$

The normalized flux, $\hat{\varphi}_1^m(u_i)$ is then substituted into the right hand side of Eq. (C.19) and the next generation approximation

to the moderator flux, $\overline{\varphi}_2^m(u_i)$, is calculated. This process is repeated utilizing the general expressions

$$\overline{\varphi}_{k+1}^m(u_i) = \frac{\overline{S}(u_i) + \int_o^{u_c} \Sigma(u_j \rightarrow u_i)\hat{\varphi}_k^m(u_j)d(u_j)}{\Sigma_s^m(u_i) + \Sigma_a^m(u_i)\left[1 + \frac{f(u_i)}{1-f(u_i)}\right]}, \qquad i = 1,2...n, \tag{C.22}$$

and,

$$\hat{\varphi}_k^m(u_i) \quad \frac{\overline{\varphi}_k^m(u_i)}{\int_o^{u_c} \Sigma_a^m(u_i)\left[1 + \frac{f(u_i)}{1-f(u_i)}\right]\overline{\varphi}_k^m(u_i)du_i} \qquad i=1,2,...n. \tag{C.23}$$

The equation is considered solved when the successive iterations satisfy the following convergence criterion at every other lethargy point:

$$\left|\frac{\hat{\varphi}_{k+1}^m(u_i)}{\hat{\varphi}_k^m(u_i)}\right| - 1 \quad \leq \epsilon \qquad\qquad i = 1,3,5,7,...,n. \tag{C.24}$$

The convergence criterion, ϵ, utilized in the COUTH calculations is $1x10^{-4}$. In general solution of the integral equation, Eq. (C.19), has taken about 13 iterations with use

of the monatomic gas model, while the use of the Nelkin water kernel with its more complicated fine structure usually requires about 27 iterations for solution.

The fuel and cladding spectra, the mean velocities, the disadvantage factors, the lifetime, the thermal utilization, ηf, L, D, and the averaged cross sections are calculated in a straightforward manner as defined in Chap. 6.

An entire lattice calculation, including the computation of the escape probabilities, the spatially averaged thermal spectra, and all of the parameters defined in Chap. 6 takes about 40 seconds of computer time with use of the Nelkin water kernel, and about 30 seconds with the monatomic gas model. Calculational times for the kernel are not included in these figures. Compiling time for the Fortran source program of COUTH runs about two and one half minutes.

APPENDIX D

INPUT-OUTPUT FORMAT FOR COUTH

A Fortran statement of the COUTH code for use with the Nelkin water kernel as a scattering model is listed in Appendix E. This section describes the input required and the output received for a typical lattice calculation. The input data is listed below, the first column being the item or data card number, the second column is the Fortran FORMAT as it appears in COUTH, the third column is the Fortran list of the input variable, and the fourth column is a description of each variable.

1.	(I4)	IND	Identification number. If IND =1, the previously calculated down scattering portion of the Nelkin water kernel at 20°C will be used in the calculation. If IND $\geq$ 2, the Nelkin water kernel will be calculated at the temperature specified in Item 2.

2.	(2F10.6,I5,E12.4)	T	The moderator temperature in degrees absolute.
		RHϕ	The moderator density at T in gm/cc.
		N	The number of lethargy intervals. N = 44 gives mesh in Table B.1. N must be $\leq$ 54.
		EPSI	Convergence criterion, ϵ, Eq. (C.24).
3.	(13F6.1)	XA(I)	U^{235} absorption cross section in barns.
4.	(13F6.1)	XF(I)	U^{235} fission cross section in barns.
5.	(7E11.3)	SK(J,I)	Downscattering portion of Nelkin model scattering matrix for 20°C.
6.	(20F4.3)	AMUBAR(I)	Average cosine of the scattering angle in water, $\bar{\mu}(E_i)$.

7.	(11F7.4)	CF(I)	Correction factors to the SK(J,I) diagonals see Sec. 7.1.
8.	(8F8.4,E16.4)	DEN	Fuel rod density in gm/cc.
		ENR	Fuel enrichment in weight per cent.
		RO	Fuel element diameter in inches.
		RCI	Fuel cladding inner diameter in inches.
		RF	Fuel rod diameter in inches.
		AMC	Cladding scatterer mass in amu.
		SSC	Cladding free atom cross section in barns.
		SAC	Cladding 2200 m/sec absorption cross section in barns.
		FNC	Cladding number density in atoms/barn-cm.
9.	(10A8)	TITLE	80 character title.

10. (2F10.5)	WΦ	The nominal water to oxide volume ratio for the lattice under consideration.
	AP	The lattice pitch or rod to rod spacing (in.) in a hexagonal lattice.

COUTH is instrumented to reread a series of items 10 until a negative value of WΦ is encountered. If this occurs, items 8 and 9 will be reread with the subsequent read in of a series of items 10. Calculation will stop when the computer encounters a negative value of WΦ, item 10, followed directly by a negative value for DEN, item 8. This allows one to calculate the scattering kernel at a given temperature, then consider a fuel element of certain specifications and calculate parameters for all of the lattices utilizing this fuel element. New fuel element specifications are then read in and the lattices utilizing this fuel element are analyzed. There is no limit on the number of fuel elements or the number of lattices for each fuel element type which may be considered.

The output for a typical 1 lattice calculation using a 45 point energy mesh is outlined below. The first column represents the page number after the execution of the source program, the second column gives the Fortran list of the output

variable, and the third column gives a description of the output variable.

1.	I	Index identifying lethargy mesh points.
	E(I)	Energy mesh point, E_i.
	DE(I)	Energy interval, $\Delta E_i = E_{i+1} - E_i$.
	V(I)	Velocity mesh point, v_i
	DV(I)	Velocity interval, Δv_i.
	U(I)	Lethargy mesh point, u_i.
	DU(I)	Lethargy interval, Δu_i.
2.	BLANK	
3. 4. 5. 6. 7.	SK(J,I)	Scattering matrix, $\sigma(U(J) \longrightarrow U(I))$, J running horizontally and I running vertically.
8.	E(I)	Energy mesh point, E_i.
	SX(I)	Moderator scattering cross section in barns.
	ST(I)	Moderator transport cross section in barns.
	SS25(I)	U^{235} scattering cross section in barns.
	SS28(I)	U^{238} scattering cross section in barns.
	SS16(I)	O^{16} scattering cross section in barns.
	AMUBAR(I)	Average cosine of the scattering angle, $\bar{\mu}(E_i)$, for water.

9. E(I) Energy mesh point, E_i.

XA(I) U^{235} absorption cross section in barns.

SF(I) U^{235} fission cross section in barns.

SIGMAF(I) Fuel absorption cross section in cm^{-1}, $\Sigma_f^f(E_i)$.

FSIGMAF(I) Fuel absorption cross section in cm^{-1}, $\Sigma_a^f(E_i)$.

AA(I) $1 + \alpha(E_i)$, $\alpha(E_i)$ = fuel capture to fission ratio.

SN(I) Slowing down source of neutrons, S(E), Eq. (7.1).

10. E(37) E(37) = .0253 eV. This page shows E = kT values for the variables used in the cladding calculations.

PR P_{rv}, Eqs. (4.8), (4.19).

FJϕ J_o, Eq. (4.22).

TT Cladding thickness in cm.

FO Solid angle factor, Eq. (4.26).

FIN Fraction of neutrons scattered in, Eq. (4.48).

SIGS Cladding scattering cross section in cm^{-1}.

SIGT Cladding total cross section in cm^{-1}.

G g, Eq. (4.45).

S T, Eq. (4.35).

PU P_u, Eq. (4.43).

PUNIF P_{unif}, Eq. (4.44).

	RSUM	$r_{in} + r_{out}$, Eq. (4.46).
	TAU	τ, Eq. (4.40).
	RHϕSUM	$\rho_{in} + \rho_{out}$, Eq. (4.47).
	CTE	Cladding absorption rate to fuel element absorption rate ratio, Eq. (4.55).
11.	BLANK	
12.	BLANK	
13.	Wϕ	Input item 10.
	T	Input item 2.
	TITLE	Input item 9.
	E(I)	Energy, E_i.
	FLUX (I)	$\bar{\varphi}^m(E_i)$, Eq. (6.1).
	FC(I)	$\bar{\varphi}_c(E_i)$, Eq. (6.4).
	FS(I)	$\bar{\varphi}^f(E_i)$, Eq. (6.3).
	AB(I)	$\Sigma_a^m(E)\left[1 + \frac{f(E)}{1-f(E)}\right]$.
14.	Wϕ	Input item 10.
	T	Input item 2.
	TITLE	Input item 9.
	E(I)	Energy, E_i.
	PS(I)	$P_s(E_i)$, Eq. (3.4).
	PM(I)	$P_m(E_i)$, Eq. (3.6).
	PR(I)	$P_{rr}(E_i)$, Eq. (4.8), (4.19).

	PE(I)	$P_e(E_i)$, Eq. (4.21).
	TU(I)	$f(E_i)$, Eq. (3.8).
	RFA(I)	f/(1-f), Eq. (3.8).
	RTE(I)	Rod abs. rate/element abs. rate, Eq. (4.53).
	FJϕ	$J_o(E_i)$, Eq. (4.22).
15.	Wϕ	Input item 10.
	T	Input item 2.
	TITLE	Input item 9.
	F	f, Eq. (6.15).
	ETA	η.
	ETAF	ηf, Eq. (6.16).
	DIS	δ_n^m, Eq. (6.8).
	DISC	δ_n^c, Eq. (6.9).
	DIFFC	D, Eq. (6.38).
	DIFFL	L, Eq. (6.39).
	AL	ℓ_t, Eq. (6.17).
	AL1	$\ell_m = \ell_t/\eta f$.
	VM	$\bar{v}_m$, Eq. (6.6).
	VF	$\bar{v}_f$, Eq. (6.6).
	VC	$\bar{v}_c$, Eq. (6.6).
	HV	$\bar{v}_h$, Eq. (6.33).
	FN25	U^{235} number density.
	FN28	U^{238} number density.
	FN16	Oxygen in UO_2 number density.

FNC	Cladding number density, input item 8.
FNM	Moderator number density.
N	Input item 2.
K	Number of iterations required to solve Eq. (6.1).
EPSI	Input item 2.
RHϕ	Input item 2.
ENR	Fuel enrichment in atom per cent.
AP	Input item 10.
R1	Equivalent cell radius, cm.
RO	Fuel element radius, cm.
VOLM	Moderator area, cm^2.
VOLC	Cladding area, cm^2.
VOLF	Fuel rod area, cm^2.
R	Actual water to oxide volume ratio.
TITLE	Input item 10.

16. Page 16 lists the effective cross sections for each region of the cell, Eq. (6.23), and for the homogenized cell, Eq. (6.31); and the mean cross sections for each region, Eq. (6.24), and for the homogenized cell, Eq. (6.32).

Pages 12 through 16 are repeated for each lattice considered, while consideration of a fuel element with new specifications will cause pages 10 and 11 to be printed with the subsequent printing of pages 12 through 16 for each lattice considered.

APPENDIX E

FORTRAN LISTING OF COUTH

This appendix lists the Fortran statement of the COUTH source program as instrumented for calculation with the Nelkin water kernel as the scattering model. SUBROUTINE FKERN, which calculates the monatomic gas model for the scattering kernel, is also listed. For calculations with the monatomic gas model, SUBROUTINE WATER, FUNCTION ONE and FUNCTION TWO are replaced by SUBROUTINE FKERN. In addition the main program of COUTH must be modified to read in the values of the transport cross section of water as calculated with the Nelkin model for use in the calculation of the moderator escape probabilities.

```
      PROGRAM COUTH
      DIMENSION U(55),E(55),PS(55),PM(55),PE(55),RFA(55),TU(55),AB(55),
     1SN(55),SK(55,55),SX(55),ALPHA(55),PHIN(55),DU(55),AA(55),FEA(55),
     2GAMMA(55),DELTA(55),SALPHA(55),SPHIN(55),FLUX(55),ZZ(55),SXA(55),
     3XA(55),XF(55),FS(55),ST(55),AMUBAR(55),KN(5),IM(5),CF(55),
     4SIGMAF(55),FSIGMAF(55),DE(55),DV(55),V(55),SS25(55),SS28(55),
     5SS16(55),D(55),DD(55),TITLE(10),PR(55),FJO(55),RTE(55),FC(55),
     6CTE(55),FB(55),TRB(55)
C      ORDER OF DATA INPUT IS AS FOLLOWS.
C          IND ---------- I4
C          T,RHO,N,EPSI ---------- 2(F10.6),I5,2X,E10.2
C          XA ---------- 13(F6.1)
C          XF ---------- 13(F6.1)
C          SK ---------- 7(E11.3)
C          AMUBAR ---------- 20(F4.3)
C          CF ---------- 11(F7.4)
C          DEN,ENR,RO,RCI,RF,AMC,SSC,SAC,FNC  8(F8.4),4X,E12.4
C          TITLE ---------- 10(A8)
C          WO,AP ---------- 2(F10.5)
C      IND = 1, NELKIN WATER KERNEL FOR 20 DEG. C READ IN.
C      IND = 2, NELKIN WATER KERNEL CALCULATED AT T.
C      T = MODERATOR TEMPERATURE IN DEGREES KELVIN.
C      RHO IS THE MODERATOR DENSITY IN GM/CC.
C      N = NUMBER OF LETHARGY INTERVALS.
C      EPSI = CONVERGENCE CRITERION FOR THE ITERATION.
C      XA IS HONECKS U235 ABSORPTION CROSS SECTION IN BARNS.
C      XF IS HONECKS U235 FISSION CROSS SECTION IN BARNS.
C      SK IS THE SCATTERING MATRIX.
C      SK IS SIGMA(U(J) TO U(I))/UNIT LETHARGY OR F(I)*SIGMA(E(J) TO
C      E(I))/UNIT EV.  SIGMA IS IN BARNS.
C      AMUBAR IS THE AVERAGE COSINE OF THE SCATTERING ANGLE.
C      CF IS THE CORRECTION FACTOR TO THE SK DIAGONALS.
C      DEN IS THE FUEL DENSITY IN GM/CC.
C      ENR IS THE FUEL ENRICHMENT EXPRESSED AS WEIGHT PER CENT.
C      RO IS THE FUEL ELEMENT DIAMETER IN INCHES.
C      RCI IS THE FUEL CLADDING INNER DIAMETER IN INCHES.
C      RF IS THE FUEL ROD DIAMETER IN INCHES.
C      AMC IS THE CLADDING SCATTERING MASS IN AMU.
C      SSC IS THE CLADDING FREE ATOM SCATTERING CROSS SECTION IN BARNS.
C      SAC IS THE CLADDING 2200 M/SEC ABSORPTION CROSS SECTION IN BARNS.
C      FNC IS THE CLADDING CONCENTRATION IN ATOMS/BARN-CM.
C      WO IS THE NOMINAL WATER TO URANIUM OXIDE VOLUME RATIO.
C      AP IS THE LATTICE PITCH IN INCHES.
   19 FORMAT (1H1)
  199 FORMAT (60H1SCATTERING KERNEL, SIGMA(U(J) TO U(I))/UNIT LETHARGY,
     1KT = F7.5,6H, J = I2,4H TO I2,/)
  200 FORMAT (I4,2X,10(E11.3))
  203 FORMAT (37H1WATER TO URANIUM OXIDE VOLUME RATIO,F5.1,7H TO 1.0,/,2
     14H ABSOLUTE TEMPERATURE = F8.2,/,27H THERMAL UTILIZATION (F) = F8.
     25,/,7H ETA = F8.5,/,9H ETA*F = F8.5,/,33H MODERATOR DISADVANTAGE F
     3ACTOR = F8.5,/,32H CLADDING DISADVANTAGE FACTOR = F8.5,/,30H DIFFU
     4SION COEFFICIENT (CM) = F8.4,/,25H DIFFUSION LENGTH (CM) = F8.4,/,
     525H LIFETIMES (MICROSECONDS),/,10X,11H THERMAL = F8.5,/,10X,8H MEA
     6N = F8.5,/,27H AVERAGE VELOCITIES (M/SEC),/,10X,13H MODERATOR = F8
```

```
     7.2,/,10X,8H FUEL = F8.2,/,10X,12H CLADDING = F8.2,/,10X,20H HOMOGE
     8NIZED CELL = F8.2)
  204 FORMAT (//,30H NUMBER OF ENERGY INTERVALS = I4,/,24H NUMBER OF ITE
     1RATIONS = I4,/,25H CONVERGENCE CRITERION = E11.3,/,29H MODERATOR D
     2ENSITY (GM/CC) = F8.5,/,24H FUEL DENSITY (GM/CC) = F8.5,/,34H FUEL
     3 ENRICHMENT (ATOM PERCENT) = F8.5,/,26H LATTICE PITCH (INCHES) = F
     48.5,//,11H RADII (CM),/,10X,19H EQUIVALENT CELL = F8.5,/,10X,16H F
     5UEL ELEMENT = F8.5,/,10X,12H FUEL ROD = F8.5,//,14H AREAS (CM**2),
     6/,10X,13H MODERATOR = F8.5,/,10X,12H CLADDING = F8.5,/,10X,12H FUE
     7L ROD = F8.5,//,46H ACTUAL WATER TO URANIUM OXIDE VOLUME RATIO = F
     88.5,/)
  206 FORMAT (4X,31HEFFECTIVE CROSS SECTIONS (1/CM),29X,26HMEAN CROSS SE
     1CTIONS (1/CM),/,4X,31(1H-),29X,26(1H-),/,2(8X,10HABSORPTION,42X),/
     2,2(12X,9HMODERATOR,F10.5,29X),/,2(12X,4HFUEL,F15.5,29X),/,2(12X,8H
     3CLADDING,F11.5,29X),/,2(8X,10HSCATTERING,42X),/,2(12X,9HMODERATOR,
     4F10.5,29X),/,2(12X,4HFUEL,F15.5,29X),/,2(12X,8HCLADDING,F11.5,29X)
     5,/,2(8X,9HTRANSPORT,43X),/,2(12X,9HMODERATOR,F10.5,29X),/,2(12X,4H
     6FUEL,F15.5,29X),/,2(12X,8HCLADDING,F11.5,29X),/,2(8X,5HTOTAL,47X),
     7/,2(12X,9HMODERATOR,F10.5,29X),/,2(12X,4HFUEL,F15.5,29X),/,2(12X,8
     8HCLADDING,F11.5,29X),/,2(8X,7HFISSION,45X),/,2(12X,4HFUEL,F15.5,29
     9X))
  207 FORMAT (//,2(8X,31HHOMOGENIZED CELL CROSS SECTIONS,21X),/,2(12X,10
     1HABSORPTION,F9.5,29X),/,2(12X,10HSCATTERING,F9.5,29X),/,2(12X,9HTR
     2ANSPORT,F10.5,29X),/,2(12X,5HTOTAL,F14.5,29X),/,2(12X,7HFISSION,F1
     32.5,29X))
  208 FORMAT (/,34H NUMBER DENSITIES (NUMBER/BARN-CM),/,10X,8H U235 = E1
     12.4,/,10X,8H U238 = E12.4,/,10X,10H OXYGEN = E12.4,/,10X,12H CLADD
     2ING = E12.4,/,10X,13H MODERATOR = E12.4)
  334 FORMAT (11(F7.4))
  815 FORMAT (6H      I,3X,6HENERGY,7X,7HDELTA E,6X,8HVELOCITY,2X,7HDELTA
     1 V,3X,8HLETHARGY,8H DELTA U,///,(2X,I4,2X,2(E11.3,2X),2(F8.1,2X),2
     22(F7.4,2X))
 1000 FORMAT (/,(1X,I4,7(E15.4)))
 1001 FORMAT (13(F6.1))
 1004 FORMAT (37H1WATER TO URANIUM OXIDE VOLUME RATIO,F5.1,8H TO 1.0,,
     124H ABSOLUTE TEMPERATURE = F6.1)
 1005 FORMAT (2(F10.5))
 1006 FORMAT (2(F10.6),I5,2X,E10.2)
 1007 FORMAT (8(F8.4),4X,E12.4)
 1008 FORMAT (10(A8))
 1009 FORMAT (/,10(A8))
 1100 FORMAT (5H1   I  ,4X,6HENERGY,7X,15HU235 ABSORPTION,2X,12HU235 FISSI
     1ON,1X,15HFUEL ABSORPTION,1X,12HFUEL FISSION,5X,9H1 + ALPHA,4X,12HS
     2LOWING DOWN,/,23X,4(13HCROSS SECTION,2X),19X,6HSOURCE,/,26X,2(7H(B
     3ARNS),8X),2(6H(1/CM),9X),/,39(3H-  ))
 1101 FORMAT (5H1   I  ,4X,6HENERGY,7X,14HH2O SCATTERING,2X,13HH2O TRANSPO
     1RT,2X,12HU235 SCATTER,3X,12HU238 SCATTER,4X,11HO16 SCATTER,7X,6HMU
     2 BAR,/,23X,5(13HCROSS SECTION,2X),/,26X,5(7H(BARNS),8X),/,39(3H-
     3))
 1102 FORMAT (3H0 I,8X,6HENERGY,9X,9HMODERATOR,6X,8HCLADDING,7X,4HFUEL,1
     13X,16HABSORPTION CROSS,/,27X,3(8HSPECTRUM,7X),2X,18HSECTION (1/CM
     2H2O),/,32(3H-  ),//,(I4,6X,4(E12.4,3X),F10.4))
 1103 FORMAT (3H0 I,8X,6HENERGY,20X,2HPS,8X,2HPM,8X,2HPR,8X,2HPE,8X,2HTU
     1,7X,3HREA,7X,3HRTF,6X,5HJ OUT,/,38(3H-  ),//,(I4,6X,F12.4,8X,8(F10
```

```
     2.4)))
 1212 FORMAT (I4)
 4000 FORMAT (7(E11.3))
 4444 FORMAT (20(F4.3))
 9198 FORMAT (5X,4HJ = ,10(I2,9X),/,3H   I)
 9199 FORMAT (I4,2X,5(E11.3))
 9298 FORMAT (5X,4HJ = ,5(I2,9X),/,3H   I)
      READ 1212,IND
      READ 1006,T,RHO,N,EPSI
      NM=N+1
      READ 1001,(XA(I),I=1,NM)
      READ 1001,(XF(I),I=1,NM)
      READ 4000,((SK(J,I),J=1,I),I=1,NM)
      READ 4444,(AMUBAR(I),I=1,NM)
      READ 334,(CF(I),I=1,NM)
      T=8.6167E-5*T
      OM1=0.205
      OM2=0.481
      OMR=0.06
      EM=18.
      EMR=2.32
      EMV =3./(1.-1./18.-1./2.32)
      FA25=10.0
      FA28=8.3
      FA16=3.76
      AM25=235.117/1.00896
      AM28=238.125/1.00896
      AM16=16.0/1.00896
      RM=238.125/235.117
      ANU=2.43
C     START CALCULATION OF ENERGY,VELOCITY,LETHARGY MESH.  CALCULATION
C     ENDS WITH STATEMENT 94.
      B=0.1*LOGF(10.)
      U(1)=0.0
      DV(1)=0.1*2200.
      V(1)=440.
      V(2)=V(1)+DV(1)
      DV(NM)=0.0
      DU(NM)=0.0
      DE(NM)=0.0
      DO 90 I=2,34
      DV(I)=DV(1)
   90 V(I+1)=V(I)+DV(I)
      DO 91 I=35,N
      DV(I)=DV(1)*EXPF(B*FLOATF(I-34))
   91 V(I+1)=V(I)+DV(I)
      DO 711 I=1,NM
      D(I)=V(I)
  711 DD(I)=DV(I)
      DO 92 I=1,NM
      V(I)=D(NM+1-I)
   92 E(I)=(V(I)**2)*.0252977/(2200.**2)
      DO 93 I=1,N
   93 DV(I)=DD(NM-I)
```

```
      DO 94 I=2,NM
      U(I)=LOGF(E(1)/E(I))
      DU(I-1)=U(I)-U(I-1)
   94 DE(I-1)=E(I-1)-E(I)
      PRINT 19
      PRINT 815,(I,E(I),DE(I),V(I),DV(I),U(I),DU(I),I=1,NM)
      PRINT 19
      DO 712 I=1,5
      KJ=10.*FLOATF(I)
      IM(I)=KJ
  712 KN(I)=KJ-9
      IF(IND-2) 222,223,223
  223 CALL WATER(E,T,N,SK)
      DO 224 I=1,NM
  224 AMUBAR(I)=AMUBAR(I)-(10.*T-.2526)/8.61637
  222 DO 110 J=2,NM
      JK=J-1
      DO 110 I=1,JK
      BB=((E(I)/E(J))**2)*EXPF((E(J)-E(I))/T)
  110 SK(J,I)=SK(I,J)*BB
      DO 951 L=1,4
      NI=KN(L)
      MI=IM(L)
      PRINT 199,T,NI,MI
      PRINT 9198,(I,I=NI,MI)
  951 PRINT 200,(I,(SK(J,I),J=NI,MI),I=1,NM)
      NI=41
      MI=45
      PRINT 199,T,NI,MI
      PRINT 9298,(I,I=NI,MI)
      PRINT 9199,(I,(SK(J,I),J=NI,MI),I=1,NM)
      DO 445 I=1,NM
  445 SK(I,I)=SK(I,I)*CF(I)
      DO 119 J=1,NM
      DO 116 I=1,NM
  116 SXA(I)=SK(J,I)
  119 SX(J)=TRAP(SXA,DU,N)
C     SX IS THE SCATTERING CROSS SECTION OF H2O IN BARNS.
      DO 447 I=1,NM
      SS25(I)=FA25*SCROSS(E(I),T,AM25)
      SS28(I)=FA28*SCROSS(E(I),T,AM28)
      SS16(I)=FA16*SCROSS(E(I),T,AM16)
C     SS25,28,16 ARE THE SCATTERING CROSS SECTIONS OF U235,U238,016
C     IN BARNS.
  447 ST(I)=.656*SQRTF(.0253/E(I))+SX(I)*(1.-AMUBAR(I))
C     ST IS THE TRANSPORT CROSS SECTION OF H2O IN BARNS.
      DO 448 I=1,NM
      DO 448 J=1,NM
  448 SK(J,I)=SK(J,I)*RHO*.60247/18.02
      PRINT 1101
      PRINT 1000,(I,E(I),SX(I),ST(I),SS25(I),SS28(I),SS16(I),AMUBAR(I),
     1I=1,NM)
      TE=T/EM+OM1/(2.*EMV)+OM2/EMV+OMR*(1./(EXPF(OMR/T)-1.)+.5)/EMR
C     TE IS THE EFFECTIVE TEMPERATURE.
```

```
      DO 8 I=1,NM
      ST(I)=ST(I)*RHO*.60247/18.02
      SX(I)=SX(I)*RHO*.60247/18.02
C     SK,ST,AND SX ARE NOW IN (1/CM).
      A1=SQRTF(E(I)/TE)
    8 SN(I)=E(I)*ERF(A1)
      BETA=TRAP(SN,DU,N)
      DO 9 I=1,NM
    9 SN(I)=SN(I)/BETA
C     SN IS THE NORMALIZED SOURCE
      T=T/8.6167E-5
  714 READ 1007,DEN,ENR,R0,RCI,RF,AMC,SSC,SAC,FNC
      IF(DEN) 41,41,715
  715 READ 1008,TITLE
      AMC=AMC/1.00896
      R0=R0*2.54/2.
      RF=RF*2.54/2.
      RCI=RCI*2.54/2.
      ENR=100.*ENR*RM/(ENR*RM+(100.-ENR))
      FN25=ENR*.60247*DEN*1.0E-2/270.26
      FN28=FN25*(100.-ENR)/ENR
      FN16=2.01*.60247*DEN/270.26
      FNM=.60247*RHO/18.02
      DO 713 I=1,NM
      SIGMAF(I)=FN25*XA(I)+FN28*2.71*SQRTF(.0253/E(I))
      FSIGMAF(I)=FN25*XF(I)
      PR(I)=PRODF(FN25,FN28,SIGMAF(I),FSIGMAF(I),DEN,RF,RCI,R0,
     1SS25(I),SS28(I),SS16(I))
  713 AA(I)=SIGMAF(I)/FSIGMAF(I)
      PRINT 1100
      PRINT 1000,(I,E(I),XA(I),XF(I),SIGMAF(I),FSIGMAF(I),AA(I),SN(I),
     1I=1,NM)
      CALL PESCF(E,FNC,SSC,SAC,AMC,RCI,R0,NM,T,PR,FJO,PE,CTE)
      DO 47 I=1,NM
   47 RTE(I)=FJO(I)*(1.-PR(I))/(PR(I)*(1.-PE(I)))
C     RTE IS THE RATIO OF THE NUMBER OF NEUTRONS ABSORBED IN THE FUEL
C     ROD TO THE NUMBER ABSORBED IN THE FUEL ELEMENT.
  301 READ 1005,WO,AP
      IF(WO) 714,714,141
  141 PRINT 19
      PRINT 1004,WO,T
      PRINT 1009,TITLE
      R1=SQRTF(((AP*2.54)**2)*1.73205/(2.*3.14159))
      Y=R1/R0
      VOLM=3.14159*((R1**2)-(R0**2))
      VOLF=3.14159*(RF**2)
      VOLC=3.14159*((R0**2)-(RCI**2))
      VOLCELL=3.14159*(R1**2)
      R=VOLM/VOLF
      RC=VOLM/VOLC
    2 DO 7 I=1,NM
      PS(I)=PSLOF(E(I),R0,Y,RHO,ST(I))
      PM(I)=PMODF(E(I),R0,Y,RHO,ST(I))
      TU(I)=((1.-PE(I))*PS(I))/(1.-PM(I)*PE(I))
```

```
C       TU IS THE RATIO OF THE NUMBER OF NEUTRONS ABSORBED IN THE FUEL
C       ELEMENT TO THE NUMBER ABSORBED IN THE CELL.
        RFA(I)=TU(I)/(1.-TU(I))
C       RFA IS THE RATIO OF THE NUMBER OF NEUTRONS ABSORBED IN THE FUEL
C       ELEMENT TO THE NUMBER ABSORBED IN THE MODERATOR.
        FEA(I)=RFA(I)*.656*RHO*.60247*SQRTF(.0253/E(I))/18.02
C       FEA IS THE FUEL ELEMENT ABSORPTION CROSS SECTION IN 1/CM.
      7 AB(I)=(1.+RFA(I))*.656*RHO*.60247*SQRTF(.0253/E(I))/18.02
C       AB IS THE TOTAL ABSORPTION CROSS SECTION IN THE CELL PER CM H2O.
C       BEGIN ITERATIVE SOLUTION OF INTEGRAL EQUATION. SOLUTION ENDS ON 36
        DO 112 I=1,NM
    112 PHIN(I)=1.000
C       INITIAL GUESS AT SPECTRUM IS A CONSTANT
        K=1
        DO 13 I=1,NM
     13 ALPHA(I)=PHIN(I)*AB(I)
        B=TRAP(ALPHA,DU,N)
        DO 23 I=1,NM
     23 PHIN(I)=PHIN(I)/B
     14 DO 15 I=1,NM
        DO 16 J=1,NM
     16 GAMMA(J)=PHIN(J)*SK(J,I)
     15 DELTA(I)=TRAP(GAMMA,DU,N)
        DO 27 I=1,NM
     27 SPHIN(I)=(SN(I)+DELTA(I))/(AB(I)+SX(I))
        DO 28 I=1,NM
     28 SALPHA(I)=SPHIN(I)*AB(I)
        C=TRAP(SALPHA,DU,N)
        DO 29 I=1,NM
     29 SPHIN(I)=SPHIN(I)/C
        DO 32 I=1,NM,2
        RA=SPHIN(I)/PHIN(I)
        ABSDIF=ABSF(RA-1.)
        IF (ABSDIF-EPSI) 32,32,38
     32 CONTINUE
        GO TO 36
     38 K=K+1
        IF (K-100) 39,39,36
     39 DO 60 J=1,NM
     60 PHIN(J)=SPHIN(J)
        GO TO 14
     36 DO 37 I=1,NM
     37 FLUX(I)=SPHIN(I)/E(I)
        DO 70 I=1,NM
     70 ZZ(I)=FEA(I)*RTE(I)*SPHIN(I)
        C1=TRAP(ZZ,DU,N)
        DO 71 I=1,NM
     71 ZZ(I)=AB(I)*SPHIN(I)
        C2=TRAP(ZZ,DU,N)
        F=C1/C2
        DO 72 I=1,NM
        FS(I)=SPHIN(I)*R*FEA(I)*RTE(I)/SIGMAF(I)
        FC(I)=FEA(I)*CTF(I)*SPHIN(I)*RC*SQRTF(E(I))/(SQRTF(.0253)*FNC*SAC)
     72 ZZ(I)=FEA(I)*RTE(I)*SPHIN(I)/AA(I)
```

```
      C3=TRAP(ZZ,DU,N)
      ETAF=ANU*C3/C2
      ETA=ETAF/F
      DO 73 I=1,NM
   73 ZZ(I)=SPHIN(I)/V(I)
      C4=TRAP(ZZ,DU,N)
      DO 74 I=1,NM
   74 ZZ(I)=FS(I)/V(I)
      C5=TRAP(ZZ,DU,N)
      DO 75 I=1,NM
   75 ZZ(I)=FC(I)/V(I)
      C6=TRAP(ZZ,DU,N)
      DIS=C4/C5
      DISC=C6/C5
      C7=TRAP(SPHIN,DU,N)
      C8=TRAP(FS,DU,N)
      C9=TRAP(FC,DU,N)
      VM=C7/C4
      VF=C8/C5
      VC=C9/C6
      DO 77 I=1,NM
   77 ZZ(I)=SPHIN(I)*.656*RHO*.60247*SQRTF(.0253/E(I))/18.02
      C10=TRAP(ZZ,DU,N)
      DO 78 I=1,NM
   78 ZZ(I)=FS(I)*SIGMAF(I)
      C11=TRAP(ZZ,DU,N)
      DO 79 I=1,NM
   79 ZZ(I)=FC(I)*SAC*FNC*SQRTF(.0253/E(I))
      C12=TRAP(ZZ,DU,N)
      DO 80 I=1,NM
   80 ZZ(I)=SPHIN(I)*ST(I)
      C13=TRAP(ZZ,DU,N)
      DO 81 I=1,NM
   81 ZZ(I)=SPHIN(I)*SX(I)
      C14=TRAP(ZZ,DU,N)
      DO 82 I=1,NM
   82 ZZ(I)=FS(I)*(SS25(I)*FN25+SS28(I)*FN28+SS16(I)*FN16)
      C15=TRAP(ZZ,DU,N)
      DO 83 I=1,NM
   83 ZZ(I)=FS(I)*(SS25(I)*FN25*(1.-2./(3.*AM25))+SS28(I)*FN28*(1.-2./
     1(3.*AM28))+SS16(I)*FN16*(1.-2./(3.*AM16)))
      C16=TRAP(ZZ,DU,N)
      T=T*8.6167E-5
      DO 86 I=1,NM
      FB(I)=(SPHIN(I)*VOLM+FS(I)*VOLF+FC(I)*VOLC)/VOLCELL
      TRB(I)=(ST(I)*SPHIN(I)*VOLM+(FS(I)*SIGMAF(I)+ZZ(I))*VOLF+(FC(I)*((
     1SAC*FNC*SQRTF(.0253/E(I)))+(FNC*SSC*SCROSS(F(I),T,AMC)*(1.-2./(3.*
     2AMC)))))/(VOLCELL*FB(I))
   86 ZZ(I)=FB(I)/TRB(I)
      C20=TRAP(ZZ,DU,N)
      C21=TRAP(FB,DU,N)
      DIFFC=C20/(3.*C21)
      DO 84 I=1,NM
   84 ZZ(I)=FC(I)*FNC*SSC*SCROSS(E(I),T,AMC)
```

```
      C17=TRAP(ZZ,DU,N)
      T=T/8.6167E-5
      C18=C17*(1.-2./(3.*AMC))
      DO 85 I=1,NM
   85 ZZ(I)=FS(I)*FSIGMAF(I)
      C19=TRAP(ZZ,DU,N)
      SBAM=C10/C7
      SBAF=C11/C8
      SBAC=C12/C9
      SBSM=C14/C7
      SBSF=C15/C8
      SBSC=C17/C9
      SBTRM=C13/C7
      SBTRF=(C11+C16)/C8
      SBTRC=(C12+C18)/C9
      SBTM=SBAM+SBSM
      SBTF=SBAF+SBSF
      SBTC=SBAC+SBSC
      SBFF=C19/C8
      V0=2200.0
      SHAM=SBAM*VM/V0
      SHAF=SBAF*VF/V0
      SHAC=SBAC*VC/V0
      SHSM=SBSM*VM/V0
      SHSF=SBSF*VF/V0
      SHSC=SBSC*VC/V0
      SHTRM=SBTRM*VM/V0
      SHTRF=SBTRF*VF/V0
      SHTRC=SBTRC*VC/V0
      SHTM=SBTM*VM/V0
      SHTF=SBTF*VF/V0
      SHTC=SBTC*VC/V0
      SHFF=SBFF*VF/V0
      DZ=C7*VOLM+C8*VOLF+C9*VOLC
      SBA=(C10*VOLM+C11*VOLF+C12*VOLC)/DZ
      SBS=(C14*VOLM+C15*VOLF+C17*VOLC)/DZ
      SBTR=(C13*VOLM+(C11+C16)*VOLF+(C12+C18)*VOLC)/DZ
      SBT=SBA+SBS
      SBF=C19*VOLF/DZ
      HV=DZ/(C4*VOLM+C5*VOLF+C6*VOLC)
      SHA=SBA*HV/V0
      SHS=SBS*HV/V0
      SHTR=SBTR*HV/V0
      SHT=SBT*HV/V0
      SHF=SBF*HV/V0
      DIFFL=SQRTF(DIFFC/SBA)
      AL=((C4*VOLM+C5*VOLF+C6*VOLC)*1.0E+4)/(C2*VOLM)
      AL1=AL/ETAF
      DO 76 I=1,NM
      FC(I)=FC(I)/E(I)
   76 FS(I)=FS(I)/E(I)
   40 PRINT 1102,(I,E(I),FLUX(I),FC(I),FS(I),AR(I),I=1,NM)
      PRINT 1004,WO,T
      PRINT 1009,TITLE
```

```
      PRINT 1103,(I,E(I),PS(I),PM(I),PR(I),PE(I),TU(I),RFA(I),RTE(I),
     1FJO(I),I=1,NM)
      PRINT 203,WO,T,F,ETA,ETAF,DIS,DISC,DIFFC,DIFFL,AL,AL1,VM,VF,VC,HV
      PRINT 208,FN25,FN28,FN16,FNC,FNM
      PRINT 204,N,K,EPSI,RHO,DEN,ENR,AP,R1,RO,RF,VOLM,VOLC,VOLF,R
      PRINT 1009,TITLE
      PRINT 1004,WO,T
      PRINT 206,SHAM,SBAM,SHAF,SBAF,SHAC,SBAC,SHSM,SBSM,SHSF,SBSF,SHSC,
     1SBSC,SHTRM,SBTRM,SHTRF,SBTRF,SHTRC,SBTRC,SHTM,SBTM,SHTF,SBTF,SHTC,
     2SBTC,SHFF,SBFF
      PRINT 207,SHA,SBA,SHS,SBS,SHTR,SBTR,SHT,SBT,SHF,SBF
      PRINT 1009,TITLE
      PRINT 19
      GO TO 301
   41 CONTINUE
      END


      FUNCTION PRODF(FN25,FN28,SIGMAA,SIGMAF,DEN,RF,RCI,RO,SS25,SS28,
     1SS16)
C     THIS CALCULATES THE ESCAPE PROBABILITY FROM THE FUEL ROD USING
C     THE PARABOLIC FLUX APPROXIMATION.  SEE K.B. CADY THESIS, PG 118.
      FN16=2.01*.60247*DEN/270.26
      SS=SS25*FN25+SS28*FN28+SS16*FN16
      SA=SIGMAA
      ST=SS+SA
      SF=SIGMAF
      C=SS/ST
      A=ST*RF
      B=1.-C
      IF(A-.5) 1,1,2
    1 CALL BESS(A,FI0,FI1,FI2,FK0,FK1,FK2)
      FI0=A*(FI1*FK0+1.-A*(FI1*FK1+FI0*FK0))
      FI1=(FI1*FK1+1.-2.*FI0)/3.
      FM00=1.-2.*FI1
      PR=1.-2.*A*B*(1.-FM00)/(1.-C*FM00)
      GO TO 3
    2 CALL BESS(A,FI0,FI1,FI2,FK0,FK1,FK2)
      FI0=A*(FI1*FK0+1.-A*(FI1*FK1+FI0*FK0))
      FI1=(FI1*FK1+1.-2.*FI0)/3.
      FI2=(FI2*FK0-1.+2.*FI0+2.*FI1)/3.
      FI21=((FI2*FK1/A)+FI1-FI2)/5.
      FI22=((FI2*FK2/(A**2))+(1./(3.*(A**2)))-2.*FI21)/7.
      FM00=1.-2.*FI1
      FM02=1.-4.*FI1+8.*FI21
      FM22=1.-6.*FI1+24.*FI21+24.*FI22-2./(A**2)
      FM0=2.*A*(1.-FM00)
      FM2=A*(1.-FM02)
      G=1.-C*(4.*FM00+4.*FM22-6.*FM02)+(C**2)*(4.*FM00*FM22-3.*
     1(FM02**2))
      PR=1.-B*(FM0-C*(FM0*(4.*FM22-3.*FM02)+6.*FM2*(FM00-FM02)))/G
    3 PRODF=(1.-RF/RCI)+RF*PR/RCI
      END
```

```
      SUBROUTINE PESCF(E,FNC,SSC,SAC,AMC,RF,RO,NM,T,PR,FJO,PE,CTE)
      DIMENSION E(55),PR(55),FJO(55),PE(55),CTE(55)
C     THIS CALCULATES THE ESCAPE PROBABILTY FROM THE FUEL ELEMENT GIVEN
C     THE ESCAPE PROBABILITY FROM THE FUEL ROD.  THIN REGION THEORY
C     IS USED AS DEVELOPED IN K.B. CADY THESIS, APPENDIX J.
   19 FORMAT (1H1)
   50 FORMAT (10H ENERGY = E12.4,/,31H FUEL ROD ESCAPE PROBABILITY = F8.
     15,/,19H ROD CURRENT OUT = F8.5,/,35H FUEL ELEMENT ESCAPE PROBABILI
     2TY = F8.5,/,27H CLADDING THICKNESS (CM) = F8.5,/,5H FO =F8.5,/,25H
     3 FRACTION SCATTERED IN = F8.5,/,20H SIGMA SCATTERING = F8.5,/,15H
     4SIGMA TOTAL = F8.5,/,5H G = F8.5,/,5H T = F8.5,/,6H PU = F8.5,/,9H
     5 PUNIF = F8.5,/,14H RIN + ROUT = F8.5,/,7H TAU = F8.5,/,18H RHOIN
     6+ RHOOUT = F8.5,/,7H CTE = F8.5)
      PI=3.14159
      GAM=.5772157
      T=T*8.6167E-5
      ZE=RF/RO
      TT=RO-RF
      FK=1.-(ZE**2)
      FO=2.*ASINF(ZE)/PI
      F1=ZE
      F2=FO+2.*ZE*SQRTF(FK)/PI
      F3=3.*ZE*(1.-(ZE**2)/3.)/2.
      D1=PI*(ZE**2)/4.
      FLAM=LOGF(4./SQRTF(FK))
      D2=(2./3.)*(1.-.75*FK-3.*(FLAM-.25)*(FK**2)/16.-3.*(FLAM-(11./
     112.))*(FK**3)/64.)
      FL1=(F2-4.*D1/PI)/F1
      FL2=(8.*F3/3.-2.*FK*F1-4.*D2)/F1
      C1=(PI*FO/2.+ZE*SQRTF(FK))/(2.*ZE)
      C2=D2/(ZE**2)
      FLL1=4.*C1/PI-ZE
      FLL2=2.*FK+8.*(ZE**2)/3.-4.*ZE*C2
      FIN=ASINF(2.*ZE/(1.+ZE))/PI
      DO 10 I=1,NM
      SIGS=SSC*FNC*SCROSS(E(I),T,AMC)
      SIGT=SIGS+FNC*SAC*SQRTF(.0253/E(I))
      SIGA=SIGT-SIGS
      S=F1-SIGT*RO*F1*FL1+.5*((SIGT*RO)**2)*F1*FL2
      X=SIGT*TT
      PU=.5*X*(GAM+LOGF(X)-1.5)+1.-(X**2)/6.+(X**3)/48.-(X**4)/360.+
     1(X**5)/2880.
      PUNIF=PU/(1.-(SIGS*(1.-PU)/SIGT))
      IF(X-.05) 31,31,32
   31 G=(1.-F1)-2.*(1.-F2)*SIGT*RO+8.*(1.-F3)*((SIGT*RO)**2)/3.
      GO TO 33
   32 G=-.0212-.0266*LOGF(X)/(ZE**2.2)
   33 CONTINUE
      RSUM=SIGS*(1.-G-S)*PUNIF/SIGT
      TAU=1.-SIGT*RO*FLL1+.5*((SIGT*RO)**2)*FLL2
      RHOSUM=SIGS*(1.-TAU)*PUNIF/SIGT
      RIN=FIN*RSUM
      ROUT=RSUM-RIN
      RHOIN=FIN*RHOSUM
```

```
      RHOOUT=RHOSUM-RHOIN
      FJO(I)=PR(I)*(S+RIN)/(1.-RHOIN*PR(I))
      PE(I)=G+ROUT+FJO(I)*(TAU+RHOOUT)
      CTE(I)=SIGA*((1.-G-S)+FJO(I)*(1.-TAU))/((1.-PE(I))*(SIGA+(SIGS*
     1PU)))
      IF(I-37) 10,40,10
   40 PRINT 19
      PRINT 50,E(I),PR(I),FJO(I),PE(I),TT,FO,FIN,SIGS,SIGT,G,S,PU,PUNIF,
     1RSUM,TAU,RHOSUM,CTE(I)
      PRINT 19
   10 CONTINUE
      T=T/8.6167E-5
      END


      FUNCTION ERF(Z)
C     ERF(Z) CALCULATES THE ERROR FUNCTION.
      AZ=ABSF(Z)
      IF (AZ-4.) 85,86,86
   86 ERF=AZ/Z
      RETURN
   85 IF (AZ-2.) 87,88,88
   87 T1=1.
      T2=T1*(Z**2)/3.
      T3=T2*(Z**2)*3./(2.*5.)
      T4=T3*(Z**2)*5./21.
      T5=T4*(Z**2)*7./36.
      T6=T5*(Z**2)*9./55.
      T7=T6*(Z**2)*11./78.
      T8=T7*(Z**2)*13./105.
      T9=T8*(Z**2)*15./136.
      T10=T9*(Z**2)*17./171.
      T11=T10*(Z**2)*19./210.
      T12=T11*(Z**2)*21./253.
      T13=T12*(Z**2)*23./300.
      T14=T13*(Z**2)*25./351.
      T15=T14*(Z**2)*27./406.
      T16=T15*(Z**2)*29./465.
      T17=T16*(Z**2)*31./528.
      T18=T17*(Z**2)*33./595.
      T19=T18*(Z**2)*35./666.
      T20=T19*(Z**2)*37./741.
      T21=T20*(Z**2)*19.5/820.
      ERF=2.*.5641896*Z*(T1-T2+T3-T4+T5-T6+T7-T8+T9-T10+T11-T12+T13
     1-T14+T15-T16+T17-T18+T19-T20+T21)
      RETURN
   88 ZA=2.*(Z**2)
      S1=1.
      S2=1./ZA
      S3=3./(ZA**2)
      S4=15./(ZA**3)
      S5=52.5/(ZA**4)
      ERF=(1.-.5641896*(S1-S2+S3-S4+S5)/(AZ*EXPF(Z**2)))*(AZ/Z)
      END
```

```
      SUBROUTINE BESS(Z,C,D,E,F,G,H)
C     BESS CALCULATES MODIFIED BESSEL FUNCTIONS OF THE FIRST AND
C     SECOND KIND.
C     C=I0(Z),D=I1(Z),F=I2(Z),F=K0(Z),G=K1(Z),H=K2(Z)
      DIMENSION B(100),BK(3)
      IF(Z-45.) 1,1,2
    1 N=XFIXF(2.*Z+10.)
      GO TO 3
    2 N=100
    3 B(N-1)=1.0E-40
      DO 8 I=N,100
    8 B(I)=0.0
      SUM=2.0E-40
      NJ=N-1
      DO 4 L=2,NJ
      NL=N-L
      B(NL)=FLOATF(NL)*2.*B(NL+1)/Z+B(NL+2)
    4 SUM=SUM+2.*B(NL)
      SUM=SUM-B(1)
      FACTOR=(EXPF(Z))/SUM
      DO 5 L=1,N
      B(L)=FACTOR*B(L)
      IF(B(L)-1.0E-307) 6,6,5
    6 B(L)=0.0
    5 CONTINUE
      C=B(1)
      D=B(2)
      E=B(3)
      IF(Z-5.) 81,82,82
   82 IF(Z-6.) 110,111,111
  110 KL=10
      GO TO 140
  111 IF(Z-7.) 112,113,113
  112 KL=12
      GO TO 140
  113 IF(Z-8.) 114,115,115
  114 KL=14
      GO TO 140
  115 IF(Z-9.) 116,117,117
  116 KL=16
      GO TO 140
  117 IF(Z-10.) 118,119,119
  118 KL=18
      GO TO 140
  119 KL=10
      GO TO 140
  140 W=1.0
      SUM2=1.0
      DO 83 I=1,KL
      W=-W*((2.*FLOATF(I)-1.)**2)/((Z*8.)*FLOATF(I))
   83 SUM2=SUM2+W
      SUM2=SUM2-W/2.
      BK(1)=(SUM2*SQRTF(3.141592654/(2.*Z)))/EXPF(Z)
      GO TO 9
```

```
   81 SUM1=0.0
      DO 7 I=3,99,2
    7 SUM1=SUM1+B(I)/FLOATF(I-1)
      SUM1=4.*SUM1
      BK(1)=SUM1-(.577215665+LOGF(Z/2.))*B(1)
    9 BK(2)=((1./Z)-BK(1)*B(2))/B(1)
      F=BK(1)
      G=BK(2)
      BK(3)=((1./Z)-BK(2)*B(3))/B(2)
      H=BK(3)
      END


      FUNCTION PMODF(E,R0,Y,RH0,SIGMATR)
C     THIS CALCULATES THE ESCAPE PROBABILITY OF NEUTRONS INCIDENT ON
C     THE MODERATOR FROM THE FUEL.  IT IS CALCULATED FROM PSLOF BY A
C     RECIPROCITY RELATIONSHIP, SEE K.B. CADY THESIS, PG 88.
C     SIGMATR IS THE TRANSPORT CROSS SECTION OF THE MODERATOR
C     FLAMBDA IS THE LINEAR EXTRAPOLATION LENGTH
C     SIGMAMA IS THE ABSORBTION CROSS SECTION IN THE MODERATOR
      R1=R0*Y
      FLAMBDA=(.623/(1.+2.48*SIGMATR*R0))+.7104
      SIGMAMA=.656*RH0*.60247*SQRTF(.0253/E)/18.02
      D=1./(3.*SIGMATR)
      DELTA=FLAMBDA/SIGMATR
      FK=SQRTF(SIGMAMA/D)
      RK1=FK*R1
      RK0=FK*R0
      CALL BESS(RK0,FI00,FI10,FI20,FK00,FK10,FK20)
      CALL BESS(RK1,FI01,FI11,FI21,FK01,FK11,FK21)
      B=(FK11*FI00+FI11*FK00)/(FK10*FI11-FK11*FI10)
      C=B+FK*DELTA
      XE=2./(C*R0*((Y**2)-1.)*FK)
      PMODF=1.-2.*SIGMAMA*R0*((Y**2)-1.)*XE
      END


      FUNCTION PSLOF(E,R0,Y,RH0,SIGMATR)
C     THIS CALCULATES THE ESCAPE PROBABILITY OF NEUTRONS APPEARING
C     AT ENERGY (E) DUE TO COLLISIONS AT OTHER ENERGIES.  DIFFUSION
C     THEORY IS USED WITH A SPATIALLY UNIFORM SOURCE AND AN ENERGY
C     DEPENDENT LINEAR EXTRAPOLATION LENGTH.
      FLAMBDA=(.623/(1.+2.48*SIGMATR*R0))+.7104
      SIGMAMA=.656*RH0*.60247*SQRTF(.0253/E)/18.02
      R1=R0*Y
      D=1./(3.*SIGMATR)
      DELTA=FLAMBDA/SIGMATR
      FK=SQRTF(SIGMAMA/D)
      RK1=FK*R1
      RK0=FK*R0
      CALL BESS(RK0,FI00,FI10,FI20,FK00,FK10,FK20)
      CALL BESS(RK1,FI01,FI11,FI21,FK01,FK11,FK21)
      B=(FK11*FI00+FI11*FK00)/(FK10*FI11-FK11*FI10)
      C=B+FK*DELTA
```

```
      PSLOF=2./(C*R0*((Y**2)-1.)*FK)
      END


      FUNCTION TRAP(S,DU,N)
      DIMENSION S(56),DU(56)
C     USES THE TRAPEZOIDAL RULE TO INTEGRATE THE N+1 DIMENSIONAL
C     VECTOR S. DU IS THE LETHARGY INCREMENT.
      C=0.0
      DO 2 I=1,N
    2 C=C+.5*(S(I)+S(I+1))*DU(I)
      TRAP=C
      END


      FUNCTION SCROSS(E,T,A)
C     CALCULATES SCATTERING CROSS SECTION/FREE ATOM CROSS SECTION FROM
C     THE MONATOMIC GAS MODEL.  E AND T ARE IN EV, A IS IN NEUTRON
C     MASSES.
      Y=E*A/T
      IF(Y-700.) 1,1,2
    1 X=SQRTF(Y)
      SCROSS=(1.+.5/Y)*ERF(X)+1./(X*EXPF(Y)*SQRTF(3.14159))
      RETURN
    2 SCROSS=(1.+.5/Y)
      END


      SUBROUTINE WATER(E,T,N,SK)
C     WATER CALCULATES THE NELKIN WATER KERNEL.  FUNCTIONS ONE AND TWO
C     ARE NECESSARY.
      DIMENSION E(55),SK(55,55),WGT(12),SKA(55),KN(5),IM(5),AMU(12)
      OM1=0.205
      OM2=0.481
      OMR=0.06
      EM=18.
      EMR=2.32
      EMV =3./(1.-1./18.-1./2.32)
   19 FORMAT (1H1)
      NM=N+1
      KN(1)=1
      KN(2)=11
      KN(3)=21
      KN(4)=31
      IM(1)=10
      IM(2)=20
      IM(3)=30
      IM(4)=40
      AMU(1)=.9602899
      AMU(2)=.7966665
      AMU(3)=.5255324
      AMU(4)=.1834346
      AMU(5)=.98940093
      AMU(6)=.94457502
```

```
      AMU(7)=.86563120
      AMU(8)=.75540441
      AMU(9)=.61787624
      AMU(10)=.45801678
      AMU(11)=.28160355
      AMU(12)=.09501251
      WGT(1)=.1012285
      WGT(2)=.2223810
      WGT(3)=.3137066
      WGT(4)=.3626838
      WGT(5)=.02715246
      WGT(6)=.06225352
      WGT(7)=.09515851
      WGT(8)=.12462897
      WGT(9)=.14959599
      WGT(10)=.16915652
      WGT(11)=.18260342
      WGT(12)=.18945061
      DO 102 I=1,NM
      DO 101 J=1,I
      BEE=E(I)+E(J)
      C=SQRTF(E(I)*E(J))
      D=0.
      H=0.
      NJ=NM+J
      NA=.5*FLOATF(NJ)
      IF(I-NA) 150,150,80
  150 KM=5
      KL=12
      GO TO 306
   80 KM=1
      KL=4
  306 IF(E(J)-.33) 300,300,301
  301 IF(E(J)-.34) 302,302,303
  300 MJ=1
      GO TO 304
  302 MJ=3
  304 OM=OMR
      AM=EMR
      LJ=3
      CM=1./EM
      GX=T/EM
      B=EXPF(OM/(2.*T))
      AI=((B**2)+1.)/(((B**2)-1.)*EMR*OMR)+1./(EMV*OM1)+2./(EMV*OM2)
      GO TO 305
  303 OM=OM1
      AM=EMV
      MJ=3
      LJ=1
      CM=1./EM+1./EMR
      GX=T/EM+OMR*(1./(EXPF(OMR/T)-1.)+.5)/EMR
      B=EXPF(OM/(2.*T))
      AI=1./(EMV*OM1)+2./(EMV*OM2)
  305 IF(I-J) 901,902,901
```

```
 902 ALPHA=E(J)/SQRTF(3.14159*GX)
     BETA=E(J)*SQRTF(16./(3.14159*T))
     GO TO 903
 901 ALPHA=0.
     BETA=0.
 903 ZOX=2.*B/(AM*OM*(B**2-1.))
     DO 151 K=KM,KL
     X=BEE+2.*C*AMU(K)
     XX=SQRTF(X)
     Z=X*ZOX
     F=ONE(E(J),E(I),X,GX,OM,CM,MJ,LJ,AI,B,Z,EMV)
     F=(2.*81.5/4.)*(F-ALPHA/XX)+(4.24/4.)*
    1(TWO(E(J),E(I),X,T)-BETA/XX)
     X=BEE-2.*C*AMU(K)
     XX=SQRTF(X)
     Z=X*ZOX
     G=ONE(E(J),E(I),X,GX,OM,CM,MJ,LJ,AI,B,Z,EMV)
     G=(2.*81.5/4.)*(G-ALPHA/XX)+(4.24/4.)*
    1(TWO(E(J),E(I),X,T)-BETA/XX)
     D=D+WGT(K)*(F+G)
 151 H=H+WGT(K)*AMU(K)*(G-F)
     IF(I-J) 70,802,70
 802 FA=((2.*81.5/4.)*ALPHA+(4.24/4.)*BETA)*2./SQRTF(E(J))
     D=D+FA
     H=H+FA/3.
  70 SK(J,I)=D
 101 SKA(J)=SK(J,I)
     PRINT 1004,I
1004 FORMAT (4HI = I3)
1005 FORMAT (19H SCATTERING KERNEL /(7(I3,E13.4)/))
     PRINT 1005,(J,SKA(J),J=1,I)
 102 CONTINUE
     DO 110 J=2,NM
     JK=J-1
     DO 110 I=1,JK
     BB=((E(I)/E(J))**2)*EXPF((E(J)-E(I))/T)
 110 SK(J,I)=SK(I,J)*BB
     DO 951 L=1,4
     NI=KN(L)
     MI=IM(L)
     PRINT 199,T
 199 FORMAT (25H1SCATTERING KERNEL, KT = F7.4)
     PRINT 9199,(I,I=NI,MI)
9199 FORMAT (7X,10(I2,9X))
 951 PRINT 200,(I,(SK(J,I),J=NI,MI),I=1,NM)
 200 FORMAT (I4,2X,10(E11.3))
     NI=41
     MI=45
     PRINT 199,T
     PRINT 9199,(I,I=NI,MI)
     PRINT 220,(I,(SK(J,I),J=NI,MI),I=1,NM)
 220 FORMAT (I4,2X,5(E11.3))
9876 CONTINUE
     END
```

```
      FUNCTION ONE(EP,E,X,GX,OM,CM,MJ,LJ,AI,B,Z,EMV)
C     THIS CALCULATES (SIGMA(UP TO U,MU)/(SIGMA BOUND ATOM/4)) FOR
C     NELKIN PROTON. EP,E,X, AND T ARE IN EV.
      DIMENSION BI(200),AA(3),CC(3)
      OM1=0.205
      OM2=0.481
      AA(1)=1.
      AA(2)=X/(EMV*OM1)
      AA(3)=(AA(2)**2)/2.
      CC(1)=1.
      CC(2)=2.*X/(EMV*OM2)
      CC(3)=(CC(2)**2)/2.
      PROD1=0.0
      SUM=0.
      D=E*SQRTF(E/(EP*X*GX*3.14159))
      N=1.5*Z+10.
      BI(N)=0.
      SUM=1.0E-20
      BI(N-1)=SUM
      NN=N-1
      DO 11 J=2,NN
      I=N-J
      BI(I)=2.*FLOATF(I)*BI(I+1)/Z+BI(I+2)
   11 SUM=SUM+BI(I)
      SUM=2.*SUM-BI(1)
      C=EXPF(Z)/SUM
      DO 12 J=1,NN
   12 BI(J)=C*BI(J)
      DO 1050 M=1,MJ
      FM=M-1
      PROD=0.
      DO 17 L=1,LJ
      EL=L-1
      SUM=0.
      DO 13 N=1,NN
      EN=N-1
      BB=E-EP+X*CM+EN*OM+EL*OM1+FM*OM2
      AZ=(BB**2)/(4.*X*GX)
      IF(AZ-705.) 112,112,113
  112 P=((B**EN)*BI(N))/EXPF(AZ)
      GO TO 114
  113 P=0.0
  114 SUM=SUM+P
      W=P/SUM
      IF(W-1.0E-4) 14,14,13
   13 CONTINUE
      PRINT 500,N
  500 FORMAT (5H N = I3)
   14 DO 15 N=2,NN
      EN=N-1
      BB=E-EP+X*CM-EN*OM+EL*OM1+FM*OM2
      AZ=(BB**2)/(4.*X*GX)
      IF(AZ-705.) 115,115,116
  115 P=(BI(N)/(B**EN))/EXPF(AZ)
```

```
      GO TO 117
  116 P=0.0
  117 SUM=SUM+P
      W=P/SUM
      IF(W-1.0E-4) 16,16,15
   15 CONTINUE
      PRINT 500,N
   16 PROD=AA(L)*SUM+PROD
   17 CONTINUE
      PROD1=CC(M)*PROD+PROD1
 1050 CONTINUE
      ONE=D*PROD1/EXPF(X*AI)
      END


      FUNCTION TWO(EP,E,X,T)
C     THIS CALCULATES (SIGMA(UP TO U,MU)/(SIGMA BOUND ATOM/4))
C     FOR A FREE GAS OF MASS 16. EP,E,X,AND T ARE IN EV.
      B=E-EP+X/16.
      D=E*SQRTF(E*16./(X*T*3.14159*EP))
      TWO=D/EXPF((B**2)*16./(4.*X*T))
      END
         END        COUTH


      SUBROUTINE FKERN(NM,SFA,T,A,E,SK)
C     SUBROUTINE FKERN CALCULATES THE SCATTERING MATRIX USING THE
C     MONATOMIC GAS MODEL.
      DIMENSION E(55),SK(55,55),W(55),RX(55),EX(55)
      ETA=(A+1.)/(2.*SQRTF(A))
      RIO=(A-1.)/(2.*SQRTF(A))
      DO 43 I=1,NM
      W(I)=SQRTF(E(I)/T)
      RX(I)=RIO*W(I)
   43 EX(I)=ETA*W(I)
      DO 10 I=1,NM
      DO 10 J=1,I
   10 SK(J,I)=.5*SFA*(ETA**2)*(F(I)/E(J))*(ERF(EX(I)-RX(J))+ERF(EX(I)+
     1RX(J))+(EXPF((W(J)**2)-(W(I)**2)))*(ERF(EX(J)-RX(I))-ERF(RX(I)+
     2EX(J))))
      END
```

APPENDIX F

NOTATION

Roman Letters

a	Fuel rod radius in mean free path, $a = \Sigma_t^f r_f$
A	Fuel element area, Eq. (2.12)
A	Ratio of scatterer mass to neutron mass, Eq. (5.1)
A	Parameter for substitution into the Nelkin Water Kernel, Eqs. (5.17) and (5.18)
A	Mass number, Eq. (7.3)
c	Ratio of the scattering to the total cross section, p. 27
C(E)	Correction factors to the diagonal terms in the Nelkin Water Matrix, p. 59
C_1	Eq. (4.36)
C_2	Eq. (4.37)
d(E)	Linear extrapolation length into the fuel element, Eq. (2.18)
$d_o(E)$	Linear extrapolation length into a black hole, Eq. (C.4)
D	Diffusion coefficient for the homogenized cell, Eq. (6.38)
D_1	Eq. (4.30)
D_2	Eq. (4.32)

$D_m(E)$	Diffusion coefficient for the moderator, Eq. (2.13)
$D_f(E)$	Diffusion coefficient for the fuel, p. 27
E	Neutron energy in eV
E_c	Thermal cutoff energy
f	Thermal utilization, Eqs. (6.13) and (6.15)
$f(\mu)$	Eq. (5.21)
f(E)	Eqs. (2.7), (2.28), and (3.8)
F_o	Eq. (4.26)
F_1	Eq. (4.27)
F_2	Eq. (4.28)
F_3	Eq. (4.29)
g	Sec. 4.3, Eq. (4.45)
G(E)	Eq. (2.17)
h	Planck's Constant
$I_n(z)$	Modified Bessel function of the first kind
$J_-(E)$	Current into the fuel element, Eq. (2.24)
$J_o(E)$	Net current entering the cladding from the fuel rod, Eq. (4.22)
$J_n(E)$	Net current entering the fuel element, Eq. (2.12)
$K_n(z)$	Modified Bessel function of the second kind
ℓ_t	Thermal lifetime, Eq. (6.17)
L	Diffusion length for the homogenized cell, Eq. (6.39)
$\bar{L}_1^{-1}$	Eq. (4.33)

$\bar{L}_1^2$	Eq. (4.34)
$\bar{\mathcal{L}}_1^1$	Eq. (4.38)
$\bar{\mathcal{L}}_1^2$	Eq. (4.39)
M	p. 47
M(E)	Maxwellian distribution, Eq. (2.6)
M_{ij}	Cylindrical moments, Sec. 4.1
M_r	p. 47
M_v	p. 47
N(E)	Spatially averaged source, Eq. (2.11)
$N(\vec{r},E)$	Neutron source, Eq. (2.11)
$\bar{N}^i(E)$	Spatially averaged energy dependent neutron density in region i, Eq. (6.5)
$\bar{N}^i$	Total neutron density in region i, Eq. (6.7)
$P_e(E)$	Fuel element escape probability, Chap. 4
$P_m(E)$	Moderator escape probability, Sec. 3.2
$P_r(E)$	Fuel rod escape probability, Sec. 4.1
$P_{rv}(E)$	Escape probability for the fuel rod and void region, Sec. 4.2
$P_s(E)$	Moderator escape probability, Sec. 3.1
P_u	Eq. (4.43)
P_{unif}	Eq. (4.44)
r_o	Fuel element radius
r_1	Equivalent cell radius
r_c	Inner radius of the cladding
r_f	Fuel rod radius

r_{in}	Sec. 4.3, Eq. (4.49)
r_{out}	Sec. 4.3, Eq. (4.50)
RR_j^i	Reaction rate of type j in region i, Eqs. (6.18) and (6.19)
$S(E)$	Neutron slowing down source, Eq. (2.3)
$\overline{S}(E)$	Spatially averaged slowing down source of neutrons, Eqs. (2.10), (5.27), and (7.1)
$S(\vec{r},E)$	Spatially dependent slowing down source of neutrons, Eq. (2.10)
t	Eq. (4.24)
T	Moderator temperature in electron volts
T	Sec. 4.3, Eq. (4.35)
u	Lethargy
v(E)	Neutron velocity
$\overline{v}_i$	Average neutron velocity in region i, Eq. (6.6)
V^i	The volume of region i
w_k	Weighting coefficients for the Gaussian quadrature integration formula, p. 50
x	Eq. (4.42)
X	Eq. (5.2)
y	p. 15, $y = r_1/r_o$
y	Eq. (5.14)
z	Eqs. (5.17) and (5.18)
z	Eq. (5.5)

Greek Letters

$\alpha(E)$	Fuel capture to fission ratio
$\beta(E)$	Eq. (4.2)
γ	Euler's Constant
δ_n^m	Moderator neutron density disadvantage factor, Eq. (6.8)
δ_n^c	Cladding neutron density disadvantage factor, Eq. (6.9)
δ_φ^m	Moderator flux disadvantage factor, Eq. (6.10)
δ_φ^c	Cladding flux disadvantage factor, Eq. (6.11)
ϵ	Convergence criterion, Eq. (C.24)
ζ	Eq. (4.20)
η	Number of fission neutrons produced per thermal absorption in the fuel, Eq. (6.16)
η	Eq. (5.7)
θ	Eq. (4.25)
κ	p. 15
κ_f	p. 28
λ	Eq. (C.4)
$\wedge$	Eq. (4.31)
μ	Cosine of the scattering angle
$\bar{\mu}(E)$	Average cosine of the scattering angle, Eq. (5.24)
μ_k	A zero of the Legendre polynomials, p. 50
ν	Number of fission neutrons produced per thermal fission
ξ	Eq. (4.23)
ξ	Eqs. (5.17) and (5.18)

π = 3.14159

ρ Eq. (5.8)

ρ_{in} Sec. 4.3, Eq. (4.51)

ρ_{out} Sec. 4.3, Eq. (4.52)

σ_b Bound atom microscopic cross section

σ_f Free atom microscopic cross section

$\sigma_j^i(E)$ Microscopic cross section expressed in barns for interaction type j in material i

$\sigma(E' \longrightarrow E, \mu)$ Differential scattering kernel, Eqs. (5.1) and (5.15)

$\sigma(E' \longrightarrow E)$ Scattering kernel, Eqs. (5.4) and (5.19)

$\sigma^*(E \longrightarrow E)$ Modified diagonals for the Nelkin water kernel, Eq. (5.26)

$\sigma_1(E' \longrightarrow E)$ First moment of the scattering kernel, Eq. (5.23)

$\Sigma_j^i(E)$ Macroscopic cross section expressed in cm^{-1} for interaction type j in material i

$\hat{\Sigma}_j^i$ Macroscopic effective cross section for interaction type j in material i, Eqs. (6.23) and (6.31)

$\overline{\Sigma}_j^i$ Macroscopic mean cross section for interaction type j in material i, Eqs. (6.24) and (6.32)

$\Sigma(E' \longrightarrow E)$ Macroscopic scattering kernel, Eq. (2.1)

τ Sec. 4.3, Eq. (4.40)

$\varphi^m(E)$ Energy dependent flux in an infinite homogeneous moderator, Eq. (2.1)

$\bar{\varphi}^i(E)$	Spatially averaged energy dependent flux in region i
$\bar{\varphi}^i_o$	Spatially averaged 2200 m/sec flux in region i
$\bar{\varphi}^i_T$	Spatially averaged thermal flux in region i
$\bar{\varphi}^m_k(u_i)$	k^{th} iteration for the moderator flux at lethargy u_i, Eq. (C.22)
$\hat{\varphi}^m_k(u_i)$	$\bar{\varphi}^m_k(u_i)$ normalized, Eq. (C.23)
$\varphi_u(\vec{r})$	Eq. (4.5)
χ	Eqs. (5.17) and (5.18)
$\chi(E)$	Eq. (2.21)
ω_r	p. 47
ω_1	p. 47
ω_2	p. 47

Subscripts and Superscripts

a	absorption
c	cladding
f	fuel
f	fission
h	homogenized cell
m	moderator
s	scattering
t	total
tr	transport

WORKS CITED

BOOKS

K. M. Case, F. de Hoffmann, and G. Placzek, Introduction to the Theory of Neutron Diffusion, Vol. I, United States Government Printing Office, 1953. (See Footnotes 28 and 35.)

H. B. Dwight, Tables of Integrals and Other Mathematical Data, The Macmillan Company, New York, 1961. (See Footnotes 87 and 90.)

S. Glasstone and M. C. Edlund, The Elements of Nuclear Reactor Theory, D. Van Nostrand Company, Inc., Princeton, Toronto, London, and New York, 1952. (See Footnotes 20 and 25.)

A. M. Weinberg and E. P. Wigner, The Physical Theory of Neutron Chain Reactors, The University of Chicago Press, Chicago, 1958. (See Footnotes 1, 23, 26, 30, 63, 76, and 83.)

JOURNALS

A. Amouyal, P. Benoist, and J. Horowitz, "Nouvelle Méthode de Determination du Facteur d'Utilization Thermique d'une Cellule," J. Nucl. Energy 6, 79 (1957). (See Footnotes 10 and 27.)

J. R. Beyster, et al., "Measurement of Neutron Spectra in Water, Polyehtylene, and Zirconium Hydride," Nucl. Sci. Eng. 9, 168 (1961). (See Footnote 54.)

K. B. Cady and M. Clark, Jr., "Neutron Transport in Cylindrical Rods," Nucl. Sci. Eng. 18, 491-507 (1964). (See Footnotes 24 and 32.)

K. B. Cady and C. R. Mac Vean, "A Simplified Formulation of Space-Energy Cell Theory," Trans. Am. Nucl. Soc. 6, 234-235 (1963). (See Footnote 70.)

G. P. Calame, "Diffusion Parameters of Water for Various Scattering Kernels," Nucl. Sci. Eng. 19, 189 (1964). (See Footnote 55.)

L. G. de Sobrino and M. Clark, Jr., "A Study of the Wilkins Equation," Nucl. Sci. Eng. 10, 388 (1961). "Comparison of the Wilkins Equation with Experiments on Water Systems," Nucl. Sci. Eng. 10, 377 (1961). (See Footnote 47.)

M. Goldstein and R. M. Thaler, "Recurrence Techniques for Calculation of Bessel Functions," Mathematical Tables and Other Aids to Computation, 13, 102 (1959). (See Footnotes 88 and 89.)

A. Hassitt, "Methods of Calculation for Heterogeneous Reactors," Progress in Nuclear Energy, Series I, Vol. 2, Pergamon Press, New York, London, Paris, and Los Angeles, 1958. (See Footnote 4.)

R. L. Hellens and H. C. Honeck, "Summary and Preliminary Analysis of the BNL Slight Enriched Uranium, Water Moderated Lattice Measurements," Light Water Lattices, International Atomic Energy Agency, Vienna, 1962. (See Footnote 75.)

H. C. Honeck, "The Calculation of the Thermal Utilization and Disadvantage Factor in Uranium/Water Lattices," Nucl. Sci. Eng. 18, 49-68 (1964). (See Footnotes 7, 15, 38, 73, 74, 77, 78, 79, and 81; Table A.3; and Figs. 8.1, 8.2, and 8.3.)

A. N. Lowan, N. Davis, and A. Levinson, "Tables of the Zeros of the Legendre Polynomials of Order 1-16 and the Weight Coefficients for Gauss's Mechanical Quadrature Formula," Bull. Am. Math. Soc. 48, 739 (1942). (See Footnote 57.)

M. S. Nelkin, "Scattering of Slow Neutrons by Water," Phys. Rev. 119, 741-746 (1961). (See Footnotes 13, 41, 46, 48, and 53.)

C. D. Petrie, M. L. Storm, and P. F. Zweifel, "Calculation of Thermal Group Constants for Mixtures Containing Hydrogen," Nucl. Sci. Eng. 2, 728-744 (1957). (See Footnote 64.)

G. C. Pomraning, "On the Energy Averaging of the Diffusion Coefficient," Nucl. Sci. Eng. 19, 250 (1964). (See Footnote 67.)

G. C. Pomraning, "On the Validity of the Constant Source Assumption for the Cell Problem," Nucl. Sci. Eng. 18, 400-403 (1964). (See Footnote 21.)

M. J. Poole, M. S. Nelkin, and R. S. Stone, "The Measurement and Theory of Reactor Spectra," Progress in Nuclear Energy, Series I, Vol. 2, Pergamon Press, New York, London, Paris, and Los Angeles, 1958. (See Footnotes 2, 18, 51, and 91.)

K. S. Singwi and L. S. Kothari, "Transport Cross Section of Thermal Neutrons in Solid Moderators," Second Geneva Conference Proceedings 16, 325 (1958). (See Footnote 65.)

N. G. Sjöstrand, "Definition of the Diffusion Constant in One-Group Theory," J. Nucl.Energy, Part A, Reactor Science 12, 151 (1964). (See Footnote 66.)

E. Starr and J. Koppel, "Determination of Diffusion Hardening in Water," Nucl. Sci. Eng. 14, 244 (1962). (See Footnote 56.)

G. W. Stuart and R. W. Woodruff, "Method of Successive Generations," Nucl. Sci. Eng. 10, 388 (1961). (See Footnote 33.)

R. S. Varga, "Numerical Methods for Solving Multi-Dimensional Multigroup Diffusion Equations," Proceedings of Symposia in Applied Mathematics, Vol. XI, Nuclear Reactor Theory, American Mathematical Society, Providence, 1961. (See Footnote 16.)

D. F. Zaretsky, "Effective Boundary Conditions for Grey Bodies," First Geneva Conference Proceedings 5, 525-530 (1955). (See Footnote 84.)

REPORTS

D. D. Clark, "The Cornell University Nuclear Reactor Laboratory," CURL-1, Cornell University (1961). (See Footnote 14 and 68 and Table A.2.)

F. D. Federighi and D. T. Goldman, "KERNEL and PAM-Programs for Use in the Calculation of the Thermal Scattering Matrix for Chemically Bound Systems," KAPL-2225, Knolls Atomic Power Laboratory (1962). (See Footnotes 49, 58, and 86.)

D. Hughes and B. Schwartz, "Neutron Cross Sections," BNL-325, 2nd Ed., Brookhaven National Laboratory (1958). (See Footnotes 60 and 72.)

H. C. Honeck, "THERMOS-A Thermalization Transport Theory Code for Reactor Lattice Calculations," BNL-5826, Brookhaven National Laboratory (1961). (See Footnotes 6, 17, and 59.)

D. C. Leslie, "The Calculation of Thermal Spectra," Proceedings of the Brookhaven Conference on Neutron Thermalization, BNL-719, Vol. II, pp. 592-609, Brookhaven National Laboratory (1962). (See Footnote 9.)

D. C. Leslie, "The SPECTROX Method for Thermal Spectra in Lattice Cells," AEEW-M211, United Kingdom Atomic Energy Authority (1962). (See Footnotes 8, 19, 22, and 85.)

Neutron Spectra in Lattices and Infinite Media, Proceedings of the Brookhaven Conference on Neutron Thermalization, BNL-719, Vol. II, Brookhaven National Laboratory (1962). (See Footnotes 3 and 5.)

A. Radkowsky, "Temperature Dependence of the Thermal Transport Mean Free Path," Physics Quarterly Report (April, May, June, 1950), ANL-4476, p. 89, Argonne National Laboratory (July, 1950). (See Footnote 42.)

The Scattering Law, Proceedings of the Brookhaven Conference on Neutron Thermalization, BNL-719, Vol. I. Brookhaven National Laboratory (1962). (See Footnote 44.)

E. P. Wigner and J. E. Wilkins, Jr., "Effect of the Temperature of the Moderator on the Velocity Distribution of Neutrons with Numerical Calculations for H as the Moderator," AECD-2275 (1944). (See Footnotes 11, 39, 45, and 52.)

J. E. Wilkins, Jr., "Effect of the Temperature of the Moderator on the Velocity Distribution of Neutrons for a Heavy Moderator, CP-2481 (1944). (See Footnotes 12, 40, 45, and 50.)

C. H. Wescott, "The Specification of Neutron Flux and Effective Cross Sections," AECL-352 (1956). (See Footnote 61.)

THESES

S. S. Berg, "Initial Experiments on the Cornell University Zero Power Reactor Cores," Cornell University Thesis (1964). (See Footnotes 69 and 80 and Table A.1.)

K. B. Cady, "Neutron Transport in Cylindrical Rods," Massachusetts Institute of Technology Thesis (1962). (See Footnotes 29, 31, 34, 36, and 37.)

J. A. Larrimore, "Temperature Coefficients of Reactivity in Homogenized Thermal Nuclear Reactors," Massachusetts Institute of Technology Thesis (1962). (See Footnote 62.)

J. Suich, "Temperature Coefficients in Heterogeneous Reactor Lattices," Massachusetts Institute of Technology Thesis (1963). (See Footnotes 71 and 82.)

thesM27
A simplified cell theory applied to the
3 2768 002 03371 4
DUDLEY KNOX LIBRARY